Maritime Sediments and Atlantic Geology

Published by

THE ATLANTIC GEOSCIENCE SOCIETY

Editors - R.K. Pickerill, S.M. Barr and G.L. Williams

Business Manager - A. Fricker

ASSOCIATE EDITORS

K.L. Currie
Geological Survey of Canada
601 Booth Street
Ottawa 4, Ontario, K1A 0E8

K. Howells
Nova Scotia Research Foundation
P.O. Box 790
Dartmouth, Nova Scotia, B2Y 3Z7

J.D. Keppie
Nova Scotia Department of Mines and Energy
1649 Hollis Street
Halifax, Nova Scotia, B3J 2X1

B.R. Pelletier
Geological Survey of Canada
601 Booth Street
Ottawa 4, Ontario, K1A 0E8

D.J.W. Piper
Geological Survey of Canada
Atlantic Geoscience Centre
Bedford Institute of Oceanography
P.O. Box 1006
Dartmouth, Nova Scotia, B2Y 4A2

J. Riva
Department of Geology
Université Laval
Ste-Foy, Québec, G1K 7P4

P.E. Schenk
Department of Geology
Dalhousie University
Halifax, Nova Scotia, B3H 3J5

G.S. Stockmal
Geological Survey of Canada
Atlantic Geoscience Centre
Bedford Institute of Oceanography
P.O. Box 1006
Dartmouth, Nova Scotia, B2Y 4A2

French Translation Editor - D. Fillion

©Maritime Sediments and Atlantic Geology (1981)
World rights reserved.

Permission to photocopy for internal or personal use or the internal or personal use of specific clients is granted by Maritime Sediments and Atlantic Geology for libraries and other users registered with the Copyright Clearance Center (CCC), provided that the stated fee per copy is paid directly to the CCC, 21 Congress Street, Salem, MA 01970. Special requests should be addressed to Maritime Sediments and Atlantic Geology, c/o Acadia University Institute, Wolfville, Nova Scotia, B0P 1X0.

ISSN 0711-1150

LETTER FROM THE PRESIDENT OF A.G.S.

Owing to the strong interest of members throughout the region, the Atlantic Geoscience Society has accepted Maritime Sediments and Atlantic Geology as the official journal of the Society. This significant step is a great opportunity and challenge for both the journal and the Society. It must offer wider opportunities and benefits for geoscientists in Atlantic Canada.

In its 22-years, the journal has demonstrated the need for the publication of papers with a regional orientation and the development of the local geological database. We are indebted to the hard work of the editors, D.J. Stanley and D.J.C. Laming (1965-6), B. Pelletier and G. Drapeau (1967-80), R.K. Pickerill and G.E. Pajari (1981-5), to the associate editors, to the production staff and to the many authors and others who have helped support and develop the journal.

The journal has not stood still, however, but has broadened its scope into all aspects of geoscience and has established itself as the regional journal. On the occasion of the change of editorship and production in 1979-80, A.G.S. as the regional society was approached to find whether some relationship with the journal could be set up. As Alasdair McKay who was President at the time wrote in Volume 17, the agreed association was an informal one. The journal since 1980 has supported the Society by publishing abstracts of papers given at A.G.S. annual meetings. In return, the Society undertook to promote the journal through its newsletter.

1986 will be another transition period. Two of the issues of Volume 22 will be special issues. Though the format for the journal is the same, the production is now in Atlantic Canada. In 1987, Volume 23 will be the first that will truly be the "Journal of the Atlantic Geoscience Society". Ron Pickerill, Sandra Barr and Graham Williams have been appointed by the Society as its first journal editors.

On behalf of the Atlantic Geoscience Society I am glad to express the support of our members for the three appointed editors and to encourage them in putting the journal on a sound and secure scientific and financial footing. I urge readers and members to make good use of the new opportunities.

Aubrey Fricker
President, A.G.S.

Contributions to the Geology of the Meguma Terrane, Nova Scotia

Edited by

J. Duncan Keppie
Department of Mines and Energy
P.O. Box 1087, Halifax, Nova Scotia, Canada B3J 2X1

Type setting and layout for this issue were funded by the Federal Government, Department of Energy, Mines and Resources, and printing costs were borne by the Nova Scotia Department of Mines and Energy under the Canada-Nova Scotia Mineral Development Agreement 1984-9.

A Special Issue

of

Maritime Sediments and Atlantic Geology

Vol. 22, No. 1

Maritime Sediments and Atlantic Geology

Vol. 22 April, 1986 No. 1

Foreword

J. Duncan Keppie
(Editor)

During the period between 1981 and 1984, the eastern end of the Meguma Terrane was investigated under the Canada - Nova Scotia Co-operative Mineral Program. This program involved geologists from both Federal and Provincial Governments and a number of universities. It provided the first comprehensive remapping since the excellent mapping undertaken by E. H. Faribault around the turn of the century. The remapping was supported by airborne gradiometry and radiometry and formed the basis for multidisciplinary studies into various aspects of the geology , especially gold metallogeny. These studies, together with those in other parts of the Meguma Terrane, formed the basis for a Symposium at the Northeastern Section of the Geological Society of America in March, 1984. The papers in this volume represent a collection of several presented at the Symposium. Other papers on the topic have already been published in the Geological Survey of Canada Papers 83-1 and 84-1, the Nova Scotia Department of Mines and Energy Papers 83-1 and 84-1, and in the Canadian Institute of Mining and Metallurgy Division, Excursion Guidebook entitled "Gold Deposits in the Meguma Terrane of Nova Scotia", 1983. A symposium on "Turbidite-Hosted Gold Deposits" was held at the Geological Association of Canada Annual Meeting in Fredericton, 1985 followed by publication of a collection of papers in a Geological Association of Canada Special Paper. Some of these papers deal with gold deposits in the Meguma Terrane. A field trip to several gold deposits in the Meguma Terrane, augmented by a field guidebook, followed the Symposium. Undoubtedly, other results of these studies will continue to be published.

Each paper in this volume was reviewed by two independent reviewers whose comments were used to determine whether the paper was acceptable for publication. The editor takes this opportunity for thanking the reviewers for their assistance; their contribution lead to improvements in the papers. The reviewers were: J. Chandra, A. K. Chatterjee, D. B. Clarke, G. Cumming, K. Currie, J. Dostal, W. Fyson, S. J. Haynes, J. Henderson, R. V. Kirkham, H. Massone, B. H. O'Brien, K. H. Poulsen, P-Y Robin, D. F. Sangster, P. K. Smith, R. Thorpe, T. Wright and M. Zentilli. I would also like to thank P. Ledwidge for translating all but one of the abstracts.

Maritime Sediments and Atlantic Geology

Vol. 22 April, 1986 No. 1

Table of Contents

Foreword i

*Constraints on the origin of gold in the Meguma Zone, Ecum Secum area, Nova Scotia
M.N. Henderson and J.R. Henderson 1

*Distribution and localization of gold in Meguma Group rocks, Nova Scotia: implications of metal distribution patterns in quartz veins and host rocks on mineralization processes at Harrigan Cove, Halifax County
J.H. Crocket, F. Fueten, A. Kabir and P.M. Clifford 15

*Formation of spaced cleavage and concurrent mass removal of SiO_2, Meguma Group metagreywackes, Goldenville, Nova Scotia
F. Fueten, P.M. Clifford, L.L. Pryer, M.J. Thompson and J.H. Crocket... 35

Structural study of highly deformed Meguma phyllite and granite, vicinity of White Head Village, S.E. Nova Scotia
C.K. Mawer and P.F. Williams 51

*A stratabound zinc-lead deposit in Meguma Group metasediments at Eastville, Nova Scotia
W.P. Binney, K.A. Jenner, A.L. Sangster and M. Zentilli 65

*Lead isotope data for gold-bearing veins and their host metasedimentary rocks of the Goldenville Formation, eastern Nova Scotia
R.M. Farquhar and S.J. Haynes 89

A re-appraisal of the alaskite/muscovite-biotite granite suite of Halifax County, Nova Scotia
T.E. Smith, D. Peck, C.H. Huang and P.E. Holm 101

*Application of airborne gamma ray spectrometric surveys, Meguma Terrane, Nova Scotia
K.L. Ford and J.M. Carson 117

*Contributions to the Canada-Nova Scotia Co-operative Mineral Program 1981-1984.

Maritime Sediments and Atlantic Geology

Vol. 22 April, 1986 No. 1

Constraints on the Origin of Gold in the Meguma Zone, Ecum Secum area, Nova Scotia

M.N. Henderson and J.R. Henderson
Geological Survey of Canada
601 Booth St., Ottawa, Ontario K1A 0E8

Gold occurs mainly in laminated bedding-parallel quartz veins in the Goldenville Formation metawacke-slate sequence. The bedding-parallel veins formed by hydraulic fracturing before the beds were folded. Subsequently, during development of the folds, en echelon quartz veins formed on the fold limbs, and perhaps in the latest stage of folding, saddle reef veins formed along fold hinges. All these vein types are locally auriferous, but gold was first deposited during formation of the bedding-parallel veins. Absence of any through-going system of "feeder" veins as well as the formation of hydraulic fractures indicate that the rocks were not permeable during vein formation, and the quartz and gold were derived locally from the host strata.

L'or présent dans la suite métawacke-schiste de la Formation Goldenville est localisé principalement dans des veines de quartz laminées et parallèles à la stratification. Ces veines parallèles à stratification furent formées par fracture hydraulique avant le plissement des lits. Par la suite, pendant l'amplification des plis, des veines de quartz en échelon furent formées sur les flancs de plis et peut-être, pendant la phase finale de plissement, des veines en "gîte de selle" se formèrent à la charnière de plis. Tous ces types de veines sont aurifères par endroit mais l'apport initial de l'or date de la formation des veines parallèles à la stratification. L'absence de système de veines nourricières ainsi que la formation de fractures hydrauliques indiquent que les roches n'étaient pas perméables à l'époque de formation de veine et que le quartz et l'or sont de provenance locale.

INTRODUCTION

Disseminated visible gold occurs in quartz veins in the Goldenville Formation of the Cambro-Ordovician Meguma Group (Fig. 1). In the Meguma Zone between Sheet Harbour and Goldenville, one principal vein set is commonly subparallel to bedding, a second vein set forms en échelon arrays within slate interbedded with thicker arenaceous metawacke, and a third set occurs perpendicular to fold hinges within some metawacke beds. The conformably overlying Halifax Formation is mainly slate with thin silty metawacke beds, and generally does not contain quartz veins. Only the bedding-parallel and en échelon veins appear to be auriferous in the study area.

Auriferous veins occur in rocks of greenschist to lower amphibolite metamorphic grade. The typical vein in greenschist terrain is composed of coarse quartz, with some carbonate, chlorite and white mica. Arsenopyrite comprises less than 10 percent of the auriferous veins, and arsenopyrite porphyroblasts are scattered throughout the adjacent wall rocks.

Our main purpose in this report is to describe the relationship of the bedding-parallel veins to the host Goldenville Formation and their development within the geological history of the Meguma Zone. Several explanations of the origin of these veins have been proposed by past workers. Since the last century, bedding-parallel veins in the Goldenville Formation have been classified as anticlinal saddle reefs, first adopted by Faribault (1899) and

MARITIME SEDIMENTS AND ATLANTIC GEOLOGY
22, 1-13 (1986)

0711-1150/86/010001-13$2.95/0

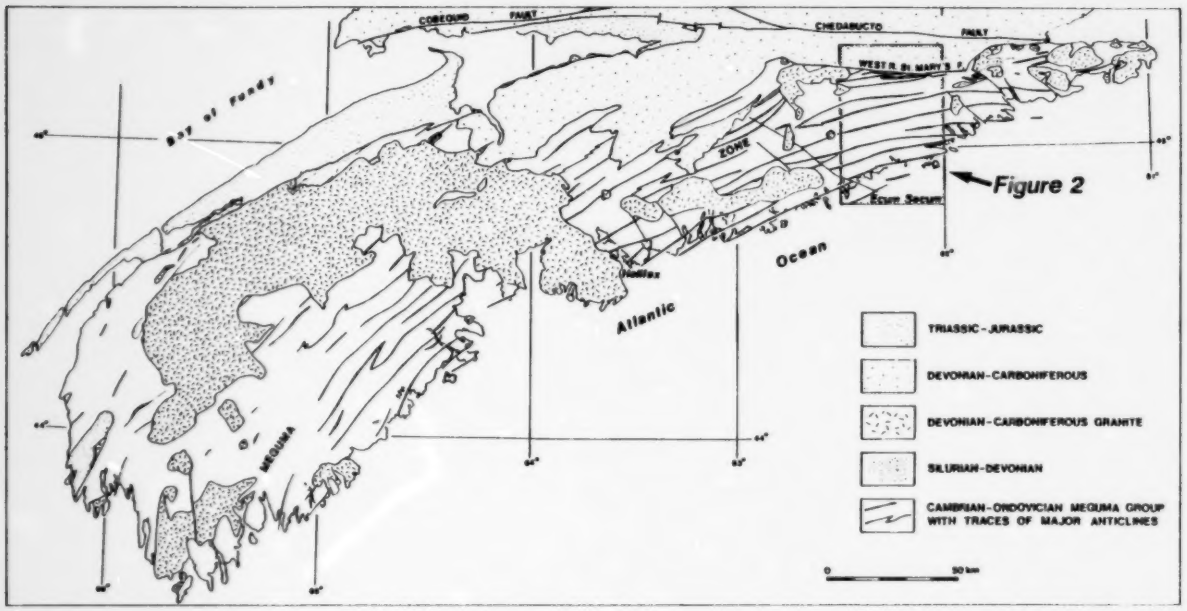

Figure 1 - Generalized geological map of part of mainland Nova Scotia showing the Meguma Zone and the location of the Ecum Secum study area.

recently accepted by Keppie (1976). It is now known that saddle reefs form late in the strain history of chevron folding, and are restricted to dilatant openings in fold hinge regions (Ramsay, 1974). Our studies show that the auriferous bedding-parallel veins in the Goldenville Formation are not restricted to fold hinge regions and that the bedding-parallel veins actually antedate the folding.

Recently it has been proposed that some or all of the bedding-parallel quartz in the Goldenville Formation originated as sea-floor hydrothermal vent-apron deposits of siliceous sinter (Haynes, 1983) or deposits from silica-rich brine (Kretschmar, 1984). Bedding-parallel quartz in the Goldenville Formation consists of centimetric crystals with their prism axes commonly aligned subnormal to the walls of the veins (Henderson, 1983a) whereas sinters are amorphous. Neither Haynes (1983) nor Kretschmar (1984) supported their hypotheses with arguments to explain the crystallization of amorphous silica to form coarse, oriented quartz crystals under greenschist grade conditions. It is noteworthy that James (1955) used grain size of crystallized chert in banded iron formation as an index to metamorphic grade: an average grain size of 0.2 mm defined the staurolite-to-sillimanite grade transition in the Penokean Orogen in northern Michigan.

Graves and Zentilli (1982) proposed that bedding-parallel veins in the Goldenville Formation resulted from hydraulic fracturing under orogenic stress during greenschist grade metamorphism. Their model assumes that fluids released by dehydration reactions could not escape rapidly enough to prevent pore fluids from exceeding the local tectonic stress. Henderson (1983a) attributed inclusion bands of white mica in quartz crystals within bedding-parallel veins in the Goldenville Formation to the crack-seal mechanism of rock deformation (Ramsay, 1980), and thus supported the hydraulic fracture model of Graves and Zentilli (1982).

Smith (1983) showed that at Cochrane Hill (Fig. 2) some auriferous quartz veins antedate and some postdate late Acadian garnet grade metamorphism, and

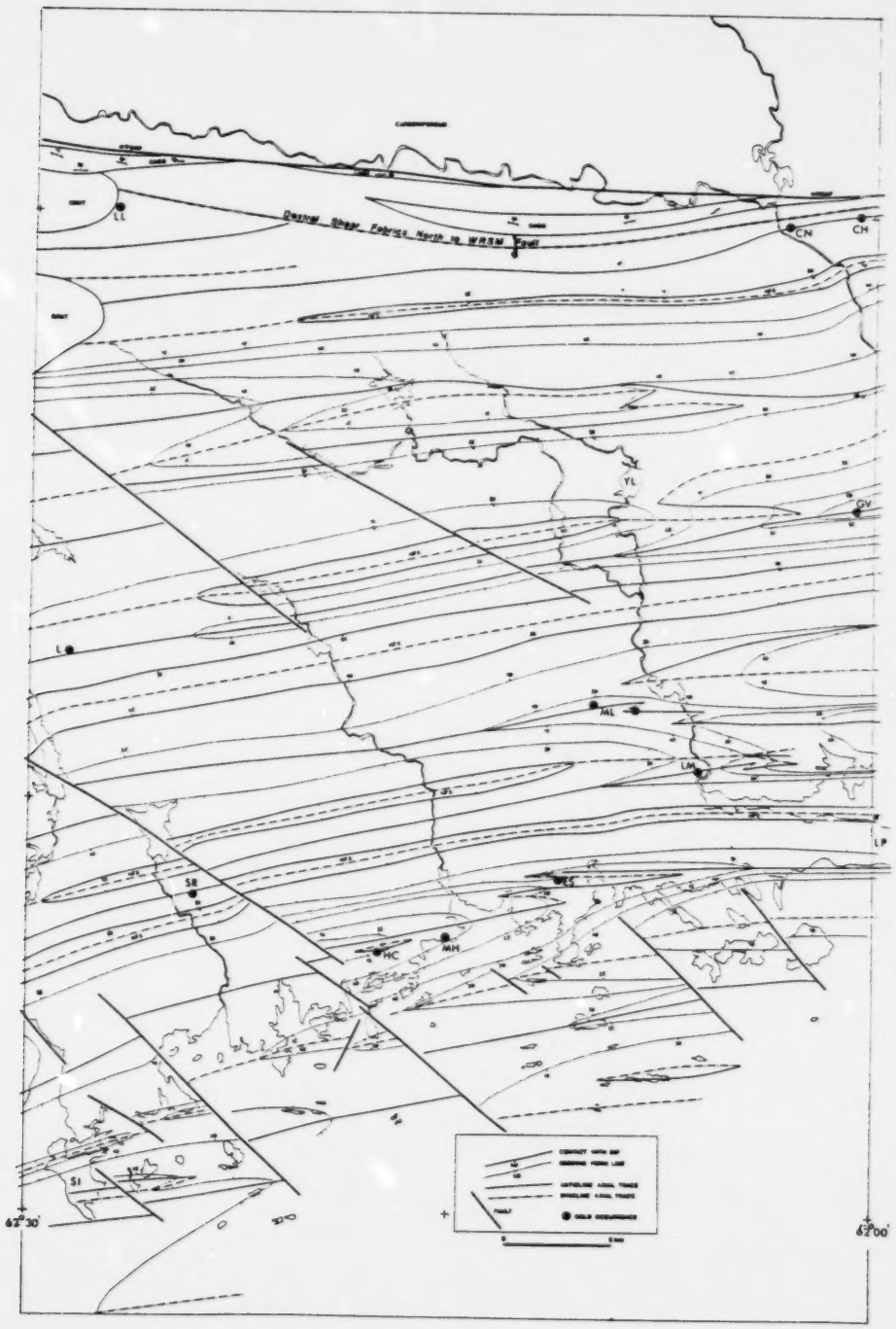

Figure 2 - Geological map of the Ecum Secum study area. Carboniferous fanglomerate (Horton Group) occurs in the St. Mary's Graben north of the West River-St. Mary's River (WRSMF). South of WRSMF the Meguma Group, composed of the Goldenville Formation overlain by the Halifax Formation (HFX), is intruded by granite bodies of two textural types: unfoliated granite (GRNT) and foliated granite (GNSS). Gold occurrences within the area are: Salmon River (SR), Harrigan Cove (HC), Moosehead (MH), Ecum Secum (ES), Liscomb Mills (LM), Miller Lake (ML), Goldenville (GV), Cochrane Hill (CH), Crow's Nest (CN), Liscomb Lake (LL), and Lochaber (L).

concluded that gold was deposited several times during the deformational and metamorphic history of Meguma Zone rocks in this area. The relative age of first development of auriferous quartz veins in the Goldenville Formation would place constraints on some genetic models that have been advanced. Once introduced into the vein network, gold may have later migrated with quartz into other sites, or alternatively, gold may have been introduced from one or more sources several times during the history of vein formation.

CLASSIFICATION OF VEINS IN THE GREENSCHIST TERRAIN

The Meguma Group in the Ecum Secum area consists of Goldenville Formation metawacke and some slate, overlain by Halifax Formation slate and thin bedded silty metawacke. The two units have been folded into tight sub-vertical regional en échelon folds (Fig. 2). Grade of regional metamorphism is lower greenschist except in the north along the West River - St. Mary's Fault where staurolite grade static metamorphism has been superimposed on folded strata which were then redeformed by dextral shear. Within the less complicated greenschist terrane to the south, we recognized three distinct geometries of veins based upon their relationships to bedding and folds, namely, bedding-parallell (BP), en échelon (EE) and ac veins (Fig. 3). In contradiction to our earlier report (Henderson, 1983b), subsequent field work showed that BP and EE veins are not contemporaneous: the BP veins antedate the folding, and the EE veins formed throughout the folding history. The ac veins formed late in the folding history and in some fold hinges ac are weakly folded as a result of vein-parallel shortening.

An example of the classical saddle-reef vein was not observed in our study area. Nevertheless, the major orebody in the Salmon River Gold District (Dufferin Mine) was a rich quartz lode 6 m thick on the crest of an anticline that pinched out within 37 m down-dip

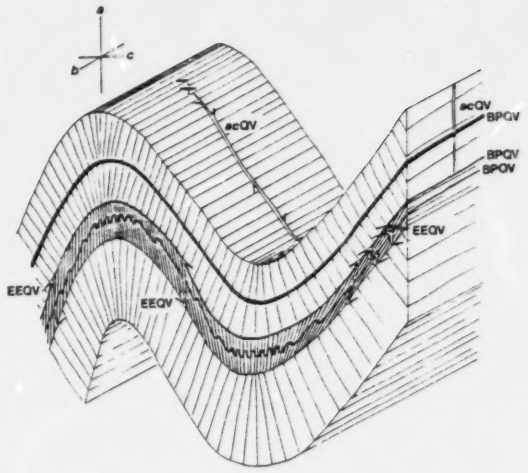

Figure 3 - Diagrammatic representation of the geometry of bedding, cleavage and the three principal vein sets: BPQV (bedding-parallel quartz veins), EEQV (en échelon quartz veins) and acQV (veins parallel to the ac or profile plane of the folds). Note that the drawing is not to scale; most veins are several centimetres wide and several hundred metres long whereas the fold wave lengths are several kilometres.

on each limb (Fig. 4), and was mined for 545 m along the fold crest (Malcolm and Faribault, 1929). Another vein type recognized by Faribault, but not directly observed in our study is the ab vein or fissure vein. At Ecum Secum Mine, the Galena Fissure Vein was coincident with the axial surface of a minor syncline (Fig. 5) and was probably an ab vein. There too, several BP veins (Cameron Leads) are thickened considerably by isoclinal folding in the hinges of a minor syncline and anticline: a process of mechanical thickening of veins which otherwise were too thin to mine with profit on the limbs of folds.

Bedding Parallel Veins (BP)

BP veins are widespread. Most commonly they occur in slate at or near the top of a complete or incomplete Bouma turbidite cycle. They also occur between thick amalgamated metawacke beds. Although BP veins commonly

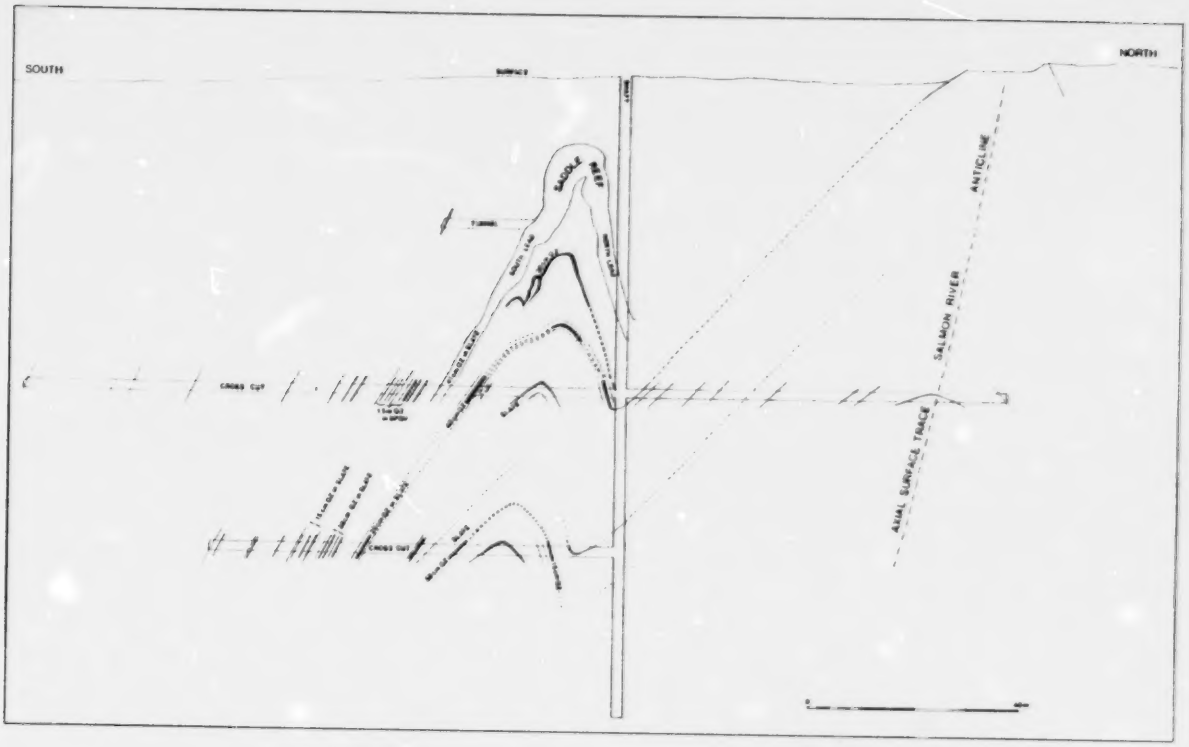

Figure 4 - Transverse-section of the Dufferin Mine, Salmon River Gold District (traced from an unpublished original drawing by E.R. Faribault, Geological Survey of Canada, 1899).

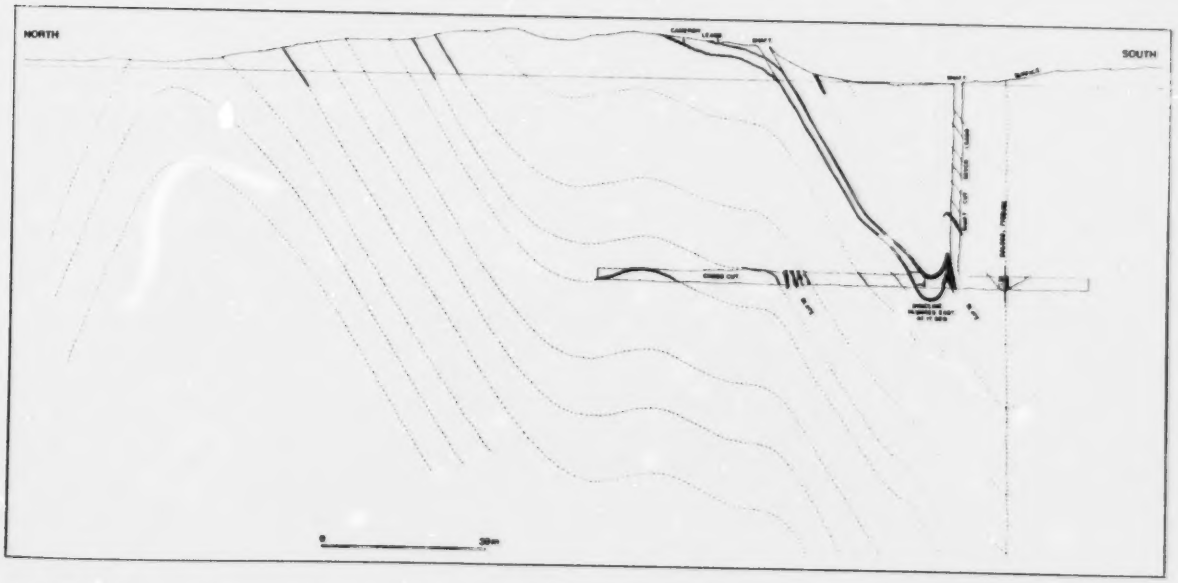

Figure 5 - Transverse-section of the Ecum Secum Mine (traced from an unpublished original drawing by E.R. Faribault, Geological Survey of Canada, 1903).

parallel bedding for considerable distances, locally they are discordant and truncate primary fabrics within the turbidites, e.g. climbing-ripples and sand filled scours. The BP veins range in width from several millimetres to a metre; most are about 10 cm thick and several veins may occur in the same slate bed.

Mesoscopically, BP veins are composed of fairly coarse, translucent quartz, and commonly are subdivided by laminations composed of dark micaceous material (inclusion bands) parallel to the vein walls (Fig. 6). In the gold districts these veins may also contain coarse carbonate, disseminated arsenopyrite, pyrite, pyrrhotite, galena and visible gold.

In some BP veins, stylolitic surfaces parallel the vein walls (Fig. 7) and, along with the micaceous inclusions, contribute to the vein-parallel fabric. The stylolitic surfaces show parallel grooves or striations that most commonly are subparallel to the dip of the veins (Fig. 8). Their micaceous and lineated character favours simultaneous development during folding by pressure solution (to produce the linear surface structure). Although striations appear on the surface of all stylolitic laminations within the veins, striations on different surfaces within the same vein may not be exactly parallel and may differ by as much as 30 degrees. In addition, some veins contain millimetric layers of alternating milky and clear quartz which are oriented perpendicular to the vein walls and appear to intersect the vein surface parallel to the surface striations (i.e. parallel to the ac plane). Marcos Zentilli (personal communication, 1983) drew our attention to this relationship, and suggested that the milky layers might have a higher density of fluid inclusions than the clear layers. Thin sections of veins cut perpendicular to both surface striations and parallel vein-normal, colour-banded quartz fabric confirm that planes of fluid inclusions are aligned normal to the vein walls, but we could see no correlation between planes of dense fluid inclusions and the colour banding. Evidence of stretching in a and b directions is present in some BP veins, including pinch-and-swell as well as boudinage with stubby quartz crystals aligned parallel to a and b.

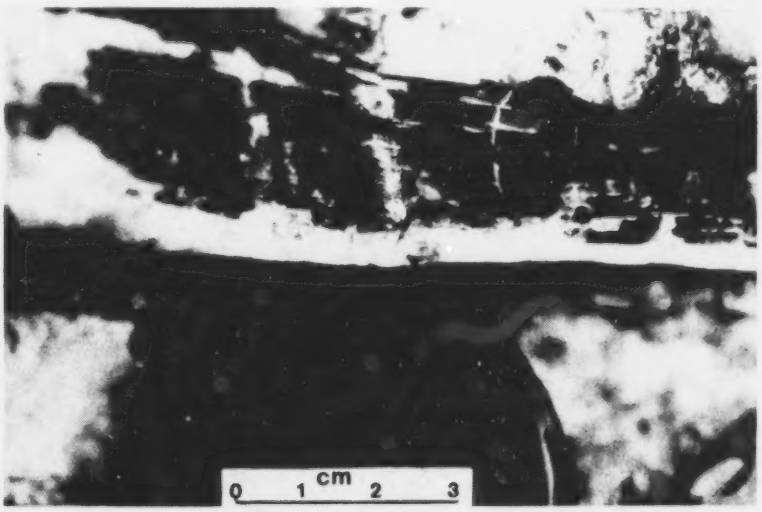

Figure 6 - Photograph showing a vertical laminated BPQV at Harrigan Cove Mine. Note the euhedral quartz crystals with numerous laminations parallel to their bases. The void space probably contained carbonate. GSC 204124-D

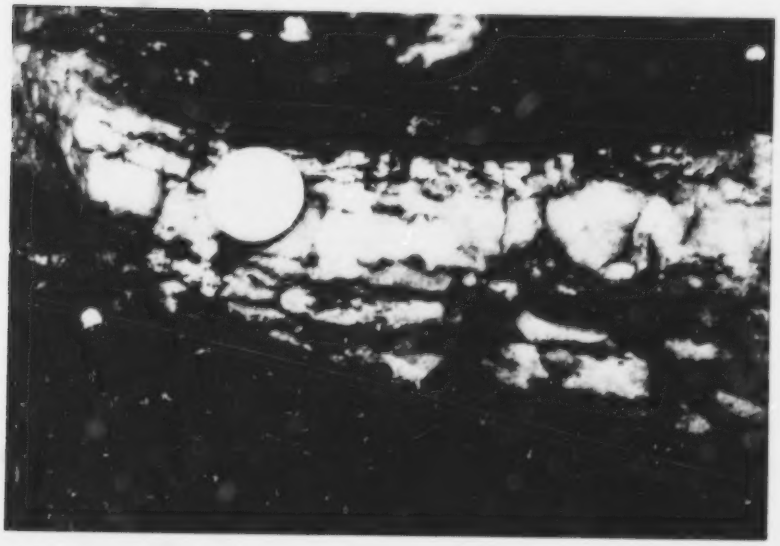

Figure 7 - Photograph of a horizontal exposure of a steeply-dipping BP quartz vein showing stylolitic laminae. Note also the down-dip pinched portion of the vein. The outcrop is located at Markie's Point on the east coast of Sober Island (SI on Fig. 2). GSC 203683-X

Figure 8 - Photograph of a vertical BP vein showing down-dip grooves on stylolitic laminae. The outcrop is located on the west coast of Liscomb Island, 2 km east of Liscomb Peninsula (LP on Fig. 2). GSC 204124-A

BP veins in slate beds are isoclinally folded on the hinges of major folds. The folded veins maintain constant thickness and are considered to be buckle folds; a few measurements of buckle shortening of veins in the ac plane ranged from 50 to 60 percent. However BP veins between amalgamated metawacke beds in fold hinges are not folded.

In thin section, primary quartz crystals in BP veins show various degrees of strain, from undulose extinction to subgrain formation and to total obliteration of primary features by recrystallization (Fig. 12). The quartz laminae and inclusion bands parallel to the vein walls (Fig. 9, 10, 11) are present in non-recrystallized quartz and are therefore primary growth features. The spacing between laminae is about 50 microns. They are separated mainly by white mica and some chlorite a few microns thick with their cleavage planes mainly subparallel to the laminae and vein wall. Also, pelitic fragments believed to be detached pieces of wall rock are contained within the laminated BP veins. The mica inclusion bands are continuous across quartz grain boundaries; the quartz grains which contain them average 5 mm in width at the vein wall and 1 cm in length. If, as described by Ramsay (1980), the inclusion band micas grew syntaxially on wall-rock micas (see also Cox and Etheridge, 1983, and van der Pluijm, 1984), it would appear that the BP veins were initiated when the wall-rock micas still possessed a bedding-parallel depositional fabric (i.e. before formation of slaty cleavage). A pre-cleavage initiation of growth of at least some BP veins is supported by a SEM scan (David Walker, Geological Survey of Canada, analyst) of a pelitic wall-rock inclusion from the vein at Harrigan Cove Mine (Fig. 6): only a weak bedding-parallel mica fabric is present.

Quartz c-axis orientation measured using a standard technique with the universal stage, and c-axis traces measured on a flat stage with a gypsum plate method (Garcia-Celma, 1982) show preferred orientation either normal to the vein wall (Fig. 9), or between 45 degrees and the normal to the vein wall (Fig. 10). The c-axes commonly parallel quartz crystal boundaries and have the same degree of obliquity to the vein walls.

In some cases, as in the BP vein shown in Figure 11, the c-axis traces make a smaller angle with the inclusion bands and the vein wall than do the crystal boundaries. In his study of various crack-seal veins, Ramsay (1980) observed that grain boundaries and c-axes of fibrous quartz are not necessarily parallel, although the orientation of long fibrous crystals may record relative motion between vein walls during crystal growth. We think that the primary quartz in the BP vein shown in Figure 6 is not fibrous (Durney, 1972; cf. Durney and Ramsay, 1973, p. 67-96), but rather the quartz crystals grew across the walls of a fluid-filled fracture that periodically opened along the contact between vein and wall rock.

In summary, we can say from our microfabric observations that the BP veins formed by incremental hydraulic fracturing at the vein-wall rock contact during bedding-normal extension at the onset of horizontal shortening that subsequently produced the slaty cleavage and later the folding. The c-axes in the least strained sample (Figs. 6 and 9) are nearly perpendicular to the vein walls; the oblique relationship between c-axes, crystal boundaries and vein walls in some samples may indicate oblique growth of quartz crystals across a fluid-filled crack, or the quartz crystals may be coarse fibres. Parallelism of bedding micaceous inclusion bands suggests that at least some of the BP veins formed when the micas still had a primary bedding-parallel fabric (i.e. before development of slaty cleavage). Steeply-dipping veins with down-dip grooves on stylolitic laminae reflect

Figure 9 - Photomicrograph of a thin section (cross nichols) of a BP vein at Harrigan Cove Mine (Fig. 6) cut normal to the vein walls, showing the traces of c-axes of quartz crystals (white and black bars). Note the tendency for the c-axes as well as the crystal boundaries to be perpendicular to the laminae which are outlined by trails of white mica, chlorite and opaque material (inclusion bands). The bar scale is 1 cm long. GSC 202510-P

bedding-parallel shear during flexural folding subsequent to BP vein formation. A more extensive petrofabric study using a universal stage on both primary and recrystallized quartz is necessary to document and interpret more completely the primary and secondary features of the BP veins.

En Échelon Veins (EE)

The EE quartz veins occur only on fold limbs; most EE veins lie within slate and silty slate and pinch out in metawacke above and below the slate. The EE veins formed throughout the folding process. Arrays of fluid-filled extension fractures became filled with quartz and later underwent bedding-parallel shear. In Figure 3 the EE veins on the right-hand limb of the syncline depict a sequence of decreasing age from right to left. During continuing deformation, a nearly planar vein became more shortened, rotated and elongated as the syncline tightened. Note that in the ac plane the orientation of the terminations or "pins" of the veins in the bounding metawacke beds reflects the original orientation of the EE vein relative to bedding and the axis of compression during fracture formation: the acute angle between bedding and the axis of the short pin indicates the shear direction of the metawacke beds bounding the slate interbed. Because the pins most commonly are not detached from the EE vein segments passing across the metawacke-slate interface we can certify that generally there was no loss of cohesion between the metawacke and slate across the contact bedding plane during folding. In Figure 13 a relatively old EE vein is shown in its present attitude relative to bedding and cleavages, as well as its apparent

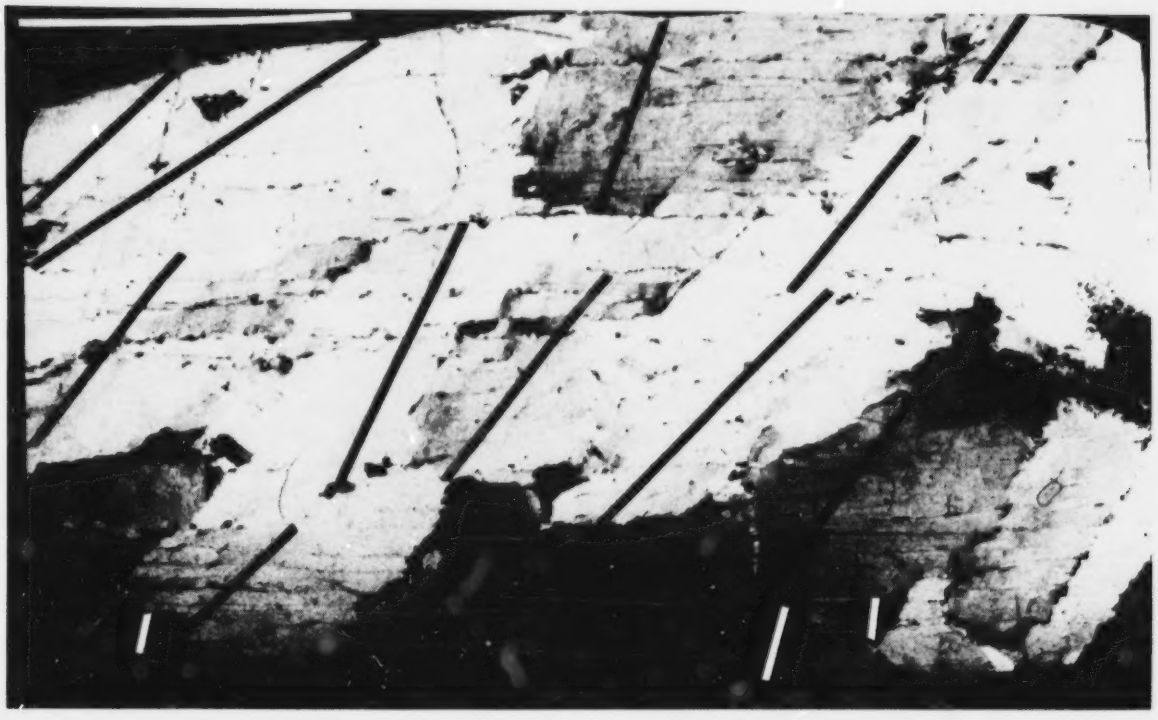

Figure 10 - Photomicrograph of a thin section (cross nichols) of a BP vein from about 2 km NW of Goldenville showing the trace of c-axes of quartz crystals. The thin section is cut parallel to the ac plane. Note the tendency for the c-axes to parallel the crystal boundaries which are oblique to the laminae. The bar scale is 1 cm long. GSC 202510-I

original relationship when bedding and cleavage were originally perpendicular. The dip of bedding at the time of fracturing in this example is not known.

Mesoscopically, EE veins are characterized by coarse milky quartz with rare scattered aggregates of coarse carbonate and chlorite. The veins are nowhere laminated or corrugated like many BP veins. As a group, EE veins have widths ranging from less than 1mm to as much as 1m. Individual EE veins themselves vary considerably in width, and commonly the widest parts are within the centre of the slate bed. The EE veins were formed during the folding and therefore postdate the BP veins.

Although we did not identify an unequivocal EE vein in any of the existing surface exposures at the specific gold deposits shown in Figure 2, we are fairly certain that Hedley's (1941) description of "angulars" in the Guysborough Mine at Goldenville corresponds to our type EE veins. It is worth noting that the richest orebodies in the Guysborough Mine occurred in angular veins near where they intersected the "leads" (our type BP veins).

ac Veins

In contrast to BP and EE veins which lie between bedding planes or are confined within slate beds, ac veins occur exclusively in metawacke beds. They are vertical and strike north-south. Traced parallel to strike, some ac veins terminate in conjugate sets of short veins aligned en échelon beyond the tip of the principal ac vein (see the diagrammatic representation in Fig. 3). In the northern half of the study area many ac veins show vein-parallel buckle shortening of 10 to 15 percent,

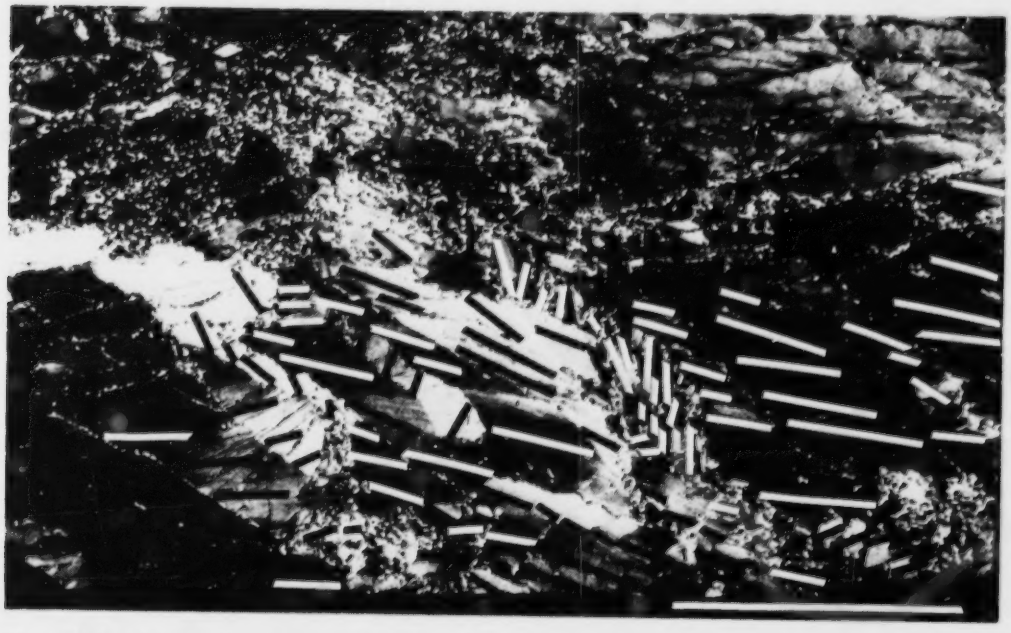

Figure 11 - Photomicrograph of a thin section (cross nichols) of a BP vein from Liscomb Island (Fig. 8) showing the trace of c-axes of quartz crystals. The thin section is cut parallel to the ac plane. Note the kinking of the laminae and the tendency for the c-axes traces to lie subparallel to the laminae whereas the primary crystal boundaries lie at a larger angle to the laminae. The bar scale is 1 cm long. GSC 202510-Q

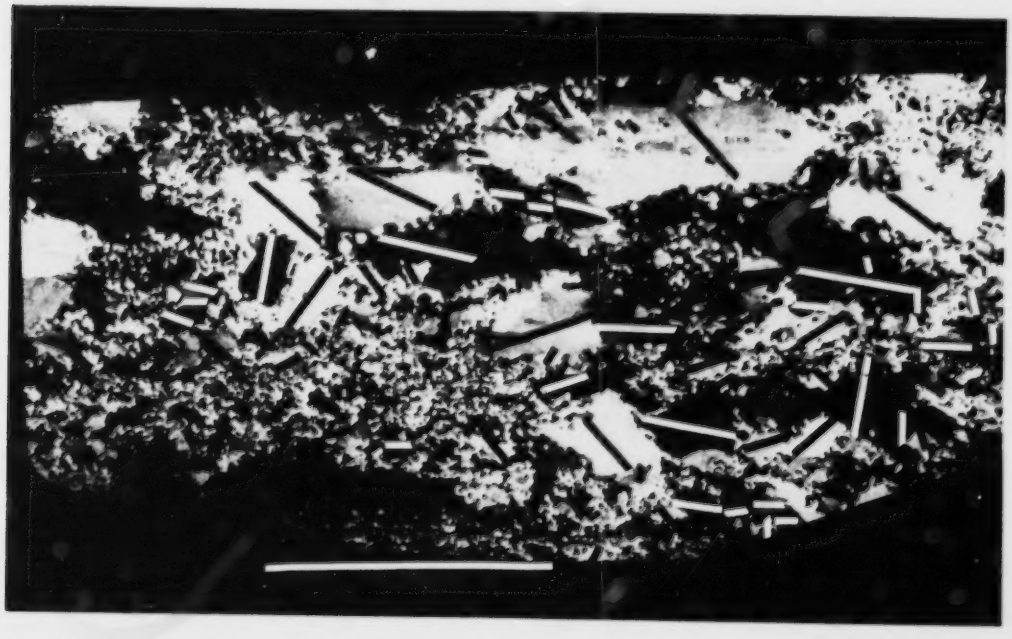

Figure 12 - Photomicrograph of a thin section (cross nichols) of a BPQ vein from the region of overturned beds 2 km west of Yankee Lake (YL on Fig. 2). The thin section is cut parallel to the ac plane. Note the apparent absence of a preferred orientation of the quartz c-axes traces in the large grains as well as the absence of laminae. The bar scale is 1 cm. GSC 202510-K

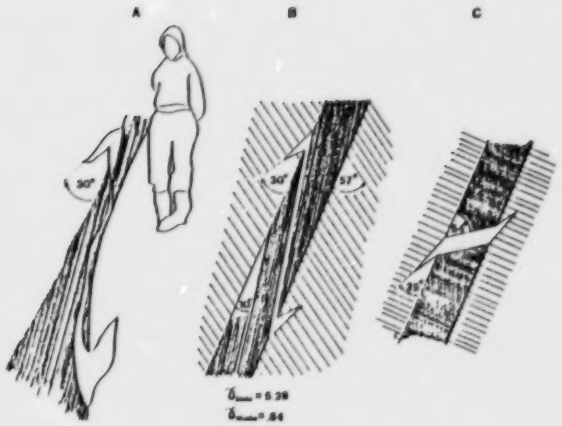

Figure 13. Deformation of an EE vein within a slate bed during flexural folding. A. Tracing from a photograph of an EE vein in slate and metawacke from the southeast coast of Goose Island (close-spaced cleavage in slate, wide-spaced cleavage in metawacke). B. Scaled drawing of bedding-cleavage-vein relations measured in the outcrop. C. Restoration of the EE vein to its original form assuming that the vein filled an en échelon extension fracture in the slate at the onset of flexural folding when bedding and cleavage were originally perpendicular (see Henderson, 1983b); simple shear strains in the slate and metawacke are indicated.

and in the southern half of the study area ac veins in fold hinge regions where bedding and cleavage are nearly perpendicular, are displaced by conjugate sets of kink bands in the vertical spaced cleavage of the metawacke.

The ac veins are composed of coarse crystals of milkly quartz commonly arranged normal to the vein walls. The veins are not laminated or grooved like the BP veins, and the quartz appears to have grown across fluid-filled extension fractures.

DISCUSSION OF CONSTRAINTS ON THE ORIGIN OF GOLD

The earliest gold is found in laminated BP quartz veins that resulted from the crack-seal mechanism of rock deformation. The veins grew by episodic vertical hydraulic extension, fracturing and concomitant vein mineral precipitation at the onset of bedding-paralliel shortening. In order for the fluid pressure to exceed the lithostatic pressure the permeability of the rocks must have been very low. Absence of permeability in both metawacke and slate is affirmed by the occurrence of the BP veins in slate just below metawacke beds as well as within the slate beds. The development of cleavage by the growth of quartz and mica beards on detrital grains within metawacke during greenschist metamorphism would have contributed to the destruction of primary pore-space. The cogenesis of cleavage and extension veins is well documented in the geological literature (see for example the references cited by Etheridge, 1983). Fueten et al. (this volume) demonstrated that formation of spaced cleavage in metawacke in the study area resulted in substantial loss of silica, some of which was probably precipitated in the veins. However, absence of slaty cleavage in a pelitic inclusion within a BP vein indicates that the vein began to be formed before the development of cleavage.

No textural evidence supports the notion that bedding-parallel quartz (and its contained gold) in the Goldenville Formation was originally a bed of amorphous silica. Epigenetic sulfur, arsenic and gold may have been deposited initially in metawacke (Crocket et al., this volume) and thence were mobilized in hydrous solution with silica, carbonate, mica, chlorite and arsenopyrite and deposited in nearby BP veins at the onset of horizontal compression and vertical extension. During folding, EE fractures formed on fold limbs, and were enriched in gold where the EE fractures intersected auriferous BP veins. Regardless of whether gold in the study area is polygenetic, we conclude that quartz, gold and other vein minerals are of local origin and probably were in a more dispersed form within the turbidites before being concentrated initially in the BP veins.

There is not evidence of "feeder" veins by which hydrothermal solutions introduced the vein minerals to the veins from some source below the Goldenville Formation.

ACKNOWLEDGEMENTS

We thank Howard K. Poulsen for improving the original manuscript, W.H. Poole and an anonymous reviewer for constructive criticisms incorporated into this version of the paper. James H. Crocket, Frank Fueten, Marcos Zentilli, Paul Clifford and Ulrich Kretschmar are thanked for sharing their ideas with us.

COX, S.F. and ETHERIDGE, M.A. 1983. Crack-seal fibre growth mechanism and their significance in the development of oriented layer-silicate microstructures. Tectonophysics, 92, pp. 147-170.

CROCKET, J.H., FUETEN, F., KABIR, A., CLIFFORD, P.M. 1986. Distribution and localization of gold in Meguma Group rocks, Nova Scotia: Implications of metal distribution patterns in quartz veins and host rocks on mineralization processes of Harrigan Cove, Halifax County. Maritime Sediments and Atlantic Geology, 22, pp. **15-33**.

DURNEY, D.W. 1972. Solution-transfer, an important geological deformation mechanism. Nature, 235, pp. 315-317.

DURNEY, D.W. and RAMSAY, J.G. 1973. Incremental strains measured by syntectonic crystal growths. In Gravity and Tectonics, ed. K.A. De Jong and R. Scholten, John Wiley & Sons (New York), pp. 67-96.

ETHERIDGE, M.A. 1973. Differential stress magnitudes during regional deformation and metamorphism: upper bound imposed by tensile fracturing. Geology, 11, pp. 231-234.

FARIBAULT, E.R. 1889. The gold measures of Nova Scotia and deep mining. Journal of the Mining Society of Canada, 2, pp. 119-128.

FUETEN, F., CLIFFORD, P.M., PRYER, L.L., THOMPSON, M.J. AND CROCKET, J.H. 1986. Formation of spaced cleavage and concurrent mass removal of SiO_2, Meguma Group metagreywackes, Goldenville, Nova Scotia. Martime Sediments and Atlantic Geology, 22, pp. **35-50**.

GARCIA-CELMA, A. 1982. Domainal and fabric heterogeneities in the Cap de Creus quartz mylonites. Journal of Structural Geology, 4, pp. 443-455.

GRAVES, M.C. and ZENTILLI, M. 1982. A review of the geology of gold in Nova Scotia; In Geology of Canadian Gold Deposits, ed. R.W. Hodder and K.W. Petruk; Canadian Institute of Mining and Metallurgy, Special Volume 24, pp. 233-242.

HAYNES, S.J. 1983. Typomorphism of turbidite-hosted auriferous quartz veins, southern Guysborough County. Nova Scotia Department of Mines and Energy, Report 83-1, pp. 183-224.

HEDLEY, P.M. 1941. Geology and structure as related to mining, Guysborough Mines Limited, Goldenville, Nova Scotia. Canadian Institute of Mining and Metallurgy, XLIV, pp. 251-258.

HENDERSON, J.R. 1983a. Harrigan Cove Mine. In Keppie, J.D., Haynes, S.J., Henderson, J.R., Smith, P.K., O'Brien, B.H., Zentilli, M., Jensen, L.R., MacEachern, I.J., Stea, R. and Rogers, P.J., C.I.M. Geology Division Excursion Guidebook: Gold Deposits in the Meguma Terrane of Nova Scotia; Canadian Institute of Mining and Metallurgy, pp. 22-31.

HENDERSON, J.R. 1983b. Analysis of structure as a factor controlling gold mineralization in Nova Scotia. Geological Survey of Canada, Paper 83-1B, pp. 13-21.

JAMES, H.L. 1955. Zones of regional metamorphism in the Pre-Cambrian of northern Michigan. Geological Society of America Bulletin, 66, pp. 1455-1488.

KEPPIE, J.D. 1976. Structural model for the saddle reef and associated gold veins in the Meguma Group, Nova Scotia. Nova Scotia Department of Mines, Paper 76-1, 34 p.

KRETSCHMAR, U. 1984. Gold in Goldenville, Nova Scotia. Abstracts with Programs, 19th Annual Meeting Northeastern Section, Geological Society of America, 16, No. 1, p. 28.

MALCOLM, W. and FARIBAULT, E.R. 1929. Goldfields of Nova Scotia. Canada Department of Mines, Geological Survey, Memoir 156, 253 p.

RAMSAY, J.G. 1974. Development of chevron folds. Geological Society of America Bulletin, 85, pp. 1741-1754.

RAMSAY, J.G. 1980. The crack-seal mechanism of rock deformation. Nature, 284, pp. 135-139.

SMITH, P.K. 1983. Geology of Cochrane Hill gold deposit. Nova Scotia Department of Mines and Energy, Report 83-1, pp. 225-256.

Maritime Sediments and Atlantic Geology

Vol. 22 April, 1986 No. 1

Distribution and Localization of Gold in Meguma Group Rocks, Nova Scotia: Implications of Metal Distribution Patterns in Quartz Veins and Host Rocks on Mineralization Processes at Harrigan Cove, Halifax County

J.H. Crocket, F. Fueten, A. Kabir and P.M. Clifford
Department of Geology
McMaster University, Hamilton, Ontario L8S 4M1

The contents of Au, As, Sb and W in metagreywacke, slate and quartz veins from Harrigan Cove, Halifax County, N.S. were determined by neutron activation analysis. The gold-bearing veins in the Goldenville Formation, the lower sandy flysch member of the Cambro-Lower Ordovician Meguma Group of eastern Nova Scotia. The Harrigan Cove metagreywacke and slate are strongly enriched in arsenic (as arsenopyrite) and weakly enhanced in gold relative to similar lithologies in barren Meguma terranes. Greywacke is the main sink for arsenic while gold occurs in highest concentration in greywacke and slate, but not in the quartz veins. Anomalous gold values occur with the same frequency in greywacke, slate and quartz veins, but anomalous quartz vein samples are much richer in gold than anomalous host rock samples.

It is suggested that the metal distributions support a polygenetic origin for the mineralization, whereby early arsenic- and sulpnur-bearing fluids introduce arsenopyrite and sulphides, mainly into greywacke. Gold is concentrated by these minerals and later mobilized along with large quantities of silica early in the history of deformation through pressure solution processes which generate a spaced cleavage. These silicic fluids and their metals are then injected by hydraulic fracture, mainly into slate, to form the gold-bearing bedding-parallel quartz veins.

La teneur de Au, As, Sb et W dans les metagrauwackes, l'ardoise, et les veines de quartz de Harrington Cove, conté de Halifax, N.E., a été déterminée par analyse d'activation de neutrons. Les veines de quartz ici contenant de l'or, sont typiques des veines de quartz de genre turoidite de la formation de Goldenville, le membre inferieur sabloneu de flysch du Groupe Meguma Cambro-Bas Ordovicien de l'est de la Nouvelle Ecosse. Le meta-grauwacke et l'ardoise de Harrigan Cove sont fortement enrichis d'arsenic, (en temps qu'arsenopyrite), et sont faiblement relevés en teneur d'or par rapport aux lithologies comparable des terrains stérile Meguma. Le grauwacke est l'entonoir principal pour l'arsenic, alors que l'or se trouve en concentration plus élevé dans les veines de quartz. L'or et l'arsenic sont en corrélation dans le grauwacke et l'ardoise, mais pas dans les veines de quartz. Des valeurs d'or anormales se trouvent avec la même fréquence dans le grauwacke, l'ardoise et les veines de quartz, mais les échantillons de quartz sont nettement plus riches en or que les échantillons des roches-hôtes.

Il a été suggéré que la distribution de métaux soutient l'idéee d'une origine polygénétique pour la minéralisation, tandis que les premiers fluides contenant de l'arsenic et du souffre introduisent de l'arsenopyrite et des sulfides, surtout dans le grauwacke. L'or est concentré par ces minéraux et est plus tard mobilisé avec de grandes quantitées de silice, tôt dans l'histoire de la déformation, par des processus de solutions de pression, qui engendrent un clivage espacé. Ces fluides silicieux et leurs métaux sont alors injectés, au moyen de fractures hydrauliques, surtout dans l'ardoise, pour former les veines de quartz contenat de l'or, au litage paralèlle.

INTRODUCTION

Recent studies of auriferous quartz veins in turbidites of the Meguma Group, Nova Scotia have provided useful new insight into the mechanisms and timing of vein emplacement (Keppie, 1976; Graves and Zentilli, 1982; Henderson, 1983a). The question of the source of vein fluids, and their

MARITIME SEDIMENTS AND ATLANTIC GEOLOGY
22, 15-33 (1986)

0711-1150/86/010015-19$3.85/0

metals, has given rise to a variety of models whose diversity indicates that vein genesis is not yet well understood. The following concepts provide examples of recent thinking. Haynes (1983) proposed a model by which some of the auriferous veins were considered to have formed in submarine hydrothermal-vent hot spring systems which tap sub-Meguma basement through faults. The basement was suggested as the source of gold. Kretschmar (1983) argued that the stratiform veins are syngenetic chemical sediments precipitated from brines in the depositional basin. Other models involve a local derivation of the vein silica and link vein formation with deformation, calling on pressure solution of quartz accompanying the development of spaced cleavage as a means of liberating silica (Clifford et al., 1983; Fueten et al., this volume). Opinions as to the source of gold and other metals are without strong consensus.

Studies which document the distribution of gold and associated metals in the various gold districts of the Meguma terrane should help constrain genetic thinking. Smith (1983a, b), for example, provided a detailed survey of the gold distribution in quartz veins and host rocks of the Cochrane Hill deposit, localized in amphibolite grade rocks. The present study was carried out on the Harrigan Cove mineralization, which is hosted in greenschist facies rocks. Good bedrock exposure is provided here by trenching and overburden stripping. Gold and associated metals, including arsenic, antimony and tungsten, were determined in metagreywacke and slate host rocks as well as in quartz veins. The metal distributions are considered with regard to a possible source of metals in local host rocks or in quartz-vein fluids. The evaluation is based primarily on gold and arsenic patterns. Little independent insight was gained from antimony values as the metal is correlated so strongly with arsenic. Tungsten was determined on a limited suite of samples only and the geochemical implications of the tungsten data are not pursued here in any detail.

GEOLOGICAL SETTING OF THE HARRIGAN COVE GOLD MINERALIZATION

The Harrigan Cove gold district is located about 100 km east of Halifax in the southeast corner of Halifax County. Trenches and stripping expose auriferous quartz veins 400 to 700 m north of Harrigan Cove post-office just off Highway No. 7 (Ecum Secum map, 11D/16). The bedrock is greywacke and slate of the Goldenville Formation, the lower member of the Cambro-Lower Ordovician Meguma Group. Gold production from the Harrigan Cove district from 1899 to 1916 was about 225 kg, somewhat less than 1% of the total production from Nova Scotia prior to 1927 according to data tabulated in Appendix 1 of Malcolm (1976). Quartz veins were the principal source of gold although some slate was milled.

The main structural elements and the distribution of quartz veins as mapped by E.R. Faribault (1906) are reproduced in Figure 1. All productive beings lay in the south limb of the South Anticline and follow the bedding. Trenches and sample locations are sketched on Figure 1. Some of the important quartz veins shown on Faribault's 1906 map are probably exposed in the trenches. These include the South Whidden and Bishop veins in the most northerly trench, the McIlrich and Galena veins in the central area and possibly the South vein in the southern trench.

Recent studies of the Harrigan Cove gold district include those of Anderle (1974), Kretschmar (1983) and Henderson (1983b). Comment below is based mainly on the latter two studies and mapping carried out by the present authors, principally F. Fueten (Fig. 2). The principal host rocks are greywacke and slate, the A and E divisions, respectively, of Bouma turbidite units. The greywackes occasionally include C division rocks toward their

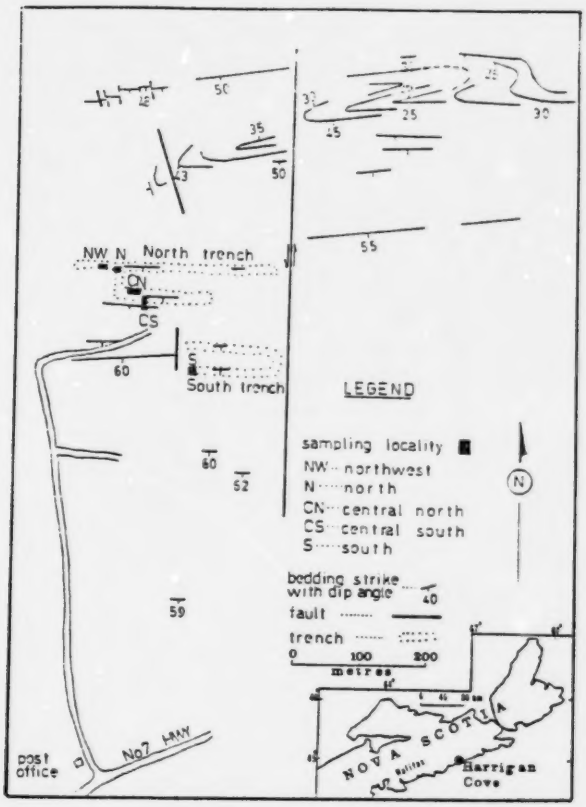

Figure 1 - Geological sketch map of Harrigan Cove showing the principal structural elements after Faribault (1906). Trenches and sample locations for this study are indicated.

stratigraphic tops. Evidence supporting the interpretation of the Meguma as a turbidite sequence deposited in one or more submarine fans is documented by Schenk (1970). At the mapped localities bedding dips 60 to 85° degrees south and strikes approximately 090°. The bedding-cleavage angle is generally less than 25° in both greywacke and slate. Most quartz veins and all those thicker than 5 cm are essentially bedding-parallel and either hosted entirely within E division slates or localized along the contacts between E divisions and the base of the overlying greywacke beds. Other veins include rare, thin (1 to 5 cm), discordant quartz veins which usually originate in thicker, bedding-parallel veins. Arsenopyrite occurs in all rock types, but is most common in greywacke beds as euhedral crystals up to 5 mm long and is often concentrated toward the coarser grained base of the bed. Pyrrhotite and pyrite occur in all lithologies, but are much less common than arsenopyrite.

Five localities (Fig. 2) representing a stratigraphic sequence about 120 m thick were mapped and sampled. For each locality (Fig. 3a, 3b, 4) the Bouma units are numbered sequentially, with the stratigraphically lowest unit designated as 1. Lithological divisions in Bouma units are identified by A for greywacke, B, C or D for slaty greywacke and E for slate. Quartz veins are indicated by Q. Where more than one sample was collected from a specific lithology they were differentiated numerically, using 1 for the stratigraphically lowest sample.

Geology of Sampled Localities

North Trench. The North trench exposes several prominent bedding-parallel quartz veins, each 20 to 30 cm thick and their sedimentary host rocks. Two areas were sampled in detail. One, designated the Northwest locality (Fig. 3a), consists of three Bouma units of approximately 4.5 m total thickness. Greywacke and slaty greywacke are dominant and several beds contain euhedral arsenopyrite crystals. A bedding-parallel quartz vein, 25 cm thick, possibly the South Whidden vein (Faribault, 1906), occurs in the basal Bouma unit. Euhedral arsenopyrite occurs sparingly in this vein at quartz vein-slate contacts. Massive nodular arsenopyrite (Sample NW1Q2a) was found where local folding apparently resulted in brecciation of the vein. The nodular arsenopyrite is highly anomalous in gold (270 ppb). The slate in contact with this vein and a thin parallel vein contains a few euhedral crystals of arsenopyrite, and is also anomalous in gold (15 to 50 ppb). Nodular arsenopyrite was observed in only one other locality where it is also anomalous in gold.

A second area in the North trench, designated the North locality (Fig.

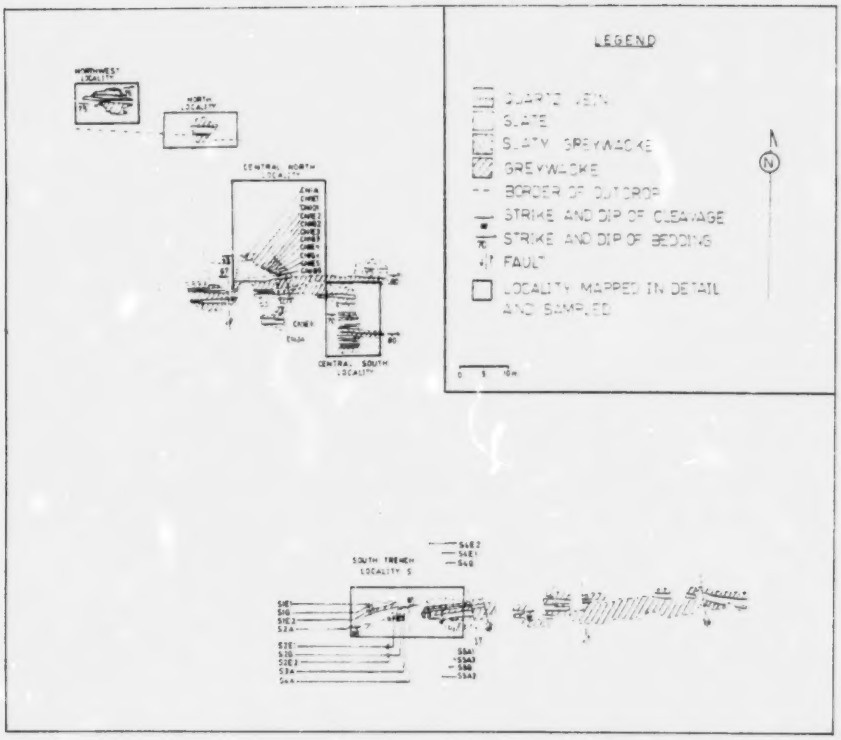

Figure 2. Harrigan Cove area, Halifax County, N.S., showing geology of some of the stripped and trenched exposures and indicating the areas sampled in detail for this study. Geology by F. Fueten.

3b), was also sampled. Although stratigraphic continuity between the North and Northwest localities is uncertain due to overburden cover, the upper greywacke of the Northwest locality, NW3A, is probably equivalent to the lowest greywacke in the North locality. This latter unit is therefore designated N3A. The North locality exposes two Bouma units, mainly of greywacke, that total 3.5 m in thickness. The lower Bouma unit includes a slate member which contains a bedding-parallel quartz vein that is 50 cm thick and is probably the productive Bishop vein (Faribault, 1906).

Central North (CN) locality in the North trench (Fig. 2) consists of a single Bouma unit of basal A division greywacke overlain by about 4.5 m of C, D and E division slate and slaty siltstone. It is unusually thick in comparison with other Harrigan Cove Bouma units. Five stratabound quartz veins are hosted in the slate unit.

Central South (S) locality in the North trench exposes a stratigraphic sequence approximately 13.2 m thick consisting of twelve Bouma units most of which are represented by A, E and occasionally C divisions (Fig. 4). The overall lithic proportion of greywacke:slate:quartz vein is 7:2.4:1. The quartz veins are predominantly bedding-parallel and average 15 cm in thickness. A few thin discordant quartz veins, generally less than 5 cm thick, cut from one to three Bouma units and appear to originate in the bedding-parallel veins. Many of the greywacke beds contain euhedral arsenopyrite crystals up to 25 cm long. Arsenopyrite is much less common in the slate beds and quartz veins. Pyrite and pyrrhotite occur occasionally in quartz veins.

South Trench (S). The west end of the South trench (Fig. 2) contains a

relatively undisturbed, continuous stratigraphic succession with several quartz veins. A sampled sequence approximately 10 m thick and containing five Bouma units consists of greywacke (A division) and slate to silty slate (C, D and E divisions). Quartz veins are bedding-parallel and occur near the top of Bouma units, commonly within slates. One particularly thick A division member, S5, represents several amalgamated beds.

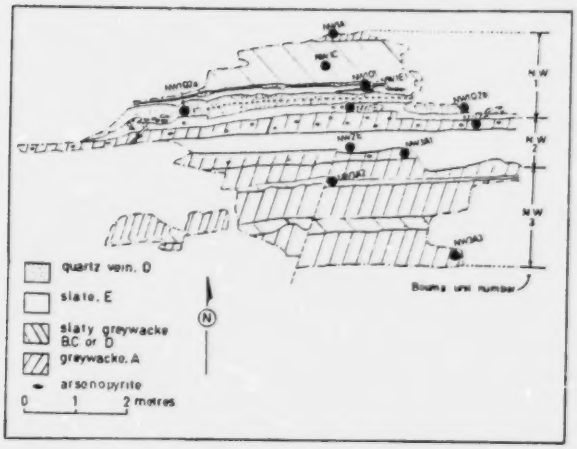

Figure 3a. Geology and sample locations in the Northwest (NW) locality in the North trench showing three Bouma units. Unit 3 ccconsists of amalgamated beds. Beds face and dip south at an average of 75°. Slaty cleavage is essentially parallel to bedding. The main quartz vein NW1Q2 is bedding-parallel. Geology by J.H. Crocket.

METHODS AND PROCEDURES

Field Sampling

Samples were collected either by hammer or by drilling with a portable diamond-bit unit which took a core 2.5 cm in diameter and up to 15 cm long. Drilling permitted precise sample location so that thin E units or the base, middle and top of specific beds could be sampled.

In the Central South locality Bouma units 1 to 8 were fractured and broken across strike by blasting nineteen holes charged sufficiently to break but not to scatter the rock fragments. Thicker greywacke beds could thus be sampled by taking several pieces across the full width of the bed. Quartz veins were usually sampled by collecting single pieces representing the full width of the vein. Samples of approximately 2 kg total weight were taken from each bed.

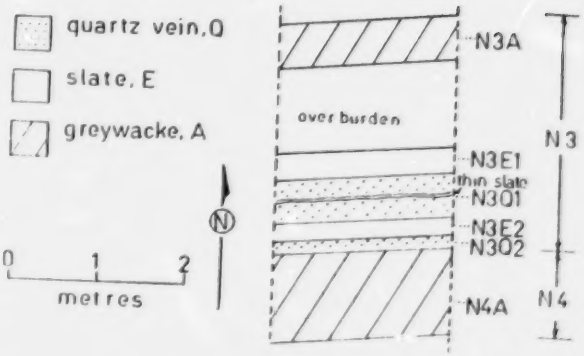

Figure 3b. Representative section across the North (N) locality in the North trench showing two Bouma units. Beds face south, strike 085° and dip 75° south. Quartz veins are bedding-parallel.

Analytical Procedures

Samples were broken in a jaw crusher to approximately 0.5 cm pieces and then pulverized in a ceramic disk grinder to a particle size of 1 mm or less. A split of 0.5 kg was then powdered in a ceramic disk grinder to pass a minus 200 mesh screen. From the minus 200 mesh powder an aliquot of 0.5 g was taken for analysis.

Instrumental epithermal neutron activation was employed for Au, As, Sb and W analyses, using a rotating cadmium shielded irradiation site in the McMaster Nuclear Reactor. Samples were irradiated in batches of fourteen plus two standards for 1 megawatt-hour (1×10^{13} neutrons/cm^2/sec) and allowed to decay for approximately 24 hours prior to counting As and W. Au and Sb were counted after further decay of 72 hours. Gamma ray spectra were taken on a coaxial intrinsic germanium detector with a resolution of 1.7 Kev and a

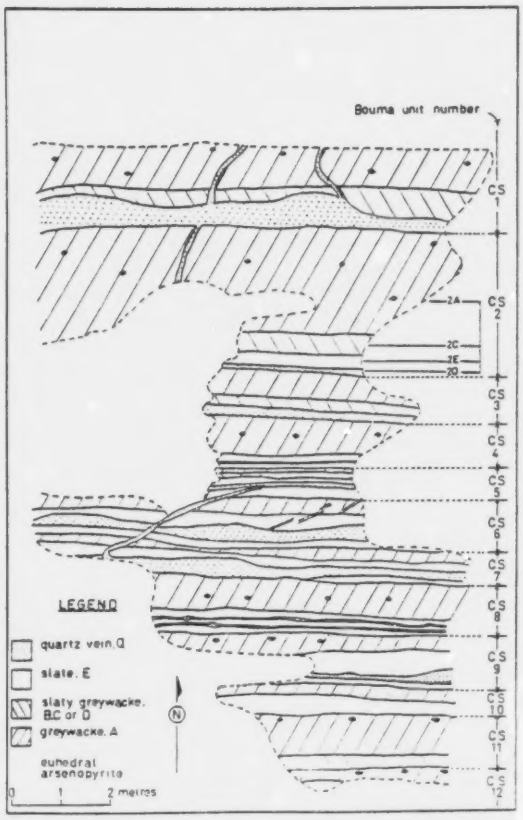

Figure 4. Geology of the Central South locality (CS) showing twelve Bouma units (e.g. CS1 -- Bouma unit 1, Central South locality). Beds face south with an average dip of 70° south. Quartz veins are mainly bedding-parallel. Some minor discordant veins are 1 to 5 cm wide. Their width on the figure is exaggerated for clarity. Geology by U. Kretschmar (1983).

peak-to-background ratio of 15:1 at 0.662 Mev. The essential analytical parameters are:

Element	Nuclide Counted	Half-Life Hours	γ-ray Energy, Kev
Arsenic	$^{96}_{As}$	26.3	559
Tungsten	$^{187}_{W}$	23.9	686
Gold	$^{198}_{Au}$	64.7	412
Antimony	$^{122}_{Sb}$	65.3	564

Standards were prepared by adding a weighed amount of weakly acidic solutions of known metal content to high purity silica powder and evaporating to dryness. Spec-Pure grade metals or oxides were used to prepare the standard metal solutions. The sensitivity of the analytical procedure is: As, 1 ppm; W, 0.1 ppm; Au, 1 ppb and Sb, 0.1 ppm.

Total carbon was determined with a LECO gas analyser which measured CO_2 adsorption in the infrared. This method yields total carbon.

RESULTS

The contents of gold, arsenic, antimony, tungsten and total carbon are presented in Table 1 with averages in Table 2. The distribution of gold in Harrigan Cove greywacke, slate and quartz veins is shown in histograms in Figure 5 which illustrate the pronounced positive skewness of the metal distribution. The main purpose of the averages (Table 2) is to recognize significant differences in metal content from one locality to another, but it is apparent from Figure 5 that a few metal-rich samples in each

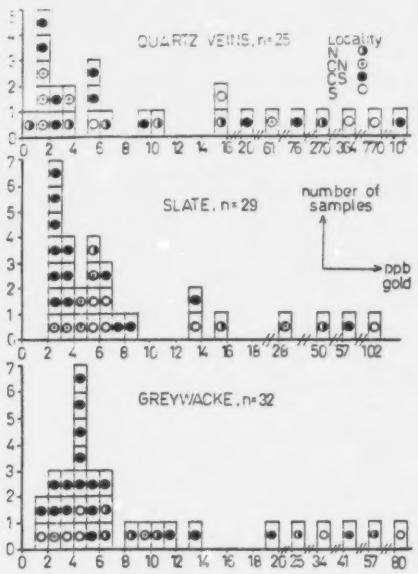

Figure 5. Histograms showing distribution of gold at Harrigan Cove in (a) greywackes, (b) slates and (c) quartz veins.

Table 1.

GOLD, ARSENIC, ANTIMONY, TUNGSTEN AND TOTAL CARBON AT HARRIGAN COVE

(a) Northwest locality (NW)

Sample	Au ppb	As ppm	Sb ppm	W ppm	CO_2 wt. %
NW1A	10	650	4.8	5.1	0.33
NW2A	57	13,900	30	-	0.23
*NW3A	8.9	1.380	8.6	4.9	0.38
NW1C	6.7	230	2.9	9.3	0.24
NW1E1	50	6,120	34	31	0.32
NW1E2	15	2,215	15	18	0.15
NW1Q1	15	540	4.1	4.1	0.15
**NW1Q2a	10	1,180	7.5	22	-
**NW1Q2a	270	35,000	84	-	-
**NW1Q2b	6.6	87	0.97	2.4	0.13

* A composite of samples NW3A1, NW3A2 and NW3A3

** NW1Q2 contains nodular arsenopyrite. Subsample 2a is an arsenopyrite-poor fraction, and subsample 2b is an arsenopyrite-rich subsample.

(b) North locality (N)

Sample	Au ppb	As ppm	Sb ppm	W ppm	CO_2 wt. %
N4A1	25	8,060	31	4.2	0.17
N4A2	6.9	960	4.1	3.2	0.17
N3E2	5.4	135	2.4	13	0.30
N3Q1	0.88	5.5	0.27	0.07	0.09
N3Q2	3.2	37	0.73	4.4	0.15

(c) Central locality (CW)

Sample	Au ppb	As ppm	Sb ppm	CO_2 wt. %
CN1A	2.7	320	2.8	0.19
CN2A	9.4	1,570	12	0.19
CN1E1	5.6	465	4.7	0.30
CN1E2	4.2	115	1.9	0.34
CN1E3	28	3,060	22	0.25
CN1E4	3.6	190	2.3	0.28
CN1E5	4.0	270	3.7	0.22
CN1E6	2.5	100	1.5	1.51
CN1Q1	1.8	110	1.5	0.15
CN1Q2	61	150	1.5	0.11
CN1Q3	3.7	6.0	0.75	0.15
CN1Q4	1.3	440	4.7	0.16
CN1Q5	1.5	2.6	0.32	0.13

TABLE 1 cont'd

(d) the Central South locality (CS)

Sample	Au ppb	As ppm	Sb ppm	W ppm	CO_2 wt. %
CS1A	13	4,170	13	15	0.21
CS2A	5.5	2,030	16	10	1.16
CS3A	5.3	1,780	6.4	10	0.16
CS4A	3.0	450	3.4	8.3	0.67
CS5A	11	2,300	8.0	13	0.21
CS6A	4.8	1,270	4.0	11	0.28
CS7A	4.1	1,260	4.2	15	0.21
CS8A	4.2	830	2.7	12	0.31
CS9A	19	2,790	16	-	0.59
CS10A	3.5	31	1.0	-	0.21
CS11A	4.9	90	0.89	-	0.29
CS12A	41	14,400	45	-	0.16
CS1C	6.8	3,650	12	25	0.27
CS2C	2.5	41	0.60	5.8	0.27
CS3C	1.7	39	0.85	12	0.20
CS5C	2.0	41	0.77	12	0.175
CS6C	5.6	160	1.9	16	0.28
CS11C	4.8	2,020	11	-	0.195
CS2E	59	68	1.0	10	0.28
CS4E	3.5	63	0.94	11	0.31
CS5E1	2.6	510	3.4	23	0.41
CS5E2	2.7	580	3.0	13	0.33
CS6E1	2.8	50	0.82	14	0.33
CS7E1	7.2	125	6.5	-	0.39
CS7E2	8.6	270	3.8	-	0.41
CS8E1	2.4	47	0.98	14	0.30
CS8E2	3.7	65	0.96	16	0.29
CS9E1	6.6	36	1.3	-	0.31
CS9E2	3.8	61	1.4	-	0.39
CS10E	2.6	38	1.1	-	0.29
CS11E2	13	1,330	7.8	-	0.29
CS1Q	76	10	0.50	0.29	0.09
CS2Q	2.9	18	0.40	7.2	0.11
CS3Q	20	1,445	9.7	10	0.14
CS4Q	5.7	410	1.6	6.8	0.13
CS5Q	9.1	400	2.7	11	0.13
CS6Q	2.0	180	1.2	16	0.10
CS7Q	1.5	5.5	0.37	14	0.10
CS8Q1	1.3	15	0.52	21	0.13
CS8Q2	10,000	90,000	190	53	0.12
CS9Q	5.8	5.3	0.50	-	0.13

(e) South Trench locality (S)

Sample	Au ppb	As ppm	Sb ppm	CO_2 wt. %
S2A	4.2	17	0.73	1.15
S3A	1.9	30	0.73	0.11
S4A	34	16	1.1	0.68
S5A1	3.4	22	0.48	0.18
S5A2	4.5	14	0.42	0.80
S5A3	80	25	0.82	0.14
S1E1	102	11,600	63	0.24
S1E2	5.1	165	1.7	0.24
S2E1	6.3	74	1.2	0.22
S2E2	5.7	47	1.5	0.24
S4E1	13	128	1.4	0.23
S4E2	6.4	17	0.93	0.21
S1Q	364	52	1.5	0.14
S2Q	15	17	1.1	0.12
S4Q	5.4	96	1.2	0.09
S5Q	770	11	0.31	0.11

Table 2.

AVERAGE METAL AND CO_2 CONTENTS AT HARRIGAN COVE

(a) by locality and lithology

Locality	Average Metal and CO_2 Contents in A, E and Q Divisions														
	Au, ppb			As, ppm			Sb, ppm			W, ppm			CO_2 wt.%		
	A	E	Q	A	E	Q	A	E	Q	A	E	Q	A	E	A
N+NW	19	24	6.4	4203	2823	167	14	17	1.5	5.3	21	2.8	.30	.26	.13
CN	6.1	8.0	14	945	228	142	7.4	2.8	1.8	-	-	-	.19	.28	.14
CS	6.0	4.8	14	1350	152	277	6.0	1.9	1.9	12	13	11	.33	.33	.12
S	21	23	289	21	86	44	0.71	1.0	1.0	-	-	-	.51	.23	.12

(b) by lithology for all samples

Lithology	Au, ppb			As, ppm			Sb, ppm			W, ppm			CO_2 wt.%		
	A	E	Q	A	E	Q	A	E	Q	A	E	Q	A	E	Q
Average	8.7	8.0	62	972	549	184	4.9	3.5	1.7	9.8	14.8	8.1	.35	.34	.12
No Samples	30	27	22	27	30	22	29	27	22	17	10	12	30	31	23

lithological population will strongly bias total population arithmetic means. The rigorous choice of a better statistical parameter to estimate the population mean is difficult as the metal populations do not fit a simple distribution (such as normal or lognormal) when tested by plotting on probability paper. Arbitrarily, the averages used in Table 2 are the arithmetic means for the data within an $\bar{x} \pm 2\sigma$ interval. This method tends to exclude one, or occasionally two, high value samples from the population averages.

Correlation plots for gold vs arsenic are presented in Figure 6 and a matrix for all interelement correlations is given in Table 4.

Gold production at Harrigan Cove from 1899 to 1916 was approximately 225 kg gold from 13, 052 tons of ore (Malcolm, Appendix 1, 1976) equivalent to an average grade of 19 ppm gold. The average gold contents of Harrigan Cove quartz veins, slates and greywackes are relatively low but are anomalous in a geochemical sense when compared with Meguma rocks from unmineralized districts or with literature averages for comparable lithologies. A similar comparison for arsenic shows the metal is also strongly anomalous in the Harrigan Cove rocks, in fact far more so than gold. The data on which these observations are based are summarized in Table 3.

Unmineralized Meguma Group greywackes and slates average 1 to 2 ppb gold (Thorpe and Thomas, 1976; Brooks et al., 1982; Crocket et al., 1983). Harrigan Cove greywackes and slates, averaging 8.7 and 8.0 ppb gold, carry at least four times the gold content of Meguma Group rocks from unmineralized areas. Although data are limited, an average arsenic content of 2.3 ppm (Crocket et al., 1983) is suggested for unmineralized greywacke, so the Harrigan Cove greywackes then average 423 times higher arsenic than unmineralized greywacke using the averages in Table 3. Unmineralized

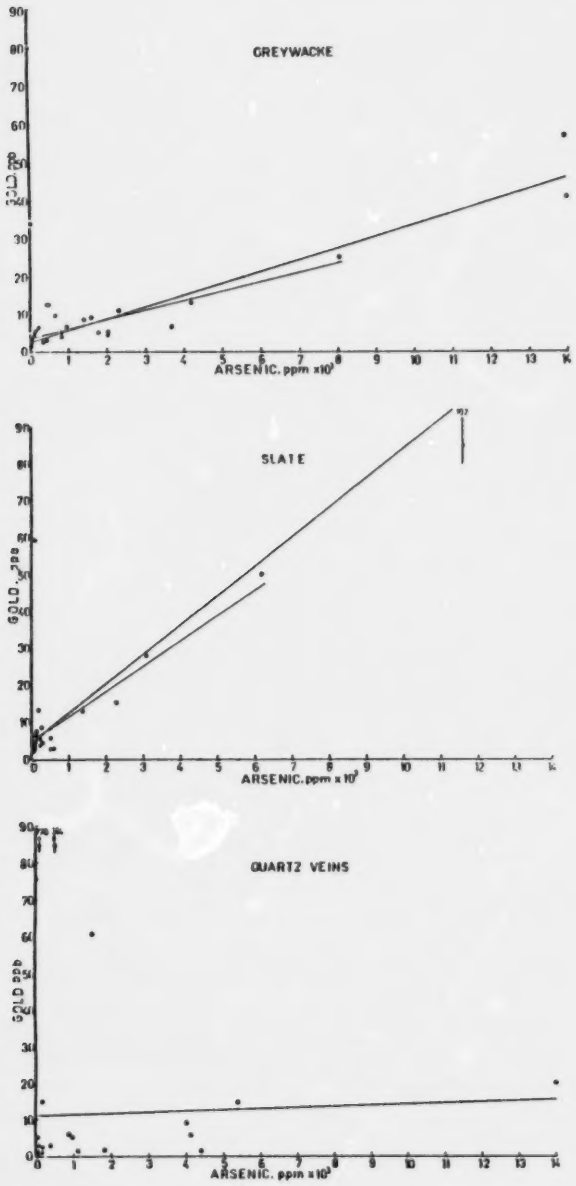

Figure 6. Gold-arsenic correlations at Harrigan Cove in (a) greywacke, (b) slate, and (c) quartz veins. Least squares fit lines are for the total (long) and $\bar{x} \pm 2$ populations (short).

Meguma Group slate from the Ecum Secum, area averages 2.5 ppm arsenic (Crocket et al., 1983), but the literature suggests a somewhat higher value, 13 ppm, may be typical of arsenic in shale (Onishi, 1969a). If an arsenic content of 10 ppm is taken as typical of slates from unmineralized areas, average Harrigan Cove slate (Table 3) is enriched in arsenic by a factor of 55.

The average antimony content of Harrigan Cove rocks does not indicate the presence of anomalous background levels of this metal. Onishi (1969b) suggested 1 to 2 ppm antimony is typical of shales and Harrigan Cove slates average 3.5 ppm antimony.

Thus, Harrigan Cove greywacke and slate, representing a mineralized district, are significantly higher in gold, and much higher in arsenic, than similar rock types from unmineralized areas. The common presence of arsenopyrite in Harrigan Cove rocks, particularly greywackes, is an obvious indication of the higher arsenic levels of the district.

The average gold content of the Harrigan Cove quartz veins is 62 ppb. Quartz veins provide the best indication of mineralization in that visible gold is occasionally seen in quartz vein outcrops, analyses return gold values of up to 10 ppm and samples are often highly anomalous in gold (i.e., 10 times the threshold level of 20 ppb). Unfortunately, no comparative body of data is available for quartz veins of an unmineralized area, and thus the gold levels characteristic of such veins cannot be estimated.

Relationship of Gold, Arsenic and Antimony to Lithology

Average metal contents (Tables 2a and 2b) indicate that greywacke and slate carry approximately the same gold contents. This equivalence is apparent whether locality averages (Table 2a) or total population averages (Table 2b) are compared. As greywacke is the most abundant lithology, it is a more important reservoir of gold than is slate. Quartz veins contain higher gold concentrations than the host rocks in three of the four localities, and on a basis of comparing averages for all data. However, gold is concentrated to variable degrees in quartz veins. In

Table 3.

COMPARISON OF AVERAGE AU AND AS CONTENTS OF ROCKS FROM HARRIGAN COVE WITH THOSE FOR UNMINERALIZED MEGUMA GROUP ROCKS AND LITERATURE VALUES FOR THESE LITHOLOGIES

Area of Sample	Lithology	Au, ppb	As, ppm	Ref.
Harrigan Cove	greywacke	8.7	972	6
	slate	8.0	549	6
Unmineralized Meguma Group Rocks				
Ruth Falls syncline	greywacke	1.2	2.3	3
Ecum Secum area	slate	1.7	2.5	3
Oldham area (core several hundred metres from nearest known mineralization)	greywacke	0.62	-	5
	slate	2.0	-	5
Sherbrooke area	whole rocks (slate, greywacke, granite)	1.0	-	1
Literature Survey	sandstones	3.0	1	2,4
	shale	2.5	13	2,4

1. Brooks et al., 1982.
2. Crocket, 1974.
3. Crocket et al., 1983.
4. Onishi, 1969a.
5. Thorpe and Thomas, 1976.
6. This study.

the Central North and Central South localities quartz veins contain about twice as much gold as do greywacke or slate, while South Trench veins contain about 10 times as much gold as the associated lithologies.

The average arsenic contents (Table 2a) of greywacke are 1.5 to 9 times greater than those of slate at three of the four localities sampled, including the North, Central North and Central South localities. The South Trench, an arsenic-poor locality shows the opposite trend. In the Central South locality, where the most extensive sampling was carried out, greywacke averages 9 times the arsenic content of slate. Average arsenic in greywacke is 4 to 25 times higher than in quartz veins, with the South Trench again an exception. In the South Trench higher arsenic is present in quartz veins than in greywacke. Thus, highest average gold contents characteristically occur in quartz veins, whereas the highest average arsenic levels occur in greywacke.

The distributions of antimony is similar to arsenic. The metal is lower in quartz veins than in slate or

greywacke, and higher in greywacke than in slate. The differences in antimony content of greywacke and slate are less than for arsenic. For example, at the Central South locality greywackes contain 3 times more antimony than do slates, whereas their average arsenic content is nine times that of slate.

Differences in Metal Contents by Locality

One of four localities, the South Trench, is characterized by different proportions of metals than the other three. Very low arsenic (21 to 86 ppm) and relatively high gold (21 to 289 ppb) prevail in South Trench samples. The one exception is a slate (S1E1) with both high gold and high arsenic contents (Table 1e), which carries 1 to 2 cm euhedral arsenopyrite crystals. The South Trench greywackes are relatively high and variable in total carbon content but there is no simple sample-by-sample correlation of high carbon with high gold. Both greywacke and slate carry abundant sulphide, mainly pyrrhotite. The South Trench is the one locality where gold does not correlate with arsenic and where a partial sulphide control of gold contents seems likely.

Relation of Total Carbon to Lithology and Gold Content

For the entire Harrigan Cove suite average carbon contents of greywacke and slate are essentially identical, and about 3 times higher than in quartz veins. On a locality by locality basis slates and veins are relatively uniform in carbon content, buy greywacke is more variable. The average carbon content of south Trench greywackes is more than twice that of South Trench slates. This is the only locality where greywacke is much higher than slate in carbon. Calcite is a common accessory mineral in greywacke, and is presumably the main source of carbon in these rocks. Calcite is also seen in slates, particularly in quartz rich clots, but some disseminated graphite is also present. For comparison, slates from unmineralized localities in the Ecum Secum area average 0.11 wt. % CO_2 (Crocket et al., 1983) or about 3 times less than Harrigan Cove slates. Gold vs carbon correlation coefficients (Table 4) show no significant correlation of these elements on a sample-by-sample basis. However, on average, the carbon-rich South Trench greywackes are also high in gold.

Interelement Correlations

Correlation coefficients for gold, arsenic, antimony and CO_2 are summarized in Table 4, and plots of gold vs arsenic in greywackes, slates and quartz veins are shown in Figure 6a, b and c. Antimony and arsenic correlate strongly in all lithologies suggesting that antimony substitutes in the arsenopyrite structure,

Table 4.

INTERELEMENT CORRELATIONS FOR AU, AS, SB AND CO_2 IN HARRIGAN COVE GREYWACKE, SLATE AND QUARTZ VEINS

	Au	As	Sb	CO_2
Au		.84	.72	.06
As			.89	.16
Sb				
CO_2				

	Au	As	Sb	CO_2
Au		.84	.88	.32
As			.97	.09
Sb				
CO_2				

	Au	As	Sb	CO_2
Au		.06	.13	.10
As			.98	.32
Sb				
CO_2				

particularly as no discrete antimony minerals were observed. Gold correlates equally strongly with arsenic in greywacke and slate, but not in quartz veins. Carbon is not significantly correlated with any metal in any rock type.

These correlations suggest that gold distribution and concentration in slates and greywacke are controlled by arsenopyrite whereas in quartz veins other minerals, probably native gold and sulphides, are additional important hosts of gold. High gold in Meguma Group arsenopyrite was documented by Brooks et al. (1982). However, correlations must be treated with some caution due to the highly skewed character of the data whereby one or two very metal rich samples contribute strongly to the correlation. The plots in Figure 6 which include the data from all four sampling areas show least squares fits for both the total and $\bar{x} \pm 2\sigma$ populations. The background portion of the population is also indicated by the area enclosed by the threshold values for gold and arsenic (see following section). Within the population represented by background values interelement correlations are very low.

The South Trench is characterized by different proportions of gold and arsenic than other localities in that samples enriched in gold are often low in arsenic. If they are included in the greywacke population r is reduced to 0.5. The greywacke correlations might be interpreted to suggest that in Harrigan Cove greywacke as a whole, gold and arsenic are only moderately correlated. Alternatively, it might be suggested that in most greywacke gold and arsenic are strongly correlated in a positive sense, probably because greywacke is the preferential reservoir for arsenopyrite which in turn is a strong concentrator of gold. Where arsenopyrite is low, as in the south Trench, some other control on gold distribution, probably sulphide, becomes significant. The latter interpretation is preferred.

Threshold Metal Values

As previously noted, the average gold and arsenic contents of Harrigan Cove rocks indicate a modest enrichment in gold and a very strong enrichment in arsenic by comparison with similar Meguma Group rocks from unmineralized areas. The gold enrichments in greywacke and slate are of geochemical, but not economic, significance. It is useful to establish the threshold values in order to identify anomalous metal values within the background represented by the Harrigan Cove rocks. The metal populations are not defined by any simple distribution. The histograms in Figure 5 suggest that much of the gold data lie in the 0 to 10 ppb range for slate and greywacke. The greywacke data show a nearly normal distribution for gold at values up to 7 ppb, with the remaining 34% of the population represented by only one sample in any one ppb interval. This break in distribution pattern at 7 ppb suggests a threshold between background and anomalous populations at about 7 ppb. For slate most of the gold data are in the range 0 to 9 ppb, with the remaining 24% represented mainly by single values in any one ppb interval. If the greywacke and slate data are plotted on cumulative probability graphs, slope discontinuities occur at 7 ppb in the greywacke plot and 10 ppb in the slate plots. A threshold value of 10 ppb gold is suggested as differentiating background and anomalous gold in both lithologies. Several clusters of data in the 0 to 20 ppb range characterize the distribution of gold in quartz veins. The most pronounced discontinuity in a cumulative probability curve is at 20 ppb and this value is taken as the threshold value for gold in quartz veins. Similar considerations suggest thresholds of 2000, 300 and 300 ppm arsenic in greywacke, slate and quartz veins, respectively. These threshold values are plotted on the correlation diagram in Figure 6.

Lithological and Spatial Associations of Anomolous Gold

Based on the threshold values just noted, 27% of the 85 analysed samples are classified as anomalous. The distribution of anomalous samples by lithology is summarized as follows:

Lithology	No. of Samples	Samples with Anomalous Gold		
		Number	Average Au, ppb	%
Greywacke	32	9	32	28
Slate	29	7	40	24
Quartz veins	24	7	1650	29

Thus, approximately the same percentage of samples from each of the three different lithologies carry anomalous gold. There are, however, significant differences in the gold content of the anomalous suites in that anomalous quartz vein samples generally exceed the threshold level far more than anomalous greywackes or slates. Another difference in the quartz vein and greywacke-slate anomalous suites is that about 70% of the anomalous greywacke-slate samples are also anomalous in arsenic whereas only 40% of the quartz vein suite is also anomalous in arsenic. This observation suggests that anomalous gold in the veins occurs as the native metal or in association with an arsenic-free phase more frequently than in the host rocks where a very close association with arsenopyrite must prevail.

DISCUSSION AND GENETIC CONSIDERATIONS

Genetic models for Meguma-hosted gold deposits are critically dependent on an understanding of the formation of the host quartz veins. They should also explain certain generalizations on the controls of mineralization many of which were noted in the early work of E.R. Faribault (1899): 1) high grade veins workable for gold are parallel to bedding planes, 2) such veins are hosted mainly in Goldenville Formation slates, 3) these veins usually occur at well defined points along anticlinal fold crests, particularly the centres of elliptical domes, and 4) such bedding-parallel veins are higher grade near the intersections with branching veins or angulars, and in minor folds or rolls. Those aspects of quartz vein formation on which consensus is lacking are the timing of vein emplacement, the mechanism of vein emplacement and the origin of the vein fluids.

The various hypotheses offered are wide ranging. In some it is proposed that the stratiform veins are essentially synsedimentary. Hunt (1868) and Hind (1869) proposed syngenetic models while recent contributions include those of Haynes (1983), who argued that the earliest stratiform veins formed as siliceous sinters in submarine, hydrothermal-vent hot-spring systems, and Kretschmar (1983) who suggested that the stratiform veins are chemical precipitates from hydrothermal silica-rich brines generated by convectively circulating seawater on the flanks of young spreading centres. In other hypotheses the veins are regarded as epigenetic and to have developed in response to deformation and/or regional metamorphism, but the timing of vein emplacement with respect to folding and metamorphism are matters on which opinions differ. Faribault (1899) directly linked vein formation and folding, and advocated that folding and vein formation occurred slowly and intermittently from solutions of local derivation. Keppie (1976) also linked folding and vein formation directly. On the other hand, Graves and Zentilli (1982) think that vein formation preceded folding, which in turn antedated cleavage development. They further argued that vein fluid introduction took place by hydraulic fracture during greenschist metamorphism and that vein mineral precipitation was rapid. Henderson (1983a) recognized three principal types of veins which were termed bedding-parallel, en échelon and AC veins. Through analysis of bedding-cleavage-vein relationship he concluded that the bedding-parallel and en échelon veins formed early in the strain history of folding at the time of cleavage formation, which was coeval with greenschist metamorphism. AC vein

formation was late in the folding history. From vein fabrics and theoretical considerations it was argued that veins were formed by fluids of local derivation that were introduced by hydraulic fracture. Henderson (1983b) also showed, using particularly well developed examples from Harrigan Cove, that the crystal fabric in some vein quartz is indicative of vein formation by repeated hydraulic extension fracturing, a mechanism that implies veins are open to fluid intermittently over a protracted period of time.

A detailed assessment of these various hypotheses is beyond the scope of this discussion. However, those models which regard quartz vein formation as an integral component of the deformational history are preferred because an expected consequence is a preferential localization of veins in specific structural environments, as for example, anti-clinal fold crests. Henderson's analysis of the timing of vein emplacement largely evolves from measurable properties of the rocks and is preferred.

The origin of the vein fluids is also highly problematic. A brief survey noting the main suggestions may be found in Keppie et al., (1983). Having advocated an emplacement of vein fluids by hydraulic fracturing early in the history of folding and in keeping with the concept that both folding and cleavage development are a response to deformation of Meguma rocks (Henderson, 1983b), it is suggested that vein fluids are also, in part at least, an integral product of the deformation (Clifford et al., 1983). The specific process is thought to be pressure solution which generated the spaced cleavage prominent in the greywackes and which is accompanied by the loss of at least 10% of the original quartz content (Fueten et al., this volume). A source of aqueous fluid is required to dissolve the quartz, but a significant proportion of the quartz in the veins is probably of local derivation.

The most significant generalizations bearing on the gold mineralization process arising from our geochemical studies are the following: 1) Harrigan Cove greywackes and slates are slightly enriched in gold and very strongly enriched in arsenic relative to similar lithologies in unmineralized Meguma terrane, 2) the highest arsenic concentrations are usually found in greywacke and the lowest in quartz veins, 3) the highest gold concentrations are usually found in quartz veins, whereas greywacke and slate contain lower and approximately equivalent gold contents, 4) strong positive correlations between gold and arsenic are typical of slates and greywackes, whereas very weak correlations are typical of quartz veins, 5) enrichment of gold can occur without a corresponding enrichment of arsenic as is found at the South Trench locality.

The first generalization is thought to reflect a fundamental aspect of the mineralization process: an early introduction of arsenic and gold leading to a large increase in arsenic and a slight increase in gold in both greywacke and slate on a district-wide scale. The formation of bedding-parallel quartz veins is also an essential element of the mineralization process. However, bedding-parallel quartz veins are common in the Meguma terrane and many are barren of gold, showing that vein formation does not necessarily lead to mineralization. It is suggested that introduction of metals on a local scale is an early and essential stage in the mineralization process of Meguma rocks. If deformation then produces favourable structures in a local area with elevated metal content, mineralized veins may result.

Initial metal enrichment at Harrigan Cove probably involved introduction of arsenic followed by gold. The timing of these events is difficult to constrain. It is thought that a syngenetic origin is unlikely because a preferential concentration of arsenic

in slate rather than greywacke would be expected. The limited discussions on the marine geochemistry of arsenic (Onishi, 1969a; Bostrom and Valdes, 1969) indicate that arsenic may be fixed in the marine environment by adsorption on ferromanganese or on fine clay-sized platy minerals or by organic concentration, all processes which would tend to result in accumulation of the metal in argillaceous members of the Meguma Group. The rapid deposition of greywacke A units from turbidity currents cannot have been favourable for any type of chem-absorption process to concentrated arsenic from the marine depositional environment. However, it is in the greywackes that the highest arsenic concentrations prevail. The explanation offered is that fluid circulation in Meguma rocks occurred mainly in greywacke, rather than in slates, because of much higher early post-lithification permeability and porosity. Thus, a preferential loading of greywacke with metals is expected if metals were introduced in fluids at some post-lithification stage after diagenesis and dewatering. Alternatively, tne slates should have been the main arsenic reservoirs if arsenic was fixed in the marine environment during sedimentation. The precise timing of this proposed arsenic introduction is uncertain but, as the deformation and metamorphism would tend to reduce primary rock porosity and permeability, it is suggested that arsenic enrichment occurred prior to, or in the very early stages, of deformation.

Migration of arsenic and gold away from veins must also be considered as a mechanism for generating metal enrichment in host rocks. The common occurrence of arsenopyrite along vein-wallrock contacts suggests that some migration of arsenic occurred, at least within the veins. However, several aspects of arsenic (and gold) distribution in the Harrigan Cove case argue against the concept that all metal introduction into host rocks is due to quartz vein formation. The proportions of arsenic and gold in the veins and greywacke host rocks are such that the arsenic-to-gold ratio in greywacke averages approximately four times that of the quartz veins. Considering the average lithic proportions of greywacke to quartz veins, about 7 to 1, the greywacke units represent an arsenic reservoir of major proportions compared to the quartz veins. If vein-forming fluids alone were responsible for arsenic in the host rocks, an extremely high initial arsenic concentration in the fluids would be required, as well as a highly efficient and selective mechanism of arsenic loss from the veins. Well defined arsenic concentration gradients from veins would be expected. None of these features are observed nor are they expected properties of the vein fluids. Also, if the veins were the sole source of metals in host rocks the high concentrations of arsenic in greywacke present difficulties. As it seems likely that vein formation was early in the strain history, and perhaps continued during folding, then vein formation must have occurred after a significant loss of primary porosity had occurred. Indeed, if hydraulic fracture is the vein fluid emplacement mechanism, porosity cannot have been high. Thus, the preferential concentration of arsenic in greywacke rather than in slate is less easily explained by emanation from veins than by an early introduction of arsenic antedating vein emplacement. The source of an arsenic-bearing fluid is of course problematical and is not directly addressed by the geochemical distribution data.

A modest gold enrichment, amounting to a four-fold increase relative to unmineralized Meguma rocks, is also characterized of the Harrigan Cove host rocks. While there is a strong positive correlation of gold with arsenic on a total sample population basis (Table 4), inspection of the averages for individual localities (Table 2a) indicates that the very strong concentration of arsenic in greywacke relative to slate does not

apply to gold. Thus, at the well sampled Central South locality average As in A units is about nine times that in E units, whereas gold is only enriched by about 1.25 times in greywacke relative to slate in these rocks. It is suggested that sufficient arsenic (and sulfur) were introduced into the host rock to crystallize discrete minerals (arsenopyrite and pyrite or pyrrhotite) which serve to concentrate gold. Although most of the arsenic crystallizes in the greywackes, sufficient arsenopyrite forms in argillaceous rocks to effectively scavenge gold in this medium as well, particularly as very small amounts of gold relative to arsenic are involved. The precise mechanism by which gold was concentrated by sulpharsenides and sulphides is unknown, but an attractive possibility is electrodeposition as advocated by Bancroft and Gilles (1982). This mechanism would allow the gold contents of sulphides (and sulpharsenides) to substantially exceed theoretical equilibrium solubility in sulphide systems (Barton, 1969). Thus, fluids which effected district-wide metal enrichments need not have had a high gold content. The critical factors leading to gold enrichment were probably related more to the volumes of fluid available, the permeability and porosity of the host rocks, and, most critically to early saturation of these fluids with respect to sulphides and sulpharsenides.

The final stage in this polygenetic mineralization process was the generation of the vein fluids in response to pressure solution, or, ultimately, to deformation. In this process, although much higher concentrations of arsenic were taken into solution than gold, the proportions of gold to arsenic in the fluids exceeded that in the host greywacke by perhaps a factor of four, leading to the relative gold enrichment in the veins. An evaluation of the pressure solution process in a gold district presents the problem of looking at a rock-vein system after metal transfer has occurred. It is suggested that an early phase of the process can be seen in unmineralized areas where spaced pressure solution cleavage has developed. The cleavage zones in unmineralized greywackes of the Ruth Falls syncline with prominent spaced cleavage that was produced by pressure solution contain 3.6 times the gold content (Crocket et al., 1983). This suggests a significantly stronger concentration of gold than of arsenic in the cleavage domains. With the development of cleavage some channelling of fluid flow along cleavage is expected. Such fluid would then leach metals in somewhat different proportions than represented by their contents in the lithon. It is suggested that fractionation of metals in the pressure solution process is one means by which higher gold-arsenic proportions are developed in vein fluids.

As assumption implicit in this hypothesis is that the gold/arsenic ratios observed in the quartz veins are the same as those of the mineralizing fluids. While the extent of gold-arsenic fractionation in the vein-forming process cannot be directly evaluated, a hydraulic fracture-fill origin of bedding-parallel veins is a mechanism which probably involved rapid fracture propagation aud rapid fluid emplacement (Graves and Zentilli, 1982; Phillips, 1972). Further, rapid crystallization from vein-filling fluids may occur (Phillips, 1972). Such characteristics would tend to minimize the potential for metal fractionation in the vein-forming process.

CONCLUSIONS

A polygenetic mineralization process is envisaged which integrates metal distributions in host rocks and veins with structural history. Vein fluid generation, spaced cleavage produced by pressure solution and folding are thought to represent response to deformation of the Meguma rocks. These processes may generate auriferous

quartz veins, but it seems that some enrichment of the host greywacke and slates in gold at, or prior to, the onset of folding is an essential element in vein genesis. At Harrigan Cove arsenopyrite plays a key role as a gold-concentrator mineral resulting in a sub-ore grade initial enrichment of gold in host rocks. Deformation further upgraded the gold concentration by selective transfer of gold to fluids that formed the quartz veins.

ACKNOWLEDGEMENTS

We gratefully acknowledge the input of Dr. J.R. Henderson (Geological Survey of Canada) in all phases of this study but particularly with regard to information pertinent to the origin of the quartz veins. Dr. U. Kretschmar helped with much of the sampling and his discussion of the metallogeny provided a simulating, if somewhat different view point, than our own.

Financing of the project through a Research Contract Award by Supply and Services Canada (Energy, Mines and Resources) is acknowledged.

ANDERLE, J.P., 1974. Geological report on the Harrigan Cove property, Halifax County, Nova Scotia. Assessment File No. 21H23(02), Nova Scotia Department of Mines and Energy, 15 p.

BANCROFT, M.G. and GILLES, J., 1982. Gold deposition at low temperature on sulphide minerals. Nature, 298, pp. 730-731.

BARTON, P.B., 1969. Solubility of gold in sulfide minerals. In Experimental Geochemistry, Geological Survey Research 1969; United States Geological Survey Professional Paper G50A, p. A108.

BOSTROM, K. and VALDES, S., 1969. Distribution of arsenic in deep-sea sediments and rocks. Lithos, 2, pp. 351-360.

BROOKS, R.R., CHATTERJEE, A., SMITH, P.K., RYAN, D.E., and ZHANG, H.F., 1982. The distribution of gold in rocks and minerals of the Meguma Group of Nova Scotia, Canada. Chemical Geology, 35, pp. 87-95.

CLIFFORD, P.M., CROCKET, J.H., and FUETEN, F., 1983. Distribution and localization of gold in Meguma Group rocks, Nova Scotia. Part 1: structural effects and pressure solution -- preliminary results. Geological Survey of Canada, Paper 83-1B, pp. 279-283.

CROCKET, J.H., 1974. Gold. In Handbook of Geochemistry, v. II/5, ed. K.H. Wedepohl; Springer-Verlag, Berlin, chapter 79, sections B-O.

CROCKET, J.H., CLIFFORD, P.M., FUETEN, F. and KABIR, A.,1983. Distribution and localization of gold in Meguma Group rocks, Nova Scotia. Part 2: Implications of background geochemistry and cleavage developement -- a preliminary report. Geological Survey of Canada, Paper 83-1B, pp. 285-290.

FARIBAULT, E.R., 1899. The gold measures of Nova Scotia and deep mining. Journal of the Mining Society of Canada, II, p. 119-128.

FARIBAULT, E.R., 1906. Plan and sections, Harrigan Cove gold district, Halifax County, Nova Scotia. Geological Survey of Canada, Map No. 945.

FUETEN, F., CLIFFORD, P.M., PRYER, L.L., THOMPSON, J., and CROCKET, J.H., in press. Distribution and localization of gold in Meguma Group rocks, Nova Scotia. Part III: Shortening and cleavage production, and widespread mass removal of SiO_2. Geological Survey of Canada.

GRAVES, M.C. and ZENTILLI, M., 1982. A review of the geology of gold in Nova Scotia. Canadian Institute of Mining and Metallurgy, Special Paper 24, pp. 233-242.

HAYNES, S.J., 1983. Typomorphism of turbidities-hosted auriferous quartz veins, southern Guysborough County. Nova Scotia Department of Mines and Energy, Report 83-1, pp. 183-224.

HENDERSON, J.R., 1983b. Harrigan Cove mine. In CIM Geology Division Excursion Guidebook Gold Deposits in the Meguma terrane of Nova scotia, by Keppie, J.D., Haynes, S.J., Henderson, J.R., Smith, P.K., O'Brien, B.H., Zentilli, M., Jensen, L.R., MacEachren, I.J., Stea, R., and Rogers, P. Canadian Institute of Mining and Metallurgy, 104 p.

HIND, H.Y., 1869. Notes on the structure of the Nova Scotia gold district, Transactions Nova Scotia Institute of National Science, II, Part 3, pp. 102-109.

HUNT, T.S., 1869. Report on the gold region of Nova Scotia. Geological Survey of Canada, 1868, p. 48.

KEPPIE, J.D., 1976. Structural model for the saddle reef and associated gold veins in the Meguma Group, Nova Scotia. Nova Scotia Department of Mines, Paper 76-1, 34 p.

KEPPIE, J.D., HAYNES, S.M., HENDERSON, J.R., SMITH, P.K., O'BRIEN, B.H., ZENTILLI, M., JENSEN, L.R., MACEACHREN, I.J., STEA, R. and ROGERS, P., 1983. CIM Geology Division Excursion Guidebook, Gold deposits in the Meguma Terrane of Nova Scotia. Canadian Institute of Mining and Metallurgy, 104 p.

KRETSCHMAR, U., 1983. Meguma-type turbidite hosted gold deposits in Nova Scotia. Unpublished report prepared for the Geological Survey of Canada, Ottawa, 133 p.

MALCOLM, W., 1976. Gold Fields of Nova Scotia. Geological Survey of Canada Memoir 385, 253 p.

ONISHI, H., 1969a. Arsenic. In Handbook of Geochemistry, v. II/4, Springer-Verlag, Berlin, chapter 51, sections B-M.

ONISHI, H., 1969b. Antimony. In Handbook of Geochemistry, v. II/4, Springer-Verlag, Berlin, chapter 51, sections B-O.

PHILLIPS, W.J., 1972. Hydraulic fracturing and mineralization. Geological Society of London, 128, pp. 337-359.

SCHENK. P.E., 1970. Regional variation of the flysch-like Megume Group (Lower Paleozoic) of Nova Scotia compared to recent sedimentation off the Scotia Shelf. In Flysch Sedimentology in North America. (Ed.) J. Lajoie. Geological Association of Canada, Special Paper 7, pp. 127-153.

SMITH, P.K., 1983a. Geology of the Cochrane Hill gold deposit, west-central Guysborough County, Nova Scotia. Nova Scotia Department of Mines and Energy, Report 83-1, pp. 225-256.

SMITH, P.K., 1983b. Cochrane Hill gold mine. In CIM Geology Division Excursion Guidebookk Gold Deposits in the Meguma Terrane of Nova Scotia, by Keppie, J.D., Haynes, S., Henderson, J.R., Smith, P.K., O'Brien, B.H., Zentilli, M., Jensen, L.R., MacEachren, K.J., Stea, R., and Rogers, P. Canadian Institute of Mining and Metallurgy, 104 p.

THORPE, R. J., and THOMAS, G.M., 1976. Gold content of greywacke and slate of the Goldenville Formation, Nova Scotia, as determined by neutron activation analysis. Geological Survey of Canada, Paper 76-1A, pp. 314-328.

Maritime Sediments and Atlantic Geology

Vol. 22 April, 1986 No. 1

Formation of Spaced Cleavage and Concurrent Mass Removal of SiO_2, Meguma Goup Metagreywackes, Goldenville, Nova Scotia

F. Fueten, P.M. Clifford, L.L. Pryer, M.J. Thompson and J.H. Crocket
Department of Geology
McMaster University, Hamilton, Ontario L8S 4M1

Increasing inequancy and decreasing fluctuation of long axes of quartz grains from lithons to cleavage zones in Meguma Group metagreywackes indicate an increase in strain. This strain increase is best ascribed to pervasive pressure solution in which quartz grains are trimmed to yield nearly rectangular sections in cleavage zones, as compared to their irregular outlines in lithons. Shortening calculated from a one-dimensional strain model reaches 60-70% in cleavage zones. Comparable values of shortening are calculated from modal analyses, and from chemical analyses of cleavages and lithons.

The implication of such shortening is that about ten percent of all the quartz in the original rock has been removed from the immediate system. This demands volumes of water about one order of magnitude greater than any likely content of connate water. The transport system was a dynamic one, involving most of the rock volume.

L'accroissement de l'inégalité et la baisse des fluctuations des longs axes des grains de quartz, des lithons jusqu'aux zones de clivage, dans les métagrauwackes du groupe Meguma, indique une hausse de tension. Cette hausse de tension est attribuée à la solution de pression pénétrante dans laquelle les grains de quartz sont taillés et donnent des sections presque rectangulaires dans les zones de clivage, comparé à leur profile irrégulier dans les lithons. Le raccourcissement, calculé à partir d'un modèle de pression unidimensionnel, atteint des valeurs entre 60 et 70% dans les zones de clivage. Des valeurs comparables du raccourcissement sont calculées à partir d'analyses modales, et d'analyses chimiques des clivages et des lithons.

L'implication de ce raccourcissement est qu'environ dix pourcent de tout le quartz de la roche originaire, a été supprimé du système immediat. Cela exige des volumes d'eau d'un ordre de grandeur plus important que n'importe quel système inné d'eau vraissembable. Ce système de transport était un système dynamique qui comprenait la majorité du volume des roches.

INTRODUCTION

An earlier report (Clifford et al.) suggested that a cleavage in metagreywackes of the Meguma Group, Nova Scotia, has been formed by pressure solution processes. New data sustain that interpretation and permit estimates of shortening in directions normal to cleavage. These in turn have implications for transport of quartz and gold.

The metagreywackes which we have examined are part of the Goldenville Formation, which is the lower division of the Cambro-Ordovician Meguma Group of Nova Scotia. Mapping in the Ecum Secum area (Fig. 1) shows that these rocks have been deformed into a series of gently, but doubly, plunging folds, commonly arranged en échelon. Axial surfaces are roughly upright and strike almost east-west. Associated with these folds is a very obvious spaced cleavage, marked by zones of high concentration of phyllosilicates. Other structures include quartz veins (see Henderson, 1983), faults which trend about 130°, and kink folds. We deal here only with the cleavage and its generation, as revealed by petrography, geometric analysis and chemistry.

MARITIME SEDIMENTS AND ATLANTIC GEOLOGY
22, 35-50 (1986)

0711-1150/86/010035-16$3.40/0

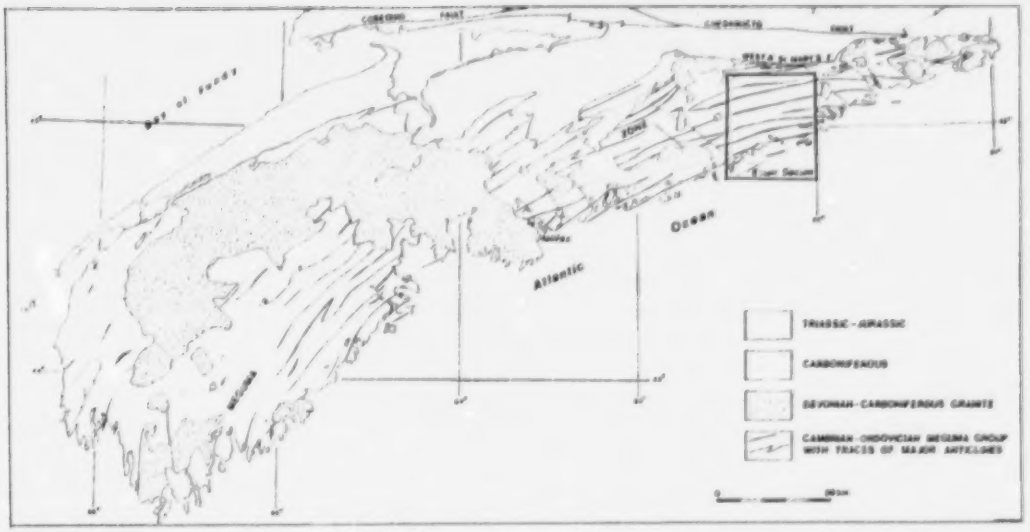

Figure 1 - Simplified geological map of Nova Scotia: Ecum Secum area is outlined. G = Goldenville.

METAGREYWACKE

The Goldenville metagreywackes occur as beds about 1-2 m thick, mainly massive, with Bouma divisions discernible in some beds. Such beds are separated by thin (ca. 10 cm) layers of meta-argillite which are recessive in most outcrops. Cleavage in the metagreywackes is widely spaced compared to a closely packed slaty cleavage in the meta-argillites. Goldenville metagreywackes are typically medium grained micaceous arenites. Quartz is the dominant mineral phase, followed by phyllosilicates. Modal analyses show that these minerals form about 95% of the rock. Other species include feldspar, carbonate and opaques.

Quartz occurs as obviously detrital grains, and also in polycrystalline aggregates which may be quartzite clasts (cf. Graves, 1976). Virtually all grains show some undulatory extinction. Most grains in lithons are irregularly sutured; but in cleavage zones (CZ), quartz grain boundaries are mainly straight and many grains are rectangular in section. Some 50% of grains have beard overgrowths of quartz and white mica.

White Mica occurs overwhelmingly as well-developed subhedral inequant crystals throughout the rock; crystals in CZ are generally a little larger than those in lithons. Small amounts of white mica are part of the beard overgrowths on quartz grains in both CZ and lithons.

Biotite occurs as anhedral crystals, usually associated with carbonate or opaque minerals in lithons. In CZ biotite crystals are larger and of better form than those of the lithons.

Taylor and Schiller (1966) noted that the regional metamorphism here is greenschist facies and this latter mineral assemblage is compatible with this metamorphic grade.

Table 1 gives modal analyses for eight thin sections, with over 2000 points per section. These include both lithons and cleavage zones. In carrying out the modal analyses, traverse lines were oriented parallel to cleavage zones and spaced 0.3 mm apart. The count "track" was recorded on a photomap of the section, and zones of different mineralogic abundances were easily defined. Because quartz and mica comprise 95% of these rocks, we ignore other components in subsequent physical analysis, with no great loss of

Table 1

MODAL ANALYSES, TWO SECTIONS FOR EACH OF FOUR SAMPLES, OF GOLDENVILLE METEGREYWACKES. OVER 2000 POINTS PER SECTION

	Quartz	White Mica	Dark Mica	Opaques	Carbonate	Feldspar
G20 753 AC	67.0	23.5	4.9	1.6	1.4	1.4
G20 753 BC	73.2	17.7	4.5	1.3	2.1	1.1
G26 415 AC	68.6	26.0	1.4	2.0	1.7	0.3
G26 415 BC	58.8	34.0	2.2	1.9	2.2	0.9
G19 354 AC	68.3	23.0	2.7	1.0	3.6	1.3
G19 354 BC	68.0	20.4	6.2	0.8	3.5	1.0
G26 353 AC	68.1	24.9	2.9	1.1	1.7	1.2
G26 353 BC	68.7	23.6	3.3	1.3	2.5	0.6
Overall Averages	68%	24%	4%	1%	2%	2%

accuracy.

PHYLLOSILICATES

Figure 2 gives the trans-cleavage variation in phyllosilicate content for a range of cleavage development, from mediocre [G20-753 AC] to exceptionally wide and sharply defined [G26-415 AC]. CZ are best defined in terms of phyllosilicate contents. Even in poorly-developed CZ, phyllosilicate content exceeds 30%, and the gradient in mica content from lithon to CZ is invariably steep. In well-developed CZ, mica content exceeds 60% and the CZ margin is very well defined. Lithons by contrast, always have phyllosilicate contents of 20% or less; the phyllosilicate grains seem to be distributed more or less uniformly throughout lithons.

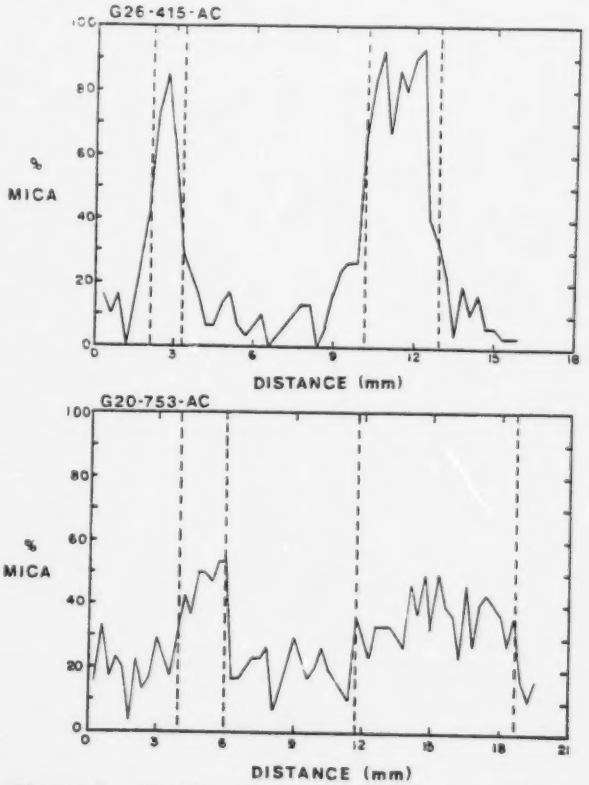

Figure 2 - Variation in phyllosilicate content across section # G26 - 415 AC, # G20 - 753 AC. Note marked changes which help define cleavage (CZ).

Throughout the lithons, white mica and biotite are about equally abundant. But in CZ, white mica content increases sharply whereas biotite content remains unchanged, relative to the modal abundances of these minerals in lithons (Fig. 3). A simple concentration of phyllosilicates should appear as an equal rise in modal abundances of both phases in CZ. This is obviously not the case. One possible conclusion is that, in addition to simple concentration, there has also occurred a production of some white mica as a new phase,

presumably at the expense of other phyllosilicates. The process also involved removal of carbonate; there is little carbonate in the rock as a whole and none in CZ.

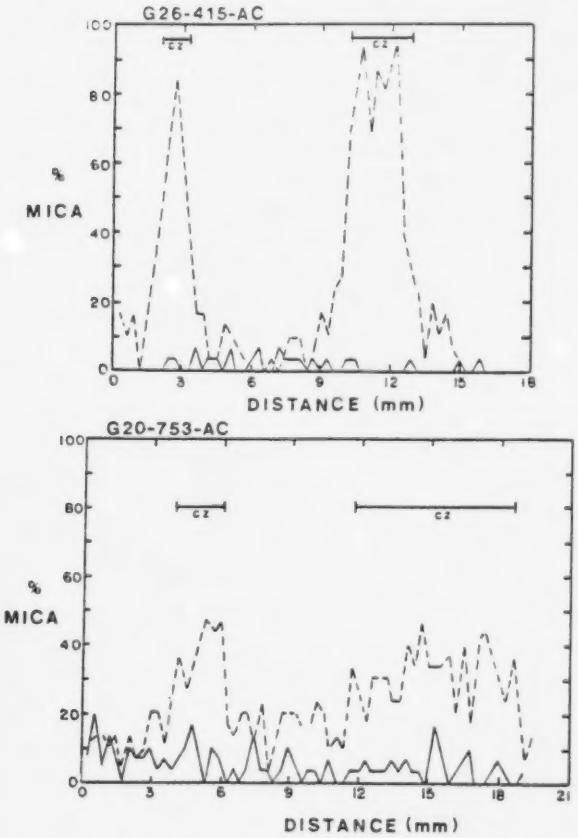

Figure 3 - Change in modal abundances of dark (continuous line) and light (dashed line) micas, sections # G26 - 415 AC, # G20 - 753 AC.

Orientation patterns of phyllosilicate grains in CZ and lithons are very similar (Fig. 4). Standard deviations of orientations in CZ are a little smaller than in lithons (Table 2), suggesting a slightly better degree of preferred orientation in CZ. However, the differences are not profound, and the mean orientations for the two kinds of sites are nearly identical, coinciding approximately with the general orientation of CZ. Better developed CZ show smaller standard deviations. One possible implication of this is that the process of cleavage formation, as it affected the orientation of phyllosilicate grains, was little more powerful in CZ than in lithons of the same sample, though the process does lead to a better degree of preferred orientation with better development of cleavage.

QUARTZ GRAIN SHAPES AND ORIENTATIONS

For the analysis ot grain shape variation, we have identified three kinds of domain in each sample. Lithons (ML) have apparently undergone least deformation. They contain more than 60% detrital quartz grains, of highly variable size and shape. Axial ratios are low, shapes range from angular to subrounded. There is a very weak preferred orientation of such grains. Intermediate zones (IM) possess a well-defined grain cleavage. Quartz exceeds 50%; quartz grains are eye-shaped with tapered ends, defining the cleavage though not very powerfully. Cleavage zones (CZ) are zones of high abundance of phyllosilicates, mainly white mica, and of straight-sided quartz grains. Micas exceed 30% and may reach 80% of the volume of the CZ. Boundaries between these domains vary from sharp to diffuse. Two examples are given in Figure 5.

For each domain, we have measured long and short axes of quartz grains, and also measured the orientation of long axes relative to an arbitrary datum (fluctuation angle, θ) for mutually perpendicular sections: (ac) sections are normal to fold axis, and (bc) sections are normal to cleavage but parallel to fold axis.

Results are plotted as "fluctuation plots" of axial ratio, A_T, versus fluctuation angle θ, for (ac) and (bc) sections (Fig. 6) (Ramsay,1967). From these plots, it is apparent that (i) quartz grains become progressively more inequant, ML → IM → CZ. (ii) long axis fluctuation is progressively more restricted ML → IM → CZ. Accompanying these changes, grain boundary geometries change from largely irregular to commonly straight-sided. In addition, there is no marked

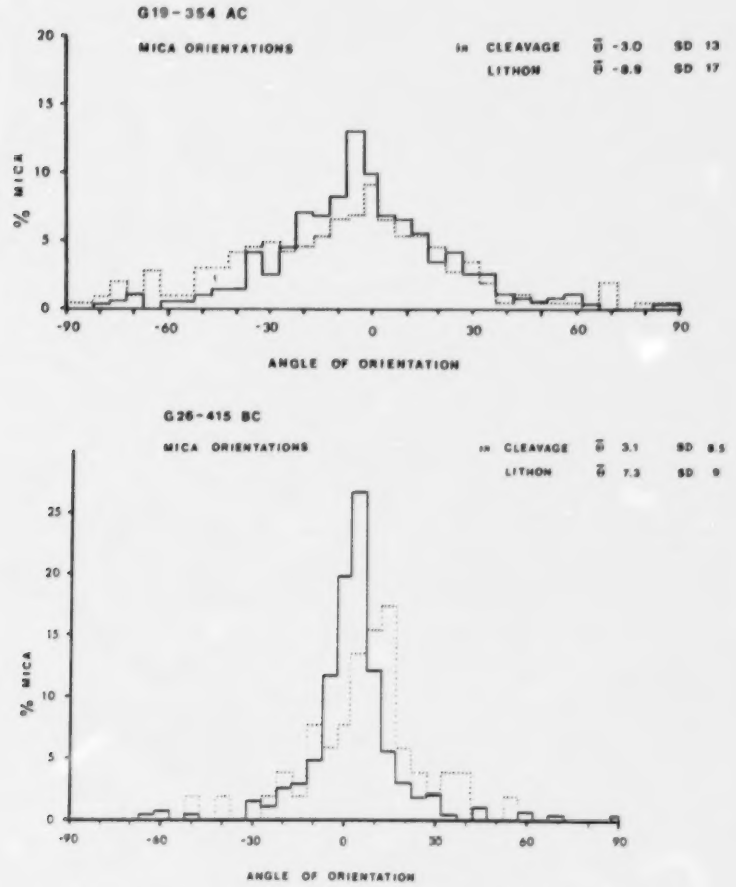

Figure 4 - Histograms of orientation of basal cleavage planes of mica (Zero = orientation of CZ). Solid line = CZ; Dotted line = Lithon. (a) Section # G19 - 354 AC; poorly defined, poorly developed CZ. Micas show highest standard deviation about mean orientation for all samples analyzed, and lowest calculated shortening -- 51%. (b) Section # G26 - 415 BC; sharply defined, well developed CZ. Micas show lowest standard deviation about mean orientations, greatest contrast between CZ and lithon for all samples analyzed, and highest calculated shortening -- 83%.

distinction in long-axis dimensions from ML to CZ, nor is there any marked increase in such things as undulatory extinction, which suggests that the changes in grain shape are not dominated by crystal plasticity.

VOLUME CHANGES

We have attempted to estimate the dimensional changes associated with this quartz grain shape change. From each fluctuation plot, we can calculate the axial ratio of the strain ellipse for that section, or a version of it where the section plane may not be exactly parallel to a plane of principal strain. This tectonic axial ratio we refer to subsequently as A_t for any given section. From such data for the mutually perpendicular sections, we calculate the axial ratio of the strain ellipsoid for each site, following the method which was outlined by Ramsay (1967) and subsequently modified by others (e.g. Dunnet, 1969). Results are given in Table 3, and illustrated in a logarithmic Flinn-type plot in Figure 7. With one exception (G26-415 lithon), all calculated strain ellipsoids suggest volume loss. The trends for all data are to greater apparent flattening from ML to CZ.

If we assume that the progression ML

Table 2.

ORIENTATION OF BASAL CLEAVAGE IN GOLDENVILLE METAGREYWACKES

Sample Number	Cleavage (CZ)	Lithon (ML)	
G19 - 354 AC	355	263	N
	- 3	- 9	M
	13	17	SD
G19 - 354 BC	357	202	N
	- 2	- 3	M
	11	11	SD
G20 - 753 AC	367	188	N
	0	0	M
	10	17	SD
G20 - 753 BC	141	192	N
	- 2	- 3	M
	11	9	SD
G26 - 353 AC	214	189	N
	- 1	- 1	M
	8	11	SD
G26 - 353 BC	224	194	N
	- 4	- 3	M
	10	9	SD
G26 - 415 AC	310	127	N
	- 2	5	M
	9	13	SD
G26 - 415 AC	273	52	N
	3	7	M
	9	9	SD

Cleavage trace is zero

N = number of observations;
M = mean orientation relative to cleavage;
SD = standard derivation

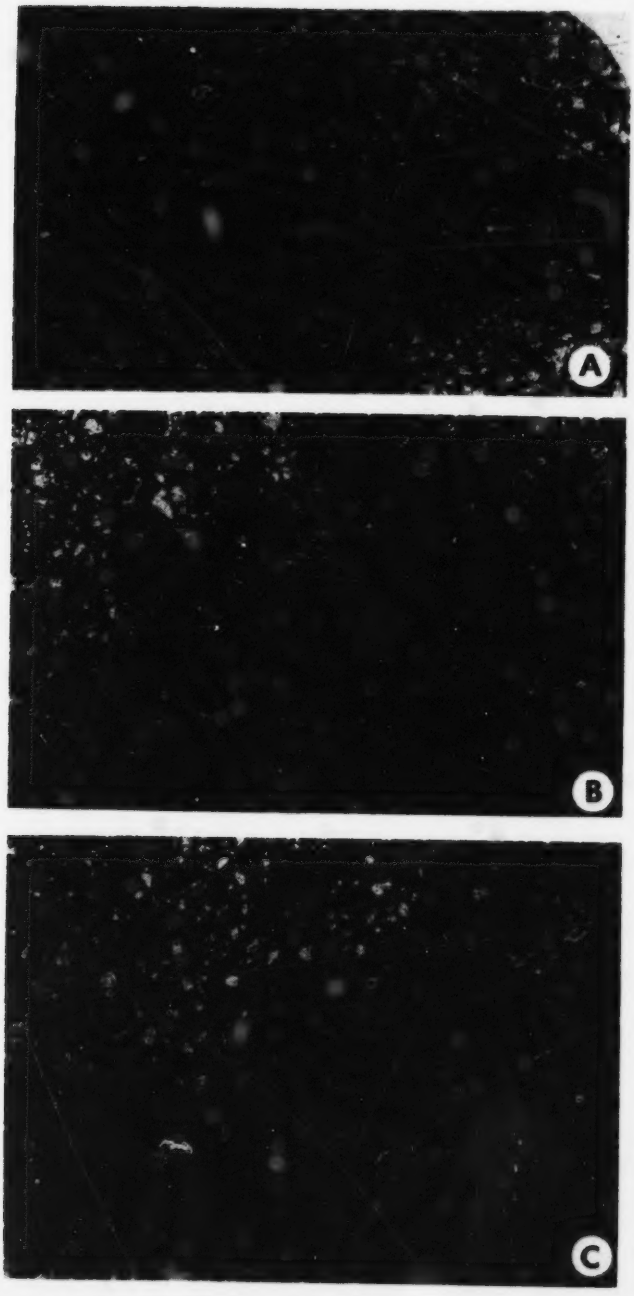

Figure 5 - Photomicrographs of (a) cleavage zone, sample # G26 - 415, (b) lithon, sample # G26 - 415, (c) sample # G20 - 753. Note differences in shapes and margins of quartz between the two domains.

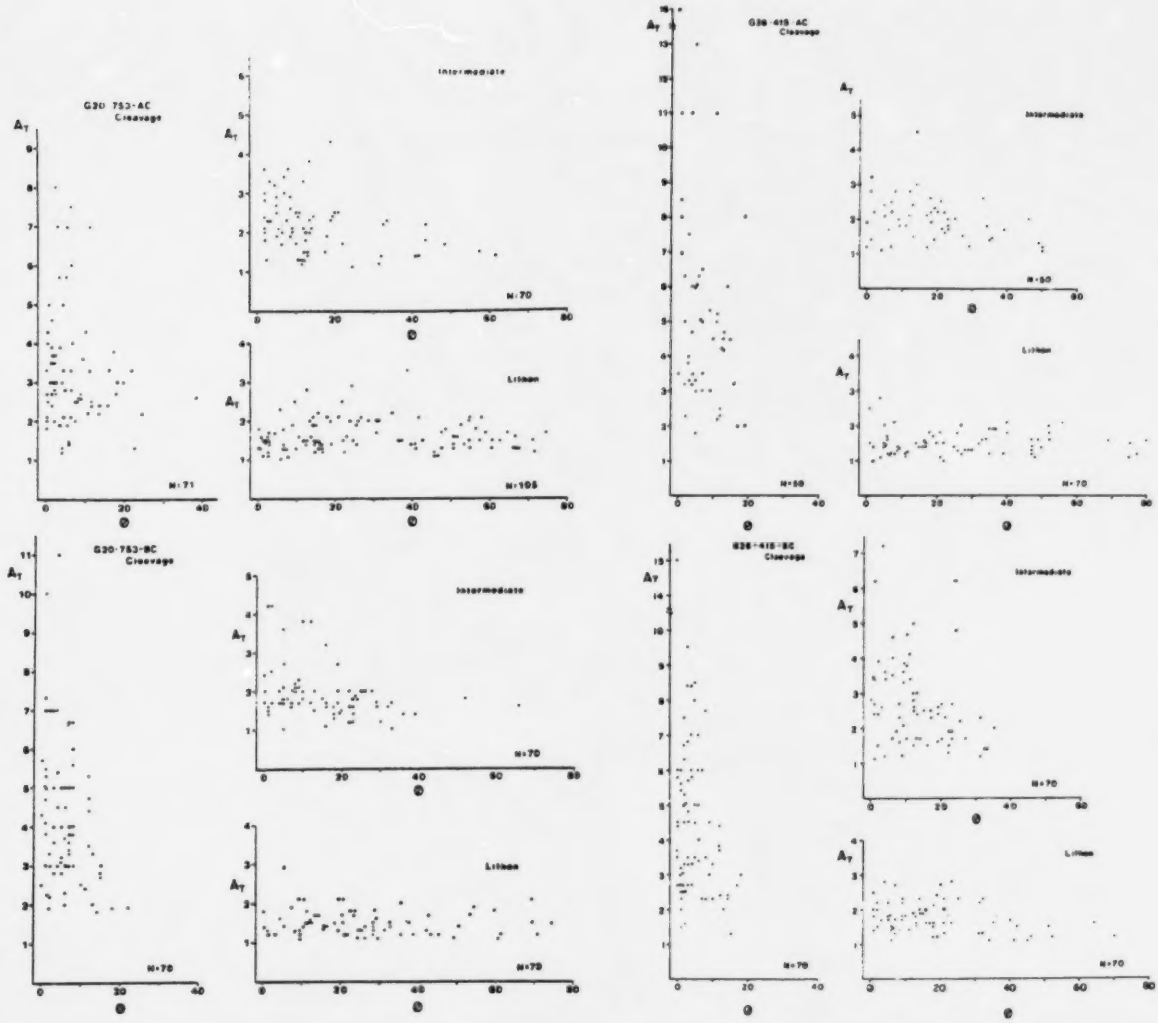

Figure 6 - Fluctuation plots: actual axial ratio, A_T, versus fluctuation angle, θ. Sample # G26 - 415 has the best defined cleavage and the highest calculated shortening. Sample # G20 - 753 has less well-defined cleavage, least calculated shortening. θ is measured from the cleavage. Diagrams should be symmetrical about zero but points have been reflected across zero to better define the distribution.

→ IM← CZ is a genuinely evolutionary one, then the deformation paths all have low k values. Following Ramsay and Wood (1973), we superimpose on Figure 7, lines of equal volume loss. These suggest that even lithons have suffered some loss of volume, up to 27%; that the loss is greater in intermediate areas; and is uniformly highest in CZ. As it happens, the highest volume losses, 71% from G26-353 and G26-415 cleavage, occurred in the anticlinal core. The least volume loss, 58% from G20-753 cleavage, occurred in the fold limb. Ranges of ΔV are least for CZ, most for ML.

A second, crude estimate of ΔV has been made, using the ratio of A_t for CZ to A_t for ML in each sample. This ratio is equivalent to the fraction of a grain, having the original dimensions of a strain ellipse for the lithon, that remains after experiencing a material volume loss accomplished by a change in one dimension only, and which

Table 3.

AXIAL RATIOS OF STRAIN ELLIPSOIDS, CALCULATED AFTER RAMSEY (1967) AND DUNNET (1969)

Sample #, Site	Axial Ratio, X_t	Strain Y_t	Ellipsoid Z_t
G26 - 353			
CZ	1.08	1.0	0.27
IM	1.03	1.0	0.56
ML	1.05	1.0	0.70
G26 - 415			
CZ	1.15	1.0	0.25
IM	1.31	1.0	0.53
ML	1.30	1.0	0.81
G20 - 753			
CZ	1.27	1.0	0.33
IM	1.15	1.0	0.56
ML	1.03	1.0	0.80
G19 - 354			
CZ	1.07	1.0	0.30
IM	1.01	1.0	0.45
ML	1.03	1.0	0.71

CZ -- Cleavage zone; IM -- Intermediate zone, ML -- Lithon

yields a strain ellipse equivalent to that found in the CZ. The equation for the elliptical case is:

$$\left[\frac{A_t \text{ (lithon)}}{A_t \text{ (cleavage)}} - 1\right] \times 100 = \text{percent area loss} \quad \text{[Eq. 1]}$$

This calculation has been carried out for (ac) and (bc) sections of each sample, and the values averaged to give a volume loss; results are listed in Table 4 alongside results from Figure 7. The numbers are remarkably similar, agreeing to within 10%. We conclude from this that the essential process of cleavage formation in these rocks involved loss of quartz by diffusional mass transfer, with the change of dimension being accomplished overwhelmingly in directions normal to the cleavage. This is supported, in our view, by the change in axial ratios in (ac) and (bc) sections without marked changes in the actual dimensions of quartz grains as measured parallel to cleavage, and by the straight margins ("neatly trimmed") of quartz grains in CZ as compared to the margins in ML.

For this second calculation, there are several assumptions:

(a) the lithons are representative of the original rock prior to deformation.

(b) volume loss affected only the Z dimension of the evolving strain ellipse; in geological terms, material was removed along axes normal to cleavage.

(c) volume loss is due solely to loss of quartz.

Of these, (c) is approximately

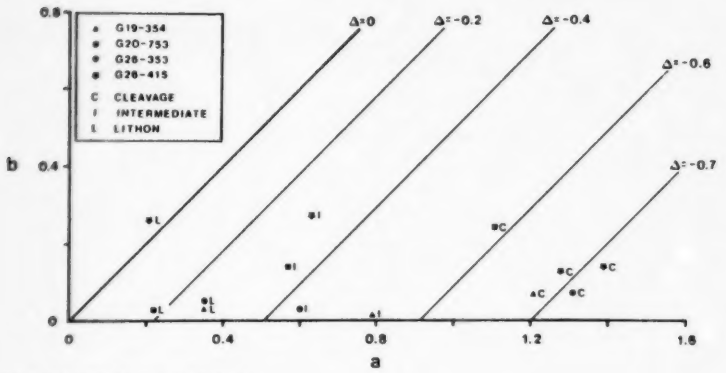

Figure 7 - Logarithmic Flinn-type plot of

$$\ln\left[\frac{1+e}{1+e_2}\right] = a \quad \underline{\text{versus}} \quad \ln\left[\frac{1+e_2}{1+e_3}\right] = b$$

for calculated strain ellipsoids in three domains in each of four samples. Lines of $\Delta = n$ are lines of implied volume loss (c.f. Ramsay and Wood, 1973). Points plot above b = 0, suggesting that deformation is not exclusively two-dimensional.

correct (ignoring any effects during compaction), because there is little of anything else but phyllosilicate in the rock. Removal of all material other than quartz and phyllosilicates would alter the numbers by, at most, ten per cent of their calculated value. Assumption (b) is probably not correct everywhere; there are some signs of crystal plasticity and preliminary calculations suggest that, in the core of the anticline, there may have been changes in both X_t and Z_t, due to constant-volume deformation. More work is to be done on this aspect. (a) is most contentious. We have no certain means of deciding what is unaltered. pristine Meguma metagreywacke. In our samples, lithons must be most nearly like the original material. However, Figure 7 implies a volume loss from litnons. This must imply that our second crude calculation is on the low side.

An alternative approach to this problem is to assume that CZ represent zones in which has accumulated phyllosilicate material, as a residue after the loss of quartz, treating lithons as unaffected. This gives a shortening across CZ only, according to the equation:

$$\left[\frac{\%\text{ mica in lithon}}{\%\text{ mica in cleavage}} - 1\right] \times 100 = \%\text{ shortening} \quad \text{[Eq. 2]}$$

Results range from 51% to 83%. This approach, dependent upon viewing lithons as original, suffers from the same drawback as mentioned above. It assumes also that all mineral phases, other than phyllosilicates, could have been involved in the volume loss episode; this is probably a safer assumption than (c) above. This calculation is unaffected by plastic deformation.

CHEMICAL ANALYSIS

Yet another approach to this problem is by chemical analysis of cleavage zones and lithons separately. Five samples of core, each approximately ten centimetres long, were selected for analysis. Each piece of core yielded one sample set, consisting of five to six cleavage planes and five to six lithons. Each cleavage and each lithon was then analysed individually, for a total of 55 samples analysed.

Table 4.

CALCULATED VOLUME CHANGES, ΔV AFTER RAMSEY AND WOOD (1973) AND ΔV_p USING EQUATION 1

Sample #, Site	ΔV	ΔV_p	$\Delta V - \Delta V_p$
G26 - 353			
CZ	-0.71	-0.62	+0.09
IM	-0.40		
ML	-0.26		
G26 - 415			
CZ	-0.71	-0.67	+0.04
IM	-0.31		
ML	+0.05		
G20 - 753			
CZ	-0.58	-0.62	-0.04
IM	-0.36		
ML	-0.18		
G19 - 354			
CZ	-0.68	-0.59	+0.09
IM	-0.54		
ML	-0.27		

CZ -- Cleavage zone; IM -- Intermediate zone; ML -- Lithon

Figure 8a shows the results of the analysis of five individual lithons of sample G26-415. As can be seen, there is a minor fluctuation in the CaO content, which probably reflects an equally minor variation in the carbonate content of the lithons of this sample. Overall, however, there is no significant variation in the major element chemistry of the lithons of individual sample sets. Other sample sets show similar agreements.

Figure 8b depicts the results of the analysis of five individual cleavage planes of sample G26-415. The chemical composition of the cleavage planes is distinctly different from that of the lithons. However, the compositions of the five different cleavage planes agree quite closely amongst themselves.

In order to determine how much the major element chemistry of cleavages and lithons of different beds varies, the average of each, cleavages and lithons, were calculated for every sample set. It is apparent from Figure 8c that the main variation in composition of the lithon average lies in their MgO content. This variation is between 0.01 wt% and 1 wt% and is likely to be due to differences in amounts of original Mg-bearing detrital phases. The bulk of the Mg may be originally derived from detrital clays; alternatively, the carbonate may have been magnesium-rich. The minor fluctuation in K_2O also can be explained by differences in the content of original K-bearing detrital phases. Overall, the chemical variation between the lithons of the five beds is quite small. The average compositions of the cleavage planes of all sample sets (Figure 8d) are also very similar to each other, especially when we consider that not every cleavage plane is

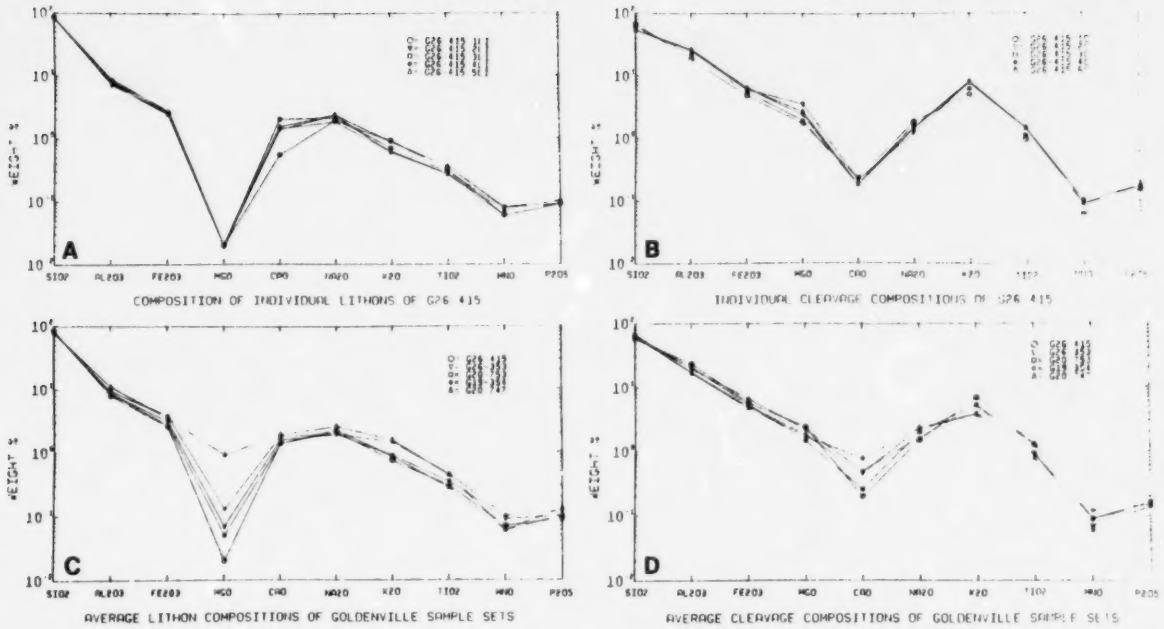

Figure 8 - Chemistry of lithons and CZ. (A) 5 lithons, sample # G26 - 415; (B) 5 CZ, sample # G26 - 415; (C) average composition of all lithons in each sample; (D) average composition of all CZ in each sample. Vertical axis has logarithmic scale.

equally well developed. Differences in the degree of development of the cleavage planes, indicated by variations in their mica content, cannot help but be reflected in their major element chemistry. The chemical composition of the lithons and cleavage planes are quite consistent and lend themselves to further investigation.

Figure 9 compares the average lithon and cleavage compositions of sample set G26-415, and indicates the following changes. The cleavage, with respect to the lithon is 26 wt% lower in SiO_2, 15 wt% higher in Al_2O_3, 3.2 wt% higher in Fe_2O_3, 2.4 wt% higher in MgO, 1.4 wt% lower in CaO, 0.6 wt% lower in Na_2O, 6.1 wt% higher in K_2O and 0.9 wt% higher in TiO_2. The amounts of MnO and P_2O_5 present and the errors associated with the XRF analysis in these oxides do not allow them to be used for quantitative results. They will therefore be ignored in the following discussion. The most interesting difference between the lithons and the cleavages is the large percentage difference in MgO and K_2O. Comparisons of other sample sets show similar results.

In an effort to determine the true losses and gains associated with the cleavage formation, the standard Gresens (1967) approach was taken. The Gresens equation is :

$$100 \left[f_v \left(\frac{g_c}{g_L}\right) C_n^c - C_n^L \right] = X_n \qquad \text{[Eq. 3]}$$

where f_v is volume factor; g_c, g_L are the densities of cleavage and lithon respectively; C_n^c, C_n^L are the amounts of any component, n, in cleavage and lithon respectively; and X_n is the actual amount of component n, lost or gained. Measurements of the densities of the cleavages and lithons showed that the differences in densities between the two was within the limits of accuracy of measurement. The density ratio used in the Gresens equation was therefore taken to be equal to one. Figure 10 shows the average volume factors for the oxides in all sample sets, assuming no loss or gain to or from the cleavage, ie. setting X_n to

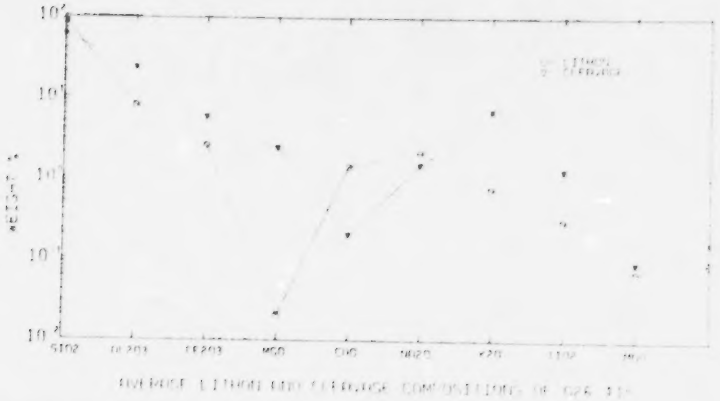

Figure 9 - Composition of the chemistry of lithons and CZ in sample # G26 - 415.

zero. Since the Gresens equation is applied to each component individually, the volume factor for each component is completely independent of the volume factor for any other component. This allows one to determine the true volume factor for the system, giving the overall bulk loss or gain the system has experienced. The criteria used to choose the true volume factor (Gresens, 1969) are as follow: one is a clustering of volume factors of several oxides, which would indicate that these oxides had been gained or lost to the same degree, or more likely, that they had been relatively immobile components; the other involves consistent component ratios of two or more oxides. If the ratios of two or more oxides is roughly the same in the lithon and in the cleavage, this indicates that these oxides were gained or lost to the same degree, or very little at all. Even though clustering may not be immediately apparent in Figure 9, TiO_2, Al_2O_3, and Fe_2O_3 are the only oxides in all five cases that are relatively close to each other. TiO_2, Al_2O_3 and Fe_2O_3 are also the only oxides that maintain relatively consistent component ratios. We therefore regard these oxides as least mobile components in this system. As the true volume factor for this system, we choose Al_2O_3, because it is located in the centre of the three relatively immobile oxides, but also because it shows the highest wt% of the three considered and is therefore least influenced by minor internal losses or gains. The true volume factors for the five cases presented here range from between 0.4 and 0.6. This implies that the cleavage represents a forty (volume factor = 0.6) to sixty (volume factor = 0.4) percent volume loss, with respect to its parental rock volume.

With the use of a true volume factor one can then use Figure 10 to determine what has been lost from or introduced to the cleavage during its formation. Any oxides to the right of the true volume factor have been lost from the cleavage during its formation, whereas oxides to the left of the volume factor were introduced to the cleavage during its formation. The distance from the true volume factor gives an indication of the degree to which this loss or gain has taken place. In all cases the results show remarkable similarities. In all cases CaO has been lost to the greatest extent during cleavage formation. It should be noted that this does not imply that the bulk of the material lost during cleavage formation was CaO but rather that this component has suffered the greatest loss with respect to its "original" lithon composition. SiO_2 shows the second greatest loss. The losses in these two components have been demonstrated in thin section by the lack of carbonate and the depletion of quartz in the cleavage plane (see above). The loss of silica is also the largest bulk loss from the cleavage plane. Other oxides

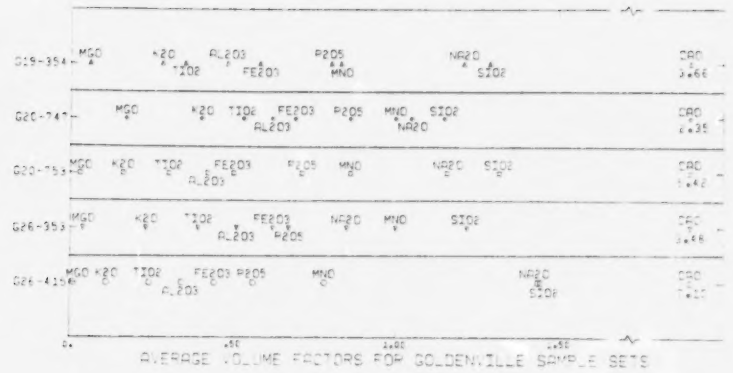

Figure 10 - Volume factor plot of Goldenville samples, using Gresens (1967) equation.

lost during the cleavage formation, in decreasing amounts, are Na_2O, MnO and P_2O_5. The sources for these oxides are likely to have been detrital clays which eventually formed the micas of the cleavage. MgO and K_2O were introduced into the cleavage plane and probably absorbed by forming micas.

These chemical changes imply that phyllosilicates [biotite, muscovite, chlorite] were actively recrystallizing during the cleavage formation period and that the chemical migrations observed took place during that period. The micas in the cleavage are different from those in the lithon as a result of these migrations. This is demonstrated by the petrography and reflected in the variations in the mica content between lithons and cleavage mentioned earlier. The similarity in the order with which the oxides plot on Figure 10, i.e. MgO on the left side to CaO on the right side, demonstrates how remarkably consistent the processes were that led to the chemical evolution of the cleavage. Furthermore, the degree to which the oxides are spaced out amongst themselves along the volume factor axis of Figure 10 is dependent upon the volume loss that has occurred. Sample G20-747, which shows the highest volume factor and therefore represents the smallest volume loss also displays the smallest spread amongst the oxides. On the other hand, sample G26-415 which shows the largest volume loss also displays the largest spread of the oxides. This demonstrates that the chemical movements that take place during the cleavage formation are not spurious and erratic, but are well controlled and follow certain definite patterns.

The fundamental assumption here is that the lithon represents the original source rock; the same assumption was used in the manipulation of the modal data earlier. Though there is a small quantity of "new" material in the lithons, in the form of beard overgrowths, this cannot alter the essential conclusion that the lithon is closer to original composition, or that it has suffered material loss. Deposition in the lithon would mean that the volume losses from CZ calculated from the chemistry are overestimates, while removal of material from lithons would lead to underestimation of losses from CZ. The close agreement of loss estimates from chemistry with loss estimates based on grain shape analysis suggests that lithons represent nearly "undiluted" source rock. This implies that material corresponding to the shortening was totally expelled from the greywackes, the bulk of this material being SiO_2.

DISCUSSION

The regional structure pattern, and the nature and geometry of quartz veins have been dealt with elsewhere (Henderson, 1983). We have concentrated on the documentation of a particular process for the two reasons: (i) we

think the process is responsible for the generation of a pervasive spaced cleavage; (ii) the process involves transfer of substantial quantities of SiO_2 from the local rocks.

Several different approaches to the problem of general mechanism of cleavage formation in these greywackes by different analyses converge on the same process, namely, pressure solution. This has produced essentially a one dimensional shortening along axes normal to CZ. Each CZ represents a shortening of at least 50% of its parent rock volume, with concurrent removal of SiO_2. Carbonate has also been removed, but is a trivial portion of the migrant material.

Our calculations of volume loss for CZ can be translated into a mass loss of SiO_2 from the system as a whole. We take the volume loss for CZ to be 50%; the lithon/CZ ratio is taken as 10:1, and the modal proportion of quartz and mica in lithon as 80 to 17. All loss is ascribed to transfer of SiO_2. These are either average figures, or, in the case of volume loss for CZ, at the low end of our range.

This converts to a mass loss of about 200 kg SiO_2 per cubic metre of dense rock. For metamorphic fluids, solubility of quartz has been put at levels of 0.1% to at most 2% by weight (Eugster, 1982). This implies rather large volumes of water to accomplish the removal of the SiO_2. For a high solubility of 2%, this works out at about 10 cubic metres of water for every cubic metre of rock affected. Naturally, this number will vary because of any or all of the following: different levels of volume loss across CZ, different lithon/cleavage ratios, different modal compositions, and variations in solubility accompanying changes in water temperature, pH, etc. The most influential of these are probably water properties and lithon/cleavage ratio. Nonetheless, even if we have overestimated by an order of magnitude, there still is a need for quantities of fluid well in excess of any plausible connate water content. The transfer system appears to have a dynamic one, involving either multiple recycling of water, or a steady supply of water from some other source (? interbedded mudstones, now slates).

This water must have circulated in such a way as to involve most of the rock volume. There is no record of a highly localized conduit or conduits with attendant alteration, such as is typical of a geothermal system. It seems probable that fluids moved mainly along all the lithons. Some redeposition in the form of straight-fibre beard overgrowths is found in the lithons, and could represent the declining stages of the process.

CONCLUSIONS

Spaced cleavage in metagreywackes of the Goldenville Formation was produced at Goldenville, Nova Scotia, primarily by removal of SiO_2 from zones in the rock as a result of pressure solution. Cleavage zones record a shortening normal to cleavage of at least 50% in the Goldenville area. This represents a loss of about 10% of the original quartz content of the total rock, equivalent to a bulk volume loss of roughly 8%, at a conservative estimate.

The removal of such a large quantity of SiO_2 appears to demand substantial quantities of water, which can be made available only by a steady recycling of water, or an equally steady supply of water from an external source. Such large quantities of water are vital for the transport of gold in amounts likely to prove exploitable.

ACKNOWLEDGMENTS

J.R. Henderson has been a constant source of advice and encouragement. A. Fyon has also offered incisive comment on some of the ideas presented here. Remarks by reviewers,especially P-Y. F. Robin, have prompted substantial

emendations to our original manuscript.

Research was funded under SSC-DEMR contract 22ST-23233-3-0354, as part of a joint Canada -- Province of Nova Scotia Co-operative Mineral Program to do with gold distribution in rocks of the Meguma Group in Nova Scotia.

CLIFFORD, P. M., CROCKET, J. H., FUETEN, F. 1983. Distribution and localization of gold in Meguma Group rocks, Nova Scotia. Part I: Structural effects and pressure solution -- preliminary results. Geological Survey of Canada Paper 83-1B, pp. 279-283.

DUNNET, D. 1969. A technique of finite strain analysis using elliptical particles. Tectonophysics, 7, pp. 117-136.

EUGSTER, H. 1982. Metamorphic solutions and reactions. Physics and Chemistry of the Earth, 13/14, pp. 461 - 507.

GRAVES, M. S. 1976. The formation of gold-bearing quartz veins in Nova Scotia: hydraulic fracturing under conditions of greenschist regional metamorphism during early stages of deformation. Unpublished M.Sc. Thesis, Dalhousie University.

GRESENS, R. 1967. Composition -- volume relationships of metasomatism. Chemical Geology, 2, pp. 47-65.

HENDERSON, J. R. 1983. Analysis or structure as a factor controlling gold mineralization in Nova Scotia. Geological Survey of Canada, Paper 83-1B, pp. 13-21.

RAMSAY, J. G. 1967. Folding and fracturing of rocks. McGraw-Hill, New York, 568 pp.

RAMSAY, J. G., WOOD, D. S. 1973. The geometric effects of volume change during deformation. Tectonophysics, 16, pp. 263-277.

TAYLOR, F. C., SCHILLER, E. A. 1966. Metamorphism of the Meguma Group of Nova Scotia. Canadian Journal of Earth Sciences, 3, pp. 959-974.

Maritime Sediments and Atlantic Geology

Vol. 22 April, 1986 No. 1

Structural Study of Highly Deformed Meguma Phyllite and Granite Vicinity of White Head Village, S.E. Nova Scotia

C.K. Mawer and P.F. Williams
Department of Geology
University of New Brunswick, Fredericton, New Brunswick E3B 5A3

A long history of dextral transcurrent shear on the Cobequid-Chedabucto Fault System is indicated by structures in Meguma Zone phyllite and granite, and late veins, which outcrop close to the present Chedabucto Fault trace. The phyllite deformed first upon collision of Meguma with Avalonia during the Acadian Orogeny, and progressively since that time by ductile deformation mechanisms for almost the total deformational history of the rocks. Its foliation is due to transposition and dynamic recrystallization. Granite was intruded syntectonically, as shown by contact metamorphic formation of syntectonic porphyroblasts in the phyllite which are rotated, and progressive development of an inhomogeneous shear zone foliation towards the phyllite-granite contact. This foliation is approximately parallel to that developed in the phyllite. Quartz veins, which overprint all earlier structures, were deformed and accomodated by ductile mechanisms while being rotated in the continued progressive dextral shear regime.

Une longue histoire de cisaillent transversale dextrale, sur les systemes de failles Cobequid-chedabucto, est indiqué par des structures dans les phylites et les granites Meguma et les jeunes veines qui affleurent pres de la trace de la faille Chedabucto actuelle. La phylite s'est d'abord deformé a la suite de la collision entre Meguma et Avalonia pendant l'orogenese Acadienne, et depuis, par des mécanismes progressifs de déformation ductile pendant presque toute la durée de l'histoire déformationelle des roches. Sa foliation est attribuée a la transposition et a la recristalisation dynamique. Le granite a été pénétré syntectoniquement, comme le demontre la formation de porphyroblastes syntectoniques par moyen de metamorphisme de contact, dans les phylites retournées, et par le développement progressif d'une foliation de zone de cisaillement inhomogene vers le contact phylite-granite. Cette foliation est plus ou moins paralelle a celle qui est développée dans la phylite. Des veines de quartz, qui surimpose toutes les structures précédentes, ont été déformées et accomodées par des mécanismes ductile, pendant qu'elles étaient retournées par le régime progressif de cisaillement déxtral.

INTRODUCTION

Meso- and microstructures of strongly deformed phyllite and granite, which outcrop close to the CHEDABUCTO fault in south-eastern Nova Scotia (Figure 1a), include a variety of features which place constraints on:

a) the style, and style variation with time, of progressive deformation of the rocks;

b) the sense of displacement of the Meguma Zone with respect to the Avalon Zone along the Cobequid-Chedabucto Fault System; and

c) the relative timing of deformation and granite emplacement in this area.

The rocks described were examined and sampled at several localities in south-eastern Nova Scotia, close to White Head Village (the granite - see Figure 1b) and approximately 4 km north of White Head (phyllites). The phyllites are thus found some 10 km south of the present surface trace of the Chedabucto Fault. In addition, outcrops of phyllites and highly deformed quartzofeldspathic rocks were studied

MARITIME SEDIMENTS AND ATLANTIC GEOLOGY
22, 51-64 (1986)

0711-1150/86/010051-14$3.10/0

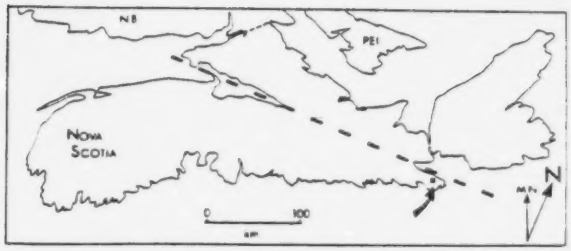

1a

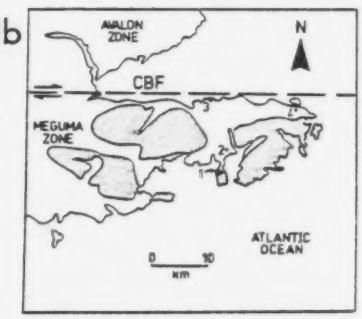

Figure 1: Location maps. 1a - Nova Scotia, showing approximate surface trace of Cobequid-Chedabucto Fault System (dashed line), and study area (arrowed square). 1b - eastern tip of Nova Scotia, showing approximate surface trace of Chedabucto Fault (dashed line). Numbers show locations of: 1 - White Head Village; 2 - transposed phyllite outcrops; 3 - Half Island Cove; 4 - Canso. Main granite bodies are stippled.

in a reconnaissance fashion at Half Island Cove, approximately 500 metres south of the present Chedabucto Fault surface trace, and at several localities between this cove and Canso to the east (Figure 1b).

With the exception of the coastal exposures, the phyllite and granite outcrops are glaciated and of limited areal extent, though sufficiently three-dimensional to allow structural analysis. After field study, oriented samples were collected and petrographic thin sections prepared, finely-ground to thicknesses of ca.25 μm for granite, and ca.10 μm for phyllites. Such very thin sections permit analysis of the microstructures of these fine-grained rocks, which are relatively uninformative and misleading in normal (30μm) thin sections. The sections were cut parallel to lineation and perpendicular to foliation (the monoclinic symmetry plane of deformation, essentially horizontal), and perpendicular to both lineation and foliation (essentially vertical).

GENERAL GEOLOGY

The Meguma Zone is a distinct lithological and tectonic entity within the Appalachian Orogen of North America, and is interpreted as African in origin, accreted to the North American craton prior to the opening of the present Atlantic Ocean (Schenk 1971, 1978). It is separated from the Avalon Zone to the north by a major steep-dipping to vertical dextral transcurrent zone of shearing, the Cobequid-Chedabucto Fault System (hereafter CCFS; Webb 1969). The Meguma Zone was first deformed during the Devonian Acadian Orogeny, as it was accreted. This was the time of formation of the CCFS and also the time of emplacement of numerous pre- to post-tectonic granitic intrusions, and regional metamorphism of generally low grade (Fyson 1966, Eisbacher 1970, Reynolds et al. 1973). Deformation due to the Carboniferous Hercynian Orogeny is considered important only along the Avalon-Meguma boundary (for example, Williams and Hatcher 1982). The present area lies within this belt, and suffered effects of both Acadian and Hercynian movements. Later movements of the CCFS during the Mesozoic led to the opening of the Bay of Fundy (for example, Keppie 1982). Thus the CCFS, as other major shear zones, has a complex and long-lived geological history.

Rocks occur along and both north and south of the CCFS trace which preserve evidence of this long deformational and metamorphic history. For example, mylonites occuring north of the Cobequid Fault trace formed solely by ductile deformation mechanisms. These mylonites were overprinted by transitional brittle fracturing and

faulting (Eisbacher 1970). The rocks described in this paper, which are found south of and close to the present trace of the Chedabucto Fault (the major eastern member of the CCFS - Figure 1b), show a similar complex developmental history.

The Meguma Zone is largely composed of rocks of the Meguma Group, a thick Cambrian - Lower Ordovician turbidite succession. This group is subdivided into two formations, the greywacke-rich, supposedly basal Goldenville Formation, and the slate/phyllite-rich, supposedly upper Halifax Formation, though these two formations may be complexly intercalated (Schenk 1976, 1978). The present study is concerned with phyllites, of various compositions, of the Halifax Formation, and their associated Acadian syntectonic granitic intrusions. The area covering the outcrops we have examined has been mapped at a scale of 1" to 1 mile by Stevenson (1964). In the area examined, the dominant foliation in both phyllites and granite is oriented approximately 078° and vertical, and the mineral elongation lineation on this foliation plunges shallowly east to horizontal. This is in accord with the data of Eisbacher (1970) gathered in the Cobequid Mountains along the CCFS to the west, and work of J.C. White (pers. commun., 1984) at Greville Bay even further west along the CCFS. These two studies plus the present work therefore sample almost the total lateral extent of exposed rocks affected by movement on the CCFS.

Major folds in the Meguma Terrane are upright or steeply inclined, and have esentially horizontal hinges at the macroscopic scale. At a finer scale the fold hinges are seen to be doubly plunging. Traces of the major fold hinges lie at a high angle to the CCFS trend in the southwestern part of the terrane, and curve smoothly towards coincidence with the CCFS trend in the north and east parts of the terrane (for example, Keppie 1979). This pattern has been explained as due to ductile reorientation of the major folds during the history of deformation which followed accretion of the terrane (Mawer 1984).

THE PHYLLITES

Mesostructural aspects

As mentioned above, phyllites were examined at several closely-spaced outcrops approximately 10 km south of the Chedabucto Fault. Several varieties of phyllite occur in these outcrops, mainly a fine-grained and occasionally porphyroblastic pelitic phyllite and a coarser-grained psammitic phyllite/schist. Intercalated with the pelitic phyllite are several very thin layers of coticule. Here we consider only the pelitic phyllite and associated coticule layers (coticules are thin, extensive, and laterally continuous layers composed of spessartine garnet and quartz, chlorite and minor amounts of several other minerals). They are interpreted as sedimentary in origin, probably volcaniclastic tuffs (Kramm 1976), and to have been deposited on oceanic crust or continental margin (Kennan and Kennedy, 1983). They are an excellent marker horizon in rocks such as the present phyllite, which often do not possess any indicators of bedding that survive deformation and metamorphism.

In outcrop, the phyllite exhibits a very well developed penetrative foliation. This is a transposed foliation (Hobbs et al. 1976, pp. 252-264); ellipsoidal pods of less deformed phyllite are occasionally found isolated within and intrafolial to this foliation. Internally, these included pods of phyllite are intricately folded (Figure 2a).

The transposed foliation is itself folded by open to tight metre-scale folds, and field evidence (fold vergence reversals and lithological patterns) indicates the existence of tens-of-metres-scale folds of bedding

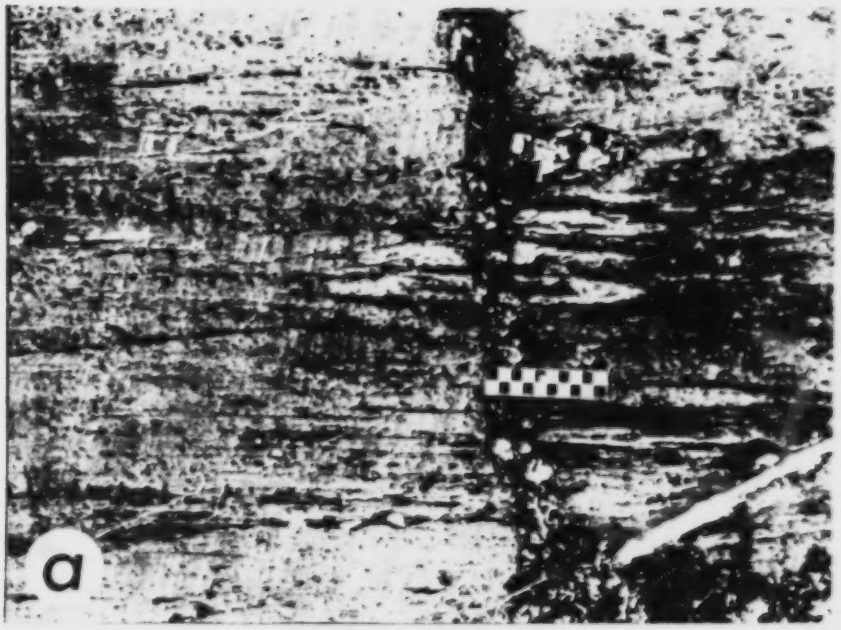
a

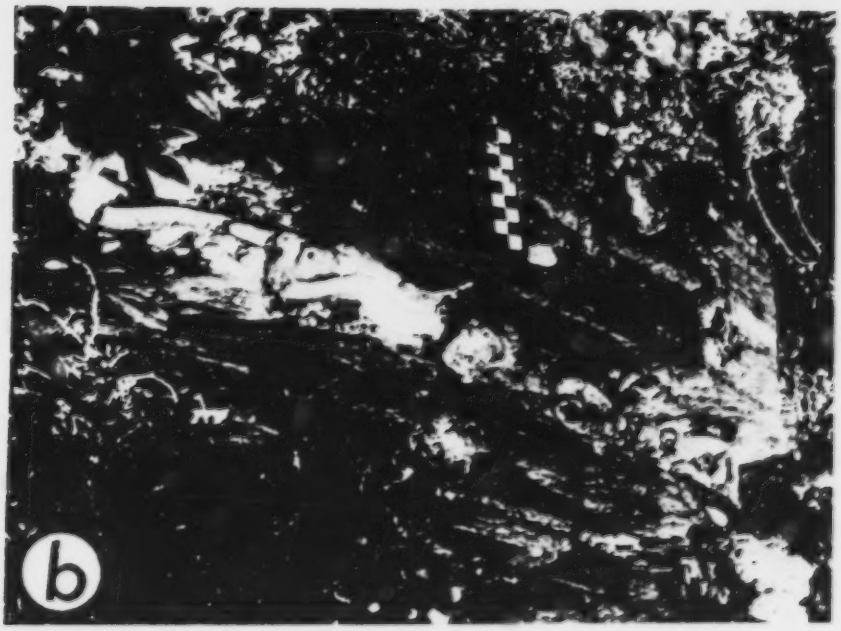
b

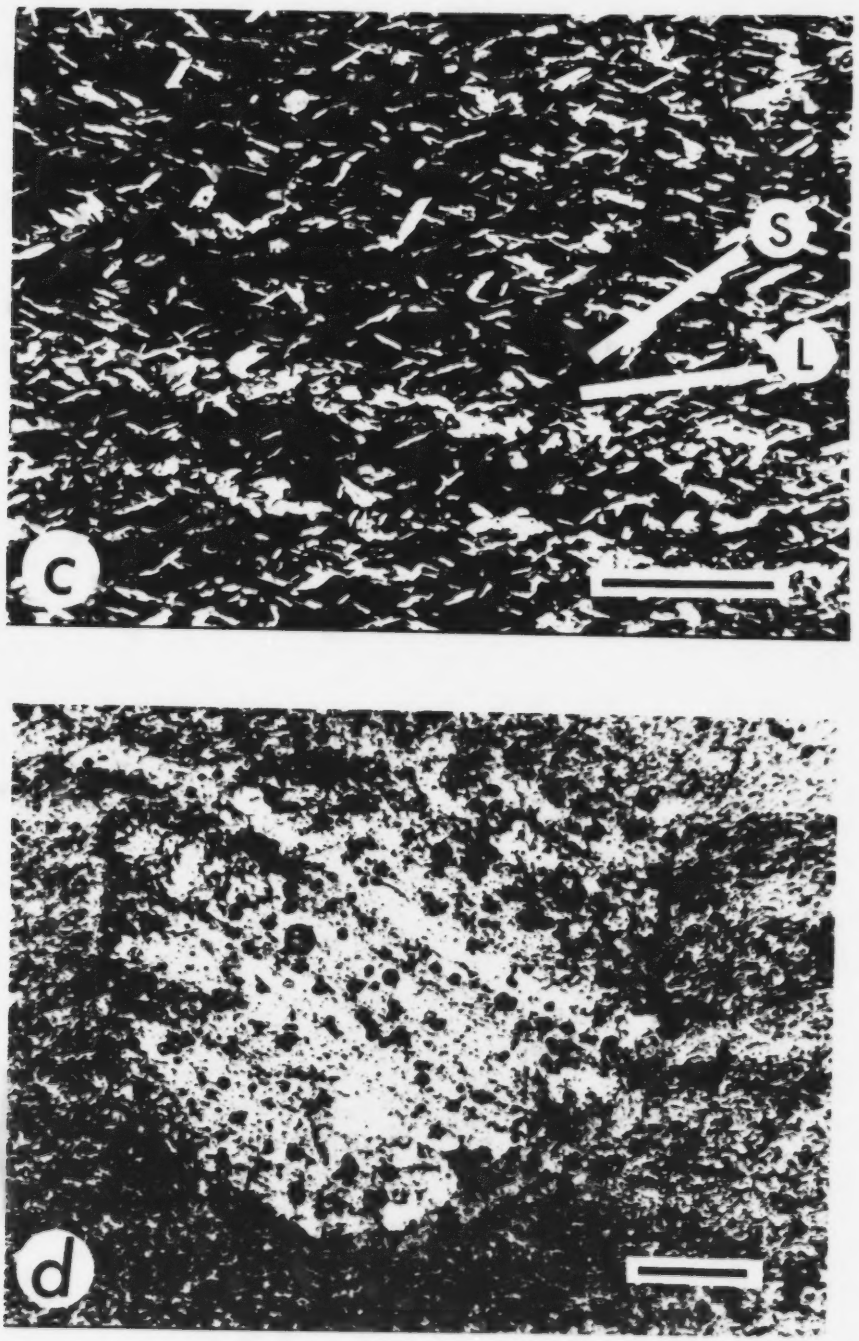

Figure 2: The transposed phyllite (Figure 1, location 2). North to top in all photographs. 2a - pod of strongly folded phyllite intrafolial to transposed foliation. Scale 10 cm long. 2b - folds of coticule layer in transposed phyllite. Scale 10 cm long. 2c - photomicrograph of kinked, transposed foliation, two dominant white mica orientations marked (L - long limb orientation, S - short limb orientation). Scale bar 200 um, NX. 2d - photomicrograph of rotated syntectonic cordierite porphyroblast. Scale bar 0.5 mm, PPL.

and transposed foliation. Outcrop was not sufficient to delineate these larger folds.

The transposition process is essentially one of rotation of pre-existing structural elements into parallelism by isoclinal folding. This is seen in the study area both on a mesoscopic scale (by folding of transposed foliation and coticule layers) and on a microscopic scale (by kinking of foliation-defining white mica - see below). In situations such as the present, with progressive non-coaxial straining of the rocks to large but unknown magnitudes of strain, and the added effect of cyclic dynamic recrystallization, this transposition produces what may be called a steady-state foliation (Means 1981). It is impossible to determine how many cycles of transposition the phyllite has undergone (cf. Williams 1983), and thus impossible to determine strain magnitudes in the phyllite.

Included coticule layers are strongly folded, and except on short limbs of larger folds, these minor folds have dextral vergence (Figure 2b). Prominent open metre-scale folds of the transposed foliation in a central outcrop also have dextral vergence. The coticule folds show a progressive sequence of development, with increasing dextral shear, from open and vertically plunging to isoclinal and horizontally plunging while remaining intrafolial to the transposed foliation.

Microstructure

In thin section, the phyllite is seen to consist mainly of well-aligned white mica and inequant quartz grains whose shapes are controlled by the mica. A subsidiary amount of equant albite is present, as is a few percent of opaques of two varieties (a very small, elongate type and a larger, equant type which often has quartz or quartz-chlorite pressure shadows). Chlorite-white mica stacks are common, and almost always have their basal plane trace at a high angle to the mica foliation. Most samples contain several percent of small idioblastic garnets, which are usually zoned with an inclusion-rich core and an inclusion-free rim. A small amount of fine grained, elongate, poikiloblastic andalusite occurs, as well as minor amounts of tourmaline and apatite. In layers of appropriate bulk composition, large pseudohexagonal or rounded highly poikiloblastic syntectonic cordierite crystals are found.

Close inspection of the mica foliation in very thin sections reveals that it is in fact defined by tightly kinked single white mica grains and aggregates of a few grains rather than simply well-aligned micas. The micas which define the kinks' long limbs are at a low angle to compositional layering, while the micas defining their short limbs are at a somewhat greater angle (Figure 2c); the kinks have dextral vergence. At an advanced state of kinking, the kinks become very tight and new white mica grows parallel to the kinks' axial surfaces. All stages of kink development are preserved in different small volumes of the phyllite, and early kinks can be redeformed at later times. This is due to the process of transposition, which nucleates at different places, and at different times, in the deforming rock mass, and is cyclic. Because of this spatial and temporal heterogeneity of development, and cyclic nature of the process, it is usual to get overprinting relationships in a progressively transposing body of rock, but they are formed during continued deformation rather than by discrete deformation events. These overprinting relationships can be on any scale, and can be very complex.

The cordierite porphyroblasts mentioned above overgrow the latest transposed foliation, preserving traces of the foliation internally. They are also rotated, again in a dextral sense, with respect to the foliation and hence are late syntectonic (Figure 2d). They are due to contact metamorphism

associated with granite intrusion, and as such offer proof that the granite was intruded syntectonically. W.K. Fyson (written commun., 1984) notes that cordierite and andalusite porphyroblasts occurring in numerous outcrops marginal to granites in this area show a consistent dextral sense of rotation.

THE GRANITE

Mesostructural aspects

Distant from its contact with the Halifax Formation phyllites, the granite appears to be undeformed (but see section (ii) below). It is pink and equigranular, and grain sizes of quartz, feldspars and micas average 0.5 cm or so. No evidence of primary structures, such as flow foliations, has been observed.

Approaching the phyllite contact, a very inhomogeneous style of deformation becomes evident. Its first manifestation is as rare, short, isolated, narrow (one to several mm) slightly curved shear zones. Towards the contact these narrow shear zones rapidly increase in number, length and planarity (though not in width), and become more closely spaced and quite periodic. They appear similar to the C surfaces (Berthe et al. 1979) often developed in mylonites at low strains, or the second transecting foliation sometimes developed in highly strained rocks with a pre-existing foliation (Vernon et al. 1983). It can be seen in the field and by optical microscopy (see section (ii) below) that in the present case the small shear zones develop progressively in unfoliated parent material, and that the apparently earlier gneissic foliation developed synchronously with them (Figure 3a). As deformation becomes more intense towards the phyllite contact, the angle between the two foliations decreases. This is an example of deformation partitioning (Lister and Williams 1983, Figure 5a), whereby alternating narrow layers of rock - the shear zones - deform by essentially progressive simple shearing (thereby effectively acting as surfaces of sliding), while the intra-shear-zone material deforms by essentially progressive pure shearing (shortening perpendicular to the shear zone boundaries and extending along their length). At the scale of the whole outcrop, though, the deformation of this granite mantle perhaps approximates to bulk progressive simple shearing.

The actural phyllite-granite contact is not exposed. At the closest granite outcrop, no more than a few metres from the contact, the narrow shear zones are very closely spaced and periodic (0.5 cm intervals) and pervasive throughout the rock. Individual shear zone widths are still approximately one mm.

Microstructure

The progressive microstructural development of the granite, from 'undeformed' parent material in the centre of the body to very inhomogeneously deformed material at the bodies' margin, considered together with the late syntectonic rotated cordierite porphyroblasts described above and the fact that the phyllite foliation is approximately parallel to the spaced shear zone foliation in the granite carapace and is not deflected by or wrapped around the granite body, indicates that the granite was emplaced syntectonically, and probably late, in the ductile deformation history of the host phyllites.

The 'undeformed' granite in thin section exhibits a wide range of ductile deformation microstructures. All minerals show moderate to strong undulose extinction, with quartz and both plagioclase and K-feldspar possessing well-developed subgrains. Plagioclase grains almost always have pervasive, fine, irregular, lenticular, mechanical polysynthetic twinning (Figure 3b). Both these deformation twins and the ubiquitous growth twins are often bent through a small angle.

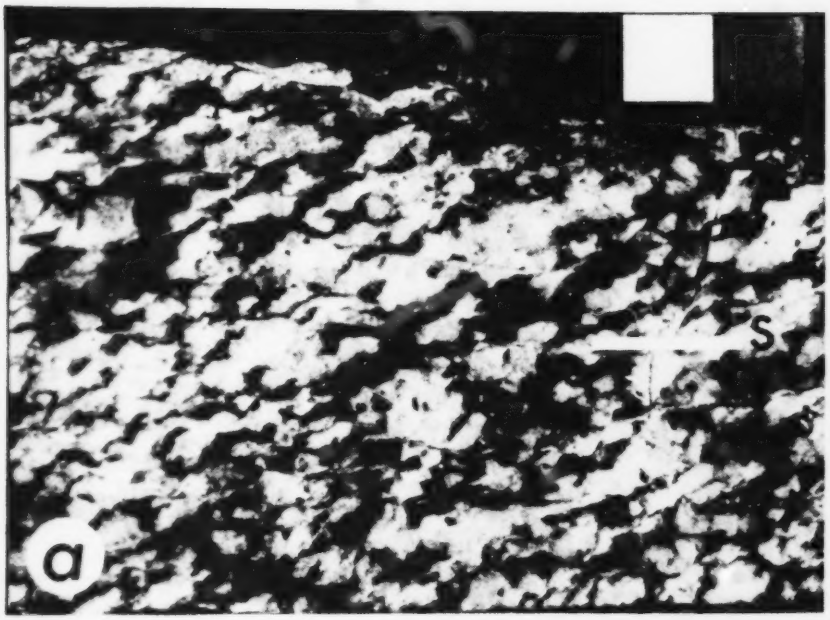
S
a

D
R
b

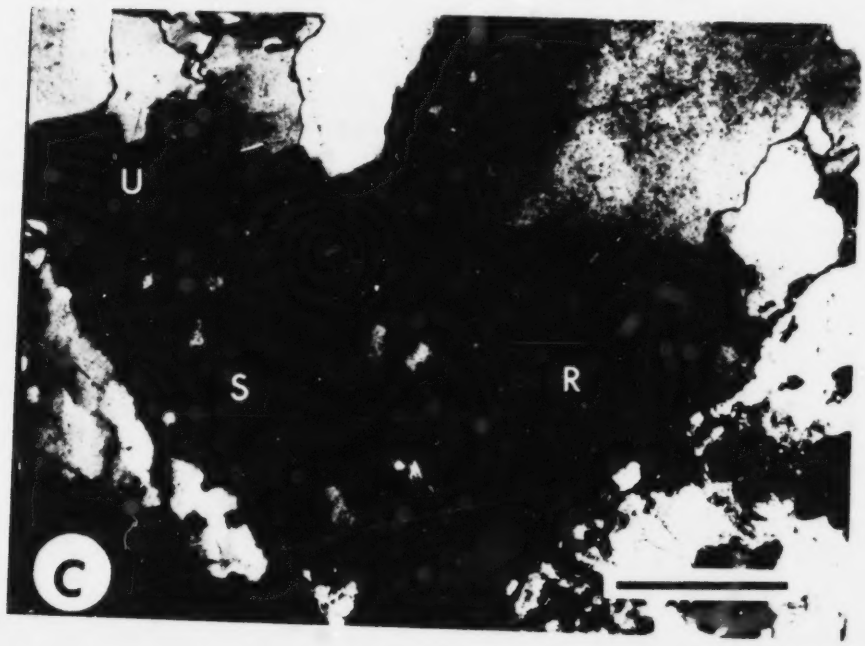

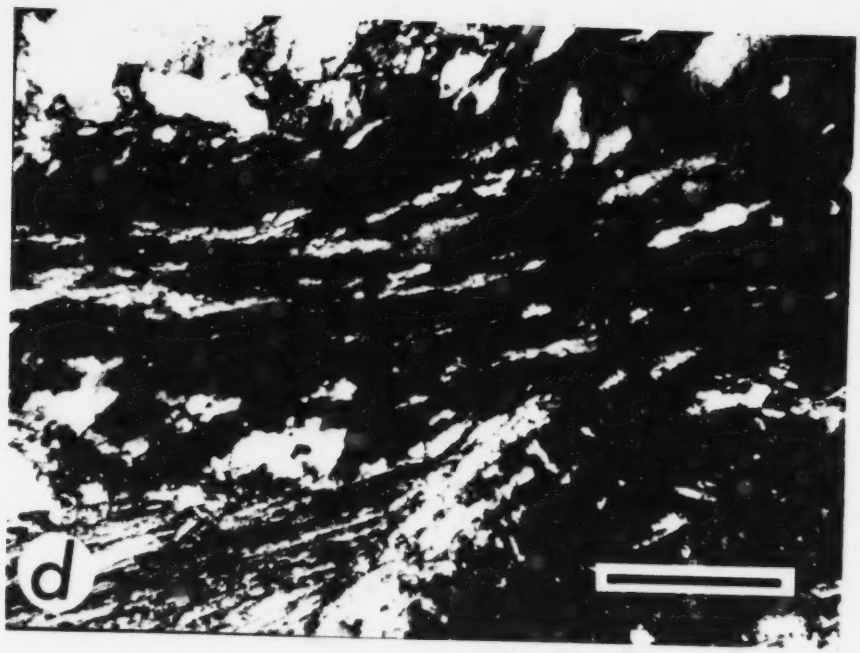

Figure 3: The granite (Figure 1, location 1). North to top in all photographs. 3a - slabbed specimen of foliated granite, shear zone foliation orientation marked S. Scale bar 2 cm. 3b - photomicrograph of plagioclase in 'undeformed' granite. Note irregular deformation twinning (D), subgrains and recrystallization along grain boundary (R). Scale bar 300 um, NX. 3c - photomicrograph of quartz in 'undeformed' granite. Note undulose extinction (U), subgrains (S), finer recrystallization along strongly sutured grain boundaries (R). Scale bar 300 um, NX. 3d - photomicrograph of quartz in shear zone foliation, same specimen as 3a. Scale bar 300 um, NX.

K-feldspar grains are microperthitic, and have pronounced but inhomogeneously developed microcline tartan twinning. K-feldspar also occasionally has minor recrystallization along grain boundaries. What appear to be original single quartz grains in hand specimen are seen in thin section to be aggregates of irregular grains with lobate and interlocking grain boundaries. Along many of these boundaries there is finer recrystallization, the new grains being inequant and showing undulose extinction (Figure 3c). Biotite and muscovite grains are generally slightly bent and have a shredded appearance due to irregularly oriented finer grains at crystal margins.

Deformation of all minerals, especially quartz and the micas, becomes more intense and markedly inhomogeneous as the granite foliation develops. In the foliated material, the foliation planes (the small shear zones) are usually defined by elongate aggregates of ribbon quartz which has often dynamically recrystallized (Figure 3d), and fine dynamically recrystallized layers of quartz and mica. That the minerals have recrystallized dynamically is shown by their fine grain size and weak undulose extinction when compared to the non-recrystallized grains, their weakly serrated or irregular grain boundaries, their slight (quartz) to moderate (mica) elongation subparallel to the small shear zones, and their pronounced crystallographic preferred orientation. All minerals in intra-shear-zone layers are very strongly deformed, both sorts of feldspars being partly recrystallized around grain margins, both types of micas being strongly bent and occasionally kinked, and original quartz grains now completely recrystallized and elongate.

All microstructural features indicate a dextral sense of shear.

LATE QUARTZ VEINS

Veins of different ages and differing mineralogical composition are found everywhere in the phyllites of the present area. At least five distinct, overprinting generations of vein types are observed; their mineralogy and structural development is the subject of a separate study. Briefly, the geological history of all types is consistent with the argument of long-lived dextral transcurrent shear in the region.

Ubiquitous in the pelitic phyllites is a family of quartz veins, of various (closely spaced) relative ages, various thicknesses and various mesoscopic structural styles. These are the latest structure, apart from joints, in the study area and as such overprint all phyllite (and granite) microstructures and earlier vein types. These veins become so numerous and so pervasive that they constitute a distinct foliation in places (a further, later foliation developed in the pelitic phyllite along the margins of thicker veins is discussed briefly below). This section will consider only these latest quartz veins.

The approximate mean trend of these latest veins is 052°, whereas that of the transposed foliation is 078° (the Chedabucto Fault trends E-W). The veins formed in tensile fractures oriented in the usual way - approximately parallel to the bulk principal compressive stress direction - probably by hydraulic fracturing, and were then rotated in a clockwise fashion by continued dextral shearing. All veins are rotated to a greater or lesser extent. All veins show mesoscopic evidence of considerable ductile deformation (for example folding, boudinage, et cetera) and all possess well-developed ductile deformation microstructures, such as subgrains, dynamically recrystallized grains, and so on. These latest quartz veins are of several different but closely-spaced ages, as some have been rotated slightly more, others slightly less, than the mean trend; those that have been rotated more than this mean trend are cut by those rotated less,

and hence are earlier.

Many of the mesoscopic structures in these veins appear to indicate a sinistral shear sense on cursory examination. In fact, all structures can be demonstrated to be formed during progressive dextral shear, and accommodated by ductile mechanisms. We will illustrate and discuss several of these structures below.

Extensional structures

All veins except those with a small length-to-width ratio show evidence of extension parallel to their length. Thick veins (5-10 cm) are boudinaged or have well-developed low amplitude pinch-and-swell, with a wavelength similar to that of boudin length - about five times vein thickness. Veins of moderate thickness (1-3 cm) have low amplitude pinch-and-swell, the wavelength of which is variable but generally about seven to ten times vein thickness. Thin veins (3-5 mm) show very low amplitude pinch-and-swell with wavelengths of about ten or several tens of centimetres which is about twenty to sixty times vein thickness. Also, small shear zones (similar geometry to 'shear bands', White et al. 1980) occasionally transect veins or vein boudins, and have a dextral sense of shear offset.

These extensional structures originated as the veins rotated into and through the extensional segment of the incremental strain ellipsoid for progressive simple shearing (Hobbs et al. 1976, p. 48), following an initial period of shortening. During this earlier period of shortening, the veins may have thickened or folded somewhat, and unfolded as they rotated into and through the extensional segment. W.K. Fyson (written commun., 1984) notes that in other places in the Meguma Terrane, quartz veins are found which lie axial planar to dextral kinks, and which are sometimes boudinaged. He suggests that veins such as are illustrated in Figures 4b and 5a could have formed in this

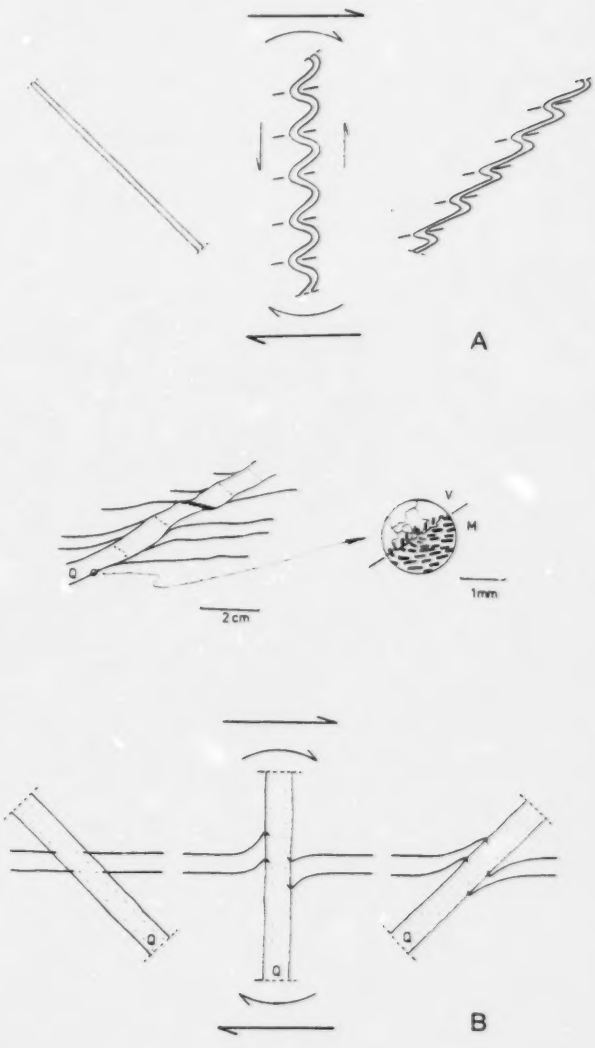

Figure 4: Diagrams of structures in latest quartz veins. 4a - model of forming sinistral-verging folds in a dextral progressive simple shear environment. 4b - top part shows sketch of slabbed specimen and part of thin section of same specimen. Note deflection of transposed foliation at vein margins. In sketch of slabbed specimen, a small shear zone is shown by the oblique ruling, and several joints by the dashed lines which traverse the vein. In sketch of thin section, note folding of transposed foliation at vein margin; V indicates vein, M indicates phyllite matrix. Individual mica grains are shown by the black bars. Lower part of figure shows the model for forming deflected foliation by dextral progressive simple shearing.

manner, mostly obscuring the kink short limb. Some of the veins we have examined may have formed in this way; as we see no remnants of kink short limbs associated with these veins, this would require that the veins consistently obliterate the entire short limb of each kink, or that the short limb remnants are destroyed by further ductile deformation.

Folds

A number of veins are folded, and the small folds possess sinistral vergence. These can be explained by antithetic shearing across the vein during rotation; the process is illustrated in Figure 4a. Some of these folded veins show pinch-and-swell, indicating extension along their length, superimposed on the earlier folds.

Deflection of foliation

Along the margins of most veins, the transposed foliation is deflected in a fashion expected from sinistral shearing across the vein (Figure 4b). Furthermore, in thin section, mica grains of the transposed foliation are observed to be overgrown in places by the quartz of the vein - see top right of Figure 4b - so that the foliation trace is folded through a large angle at the vein margin. Both features are due to rotation of the veins during progessive dextral shearing (lower part of Figure 4b).

One further important feature is the new foliation developed along the margins of some veins, especially those with small length-to-width ratios. This foliation is due to crenulation of the transposed foliation, and is in fact a differentiated crenulation cleavage (see feature 6, Figure 5a). It is a product of antithetic shearing which occurred along the quartz vein margins as they were rotated during the progressive dextral shearing history (Figure 4). As shown in Figure 5a, it is in essentially conjugate relationship to small shear zones developed in the quartz veins. Thus,

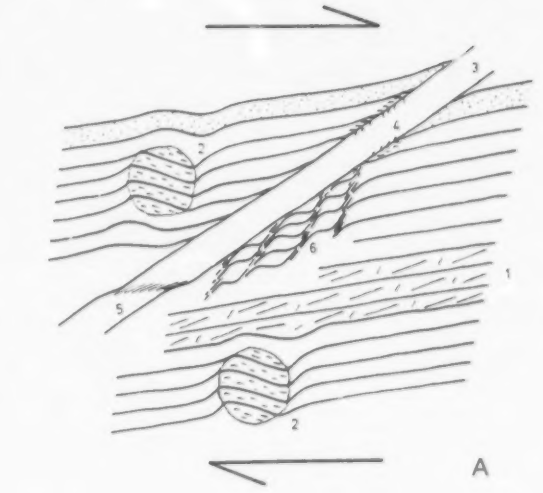

Figure 5: Summary. 5a - composite diagram of microstructural shear asymmetry indicators in transposed phyllite. Numbers are: 1 - dominant orientations of limbs of asymmetric kinks of white mica (see Figure 2c); 2 - rotated syntectonic cordierite porphyroblasts; 3 - quartz vein; 4 - deflected and partly overgrown transposed foliation at quartz vein margin; 5 - small shear zone in quartz vein; 6 - differentiated crenulation cleavage at vein margin. 5b - deformation history of study area. Time axis is non-linear.

in summary, all structural features associated with these latest quartz veins indicate a continuation of the progressive dextral shearing deformation history, and all features are accommodated by ductile mechanisms.

DISCUSSION AND CONCLUSIONS

The various microstructural features of the transposed pelitic phyllite which indicate a deformation history of

progressive, long-lasting dextral transcurrent shear over the study area are summarized in Figure 5a. Together with the mesostructural indicators discussed previously (folds in coticule layers, shear zones developed in syntectonic granite, various structures defined by quartz veins), they offer evidence of movement sense along the CCFS covering much of its history. Furthermore, latest brittle structures such as faults and joints which overprint all earlier structures, from almost the total exposed length of rocks affected by movement on the CCFS (Eisbacher 1970, J.C. White, pers. commun., 1984, unpublished results of the present authors from along the SE coast of Chedabucto Bay), also indicate a continued dextral sense of displacement.

It has been shown that the various mesoscopic and microscopic structures which are found in the granite, the pelitic phyllite and the latest quartz veins, have been formed by (or in the case of vein rotation, accommodated by) ductile deformation mechanisms. Evidence for dislocation mechanisms exists in the form of dynamic recovery (which causes subgrain development) and dynamic recrystallization in quartz, K-feldspar and plagioclase feldspar, deformation-induced twinning in K-feldspar and plagioclase feldspar, bending and kinking of the crystal lattice in biotite and muscovite micas, and ubiquitous undulose extinction of all minerals. Evidence for diffusion mechanisms occurs in the form of quartz and quartz-chlorite pressure shadows on opaque mineral grains and the formation of a differentiated crenulation cleavage at vein margins following their rotation through large angles. Therefore, ductile deformation mechanisms were operative throughout and up until the latest stages of the history of the rocks.

The granite body within the study area was emplaced syntectonically, probably fairly late in the history of the host phyllites. This is shown by the formation, due to contact metamorphic effects, of cordierite porphyroblasts in the surrounding phyllite, which overgrow the latest transposed foliation and are themselves rotated; by the fact that the phyllite foliation is approximately parallel to that developed in the granite mantle and is not deflected by the granite body; and by the progressively increasing intensity of deformation from slightly deformed core to strongly and inhomogeneously deformed mantle of the body.

The proposed structural history of the present area is summarized in Figure 5b. The time axis is non-linear. The bulk deformation of the studied area can be divided into that occurring in three subsystems, those of the phyllite, the granite and the quartz veins. Figure 5b shows this subdivision, and emphasises that the deformation effects in each subsystem develop together through time, as each subsystem is interrelated with the others. Thus, the phyllite began deforming upon accretion of the Meguma Terrane, and continued deforming until the latest stages of ductile deformation. Early-formed foliations were transposed and their component grains recrystallised, and folds were generated, rotated, tightened and refolded. During this ductile deformation history (and, it is argued previously, late in this history) the granite intruded the phyllites and was deformed with deformation concentrated at the margin of the cooling body. Subsequent to granite intrusion and some deformation, quartz veins were formed. These cut all earlier structures in the phyllite and the granite, and are themselves deformed by ductile mechanisms. Significant ductile deformation in the granite ceased (the box "granite 'locks up'" on Figure 5b), though deformation in the phyllite and its quartz veins continued. Finally, ductile deformation in the whole system ceased. It does not seem useful to attempt to separate 'Acadian' deformation from 'Hercynian' deformation (cf. Williams and Hatcher 1982) in this area, as

structural evidence is compatible with a single progressive deformation history rather than one which is episodic.

ACKNOWLEDGEMENTS

We thank Bill Fyson (University of Ottawa) and Jack Henderson (Geological Survey of Canada) for reviews and comments.

BERTHE, D., CHOUKROUNE, P., and GAPAIS, D. 1979. Orientations preferentielles du quartz et orthogneissification progressive en regime cisaillant: l'example du cisaillement sud-amoricain. Bulletin Minéralogie, 102, pp. 265-272.

EISBACHER, G.H. 1970. Deformation mechanisms of mylonitic rocks and fractured granites in Cobequid Mountains, Nova Scotia, Canada. Geological Society of America Bulletin, 81, pp. 2009-2020.

FYSON, W.K. 1966. Structures in the Lower Palaeozoic Meguma Group, Nova Scotia. Geological Society of America Bulletin, 77, pp. 931-944.

HOBBS, B.E., MEANS, W.D., and WILLIAMS, P.F. 1976. An Outline of Structural Geology. John Wiley and Sons, Inc., 571 pp.

KENNAN, P.S., and KENNEDY, M. J. 1983. Coticules - a key to correlation along the Appalachian-Caledonian Orogen? In 'Regional Trends In The Geology Of The Appalachian-Caladonian-Hercynian-Mauritanide Orogen', ed. P.E. Schenk, pp. 355-361.

KEPPIE, J. D. 1979. Geological Map of Nova Scotia, 1:500,000 scale. Nova Scotia Department of Mines and Energy.

KEPPIE, J.D. 1982. The Minas Geofracture. In 'Major Structural Zones and Faults of the Northern Appalachians', ed. p. St. -Julien and J. Beland, Geological Association Of Canada, Special Paper24, pp. 263-280.

KRAMM, U. 1976. The coticule rocks (spessartine quartzites) of the Venn-Stavelot Massif, Ardennes, a volcanoclastic metasediment? Contributions to Mineralogy & Petrology, 56, pp. 135-155.

LISTER, G.S., and WILLIAMS, P.F. 1983. The partitioning of deformation in flowing rock masses. Tectonophysics, 92, pp. 1-33

MAWER, C.K. 1984. The Meguma Terrane Shear Zone. 4th Annual Canadian Teotonics Group Meeting, Program with Abstracts, p. 21.

MEANS, W.D. 1981. The concept of steady-state foliation. Tectonophysics, 78, pp. 179-199.

REYNOLDS, P.H., KUBLICK, E.E., and MUECKE, G.K. 1973. Potassium-argon dating of slates from the Meguma Group, Nova Scotia. Canadian Journal of Earth Sciences, 10, pp. 1059-1067.

SCHENK, P.E. 1971. Southeastern Atlantic Canada, northwestern Africa, and continental drift. Canadian Journal of Earth Sciences, 8, pp. 1218-1251.

SCHENK, P.E. 1976. A regional synthesis (of Nova Scotia geology). Maritime Sediments, 11, pp. 17-24.

SCHENK, P.E. 1978. Synthesis of the Canadian Appalachians. Geological Survey of Canada, Paper 78-13, pp. 111-136.

STEVENSON, I.M. 1964. Chedabucto Bay, 1" to 1 mile geological map sheet. Map 1156A, Geological Survey of Canada.

VERNON, R.H., WILLIAMS, V.A. and D'ARCY, W.F. 1983. Grain-size reduction and foliation development in a deformed granitoid batholith. Techonophysics, 92, pp. 123-145.

WEBB, G.W. 1969. Paleozoic wrench faults in Canadian Appalachians. In 'North Atlantic Geology and Continental Dritt'. ed. M. Kay, American Association of Petroleum Geologists, Memoir 12, pp. 754-786.

WILLIAMS, H., and HATCHER, JR., R.D. 1982. Suspect terranes and accretionary history of the Appalachian orogen. Geology, 10, pp. 530-536.

WILLIAMS, P.F. 1983. Large scale transposition by folding in northern Norway. Geologic Rundschau, 72, pp. 589-604.

Maritime Sediments and Atlantic Geology

Vol. 22 April, 1986 No. 1

A Stratabound Zinc-Lead Deposit in Meguma Group Metasediments at Eastville, Nova Scotia

W.P. Binney, Falconbridge Ltd.
P.O. Box 1140, Timmins, Ontario P4N 7H9

K.A. Jenner, Gulf Canada Resources Inc., Coal Division
401 9th Ave. S.W., Calgary, Alberta T2P 2H7

A.L. Sangster, Geological Survey of Canada
Ottawa, Ontario K1A 0E8

M. Zentilli, Department of Geology
Dalhousie University, Halifax, Nova Scotia B3H 3J5

The Eastville zinc-lead deposit, discovered by soil sampling in 1976, occurs near the contact of the Goldenville and Halifax Formations, the two divisions of the Cambro-Ordovician Meguma Group. The stratigraphic succession in the contact zone comprises an assemblage of quartz metawacke, calcareous quartz metawacke and slate. Quartz metawacke is predominant in the Goldenville Formation and slate is the dominant lithology in the overlying Halifax Formation. These rocks are interpreted as the middle to outer fan and basin plain deposits of a submarine fan complex. Pyrrhotite and pyrite, the predominant sulphide minerals in all lithologies in the contact zone, were deposited by reduction of iron in the sediments, independent of the mineralizing process.

Sphalerite and galena occur in rocks over a 10 km strike length in elongate blebs, 2 to 5 mm long, distributed parallel to bedding and in cross-cutting fractures. The deposit is stratabound and generally occurs in black slate beds near the Goldenville-Halifax contact. Geochemical analyses of the rocks have indicated a concentration of Mn in the calcareous quartzite member, the upper unit of the Goldenville Formation. A relationship between the Mn enrichment and the abundance of sphalerite and galena in the section has not been established. The sulphide mineralogy, laterally continuous stratigraphy and lack of metal zonation and underlying feeder structures indicate the sphalerite and galena were syngenetically deposited from metal-rich brines at a site distant from where the brines entered the basin of deposition.

Le dépot de plomb et de zinc de Eastville, qui a été découvert par des prises d'échantillons de terre en 1976, est situé près du contact des formations Goldenville et Halifax (les deux unites du groupe Meguma). La succession stratigraphique dans la zone de contact est constitué d'un assemblage de métagrauwacke de quartz, de métagrauwacke calcaire de quartz, et d'ardoise. Le métagrauwacke de quartz est prédominant dans la formation Goldenville et l'ardoise est la lithologie dominate de la formation de Halifax, qui est superposé sur la premiére. Ces roches sont expliquées comme étant le cône central ou exterieur et des dépots de la plaine d'un basin d'un complexe de cône. La pyrrhotite et la pyrite, les mineraux sulfides principaux dans toutes les lithologies de la zone de contact, ont été déposés par une réduction de fer dans les sédiments, indépendement des processus de minéralisation.

La sphalérite et la galène se trouvent dans les roches sur une longueur de 10 kilométres le long de la couche en temps que soufflures de 2 à 5 mm de longueur, réparties paralléllement à la couche et dans les fractures à trafers banc. Le dépot est limité aux strates et se trouve en général dans de l'ardoise noire prés du contact Goldenville-Halifax. Des analyses géochimiques des roches ont indiqué une concentration de Mn dans les quartzites calcaires, l'unité la plus élevé de la formation Goldenville. Un rapport entre l'enrichissement en Mn et l'abondance de la sphalérite et de la galène dans la section, n'a pas été établie. La minéralogie des sulfides, la stratigraphie latérale continue, et le manque de zonation de métaux et de structures de conduite d'alimentation, indique que la sphalérite et la galéne ont été déposées sygénétiquement à partir de saumures riches en métaux dans un site éloigné de l'endroit où les saumures pénètrent le basin de dépot.

MARITIME SEDIMENTS AND ATLANTIC GEOLOGY
22, 65-88 (1986)

0711-1150/86/010065-24$4.60/0

INTRODUCTION

The Eastville deposit, discovered by St. Joseph Explorations Limited in 1976, represents the first reported occurrence of extensive zinc and lead sulphides in the Meguma Group metasedimentary rocks of Nova Scotia. The Cambro-Ordovician Meguma Group underlies a large area of Nova Scotia south of the Glooscap Fault. It comprises a thick (up to 14 km) assemblage of quartz metawacke turbidites interstratified with black slate. The basal half (Goldenville Formation) is mainly thick sandy turbidites; the upper half (Halifax Formation) is mainly black slate (Schenk, 1978). At Eastville, sphalerite and galena occur in stratabound disseminations and in small cross-cutting veinlets within 100 m of the contact of the Goldenville and Halifax Formations. The deposit is located between latitude 45 15'30" and longitude 62 52'30" on the west to latitude 45 17'45" and longitude 62 44'30" on the east within map area NTS 11E7. The deposit is accessible by a good quality gravel road from Eastville in the Stewiacke River valley.

This paper describes the lithology and stratigraphy of the Meguma Group in the Eastville area and the occurrence and distribution of sulphides and selected elements. An account of the exploration history of the deposit is presented and exploration guidelines for similar deposits are suggested.

The Eastville area was originally mapped by H. Fletcher and E.R. Faribault (1902) at a scale of 1:63,360. The lack of access, low relief and few outcrops in the eastern part of the area hampered accurate mapping. Benson (1967) remapped the area, placing most of the rocks southeast of Eastville in the Goldenville Formation of the Meguma Group. More recent mapping by Binney at a scale of 1:10,000 used a network of logging roads for access and the results of diamond drilling and geophysical surveys in areas of poor outcrop to determine the extent of the Goldenville and Halifax Formations (Figure 1). This work has confirmed much of Fletcher and Faribault's early mapping.

The only previous exploration activity in the Meguma Group rocks of the area prior to 1976 was assessment of the potential for gold mineralization in the quartz veins exposed on Fulton and Cox Brooks.

EXPLORATION HISTORY

The zinc-lead deposit, located immediately south and east of Eastville, Colchester County, was discovered in 1976 during exploration for gold in regional structures cutting the Meguma Group. A significant AFMAG (electromagnetic) anomaly has been noted on Geological Survey of Canada map 762G (1960) and this anomaly was thought to represent a regional fault. No previous exploration work was recorded for the area when St. Joseph Explorations Limited undertook a reconnaissance soil sampling program. Initially, in addition to gold, analyses for copper, lead and zinc were carried out for samples taken every 30 m on lines spaced one kilometre apart along strike. The initial two sample lines included lead values in excess of 1,000 ppm delineating the rough shape of a west-trending anomaly coincident with the contact of the Goldenville and Halifax Formations. Anomalous gold values were not detected. The area was staked by St. Joseph Explorations Limited and has been held since 1981 by a successor company, Sulpetro Minerals Limited.

The unrecorded presence of significant zinc and lead occurrences in the metasedimentary rocks of the Meguma Group resulted in a cautious program of exploration with B-horizon soil sampling and an electromagnetic survey (Crone CEM) on widely-spaced, uncut lines. A strong electromagnetic anomaly was located over the length of the claim group and strong geochemical

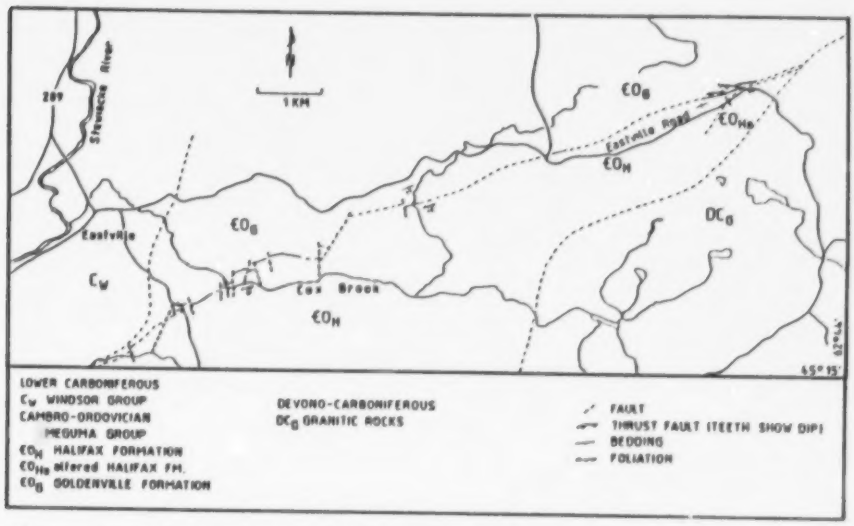

Figure 1 - Geological map of the Eastville area of Nova Scotia.

anomalies for lead and zinc were delineated in two areas coincident with the electromagnetic anomaly. As a result of these data three shallow holes were diamond drilled in 1977. Black graphitic slate was encountered at the base of the Halifax Formation, which explained the electromagnetic anomaly. Detailed examination of the drill core from the contact zone of the Goldenville and Halifax Formations revealed fine grained sphalerite and galena. Recovery of drill core was poor in hole 1 but chips recovered from a 7.0 m section assayed 3.26 per cent combined zinc-lead. Drill hole 2 included a 14.9 m section with a combined zinc-lead grade of 1.32 per cent. Hole 3 was drilled on a geochemical anomaly with no coincident electromagnetic anomaly and was completely within barren quartz metawacke of the Goldenville Formation.

Once the presence of mineralization was established a more ambitious exploration program was initiated. Grids were cut over the major geochemical anomalies with lines spaced 100 m apart. A total-field magnetic survey, horizontal-loop electromagnetic survey (Max-Min II) and detailed soil sampling were carried out along all cut lines. The geophysical surveys provided information on the location of the graphitic slate at the base of the Halifax Formation, essential for stratigraphic control of diamond drilling. Soil geochemistry outlined areas of potential zinc and lead sulphides along the Goldenville-Halifax contact. Concurrent with the geophysics and soil sampling, an orientation survey of organic-bank stream sampling was undertaken to assess the practicality of this method in regional data collection. Anomalous lead and zinc results were obtained in highly organic samples up to 1 km downstream from the mineralized area.

Between 1977 and 1982, twenty-eight diamond drill holes between 30 m and 260 m long were used to explore the Eastville deposit. Early drill holes were concentrated in areas where geochemical anomalies were coincident with the Goldenville-Halifax contact as located by geophysical surveys. Later drilling included: 1) deeper holes to test the rocks below better mineralized sections, and 2) systematic drilling of holes to examine the zinc-lead content of rocks along the length of the Goldenville-Halifax contact. Not all drill holes containing sphalerite and galena coincide with geochemical anomalies. Drilling was monitored continuously with sludge samples analysed for zinc and lead. The

analytical results were used to confirm the assay sections chosen on the basis of visual examination of the drill core.

In 1980, a program of overburden drilling and drill core analysis was completed in an effort to outline geochemical trends which might indicate untested areas of potential mineralization. Some of the analytical results are presented in this paper. The till drilling data reflect the element abundances in the underlying rocks but no new areas of mineralization were detected.

The exploration work to date has failed to outline an economic deposit of zinc and lead. Most drill holes include 2 m to 10 m sections of 1 to 3 per cent combined zinc-lead at various stratigraphic positions. Drill holes with the better grades include hole 7 with 3.34 per cent combined zinc-lead over 6.1 m of black slate and hole 28 with 4.09 per cent combined zinc-lead over 9.33 m in fault gouge at the contact between the Goldenville and Halifax Formations. The property remains of interest for base metal exploration and represents a new type of occurrence in Meguma Group metasediments.

GENERAL GEOLOGY

Low relief and bogland in the Eastville area result in poor exposures of the rock units and their contact relationships. Only in the deeply incised valleys of Fulton Brook and Cox Brook with its tributary Little Brook, are there extensive outcrops of the Meguma Group rocks (Fig. 1). The distribution of rock units shown in Figure 1, and in detail in Figures 2 and 3, is based primarily on drill results and geophysical survey.

The oldest rocks exposed in the Eastville area are massive quartz metawacke and minor interbedded slate (Fig. 4) of the Cambro-Ordovician Goldenville Formation, the basal member of the Meguma Group (Fig. 1, 2, 3). This formation is in fault contact with younger Carboniferous clastic sedimentary rocks to the north. The base of the formation is not exposed at Eastville or at other locations in Nova Scotia. Benson (1967) measured a 700 m stratigraphic section of Goldenville Formation rocks on Cox Brook. He noted that regionally a stratigraphic thickness of up to 5,400 m of the formation is recognized.

The Goldenville Formation is overlain to the south by the Halifax Formation, the upper unit of the Meguma Group. Slate, argillite and interbedded quartz metawacke and metasiltstone form the Halifax Formation in the Eastville area where it exceeds 2,000 m thickness (Fig. 1 and 5). The slate is locally graphitic, and pyrrhotite and pyrite are common throughout. At Eastville, sphalerite and galena occur near the contact of the Goldenville and Halifax Formations.

The rocks of the Meguma Group are truncated by a Devono-Carboniferous intrusion to the east (Fig. 1 and 3). Granodiorite and granite are recognized as two phases of this pluton. North of the intrusion the slates of the Halifax Formation show effects of contact metamorphism with the development of secondary biotite, almandine garnet and andalusite crystals as much as 1.5 cm across. Light grey to white, chlorite-blotched, muscovite schist occurs in the immediate contact area of the intrusion. In some drill sections mineral segregation and gneissic textures have been developed.

South and west of Eastville (Fig. 1 and 2) the Goldenville Formation and the contact zone with the Halifax Formation are unconformably overlain by the lower Carboniferous Windsor Group. Within the mapped area the group comprises a basal limonite-cemented, quartz metawacke clast conglomerate overlain by limestone, red siltstone and thick gypsum beds.

The Eastville area is on the north

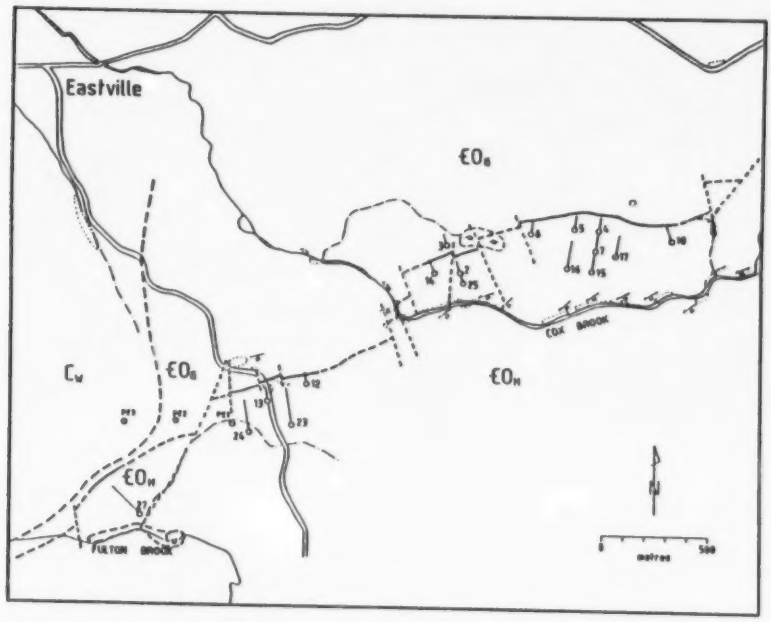

Figure 2 - Map of the weatern part of the Eastville zinc-lead deposit showing geology and diamond drill locations. Drill holes prefixed PE are vertical holes for exploration of the Carboniferous basal Windsor Limestone. Holes with no prefix were drilled by St. Joseph Explorations Ltd./Sulpetro Minerals Ltd. for exploration of the Eastville zinc-lead deposit. For an explanation of rock divisions and symbols refer to Figure 1.

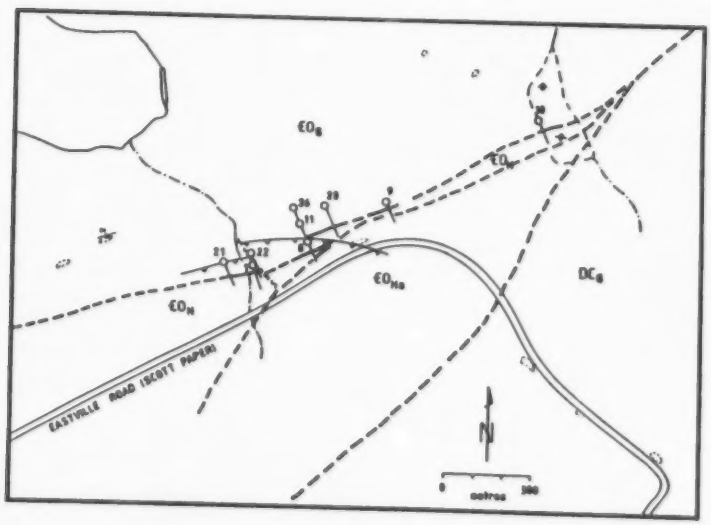

Figure 3 - Map of the eastern part of the Eastville zinc-lead deposit showing geology and diamond drill hole locations. All holes were drilled by St. Joseph Explorations Ltd./Sulpetro Minerals Ltd. For an explanation of rock divisions and symbols refer to Figure 1.

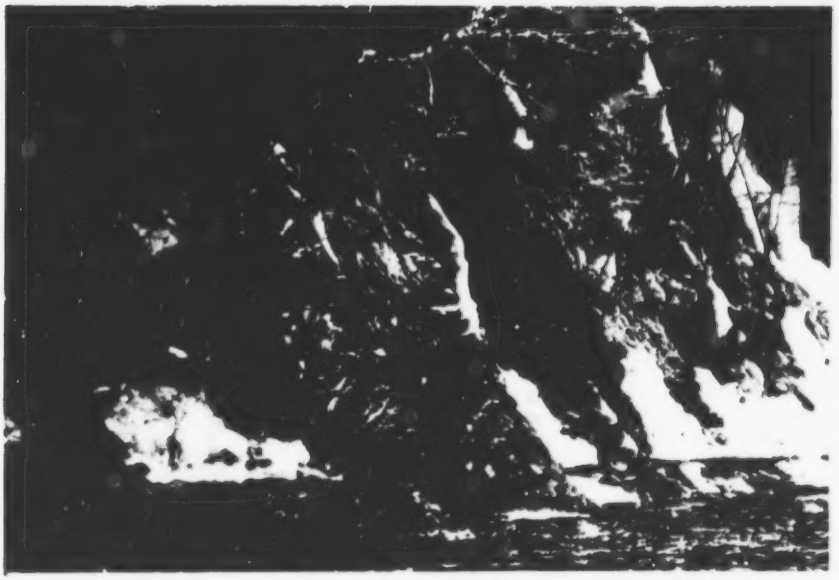

Figure 4 - Massive quartz metawacke beds of the Goldenville Formation exposed on Cox Brook. Bedding is outlined by partings and weathered argillaceous interbeds.

limb of a large east-northeasterly-trending syncline in the Meguma Group. The contact of the Goldenville and Halifax formations dips 45 to 80 degrees south in the western exposures (Fig.2). To the east the angle of dip increases to 90 degrees and locally the rocks are overturned and dip north (Fig. 3).

Two sets of steeply-dipping faults cut the contact. The first set comprises faults trending about 160 degrees which offset the Goldenville-Halifax contact from 10 to 150 m. Offsets on most faults are left lateral. Larger offsets of 200 m to greater than 500 m occur along the second set of faults trending 010 to 030 degrees (Fig. 1 and 2). In the eastern area of closer spaced drill holes (Fig. 3), a low angle thrust fault forms the boundary of a normal stratigraphic succession to the west and a sheared contact between the Goldenville and Halifax Formations to the east. In the sheared contact area at least 20 m of the section is absent as a result of a fault sub-parallel to the Goldenville-Halifax contact. The juxtaposition of the two types of contact and the continuation of the metamorphic aureole from one side of the thrust fault to the other suggests that the fault pre-dated the emplacement of the granite. Compression from the southwest could have initiated faulting along the Goldenville-Halifax contact in the east and later have thrust undisturbed rocks from the west over the brecciated contact. The thrust fault is offset by a later fault trending 150 degrees.

In outcrop, a penetrative cleavage sub-parallel to the bedding plane of slates of the Halifax Formation has obscured primary bedding features (Fig. 5). In drill core bedding is visible and the main evidence for this cleavage is the redistribution of sulphide minerals into elongate millimetric blebs. A less developed secondary cleavage perpendicular to bedding is observed both in drill core and outcrops along Cox Brook.

STRATIGRAPHY AND LITHOLOGY OF THE MEGUMA GROUP AT EASTVILLE

The detailed stratigraphy of the Meguma Group at Eastville is based on twenty-eight drill holes of St. Joseph

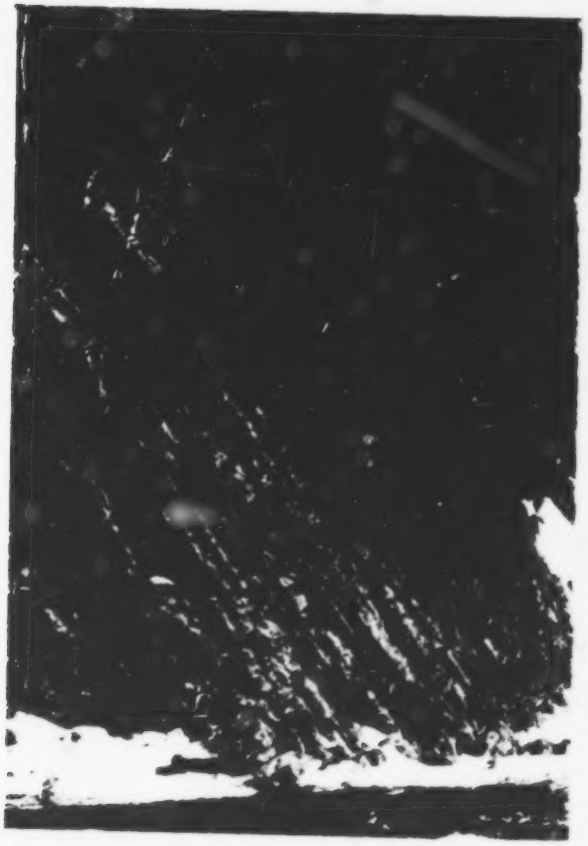

Figure 5 - Outcrop of the Halifax Formation on Cox Brook with black slate and thin interbeds of quartz metawacke. Bedding is obscured by the cleavage.

Explorations Ltd. and Sulpetro Minerals Ltd. The maximum thickness of the stratigraphic sequence represented by diamond drill cores is the upper 100 m of the Goldenville Formation and the basal 200 m of the overlying Halifax Formation. More extensive exposures exist along Cox and Fulton Brooks but faults and a pervasive cleavage subparallel to bedding have obscured the detailed stratigraphic relationship. The units defined in drill core have not been recognized in outcrops; only the gross division between the Goldenville and Halifax Formations can be mapped. A stratigraphic column is presented in Figure 6. Two drill sections (Fig. 7 and 12) illustrate the variability of the contact relationships between the Goldenville and Halifax Formations.

Three members of the Goldenville Formation have been recognized in drill cores through the Eastville deposit (Fig. 6). The basal member is a massive, grey to greenish-grey quartz metawacke. Up to 100 m of the member has been drilled (hole 3) with no slate interbeds and no base metal mineralization observed. The rock constituents include recrystallized quartz, muscovite, plagioclase, garnet, biotite, chlorite and minor iron sulphides. The idiomorphic garnets coexisting with biotite and chlorite in the rock indicate a regional metamorphic grade of middle greenschist facies (Jenner, 1982).

Overlying the basal massive quartz metawacke is the transition zone (Fig. 6), a 30 to 35 m-thick section of interbedded massive, structureless, grey quartz metawacke and finely laminated, graphitic, black slate. The base of the transition zone member is defined as the first black slate interbed (Fig. 7). Slate interbeds range from 1 cm to several metres in

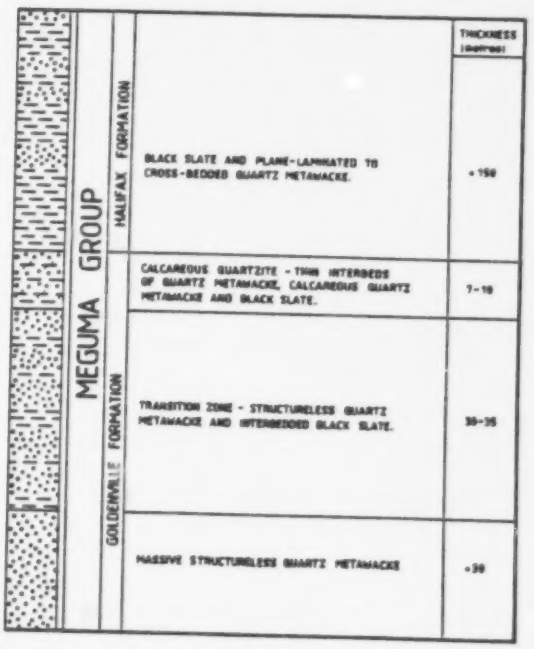
MEGUMA GROUP
HALIFAX FORMATION
GOLDENVILLE FORMATION
BLACK SLATE AND PLANE-LAMINATED TO CROSS-BEDDED QUARTZ METAWACKE.
CALCAREOUS QUARTZITE - THIN INTERBEDS OF QUARTZ METAWACKE, CALCAREOUS QUARTZ METAWACKE AND BLACK SLATE.
TRANSITION ZONE - STRUCTURELESS QUARTZ METAWACKE AND INTERBEDDED BLACK SLATE.
MASSIVE STRUCTURELESS QUARTZ METAWACKE

Figure 6 - Stratigraphic column of the Meguma Group rocks at Eastville based on diamond drill cores.

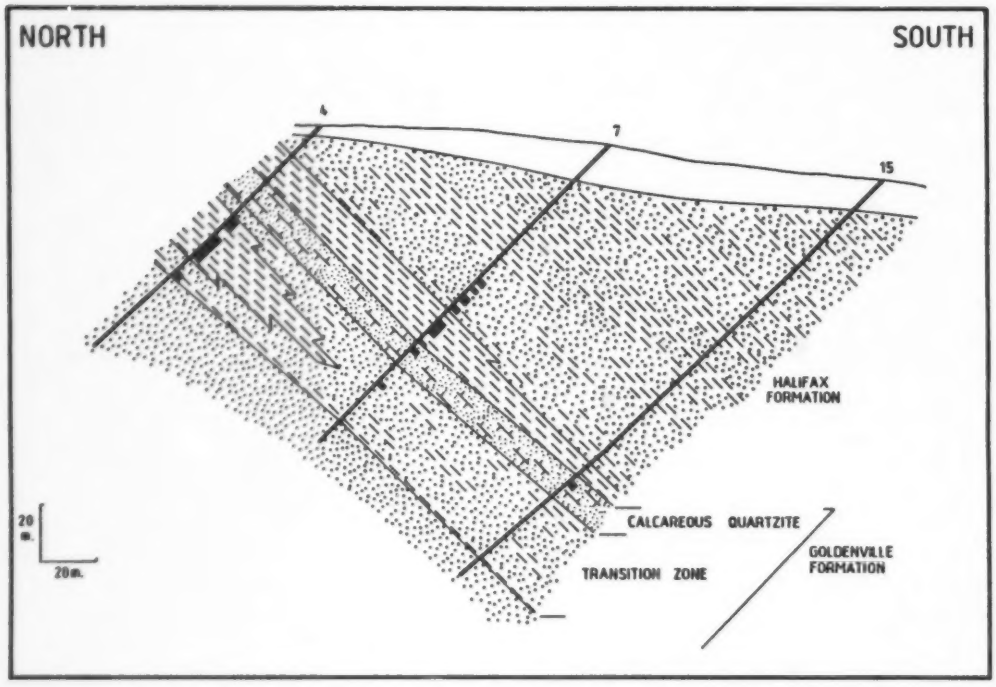

Figure 7 - Section through drill holes 4, 7 and 15 (for location see Figure 2). Major stratigraphic divisions are noted. Heavy bars beside drill holes represent sections with combined zinc-lead grades in excess of 1 per cent.

thickness and comprises from 10 to 50 per cent of the member. The total free carbon content is not accounted for solely by graphite in the black slate; accumulations of bituminous matter occur in some quartz metawacke interbeds (Zentilli and MacInnis, 1983). The restricted distribution of individual thick slate beds in the transition zone member is illustrated by the rapid lateral facies change between drill holes 5, 6 and 2 (Fig. 2). Pyrrhotite and pyrite, the principal sulphide minerals, are concentrated in the slate interbeds with few sulphides in massive quartz metawacke. Figure 7 illustrates that sphalerite and galena are also concentrated in the slate interbeds of the transition zone. In individual drill holes combined zinc-lead grades in excess of 1 per cent occur over thicknesses as great as 14 m. Drill holes with fewer slate interbeds have thinner and lower grade mineralized transition zone section. Mineralogically, the transition zone member is similar to the underlying quartz metawacke member. Quartz, muscovite, biotite, plagioclase and chlorite form an equigranular matrix enclosing disseminated blebs of pyrrhotite. Graphite occurs in the slate interbeds. Garnets are rarely observed in this lithological division.

The transition zone member is overlain by the well bedded calcareous quartzite member (Fig. 6). This marker unit, which forms the top of the Goldenville Formation in the Eastville area, comprises 7 to 10 m of interbedded quartz metawacke, calcareous quartz metawacke and black slate. Distinctive features of the member include the calcareous nature, the thin 1 to 15 mm interbeds of the different lithologies and the highly contorted bedding (Fig. 8). The base of the member is chosen as the lower limit of visible deformed bedding and both upper and lower contacts are gradational over 0.5 to 1.5 m into the adjacent units. The proportion of each lithology varies vertically within the calcareous quartzite member with slate

Figure 8 - Core sample of the calcareous quartzite member showing the contorted fine laminae of black slate (dark grey), quartz metawacke and calcareous quartz metawacke (medium grey) and pyrrhotite (light grey). White block is 1 cm square.

interbeds prominent at the top, and quartz metawacke interbeds prominent at the base. Pyrrhotite is a major component of the member, forming more than 10 per cent by volume of the rock in the slate-rich upper section. Iron sulphides (pyrrhotite and pyrite) form distinct beds or occur dispersed in other lithologies (Fig. 8). The distribution of sphalerite and galena is fracture-controlled in most drilled sections of the calcareous quartzite member. The member includes: quartz metawacke with recrystallized quartz, biotite and spessartine garnet; calcareous quartz metawacke with 0.5 mm calcite crystals intermixed with recrystallized quartz; and black slate with alternating bands of carbon-rich and quartz-rich detritus. Spessartine garnet porphyroblasts are present in all lithologies. Fine scale bedding in some sections results from different concentrations of garnets in adjacent beds and is thought to reflect original element distributions in the sediments.

The Halifax Formation overlies the Goldenville Formation in all drill holes (Fig. 6 and 7). A bed of black, pyrrhotitic, graphitic slate 5 to 15 m thick forms the base of the Halifax Formation in the Eastville area. The rock contains 5 to 10 per cent pyrrhotite, both disseminated and in distinct beds. Jenner (1982) recognized pressure shadows of aligned muscovite and quartz grains surrounding pyrrhotite blebs and suggested the sulphides had crystallized before the development of the slaty cleavage. Sphalerite and galena concentrations occur in the basal black slate beds. Although the unit is laterally extensive and has been traced by drilling for 10 km of strike length, the sphalerite and galena are not laterally continuous and occur principally in the western drill holes. The black slate includes chlorite and spessartine garnet (Fig. 9) in a groundmass of quartz, muscovite and graphite.

The remainder of the Halifax Formation intersected in drill holes consists of black graphitic slate with quartz metawacke interbeds. The latter comprise 20 to 50 per cent of the stratigraphic section. Bouma sequences (Walker, 1979) and load casts on basal contacts indicate that the quartz metawacke beds were deposited from turbidity currents (Fig. 10). Individual metawacke interbeds may contain calcite, either in structureless beds of calcareous quartz metawacke or on foreset laminae of ripples in quartz metawacke. These calcareous sections are not common in the Halifax Formation. The internal laminations in the quartz metawacke interbeds serve to distinguish this formation from the massive structureless quartz metawacke beds of

Figure 9 - Photomicrograph of spessartine garnet within the basal black graphitic slate bed of the Halifax Formation (plane light). Dark inclusions within the garnet are carbonaceous matter.

with black slate partings. The quartz-rich interbeds are conformable with other bedding on the scale of a drill hole but lateral continuity of individual beds between drill holes has not been established. Pyrrhotite and pyrite are common and locally abundant in both slate and quartz metawacke of the Halifax Formation. Both bedding-controlled and fracture-controlled sphalerite and galena occur in the section. Slate and quartz metawacke contain quartz, muscovite, chlorite, garnet and sulphides. Black slate contains laminae of carbonaceous material (now qraphite), probably of detrital origin, finely interbedded with more quartzose laminae.

This typical stratigraphic assemblage from quartz metawacke beds in the Goldenville Formation through to the Halifax Formation has been traced for 10 km of strike length from hole 27 the transition zone in the Goldenville Formation. Quartz-rich interbeds approximately 10 to 15 cm thick (Fig. 11) occur locally in the drilled section of the Halifax Formation. These siliceous interbeds comprise thin quartz-rich layers finely interbedded near Fulton Brook in the west (Fig. 2) to hole 8 adjacent to the thrust fault in the east (Fig. 3). The drill section in Figure 7 illustrates the lateral continuity of beds and the uniform thickness of beds between drill holes. In individual drill holes, faults have caused local repetition or truncation of beds.

Conformable contact relationsnips between the Goldenville and Halifax Formations are not observed east and north of the low angle thrust fault (Fig. 3). A drill section that includes holes on both sides of this fault is illustrated in Figure 12. The Goldenville Formation includes quartz metawacke with slate interbeds (correlative with the transition zone) and brecciated quartz metawacke with minor fluorite. In deeper drill holes close to the granitic intrusion, mineral segregation occurs with discrete layers of quartz and ferro-magnesian silicates. The calcareous quartzite member is absent in all these drill holes and the transition zone varies in thickness due to faulting in the section (Fig. 12).

The contact between the Goldenville

Figure 10 - Quartz metawacke interbed in black slate. Plane lamination and load casts on the basal contact of the beds are features of many interbeds in the Halifax Formation. Pyrrhotite in small pods and in cubic habit (after pyrite) disrupts the bedding.

and Halifax Formations is defined in this section by a fault zone. The basal part of the Halifax Formation comprises quartz metawacke and slate blocks in a matrix of black, graphitic fault gouge. Sphalerite and galena occur within the competent blocks and in the gouge, and iron sulphides are ubiquitous as in other sections of the Halifax Formation. Contact metamorphism by the granitic intrusion has produced biotite, almandine garnet and andalusite crystals up to 1.5 cm in cross section in the Halifax Formation. At the base of the drill holes (Fig. 12) a schist with pink garnetiferous layers in a medium-grey siliceous matrix occurs in contact with the slate. This schist could be a highly metamorphosed equivalent of the Halifax Formation and the contact between the two units a fault. The schist does not contain sulphides.

METALLIC MINERALS: HABIT AND INTERGROWTHS

Both sulphide and oxide minerals have been recognized in the Meguma Group metasedimentary rocks at Eastville. Sulphide minerals are quantitatively and economically more significant and include, in decreasing order of abundance, pyrrhotite, pyrite, sphalerite, galena, chalcopyrite and arsenopyrite. Jenner (1982) recognized both pyrite partly replaced by pyrrhotite in elongate 1 to 10 mm sulpnide blebs and pyrite that is

Figure 11 - Quartz-rich layers within the Halifax Formation. Thin interbeds of quartz-rich laminae and black slate partings occur in the slate sequence.

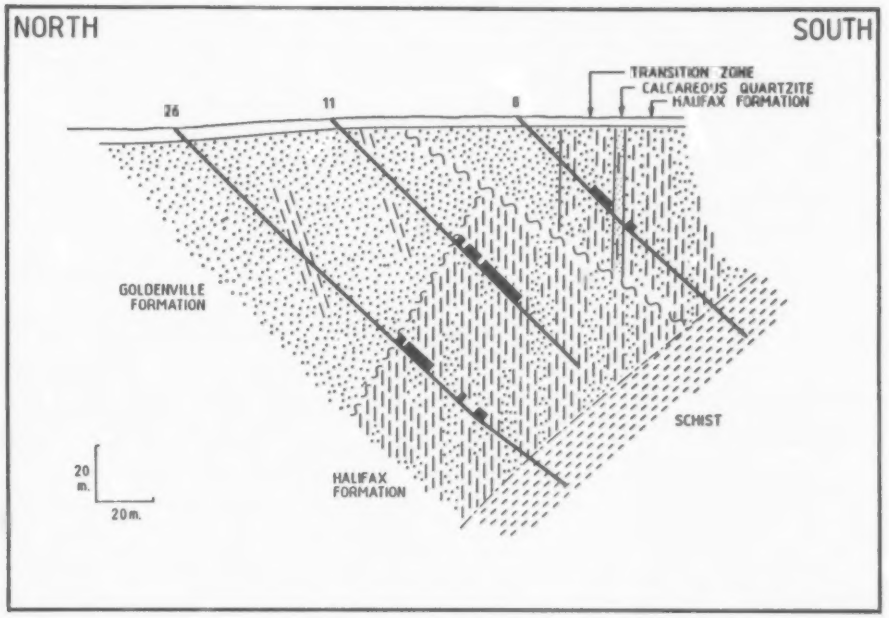

Figure 12 - Section through drill holes 26, 11 and 8 (for location see Figure 3). Hole 8 is above the thrust fault and contains a typical stratigraphic succession. In holes 26 and 11 the Goldenville and Halifax Formations are in fault contact. Bedding orientations are indicated by the attitude of the lithological patterns. Heavy bars beside the drill holes represent sections with combined zinc-lead grades in excess of 1 per cent. Drill hole 26 includes 15.7 m of 2.61 per cent Zn+Pb, and drill hole 11 includes 19.8 m of 2.19 per cent Zn+Pb. The sulphide distribution is governed by the position of the fault on the formational contact.

secondary after pyrrhotite in cross-cutting veins. The replacement textures record regional metamorphic conditions rather than primary sulphide deposition. The replacement texture, however, does suggest that much of the pyrrhotite was originally deposited as pyrite. Sphalerite and galena occur as discrete mineral grains or intergrowths with each other, and as replacement grains engulfing pyrrhotite. Chalcopyrite forms anhedral masses enclosed in pyrrhotite or sphalerite, and arsenopyrite has been observed only in a few locations in veins in the calcareous quartzite member.

Oxides include ilmenite and rutile which occur as discrete crystals in the metasediments. Ilmenite crystals (Fig. 13) in the slate of the Halifax Formation contain significant MnO. Rutile occurs as small needle-like crystals in the calcareous quartzite member and appears to outline pressure shadows around garnet porphyroblasts (Fig. 14). Both ilmenite and rutile formed during metamorphism of the sedimentary rocks and have not been observed intergrown with the sulphides.

Two principal styles of sulphide occurrence have been noted. Conformable sulphides are the most common. Pyrrhotite and lesser amounts of pyrite, galena and sphalerite occur in small blebs 1 to 2 mm thick and 2 to 5 mm long, elongate parallel to bedding (Fig. 15). Pyrrhotite also forms 1 mm to 1 cm thick beds in the slate and quartz metawacke and irregular pods on foreset laminae and plane laminae in the quartz metawacke. Nodules of pyrrhotite, up to 1 to 3 cm in size occur in all lithologies. The nodules have sharp boundaries with the enclosing sediment and in some cases are surrounded by a halo of disseminated pyrrhotite.

Redistribution of sulphides has

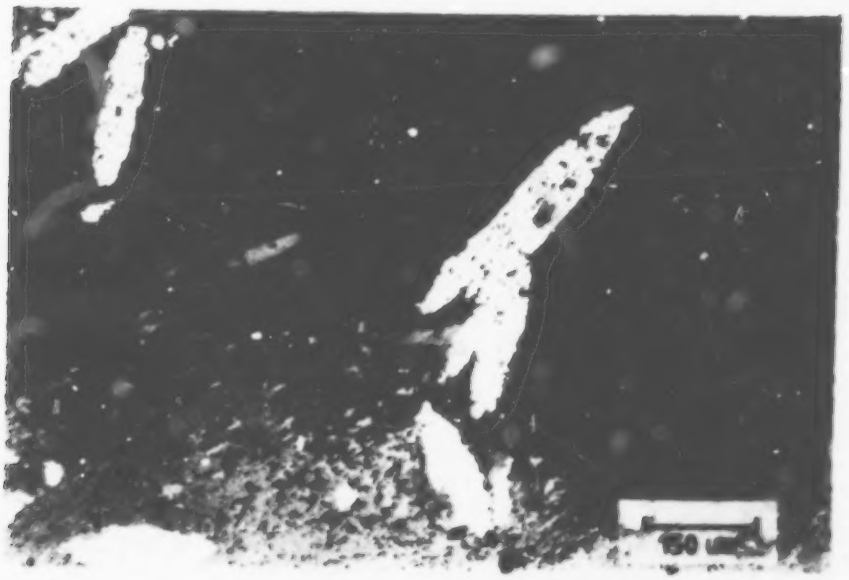

Figure 13 - Ilmenite crystal porphyroblasts dispersed in slate of the Halifax Formation (reflected light).

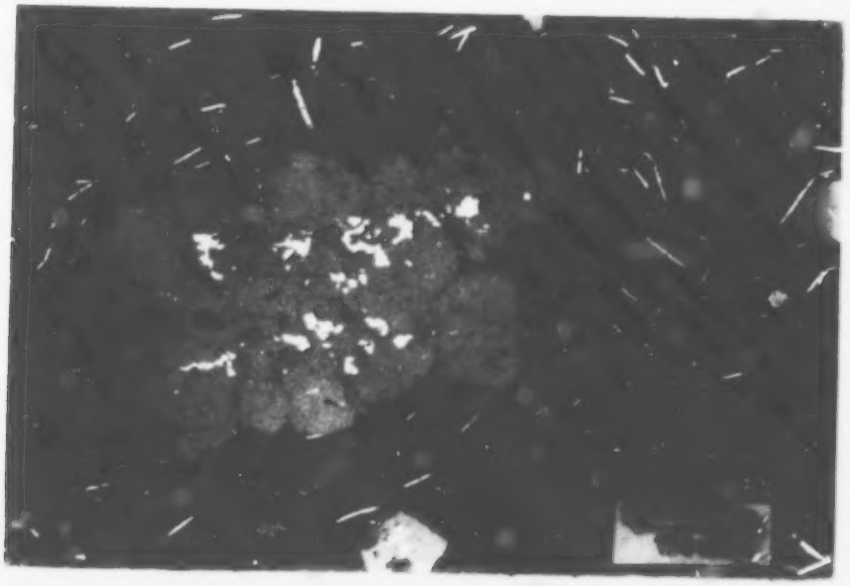

Figure 14 - Calcareous quartzite member containing small rutile needles with a preferred orientation around a porphyroblast of garnet (grey) enclosing minor sphalerite (white) (reflected light).

occurred. Pyrrhotite replaces pyrite in quartz metawacke interbeds in the Halifax Formation. Cleavage redistribution of sulphides has formed a series of elongate, disconnected millimetric blebs on one lithological horizon but with each bleb at a slight angle to the bedding. Pronounced redistribution of iron sulphides in beds that are cross-cut by the cleavage is common (Fig. 16). Sphalerite coats cleavage planes in the black slate beds.

Conformable sphalerite and galena are

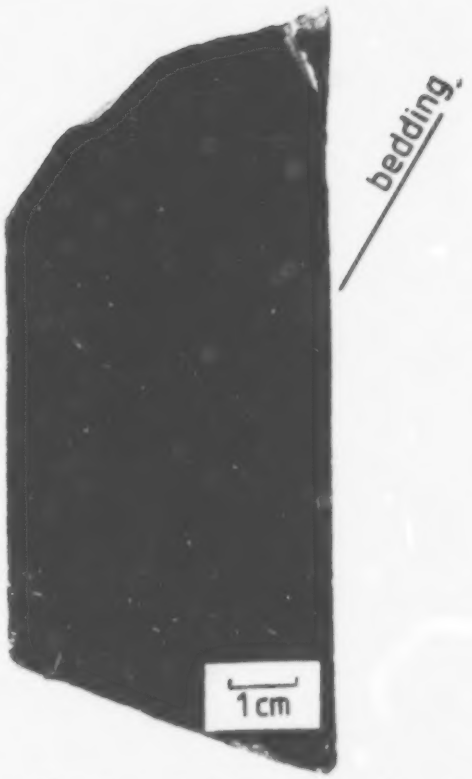

Figure 15 - Core sample of conformable galena and sphalerite (grey) in black slate. Small cross-cutting veinlets contain sphalerite. The section that includes this sample assayed 2.24 % Pb and 5.36 % Zn.

concentrated in the argillaceous and carbonaceous slate beds of the transition zone of the Goldenville Formation and in the Halifax Formation. Individual mineral grains occur in the calcareous quartzite member but the concentration is very low. Conformable iron sulphides (pyrrhotite and pyrite) are ubiquitous in the transition zone member and calcareous quartzite member of the Goldenville Formation and throughout the Halifax Formation.

Fracture-controlled sulphides account for the remainder of the ore minerals, and include pyrite and sphalerite with lesser amounts of pyrrhotite, galena and arsenopyrite. The sulphides occur in networks of 0.1 to 1 mm thick veinlets cross-cutting bedding or with quartz in 5 mm to 2 cm wide veins. In the larger veins the principal sulphides are pyrite and pyrrhotite. Sphalerite and galena in fractures (Fig. 17) occur in black slate near conformable galena and in quartz metawacke and calcareous quartz metawacke beds where fractures are the only depositional site for sphalerite and galena.

In that part of the deposit north and east of the thrust fault (Fig. 3), the style of sulphide mineralization is the same, even though the rocks have been highly brecciated. Individual blocks within the fault gouge at the base of the Halifax Formation contain both conformable galena and fracture-controlled sphalerite. The fracture-controlled veinlets terminate at the fragment boundaries. Fault gouge between the blocks contains sphalerite

Figure 16 - Transposition of a pyrrhotite bed along the cleavage in the Halifax Formation. The sulphide bed is at a high angle to the cleavage and parallel to the drill core at this location.

and galena, but these sulphides have probably been mechanically redistributed during brecciation of slate, rather than having been introduced during or after faulting.

ROCK GEOCHEMICAL STUDIES

As part of the 1980 exploration program of the Eastville property all available drill core was split and analysed by Bondar-Clegg and Company Ltd., Ottawa, by atomic absorption of acid extractable Pb, Zn, Fe, Mn, As, Sb, Ba and Sr. Usually, 3 m intervals of core of the Halifax Formation and transition zone and 2 m intervals of core of the calcareous quartzite member were split for analysis. The basal massive quartz metawacke was not analysed in a systematic manner.

Figure 17 - Discontinuous sphalerite and galena veinlets and adjacent disseminations in black slate.

In 1983, 50 selected samples from holes 24 and 25 were analysed by X-Ray Assay Laboratories Limited, Don Mills, for 48 major and trace elements using X-ray fluorescence techniques. A program of small scale analyis of individual beds was initiated by Zentilli in 1983 and is continuing.

The 1980 exploration data represents the most complete data set applicable to all drill holes; analytical results from selected drill holes are presented in this paper. Preliminary results of the 1983, more detailed, geochemical analyses are outlined.

Two distinct groups of drill holes are noted. Holes 1, 2, 4-8, 12-25 and 27, forming the first group, each intersected a complete stratigraphic section with slate, calcareous quartzite and transition zone rocks. Some of the units may be in fault contact but extensive brecciation has not taken place. While individual beds contain distinctive amounts of particular elements, the most obvious partitioning is shown by Mn and Sr. Drill hole 13 (Fig. 2 and 18) is representative of the element distributions within this group of drill holes.

The second group of drill holes, all at the east end of the property, include holes 9-11, 26 and 28. In these holes, the contact of the Goldenville and Halifax Formations is a zone of intense faulting. The calcareous quartzite member is absent from the core and only parts of the transition zone occur in the section north and east of the fault (Fig. 12). Drill hole 9 is an example of these holes, in which the distribution of elements is not governed by rock lithology but is fault controlled.

For drill hole 13, representing the first group of drill holes with normal stratigraphic sequences, the Sr, Ba, Mn and Pb+Zn profiles are shown in Figure 18. At the base of the exposed stratigraphic section, the quartz metawacke unit of the Goldenville

Formation was not analysed in drill hole 13, but in drill hole 3 (Fig. 2) the quartz metawacke contains from 100 to 170 ppm Sr. In the overlying transition zone rocks in hole 13, Sr contents range from 40 to 80 ppm. The Sr levels in the rocks decrease to 20 to 50 ppm in the calcareous quartzite member and then increase rapidly across the contact of the Goldenville and Halifax Formations. Within the Halifax Formation, Sr content ranges from 200 to 400 ppm with a gradual decrease in levels from the base to the top of the section.

Mn trends are opposite to those of Sr. In the massive quartz metawacke in drill hole 3, Mn values range from 400 to 750 ppm. In the overlying transition zone the distribution of Mn is erratic, ranging from 1,000 to 4,000 ppm Mn. The calcareous quartzite member is markedly enriched in Mn with contents of 5,000 to 17,000 ppm or 0.5 to 1.7 per cent Mn. From these high contents the Mn values drop to 1,000 to 2,000 ppm in the overlying Halifax Formation. The Mn content of the rocks is slightly lower at the base of the formation, immediately above the calcareous quartzite member.

The 1983 analyses of rock powders show a major discrepancy in Mn levels between whole rock (XRF) date and acid extractable metal data. In drill hole 24, which was chosen for detailed analysis since it contains more than 150 m of the Meguma Group section, the Mn analyses by acid extraction are within 75 to 95 per cent of the whole rock (XRF) values for rocks in the transition zone and Halifax Formation. In the calcareous quartzite member, acid extraction accounts for only 10 to 35 per cent of the whole rock values; the 1983 analyses indicate Mn levels between 6.9 and 8.6 per cent. Analysis of individual beds in the calcareous quartzite has given values up to 13 per cent Mn. The level of Mn in the calcareous quartzite member of the Goldenville Formation has, therefore, been greatly underestimated in the exploration data.

The discrepancy between the analytical results has been resolved by microscopic examination and microprobe analysis. Jenner (1982) demonstrated that the average Mn content is 22.6 per cent in spessartine garnets in the calcareous quartzite member. Calcite grains in this member contain 1.0 to

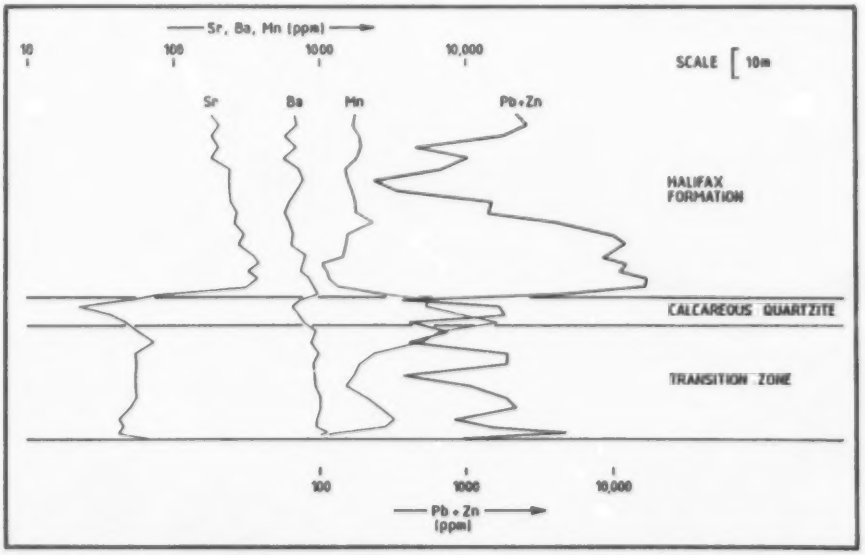

Figure 18 - Distribution of Sr, Ba, Mn and Pb+Zn in a typical stratigraphic succession of Meguma Group rocks (drill hole 13) (Fig. 2). Note that the scale for Pb+Zn data is offset by a factor of 10 for clarity. The drill hole is approximately perpendicular to the strata.

2.4 per cent Mn. In the overlying black slate of the Halifax Formation only 0.3 per cent Mn was detected in the graphitic slate but pyrrhotite-rich samples of slate contained up to 1.1 per cent Mn. Spessartine garnets in the slate beds immediately overlying the calcareous quartzite member contain an average of 17 per cent Mn.

The results indicate that most of the Mn in the calcareous quartzite member is contained in spessartine garnets which would be weakly attacked by an acid leach. The values in the transition zone (Goldenville Formation) and slate beds of the Halifax Formation are in close agreement for the two analytical methods and indicate that most Mn in these units occurs with pyrrhotite, other sulphides and perhaps calcite. Although garnets are abundant in all units, except in the calcareous quartzite and immediately overlying black slate, they are not necessarily spessartine garnets. The Mn distribution probably reflects the original composition of the sediments with the primary Mn concentration preserved in spessartine garnets, as it also is in association with other metamorphosed stratabound base metal deposits (Stumpfl, 1979).

Ba contents show only minor variation between lithologies of the Meguma Group. The content of Ba in the massive quartz metawacke of the Goldenville Formation ranges from 600 to 800 ppm (drill hole 3). In drill hole 13 the transition zone contains 900 to 1,000 ppm Ba. The levels are slightly depressed in the calcareous quartzite member, with 600 to 800 ppm Ba, but rise again at the base of the Halifax Formation. The Ba content of the Halifax Formation ranges from 600 to 1,000 ppm with the higher values toward the base of the section (Fig. 18). If Ba distribution is primary, and has not been affected by regional metamorphism, then the Ba content of the rocks appears related to lithology and independent of the base metal distribution.

In contrast to Sr, Mn and Ba, the total amount of Pb+Zn is highly variable both within and between units. In drill hole 13 (Fig. 18) the combined Pb+Zn content ranges from 240 ppm up to 18,000 ppm or 1.8 per cent. Higher values occur in a thin slate bed at the base of the transition zone and in black slate beds at the base of the Halifax Formation. The distribution of Pb+Zn is completely independent of that of Sr, Mn and Ba. Figure 7 indicates some of the local variation in the stratigraphic position of higher grade sections between adjacent drill holes.

The variation in the ratio of Pb/Zn with respect to the content of Mn and Fe for drill hole 13 is shown in triangular diagrams (Fig. 19 and 20). If Mn or Fe are related to the mineralizing process, then a variation in the Pb/Zn ratio might be expected with changing contents of Mn or Fe. In many exhalative Pb-Zn deposits the ratio of Pb/Zn increases closer to the exhalative vent of the ore solutions (Large, 1983; Franklin et al., 1981). On the Mn-Pb-Zn plot (Fig. 19) the ratio of Pb/Zn varies slightly due to possible post-depositional remobilization of Zn into fractures, enhancing the Zn content in some areas while depleting it in others. Despite this remobilization, the data clusters about a Pb/Zn ratio of 1:2.2 for all values of Mn and Fe (Fig. 19 and 20). This pattern of constant Pb/Zn ratios occurs in all drill holes of the first group with typical stratigraphic assemblages.

The detailed analytical work on drill holes 24 and 25 indicates some elements that do correlate with Pb and Zn (Fig. 21). In the transition zone Cd, Ag, Nb and Sb contents do correlate with those of Zn and Pb. In the Halifax Formation the Cd and Ag contents correlate strongly with Pb. In neither lithological unit are the major element distributions related to the Zn and Pb contents.

The element distributions for all drill holes with typical stratigraphic

successions are similar to those described for drill hole 13. The levels of individual elements may differ by up to a factor of 10 but the pattern of element distribution between units remains constant.

In the second group of drill holes (9-11, 26, 28) (Fig. 3) the calcareous quartzite member, parts of the transition zone and an undetermined amount of the Halifax Formation are absent. The contact of the Goldenville and Halifax Formations is a zone of intense faulting. Additional areas of fault gouge occur within the Halifax Formation disrupting the stratigraphic succession. The element distribution patterns for drill hole 9 are illustrated in Figure 22. The distribution of Sr, Ba Mn and Pb+Zn is in marked contrast to the variations of elements by lithology observed in drill hole 13 (Fig. 18). Sr levels range from 100 to 150 ppm throughout the hole, except in the contact zone where only 50 ppm Sr is present. Mn content is more variable with 200 to 500 ppm in rocks of both formations and a peak of 1,300 ppm at the faulted contact of the Goldenville and Halifax Formations. Average Mn values are slightly higher in the quartz metawacke than in the slate-rich section. The absolute levels of Mn are about one-tenth those in the sections with typical, unfaulted stratigraphic sequences. This may

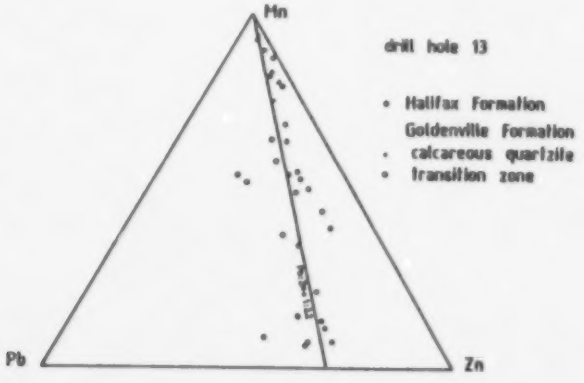

Figure 19 - Triangular plot of Mn-Pb-Zn for rocks of a typical stratigraphic succession (drill hole 13).

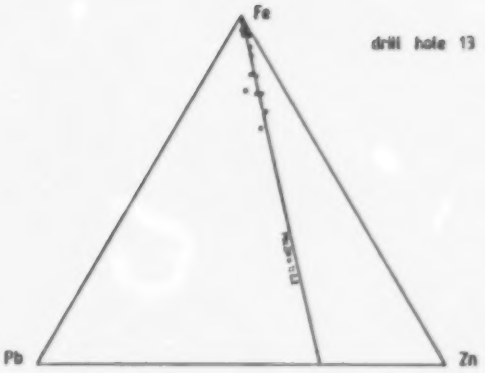

Figure 20 - Triangular plot of Fe-Pb-Zn for rocks of a typical stratigraphic succession (drill hole 13).

reflect an analytical problem with most of the Mn in spessartine garnets which were not attacked by the acid extraction techniques used on these samples. Whole rock analyses have not been done on these faulted sections. Ba levels are between 650 and 900 ppm with a small peak of 1,450 ppm at the fault contact. Ba and Sr levels, unlike that of Mn, are of the same order to magnitude as in the drill holes of the first group.

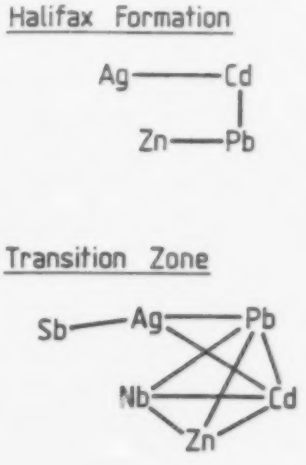

Figure 21 - Diagram showing those elements whose distributions correlate with those of Pb and Zn in rocks of the transition zone and Halifax Formation (drill holes 24 and 25) (Fig. 2).

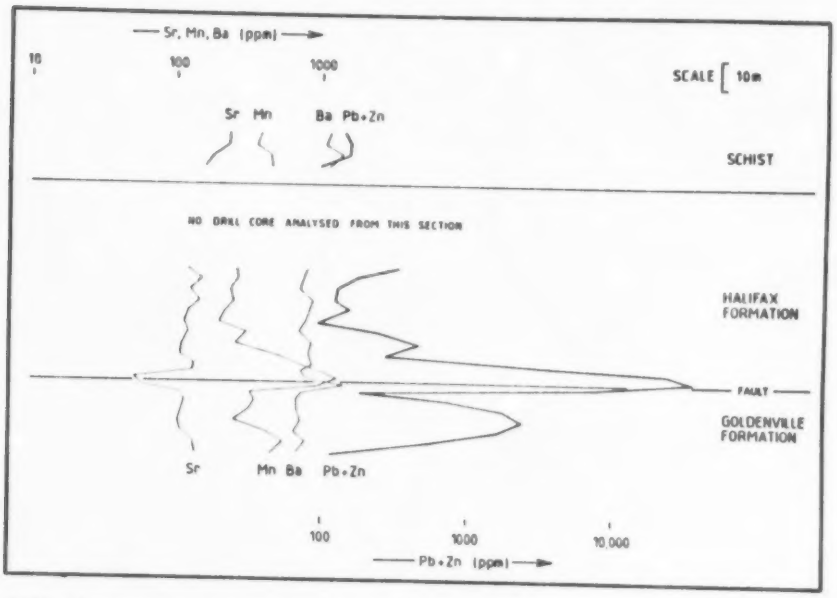

Figure 22 - Distribution of Sr, Ba, Mn and Pb+Zn in a section through the Meguma Group east of the thrust fault (Fig. 3) where the stratigraphic assemblage has been truncated by a fault at the contact of the Goldenville and Halifax Formations. Note that the scale for Pb+Zn data is offset by a factor of 10 for clarity. Drill hole 9 is plotted in reverse of the sequence drilled so that information is in the appropriate stratigraphic order. The drill hole cut the rocks at approximately a 45° angle so that true stratigraphic thickness is not represented.

The distribution of Pb+Zn in drill hole 9 is also independent of other elements. In this drill hole Pb+Zn is in excess of 3 per cent at the faulted contact between the Goldenville and Halifax Formations. Although the highest grade section of Pb+Zn is in the Halifax Formation above the fault contact, a significant amount of Pb+Zn (0.2%) occurs in quartz metawacke with slaty interbeds below the fault. This weakly mineralized section is interpreted as correlative with part of the transition zone.

In the schistose rocks at the base of the drill hole, Sr, Ba and Mn contents are slightly elevated above the adjacent, less altered rock.

Triangular plots of Mn-Pb-Zn for two drill holes cutting the faulted Goldenville-Halifax contact are presented in Figures 23 and 24. In these drill holes Mn levels are relatively constant while variation in the Pb and Zn contents of the rocks defines the graphical relationship. Two patterns have been observed depending on the location of the drill holes. The western drill holes (11, 26; 28 not analysed) (Fig. 3) represented by drill hole 26 (Fig. 23) have two groupings of data. Samples from the Goldenville Formation, which is generally poorly mineralized, group about the Mn apex of the diagram. Mineralized areas of the Halifax Formation, although they contain the same amounts of Mn, plot in the Pb-Zn part of the diagram. All data are dispersed about a Pb/Zn ratio of 1:2.2, identical to the ratio for the drill holes in the typical undisturbed stratigraphic successions to the west of the thrust fault.

The two eastern drill holes (9, 10) (Fig. 3, are lower in Pb except in the mineralized sections. As in the other areas, the absolute Mn levels are constant and the variations of Mn-Pb-Zn contents are determined by variation in the relative amounts of Zn and Pb (Fig.

24). Data for both the Goldenville and Halifax Formations plot on the Mn-Zn side of the triangular diagram. Only two samples from the extreme base of the Halifax Formation plot on the Pb-Zn side of the diagram. These two samples are from a relatively well mineralized section where the combined zinc-lead grade is 3.10 per cent over 4 m.

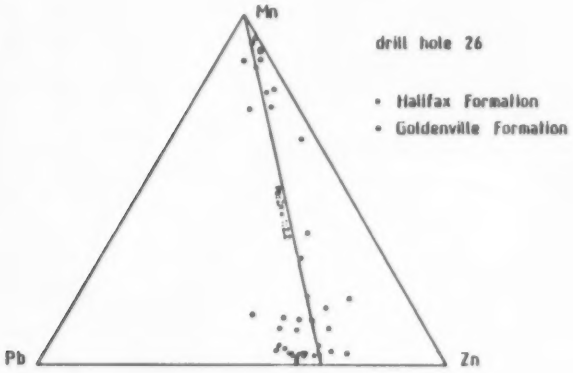

Figure 23 - Triangular plot of Mn-Pb-Zn for rocks of the faulted stratigraphic succession east of the thrust fault in drill hole 26.

In summary, element distribution patterns for two groups of drill holes have been described. In the first group, represented by hole 13, typical stratigraphic sections contain contents of Sr, Mn and to a lesser extent Ba, that are controlled by rock types. The calcareous quartzite member, a distinctive marker horizon at the top of the Goldenville Formation, is depleted in Sr but enriched in Mn with values up to 13 per cent Mn in individual beds. Zn and Pb are present in black slate beds immediately above the calcareous quartzite member and in slate beds within the transition zone. In the second group of drill holes, represented by hole 9, Sr, Mn and Ba values are relatively constant in all lithologies in faulted sections east of the thrust fault (Fig. 3). At the fault contact of the Goldenville and Halifax Formations Mn and Ba contents are higher and Sr is lower. Zn and Pb contents in excess of 1 per cent occur

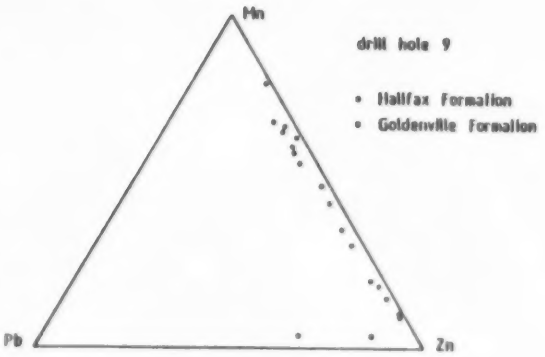

Figure 24 - Triangular plot of Mn-Pb-Zn for rocks of the faulted stratigraphic succession east of the thrust fault in drill hole 9. Note the depletion of Pb in most rocks in the section.

in the basal Halifax Formation, adjacent to the fault.

Triangular plots of Mn-Pb-Zn indicate a ratio of Pb/Zn of 1:2.2 in all drill holes with the exception of two holes (9, 10) in the extreme east end of the exposed contact area close to the granite intrusion. These latter holes are lower in Pb and do not have a regular ratio of Pb/Zn.

The rocks along the faulted contact of the Goldenville and Halifax Formations in the eastern area tend to be higher grade than those in the undisturbed sections to the west, although Mn levels are lower and no zoning of elements by lithology has been recognized. The lack of zoning suggests a pervasive alteration of the rocks east and north of the thrust fault with destruction of pre-existing element patterns. This alteration is not related to the granite intrusion since drill holes above the thrust fault, which contain schistose sections metamorphosed by the granite, retain typical element distributions.

DISCUSSION AND CONCLUSIONS

The metasedimentary rocks of the Meguma Group have been interpreted by Harris and Schenk (1975) and Schenk

(1978) as a eugeoclinal complex with abyssal plain, coalescing submarine fan and overlying continental rise deposits on a passive Atlantic-type continental margin.

The Goldenville Formation regionally includes the following rock types or their metamorphosed equivalents: massive sandstone, pebbly sandstone, conglomerate and minor interbedded black shale. The association of these rocks and the identification of sedimentary features such as flute casts, prod marks and dewatering structures indicates mid-fan deposition of turbidites in a submarine fan complex (Harris and Schenk, 1975; Walker, 1979). At Eastville, drill core has not proved adequate for a detailed sedimentological study of the Goldenville Formation. The general facies association of massive structureless quartz metawacke overlain by quartz metawacke and intercalated slate (transition zone) agrees with deposition in a mid-fan position with suprafan lobes of well-sorted sand and intervening shale between the lobes.

The Halifax Formation at Eastville, with its predominance of black slate containing plane-laminated to cross-bedded sandy turbidite interbeds, is interpreted as part of the outer fan and basin plain deposits. The black slate bed at the base of the Halifax Formation may represent a termination of supply of coarse sediment to a particular lobe of the submarine fan complex, a hiatus in supply of coarse detritus to the whole basin, or the development of a local sub-basin within the larger Meguma eugeocline.

The calcareous quartzite member of the Goldenville Formation contains calcite and a high content of manganese and does not readily fit the model of submarine fan deposition. The regional extent of the calcareous quartzite outside the Eastville area is unknown as the unit is thin relative to the entire stratigraphic succession and difficult to identify in outcrop. Except in the gold mining areas of Nova Scotia, subsurface exploration of the Meguma Group has been limited. The calcareous quartzite may represent a chemical precipitate in a local sub-basin within the more extensive Meguma basin. Further drilling of a regional nature is needed to establish the lateral extent of both the calcareous quartzite and the overlying black slate section of the Halifax Formation.

Many features, both sedimentological and metallogenic, bear on the genesis of the Eastville deposit. The deposit is laterally extensive with zinc+lead in excess of 1 per cent in drill holes over 10 km of strike length. The zinc and lead sulphides are stratigraphically restricted to rocks of the transition zone and calcareous quartzite members of the Goldenville Formation and the basal part of the Halifax Formation, about 100 m of section. No volcanic rocks have been recognized in the sequence which, as outlined, comprises mid-to outer-fan and basin plain turbidity current deposits and intercalated black slate.

Pyrrhotite and pyrite are the dominant sulphides in all lithologies. Rock lithology has determined their distribution, abundance and habit, and their distribution is independent of that of galena and sphalerite. Most iron sulphides probably formed by reduction of iron in the carbonaceous sediment as an early diagenetic process and were later deformed and metamorphosed.

Sphalerite, galena and minor chalcopyrite and arsenopyrite occur in conformable accumulations and in fractures due to possible post-depositional redistribution of sulphides. No barite has been observed in drill core and the continuity of the stratigraphic section indicates that no major accumulations of barite existed prior to regional metamorphism. The ratio of lead to zinc is constant both laterally and vertically throughout the deposit.

These features of the Eastville zinc-

lead deposit all serve to class it as a sediment-hosted stratabound lead-zinc deposit as described by Morganti (1981) and Large (1983). The independent distribution of iron and zinc and lead, the grossly stratiform nature of the deposit and the affinity of base metal sulphides for graphitic black slate (shale) are similar to features of other stratiform lead-zinc deposits. Insufficient information about the stratigraphy in the environs of the deposit inhibits speculation on any underlying or marginal graben feeder structures to account for the input of metal-bearing brines into the basin. The lack of metal zonation throughout the deposit suggests a distal exhalative vent area for ore fluids.

In sediment-hosted lead-zinc deposits at Meggen, McArthur River and Tynagh, manganese is concentrated in carbonate rocks at the same stratigraphic level as the stratiform sulphides (Large, 1983). Zentilli et al. (1984) suggested that the manganese-enriched beds at the Goldenville-Halifax contact are associated with sphalerite and galena at Eastville. The calcareous quartzite member of the Goldenville Formation contains 6 to 9 per cent Mn versus background levels of 800 ppm (0.08 per cent) for slate and quartz metawacke in the Meguma Group (Liew, 1979). Although the calcareous quartzite member is enriched in manganese, most zinc and lead occurs either stratigraphically lower in the transition zone or in the overlying Halifax Formation. The manganese content of the calcareous quartzite member bears no relation to the lead and zinc grades or to the ratio of these metals.

Deposition of the sediments and zinc and lead sulphides was followed by metamorphic and structural events. The regional greenschist metamorphic assemblage consists of recrystallized quartz, biotite, chlorite and garnet. The high manganese content of the calcareous quartzite is reflected in spessartine garnets, ilmenite and calcite. During regional metamorphism pyrrhotite formed from pyrite in the carbonaceous sediments.

The Eastville area is on the north limb of a regional syncline. The Goldenville-Halifax contact at the east end of the deposit was faulted, and undeformed rocks from the southwest were thrust over underlying units. During this deformation and metamorphism some sulphides were redistributed into veins and fractures and elongate blebs parallel to cleavage.

After the main disturbance, the Meguma Group rocks at the east end of the map area were intruded by granite. Contact metamorphism of the Halifax Formation slate developed andalusite, garnet and biotite. Mineral segregation and schistosity developed in rocks in close proximity to the intrusion.

Late north-trending faults cut the rocks of the Meguma Group and offset earlier structures. Filling of post-orogenic Carboniferous basins with clastic sediments, marine carbonate and evaporites produced the Windsor Group which unconformably overlies the Meguma Group to the west of Eastville.

Exploration guidelines for zinc-lead deposits in the Meguma Group must be preliminary in nature as many features of the Eastville deposit are still poorly understood and undergoing further research. Stream and soil geochemical sampling can outline potential areas for zinc and lead sulphides. Acid groundwater caused by the abundance of iron sulphide in the Halifax Formation ,and the mobility of zinc in solution, result in removal of zinc from the immediate area and result in geochemical anomalies with lead more abundant than zinc close to the bedrock source. Zinc is twice as abundant as lead in the rock. Till sampling provides a direct indication of base metals in the underlying rock.

Exploration at Eastville has shown the importance of detailed correlation

between drill holes. Individual quartz metawacke beds in the slate should correlate as turbidity current deposits are not laterally confined on the scale of drilling; the gross similarities between beds make such correlations difficult by visual means. The correlation could best be accomplished by geophysical logging of holes to determine the stratigraphic succession. Vertical gradiometric magnetic surveys can provide more detailed stratigraphic information (Waldron and Jenson, 1983) than the total field magnetic surveys and ground electromagnetic surveys used for stratigraphic information at Eastville. Detailed stratigraphic information permits a better assessment of any surficial geochemical anomalies as potential indicators of base metals. As an example, a high proportion of slate in the section may reflect a suitable depositional environment for zinc and lead. With detailed stratigraphic information the question of whether or not the deposit is truly conformable could also be addressed.

Regionally, the black graphitic slate can be a potential host for sphalerite and galena (Sangster, 1981). The presence of black slate does not indicate mineralization will be present, but, as demonstrated at Eastville, without the black slate significant accumulations of base metal sulphides will not be found. The manganese-enriched calcareous rocks may also be an important indicator of base metals (Zentilli et al., 1984). At Eastville no direct correlation exists between manganese and lead and zinc, but the area is enriched in these elements relative to other parts of the Meguma Group. The implications of this feature are being assessed by Zentilli with further work on the carbonate-manganese units both at Eastville and in other parts of the Meguma Group (Zentilli and MacInnis, 1983).

ACKNOWLEDGEMENTS

The authors wish to thank Sulpetro Minerals Limited, Toronto and CRA Limited of Australia for permission to publish this paper. Zentilli wishes to thank the Nova Scotia Department of Mines and Energy for their funding of detailed analytical work on selected split drill core sections. The interpretation of the geochemical data owes much to the enthusiasm and ability of Ian MacInnis.

This paper was prepared largely by W.P. Binney under contract to the Geological Survey of Canada (09GR.23233-3-1836) as a contribution to the Canada-Nova Scotia Co-operative Mineral Program, 1981-1984. W.P. Binney and A.L. Sangster were employed by Sulpetro Minerals Limited during exploration of the Eastville deposit. K.A. Jenner studied the Eastville (Gold Brook) deposit for a B.Sc thesis, Dalhousie University.

R.V. Kirkham, R. I. Thorpe, D. F. Sangster and W.H. Poole read the manuscript and made many useful comments and suggestions.

BENSON, D.G. 1967. Geology of Hopewell map-area, Nova Scotia. Geological Survery of Canada, Memoir 343, 58 p.

FLETCHER, H. and FARIBAULT, E.R. 1902. Eastville sheet no. 48. Geological Survey of Canada, map 633.

FRANKLIN, J.M., LYDON, J.W. and SANGSTER, D.F. 1981. Volcanic-associated massive sulfide deposits. In Economic Geology, 75th Anniversary Volume, ed. B.J. Skinner; The Economic Geology Publishing Company, pp. 485-627.

GEOLOGICAL SURVEY OF CANADA 1960. Aeromagnetic map 762G, Hopewell, Nova Scotia.

HARRIS, I.M. and SCHENK, P.E. 1975. The Meguma Group. In Ancient Sediments of Nova Scotia, ed. I.M. Harris; Society of Economic Paleontologists and Mineralogists, 1975 field trip, pp. 17-38.

JENNER, K.A. 1982. A study of sulphide mineralization in the Meguma Group sediments, Gold Brook, Colchester County, Nova Scotia. Unpublished B.Sc. thesis, Dalhousie University, Halifax, Nova Scotia, 60 p.

LARGE, D.E. 1983. Sediment-hosted massive sulphide lead-zinc deposits: an empirical model. In Sediment-hosted Stratiform Lead-

Zinc Deposits, Short Course Handbook; Mineralization Associaion of Canada, vol. 8, ed. D.F. Sangster, pp. 1-29.

LIEW, M. 1979. Geochemical studies of the Goldenville Formation at Taylor Head, Nova Scotia. Unpublished M.Sc. thesis, Dalhousie University, Halifax, Nova Scotia.

MORGANTI, J.M. 1981. Sedimentary type stratiform ore deposits: some models and a new classification. Geoscience Canada, 8, pp. 65-75.

SANGSTER, D.F. 1981. Three potential sites for the occurrence of stratiform shale-hosted lead-zinc deposits in the Canadian Arctic. In Current Research, Part A; Geological Survey of Canada, Paper 81-1A, pp. 1-8.

SCHENK, P.E. 1978. Synthesis of the Canadian Appalachians. In Canadian-Appalachian Orogen of the North Atlantic Region. Geological Survey of Canada, Paper 78-13, pp. 111-136.

STUMPFL, E.F. 1979. Manganese haloes surrounding metamorphic stratabound base metal deposits. Mineralium Deposita, 14, pp. 207-217.

WALDRON, J.W.F. and JENSON, L.R. 1983. Stratigraphic correlation of Goldenville sediments by gradiometer. In Seventh Annual Open House and Report of Activities, Program and Summaries; Nova Scotia Department of Mines and Energy, Information Series no. 6, pp. 43-45.

WALKER, R. G. 1979. Turbidites and associated coarse clastic deposits. In Facies Models, ed. R.G. Walker; Geoscience Canada, Reprint Series 1, pp. 91-103.

ZENTILLI, M. and MACINNIS, I. 1983. Geochemical investigation of manganiferous beds associated with stratabound lead-zinc mineralization in the Meguma Group. In Seventh Annual Open House and Report of Activities, Program and Summaries; Nova Scotia Department of Mines and Energy, Information Series No. 6, pp. 65-68.

ZENTILLI, M., WOLFSON, I., SHAW, W. and GRAVES, M. 1984. The Goldenville-Halifax transition of the Meguma Group as a control for metallic mineralization. Geological Society of America, Abstracts with Programs 1984, 16, No. 1, pp. 73.

Maritime Sediments and Atlantic Geology

Vol. 22 April, 1986 No. 1

Lead Isotope Data for Gold-Bearing Veins and Their Host Metasedimentary Rocks of the Goldenville Formation, Eastern Nova Scotia

R.M. Farquhar, Department of Physics
University of Toronto, Toronto, Ontario M5S 1A7
S.J. Haynes, Nova Scotia Department of Mines and Energy
P.O. Box 1087, Halifax, Nova Scotia B3J 2X1
Present address: Department of Geological Sciences
Brock University, St. Catherines, Ontario L2S 3A1

Lead isotope analyses have been determined for galenas which occur in small quantities in quartz veins in the Goldenville Formation of the Meguma Terrane, and also for five whole rock samples from this formation. The ten least radiogenic galenas are homogeneous in isotopic composition, and they plot close to the average terrestrial growth curve of Stacey and Kramers and the "orogene" curve of Doe and Zartman. The mean model ages are 550 Ma (Stacey and Kramers) and 600 Ma (Doe and Zartman), which are in approximate agreement with the Cambro-Ordovician age of deposition of the sediments. The close position of the galena compositions to these average growth curves suggests that these compositions were established by mixing processes as envisaged in the Doe and Zartman "plumbotectonics" model. The isotopic analyses of the whole rocks indicate that small amounts of radiogenic lead are present in non-mineralized sections of the sedimentary sequence. Three galenas from veins in rocks metamorphosed to biotite and staurolite-andalusite grades, and from late veins (post-dating deformation, metamorphism and plutonism) are significantly more radiogenic than the majority of the samples. We interpret the isotopic characteristics of these galenas to be the result of extraction of lead from Meguma metasediments or of additions of radiogenic lead to less radiogenic lead during remobilization. Other interpretations consistent with the isotopic data are possible.

Des analyses aux isotopes de plomb ont été déterminé pour les galènes qui se trouvent en petite quantités dans les veines de quartz de la formation Goldenville du terraen Meguma, et aussi pour cinq échantillons de roches entières de cette formation. Les dix galènes les moins radiogeniques sont homogènes en composition isotopique, et elles ont une tracé proche de la courbe de croissance terreste moyenne de Stacey et Kramers, et de la courbe "orogène" de Doe et Zartman. Le âges moyens des modèles sont de 550 Ma (Stacey et Kramers) et de 600 Ma (Doe et Zartman), ce qui s'accorde approximativement avec l'âge Cambro-Ordovicien du dépot des sédiments. La position proche des compositions de la galène avec ces courbes moyennes de croissance, indique que ces compositions ont été établies par un processus de mélanges, comme le propose le modèle "Plumbotectonique" de Doe et Zartman. Les analyses isotopiques de roche entière indiquent que de petites quantités de plomb radiogénique sont présentes dans les sections non-minéralisées de la sequence sèdimentaire. Trois galènes, provenant de veines de roches métamorphosée au degrés de biotite et de staurolite-andalusite, et de veines avancées (post-datant la déformation, le métamorphisme et le plutonisme) sont d'une manière significative plus radiogéniques que la majorité des échantillons. Nous interprétons les caractéristiques isotopiques de ces galènes comme le résultat de l'extraction de plomb des metasédiments Meguma, ou a l'addition de plomb radiogénique au plomb moins radiogénique durant la remobilisation. D'autres interpretations en accord avec les donnés isotopiques sont possible.

INTRODUCTION

The Meguma Group is a metamorphosed sequence of alternating sandstones and shales of Cambro-Ordovician age which underlie much of southern Nova Scotia. The sequence contains gold and sulphide deposits and occurrences of stratabound, stratiform and vein types, the occurrence and relative ages of

MARITIME SEDIMENTS AND ATLANTIC GEOLOGY
22, 89-99 (1986)

0711-1150/86/010089-11$2.65/0

which are being studied in detail as part of a joint Nova Scotia Department of Mines and Energy - Geological Survey of Canada mineral resources project.

The mineral assemblages in a number of the deposits include small quantities of galena. In many other areas the lead isotopic composition of galena has been used to estimate mineralization age and to define, in a broad way, the source region (or regions) from which the lead has been derived. To date, the majority of the data on lead isotope abundances in galena have been obtained for massive sulphide deposits and vein occurrences. Many of the massive sulphides have been clearly volcanogenic. The host rocks of the sulphides in the Meguma Terrane appear to have been originally continentally-derived sediments, thus we have the opportunity of determining whether lead isotope ratios can be used to define a mineralization age and metal sources in a depositional environment very different from that for the host rocks of the massive sulphide deposits. Specifically, we have determined lead isotope abundances in the eastern Meguma Terrane for (1) galenas in gold-bearing quartz veins hosted by the Goldenville Formation, and, (2) a limited number of whole-rock samples of Goldenville metasedimentary rocks both adjacent to and distant from auriferous quartz veins.

GEOLOGICAL SETTING

The locations of gold deposits in the Meguma Terrane, and of the sample areas are given in Figure 1. The Meguma Terrane (Schenk, 1978) comprises a thick metasedimentary sequence (Meguma Group consisting of the Goldenville Formation overlain by the Halifax Formation). The Goldenville Formation is a thick flyschoid sequence of wackes with thin silt and slate interbeds. The Halifax is a thick slate succession with minor sand and silt units. The Meguma Group is considered to be turbiditic in origin but details of deposition are controversial (Phinney, 1961; Schenk, 1970, 1971; Harris and Schenk, 1975; Smith, 1981; Stow, 1982; Waldron, 1983). The gold deposits are located mainly in the upper part of the Goldenville Formation (Faribault, in Malcolm, 1929).

In the Eastern Meguma domain, (Figure 2) low pressure-high temperature pyreneean metamorphism (Keppie and Muecke, 1979) ranges from chlorite grade in the southwest (Wine Harbour) through biotite (Isaacs Harbour, Goldenville) and garnet to staurolite-cordierite-andalusite isograds (Forest Hill). The chlorite grade metamorphism is associated with the deformations accompanying Acadian folding (O'Brien, 1983). However, at higher grades the characteristic mineral isograds are associated with a later period of static metamorphism (Smith, 1981). This metamorphism may be related to the same tectono-thermal event that resulted in post-folding intrusion of Devonian granitoid plutons. In the north (amphibolite facies), these plutons and the Meguma Group metasedimentary rocks were subsequently strongly deformed by east-west zones of ductile shear (Keppie, 1983; Haynes, 1984).

The last major tectonic event was brittle deformation related to left-lateral movement on the Country Harbour fault. At Widow Point (Figure 1) this is associated with stockwork chlorite-carbonate veining and retrograde alteration of amphibolite facies assemblages (Haynes, 1984).

QUARTZ VEINS

In the area of greenschist facies metamorphism, eleven different quartz-vein polytypes are present (Haynes, 1983). The earliest vein polytypes predate the cleavages associated with Acadian folding, and include the most auriferous polytypes (stratiform, stratabound and side). Other vein polytypes were emplaced syn- or post-folding and are essentially devoid of gold.

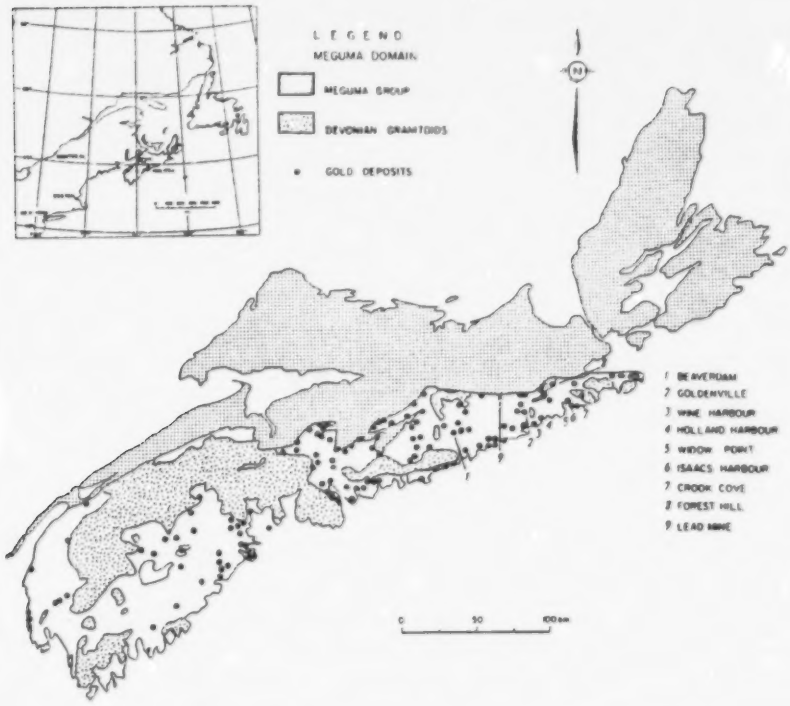

Figure 1. Gold deposits in the Meguma domain, and sample locations from which galena and rock specimens were obtained.

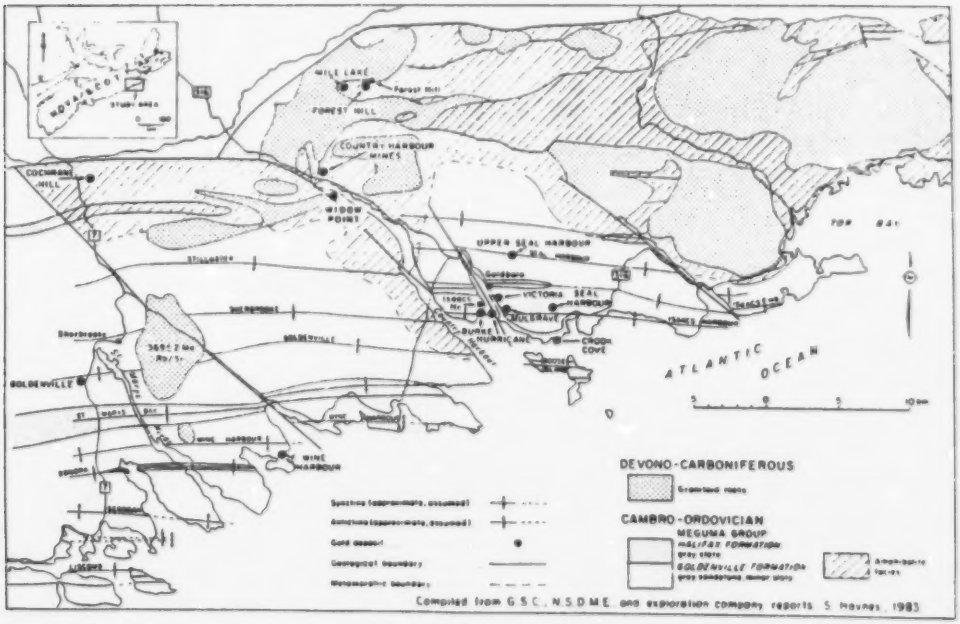

Figure 2. Gold deposits and sample locations in the Eastern Meguma region showing locations in more detail.

In the northern part of the eastern Meguma Terrane (amphibolite facies) a further period of quartz veining and gold mineralization is associated with intrusion of the granitoid plutons (Smith, 1983; Haynes, 1984). In this region the quartz veins are strongly deformed (bedding-parallel transposition) by the post-granitoid ductile shear, although remnants of the original relationships of quartz veins to Acadian fold structures are preserved at Forest Hill in thick wacke units which acted as semi-rigid blocks during ductile shear deformation (Haynes, 1984).

The final period of quartz vein formation is evident as several sets of post-folding/metamorphism veins in the greenschist facies (late and ac veins of Haynes, 1983), veins that postdate ductile shear in the amphibolite facies (ac veins of Smith, 1983), quartz stringers associated with the chlorite-carbonate veins and alteration adjacent to the Country Harbour fault (Haynes, 1984), and a cross-cutting lead vein on the East St. Mary's River (Lead Mine, Figure 1). Although there is no direct evidence, all these late veins may be equivalent in age, possibly related to the tectonic event that resulted in the extensive northwest-southeast strike-slip faulting (Hercynian ?) prevalent throughout the Meguma Terrane.

Descriptions of the veins sampled and their locations are given in Table 1. Galena was only observed in stratiform, stratabound and side veins. Stratiform veins are bedding-parallel quartz-carbonate veins displaying fine laminar textures and, often, columnar cstructures. Typically, they contain silicate mineralogies identical to the regional metamorphism isograd (e.g. chlorite at Wine Harbour; andalusite at Forest Hill). Stratabound veins are restricted to specific horizons, but may locally crosscut bedding. Typically, they are massive and their wallrocks and inclusions exhibit marked arsenopyritization, sericitization and silicification. Side veins are veins tapering away from T-junctions with stratiform or stratabound polytypes. Normally, they are present on the stratigraphically lower wall of stratiform veins and on both walls of stratabound veins. They display mineralogies and wall rock alteration effects which are similar to their "parent" vein.

GOLDENVILLE METASEDIMENTS

Samples F4WH23 and 25 (Table 1) represent arsenopyrite-sericite-silica flooding alteration of Goldenville Formation wallrocks about an auriferous stratabound vein at Wine Harbour. Samples F4HR3DH5, 7 and 14 (Table 1) are different types of Goldenville Formation metasedimentary rocks collected at Holland Harbour, distant from known gold mineralization.

These samples were analyzed to compare lead isotope values resulting from the addition of radiogenic lead from <u>in situ</u> decay of uranium and thorium in unmineralization Goldenville sedimentary rocks, with those for vein galenas and possible "overprint" effects in the alteration zones of stratabound veins.

ISOTOPIC ANALYSES

In most of the specimens visible galena occurred as discrete blebs, which were hand picked to provide sufficient material for analysis. Galenas were dissolved in ultra-pure HCl and HNO_3, and the lead separated from other metals in ion exchange columns. Approximately 800 nanograms of lead were deposited with phosphoric acid on a silica gel substrate mounted on a single rhenium filament. The mass spectrometer used for the isotopic measurements was an instrument using 90° deflection, and a radius of curvature of 30 cm. Each analysis consisted of 50-70 scans over the Pb mass spectrum, and all data have been adjusted by applying a mass fractionation correction of 0.098% per

TABLE 1

DESCRIPTION AND LOCATION OF ANALYZED SAMPLES

Sample #	Deposit	Description and Sample Type
Chlorite Grade metamorphic zone		
F4BI8	Wine Harbour	Au Stratiform vein in slate, galena
F4WH26	"	Au stratabound vein in altered
F4WH23	"	Hanging wall alteration zones to
F4WH25	"	Footwall alteration zone to F4WH26, rock lead
F4HR3DH5	Holland Harbour	Laminated meta-siltstone with pyrite, rock lead
F4HR3DH7	"	Fe/Mn concretions, in meta-wacke, rock lead
F4HR3DH14	"	Coarse meta-wacke, rock lead
Biotite Grade metamorphic zone		
HGV1	Goldenville	Au stratiform, galena
F4BH10	Isaacs Harbour (Bakers House)	Au stratiform, galena
F4BL21	Isaacs Harbour (Burke Lead)	Side vein to Au stratiform vein, galena
F4GF5	" (Goldfinch, dump sample)	Stratabound?, galena
F4GF14	" " "	Qtz-carbonate vein (stratiform?), galena
Staurolite-Andalusite Grade metamorphic zone		
FHL3N8/8	Forest Hill (School House Lead)	Au stratiform in metawacke, galena
FH9N15	" (Kennedy Lead)	Au stratiform in slate, galena
(Granite Contact Aureole)		
HBDV23	Beaverdam	Au Stratiform, galena
Chlorite Retrograding of Staurolite-Andalusite metamorphic zone		
WP2	Widow Point	Au stratiform, galena
Post-Folding/Metamorphism		
F4SB2	Isaacs Harbour (Ragged Point)	late quartz vein, galena
HLM1	Lead Mine	Pb-quartz, galena

mass unit, determined by replicate analyses of standard lead SRM-981. Details of the procedure are given by Fletcher (1979).

The isotopic ratios for the galenas and sulphides are listed in Table 2. Several of the samples (F4GF5, HBDV23 and HLM1) are significantly different in isotopic composition from the remainder. Because the Meguma Group has been deformed and metamorphosed, it seemed possible that these differences in isotopic composition could have been produced by the addition of radiogenic lead to primary galena. To estimate the amounts of radiogenic lead in the sedimentary rocks, five whole rock samples were analysed for lead (by isotope dilution), and their isotopic ratios determined. Lead was extracted by dissolving, in HF and HNO_3, approximately 300 mg splits of slices cut from drill cores. Although the

TABLE 2

LEAD ISOTOPE RATIOS FOR ANALYZED SAMPLES

	Sample	Pb(p.p.m)	$^{206}Pb/^{204}Pb$	$^{207}Pb/^{204}Pb$	$^{208}Pb/^{204}Pb$
Chlorite Metamorphic Zone	F4B1B	galena	$17.74_5 \pm .02_5$	$15.56_3 \pm .02_4$	$37.81 \pm .08$
	F4Wh26	"	$17.77_5 \pm .02_5$	$15.56_2 \pm .02_4$	$37.83 \pm .08$
	F4WH23	17.0	$18.11 \pm .07$	$15.61 \pm .06$	$38.21 \pm .14$
	F4WH25	9.5	$18.56 \pm .17$	$15.64 \pm .13$	$18.6 \pm .4$
	F4HR3DH5	7.3	$18.94 \pm .03$	$15.64 \pm .02$	$39.60 \pm .08$
	F4HR3DH7	38.7	$17.91 \pm .02$	$15.56 \pm .02$	$38.02 \pm .07$
	F4HR3DH14	ND	$19.01 \pm .07$	$15.65 \pm .05$	$39.22 \pm .16$
Biotite Metamorphic Zone	HGV1	galena	$17.78_9 \pm .02_0$	$15.56_8 \pm .02_1$	$37.82 \pm .08$
	F4BH10	"	$17.77_0 \pm .01_7$	$15.54_8 \pm .01_6$	$37.80 \pm .05$
	F4BL21	"	$17.77_0 \pm .01_8$	$15.55_0 \pm .01_9$	$37.82 \pm .07$
	F4GF5	"	$17.92_8 \pm .02_3$	$15.56_2 \pm .02_2$	$37.97 \pm .07$
	F4GF14	"	$17.78_4 \pm .02_2$	$15.56_4 \pm .02_3$	$37.86 \pm .07$
Staurolite-andalusite Metamorphic Zone	FHL3N8/B	galena	$17.81_7 \pm .01_8$	$15.56_7 \pm .02_0$	$37.88 \pm .07$
	FH9N15	"	$17.78_2 \pm .01_8$	$15.56_7 \pm .01_9$	$37.87 \pm .07$
	HBVD23	"	$18.23_9 \pm .02_0$	$15.60_3 \pm .02_0$	$38.06 \pm .07$
Chlorite retrograde Staurolite-andalusite Metamorphic Zone	WP2	"	$17.77_6 \pm .03_5$	$15.55_1 \pm .02_3$	$37.78 \pm .08$
Post folding veins	F4SB2	"	$17.83_9 \pm .01_9$	$15.56_8 \pm .02_0$	$37.94 \pm .07$
	HLM1	"	$18.22_2 \pm .02_0$	$15.60_6 \pm .02_1$	$38.35 \pm .07$

precision of the isotopic data is not as high for the whole rocks as for the galenas, the results indicate that significant amounts of radiogenic lead have been generated in the sedimentary rocks. The lead concentrations and isotopic ratios are included in Table 2.

LEAD ISOTOPIC DATA

The isotopic data for the Meguma galenas and sulphides are plotted on Figures 3a and 3b as ratios of $^{207}Pb/^{204}Pb$ and $^{208}Pb/^{204}Pb$ against $^{206}Pb/^{204}Pb$. On both figures most of the points lie in compact groups, but several analyses have substantially higher $^{206}Pb/^{204}Pb$, and $^{207}Pb/^{204}Pb$ ratios. Shown for reference on Figures 3a and 3b are growth curves from Doe and Zartman (1979). These curves define the average lead isotopic evolution of three reservoirs, the upper crust, the mantle and the orogene. In Doe and Zartman's "plumbotectonics" model, the orogene is composed of materials input from the mantle, upper crust and lower crust, and is considered to represent

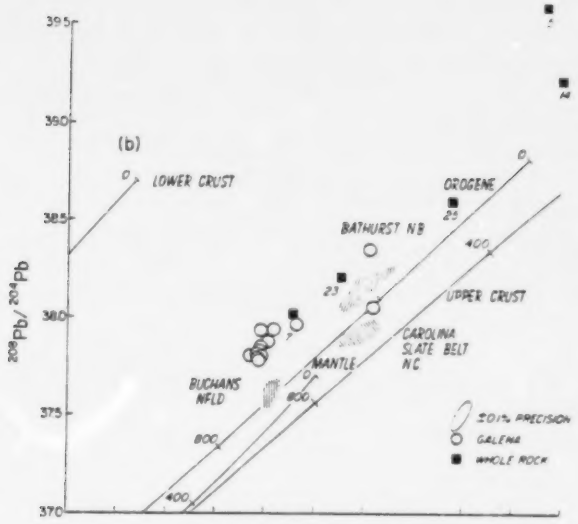

Figure 3a. $^{207}Pb/^{204}Pb$ - $^{206}Pb/^{204}Pb$ plot for Meguma galena and whole rocks. The ±0.1% error ellipse denotes the typical uncertainty in accuracy (2σ) of the isotopic ratios. The uncertainties for samples 23 and 25 are substantially larger (see Table 2). Growth curves are plotted from the data of Doe and Zartman (1979). Isotopic data fields for Bathurst, Buchans and the Carolina Slate Belt are included for comparison. See text for data sources.

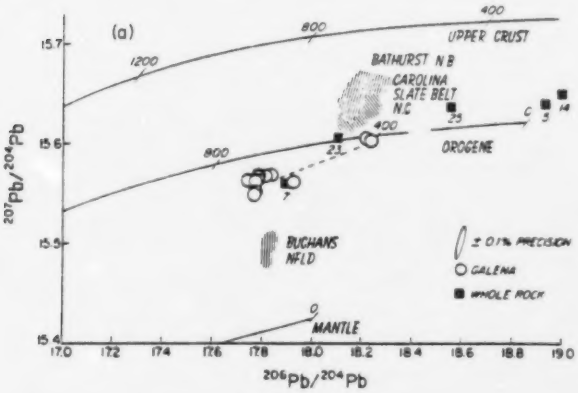

Figure 3b. $^{208}Pb/^{204}Pb$ - $^{206}Pb/^{204}Pb$ plot for Meguma galenas and whole rocks. The ±0.1% error ellipse denotes the typical uncertainty in accuracy (2σ) of the isotopic ratios. The uncertainties for samples 23 and 25 are substabtially larger (see Table 2). Growth curves are plotted from the data of Doe and Zartman (1979). Isotopic data fields for Bathurst, Buchans and the Carolina Slate Belt are included for comparison. See text for data sources.

the reservoir from which many ore deposits have been derived. To put the Meguma isotopic data in the context of similar data from relatively nearby deposits, Figures 3a and 3b also include the fields (but not individual analyses) defined for the volcanic and volcano-sedimentary-hosted sulphides at Buchans Mine, Newfoundland (Doe and Rohrbough, 1977; Farquhar and Fletcher, 1980), at Bathurst, New Brunswick (Ostic et al., 1967; Farquhar, unpublished data, Swinden and Thorpe, in press), and in the Carolina Slate Belt (Kisn and Feiss, 1982).

The rock lead isotopic data are shown on 207-206-204 and 208-206-204 plots in Figures 3a and 3b. Although the radiogenic enrichments of the lead in these rocks are not large, a linear fit to the 207-206-204 data can be made and the slope of the line determined. The value of the slope (0.078 ± .017 (1σ) York, 1969) is based on the data for the samples F4HR3DH5, 7, and 14. Although this value is not well defined, it can serve to place limits on the age of some of the detrital minerals in the original sediments.

DISCUSSION

Sediments of the Meguma Terrane were deposited in late Cambrian - early Ordovician times and consist of sequences of turbidites, slates, siltstones and sandstones. Following deposition these sequences were multiply deformed, metamorphosed and intruded by granitic plutons. Poole (1971) reports K-Ar ages of 475 - 500 Ma on two "detrital" muscovites from the Goldenville Formation (which hosts the galenas analysed in this study). An age of 400 - 415 Ma for the metamorphism associated with the Acadian orogeny was determined by Reynolds and Muecke (1978), through K-Ar stepwise outgassing measurements on slates. Intrusion of the granitic plutons followed at 369 ± 2 Ma, as defined by Rb-Sr whole rock isochron measurements (Keppie, 1983).

The rock samples for which we have isotopic data (Table 2) are from the chlorite grade metamorphic zone. If alteration of detrital minerals has taken place, the degree of this alteration will be minimal at this level of metamorphism. If we interpret the isotopic variations among these rock samples to result from radiogenic lead generated in small amounts of detrital minerals, then the slope of the 207-206-204 rock lead plot (Figure 3a) gives the primary age of these minerals. The value we compute for this age is approximately 1.2 ± 0.5 (1σ) Ga. The very large uncertainty in this figure is mainly a result of the relatively small proportion (less than approximately 4%) of radiogenic lead in the rocks.

Detailed studies have been made of the formation of the gold-bearing veins in relation to the structural deformations and metamorphic alterations which have modified the rocks of the Goldenville Formation (Haynes, 1983). These indicate that the earliest, Au-bearing stratiform and stratabound veins predated or accompanied the earliest deformation events. The isotopic compositions of the galenas associated with these veins are uniform and define a cluster of least radiogenic values. Using the time-scales on the orogene growth curves in Figures 3a and 3b, the mean "model" age for this cluster is 600 ± 50 Ma. This value is, of course, model-dependent. The Stacey and Kramers (1974) average growth curve, which is based on a much less complex evolutionary development scheme than that proposed by Doe and Zartman, gives a mean "model" age of 550 ±50 Ma for the least radiogenic Meguma galenas. Considering that both models are based on world-wide data and only represent the average evolution of lead isotope ratios, the mean "model" age computed using either approach seems remarkably close to the known age of deposition of the sedimentary rocks which enclose the mineral deposits. For two of the three other lead isotope fields outlined on Figure 3a, the time scale of the plumbotectonics model appears to give ages for the mineral deposits which are not grossly different from the ages of the host rocks. Buchans, Newfoundland, associated with well-dated Silurian volcanic rocks (Bell and Blenkinsop, 1981) has a "model" age of 400 ± 50 Ma. The age for Bathurst, New Brunswick (middle Ordovician) is 550 ± 50 Ma. The model age for the least radiogenic Carolina Slate Belt ores is about 480 Ma, less than the accepted middle Cambrian age of the enclosing sedimentary rocks. Kish and Feiss (1982) presented an alternative model to explain this discrepancy.

By comparison with the other data sets on Figures 3a and 3b, the majority of the Meguma galenas have slightly lower $^{206}Pb/^{204}Pb$ and $^{207}Pb/^{204}Pb$ ratios, and higher $^{208}Pb/^{204}Pb$ values. No lead isotopic data are available for similar sediment-hosted mineral deposits with which to compare these characteristics, and hence it is not possible to determine whether the differences are significant clues to the type of source rocks from which the lead has been derived.

Most of the galenas in the rocks of the Goldenville Formation have a single isotopic signature. However, three samples have significantly more radiogenic isotopic ratios, and all of these are located in metamorphic zones at biotite or higher grade or in late veins. There are three different models for interpreting these more radiogenic galenas. They could result from the mixing of lead of the less radiogenic type with lead from another source, at the time of intrusion of the late quartz veins. Two component mixtures will give rise to linear distributions on isotopic plots such as Figures 3a and 3b. Although the isotopic ratios are linearly distributed (within the limits of accuracy) on Figure 3a, the $^{208}Pb/^{204}Pb$ ratios do not lie on a straight line. A mixing process seems to be an unlikely hypothesis. A second possibility is that all of the leads (radiogenic and non-radiogenic) were deposited essentially simultaneously

after being extracted from underlying rock units within the sedimentary pile. The $^{207}Pb/^{204}Pb$ - $^{206}Pb/^{204}Pb$ ratios for the whole rocks (Figure 3a) are linearly related and extend over approximately the same range of values as the radiogenic galenas. The data distribution for these galenas has a ^{207}Pb - ^{206}Pb slope of .14 ± .09 (1σ) (York, 1969), a value which could result from uranium decay between approximately 1.9 Ga and .5 Ga. If we consider only the isotopic data and the very large uncertainties in the age estimates it is conceivable that the radiogenic galenas could have been extracted approximately 500 Ma age from nearby Meguma sediments. The $^{208}Pb/^{204}Pb$ - $^{206}Pb/^{204}Pb$ ratios in the whole rocks are variable to roughly the same degree as observed in the radiogenic galenas. However, our whole rock isotopic data also suggests that the Meguma units have remained at least partially closed to uranium, thorium and lead losses under low grade metamorphic conditions. This suggests that a thermal energy source would be necessary to extract substantial amounts of lead from the sediments and there is no evidence that a source of this kind existed within or adjacent to the Meguma sedimentary rocks at the time the earliest stratiform and stratabound deposits were emplaced. This problem leads us to consider a variant of this hypothesis, that the more radiogenic galenas were generated later than those of less radiogenic composition. The whole rock data shown in Figures 3a and 3b suggest that lead of isotopic compositions similar to those in the more radiogenic galenas was available in Meguma sandstones. The isotopic data for these rocks are not sufficiently precise to define accurately the time at which the extraction of the lead could have taken place. We favour this "later-extraction" hypothesis because the more radiogenic galenas occur in the biotite and higher grade metamorphic rocks and post-folding veins. The metamorphism is an indication that energy sources must have existed in the areas or at the times when the more radiogenic galenas were being deposited. The lead in these galenas could be the product of complete extraction from the sedimentary rocks, or a mixture of radiogenic lead selectively removed from these rocks and mixed with lead dissolved from pre-existing galenas of less radiogenic composition.

CONCLUSIONS

Field studies of the mineralization in the quartz veins in the Goldenville Formation (Haynes, 1983) indicate that the stratiform, stratabound and side veins predate the main period of Acadian deformation. The lead in galenas which occur in the least metamorphosed of these vein types, have a Pb isotopic homogeneity which suggests that the metal source or sources were well-mixed prior to deposition in their primary sites. The position of the isotopic ratios of these galenas close to the orogene growth curve, implies that a significant fraction of the lead has been derived from crustal sources, and lends weight to the usefulness of the orogene concept as a basis for interpreting ore deposition in sedimentary environments. The time scale associated with the orogene growth curve appears to give the approximate age of sedimentation and primary ore deposition if the least radiogenic lead isotopic ratios are used.

We interpret the lead isotope data to suggest that in the Goldenville Formation more recent geological events have given rise to some alteration of lead isotope ratios. The more radiogenic galenas occur in metamorphic zones at biotite, and staurolite-andalusite grades, and in late veins, and the isotopic data for these galenas and for whole rocks are consistent with either local derivation and redeposition or extraction and mixing of radiogenic lead with primary galena. In theory it is possible to put limits on the time at which the extraction process took place. However, the

amounts of radiogenic lead incorporated are small and the data are rather imprecise with the result that the time resolution of the method is too low to be useful. Remobilization during metamorphism could have resulted in the alteration of some but not necessarily all of the galenas, so there is not a one-to-one correspondence between isotopic alteration and those veins which are recognizably later than the primary polytypes.

It should be recognized that the isotopic data set is still rather small, and that several alternative interpretations of the isotopic results are possible. This is particularly true for the more radiogenic galenas, which might be contemporaneous with the less radiogenic sulphides or be derived later from the Meguma sedimentary rocks through complete extraction or mixing with earlier deposited galenas. Futher isotopic work would be necessary to determine which of these alternatives is correct.

ACKNOWLEDGEMENTS

Funding for this project was provided under the 1981-84 Canada-Nova Scotia Mineral Agreement, and through an NSERC grant to RMF. We thank P.R. Kuybida and P.E. Smith for assistance with sample preparation, and R.I. Thorpe for a helpful review of the original manuscript.

BELL, K. and BLENKINSOP, J. 1981. A geochronological study of the Buchans area, Newfoundland. In The Buchans ore bodies: fifty years of geology and mining, eds. E.A.Swanson, D.F. Strong, and J.G. Thurlow; Geological Association of Canada, Special Paper 22, pp. 91-111.

DOE, B.R. and ROHRBAUGH, R. 1977. Lead isotope data bank. United States Geological Survey, Open-file report 79-661, 137 p.

DOE, B.R. and ZARTMAN, R.E. 1979. Plumbotectonics, the Phanerozoic. In Geochemistry of hydrothermal ore deposits, 2nd ed., ed. H.L. Barnes, Wiley-Interscience, New York, pp. 22-70.

FARQUHAR, R.M. and FLETCHER, I.R. 1980. Ore-lead isotopes and Grenville plate tectonics. In The continental crust and its mineral deposits, ed. D.W. Strangway, Geological Association of Canada, Special Paper 20, pp. 771-788.

FLETCHER, I.R. 1979. A lead isotope study of lead-zinc mineralization associated with the Central Metasedimentary Belt of the Grenville province. Ph.D. thesis, Department of Physics, University of Toronto, Toronto, Ont. 165 p.

HARRIS, I.M. and SCHENK, P.E. 1975. The Meguma Group. In Ancient sediments of Nova Scotia; Eastern Section, ed. I.M. Harris, Economic Paleontologists and Mineralogists, Guidebook.

HAYNES, S.J. 1984. Polygenesis of gold deposits, eastern Meguma Terrane. Nova Scotia Department of Mines and Energy Report 84-1, pp. 215-224.

HAYNES, S.J. 1983. Typomorphism of turbidite-hosted auriferous quartz veins, southern Guysborough County, Nova Scotia Department of Mines and Energy Report 83-1, pp. 183-224.

KEPPIE, J.D. 1983. Introduction to the geology of Nova Scotia and the Meguma Terrane; Guidebook, Gold Deposits in the Meguma Terrane of Nova Scotia; Canadian Institute of Mining and Metallurgy, pp. 7-17.

KEPPIE, J.D. and MUECKE, G.K. 1979. Metamorphic map of Nova Scotia; Nova Scotia Department of Mines and Energy, Scale 1:1,000,000.

KISH, S.A. and FEISS, P.G. 1982. Application of lead isotope studies to massive sulfide and vein deposits of the Carolina Slate Belt. Economic Geology, 77, pp. 352-363.

MALCOLM, W. 1929. Gold fields of Nova Scotia. Geological Survey of Canada Memoir 156, 253 p. (reprinted 1976 as Memoir 385).

O'BRIEN, B.H. 1983. The structure of the Meguma Group between Gegogan Harbour and Country Harbour, Guysborough county. Nova Scotia Department of Mines and Energy Report 83-1, pp. 145-182.

OSTIC, R.G., RUSSELL, R.D. and STANTON, R.L. 1967. Additional measurements of the isotopic composition of lead from stratiform deposits. Canadian Journal of Earth Sciences, 4, pp. 245-269.

PHINNEY, W.C. 1961. Possible turbidity-current deposit in Nova Scotia. Geological Society of America Bulletin, 72, pp. 1453-1454.

POOLE, W.H. 1971. Graptolites, copper and potassium-argon in Goldenville Formation, Nova Scotia. Geological Survey of Canada, Paper 71-1A, p. 9.

REYNOLDS, P.H. and MUECKE, G.K. 1978. Age

studies on slates: applicability of the $^{40}Ar/^{39}Ar$ stepwise outgassing method. Earth and Planetary Science Letters, 40, pp. 111-118.

SCHENK, P.E. 1970. Regional variation of the flysch-like Meguma Group (Lower Paleozoic) of Nova Scotia; compared to recent sedimentation off the Scotia Shelf. Geological Association of Canada Special Paper, 7, pp. 127-153.

SCHENK, P.E. 1971. Southeastern Atlantic Canada, northwestern Africa and continental drift. Canadian Journal of Earth Sciences, 8, pp. 1218-1251.

SCHENK, P.E. 1978. Synthesis of the Canadian Appalachians; Geological Survey of Canada, Paper 78-13, pp. 111-136.

SMITH, P.K. 1981. Geology of the Sherbrooke area, Guysborough County, Nova Scotia. Nova Scotia Department of Mines and Energy Report 81-1, pp. 77-94.

STACEY, J.S. and KRAMERS, J.D. 1974. Approximation of terrestrial lead isotope evolution by a two-stage model. Earth and Planetary Science Letters, 26, pp. 207-221.

STOW, D.A.V. 1982. Toward an anatomy of fine-grained sediments. Episodes, 1982, No. 3, pp. 3-4.

SWINDEN, H.S. and THORPE, R.I. In press. Variations in style of volcanism and massive sulfide deposition in early-middle Ordovician island arc sequences of the Newfoundland central mobile belt. Economic Geology.

WALDRON, J.W.F. 1983. Sedimentary features of some Goldenville Formation sandstones, Sherbrooke area, Eastern Nova Scotia. Nova Scotia Department of Mines and Energy Report 83-1, pp. 257-261.

YORK, D. 1969. Least squares fitting of a straight line with correlated errors. Earth and Planetary Letters, 5, pp. 320-324.

Maritime Sediments and Atlantic Geology

Vol. 22 April, 1986 No. 1

A Re-Appraisal of the Alaskite/Muscovite-Biotite Granite Suite of Halifax County, Nova Scotia

T.E. Smith, D. Peck, C.H. Huang and P.E. Holm
Department of Geology
University of Windsor, Windsor, Ontario N9B 3P4

New mapping, petrography and geochemistry, including REE analyses, indicate that a much larger area of muscovite-biotite granite and fewer alaskite dykes occur in the Halifax - St. Margarets Bay area than was originally thought. The rocks of this area were formed by fractional crystallization of quartz, plagioclase, biotite, zircon, ilmenite, apatite, and monazite. The presence of monazite in the fractional crystallization assemblage is essential to account for the strong depletion of the rare earth element contents and fractionation of the light rare earth elements noted in these rocks. They have been affected by a pervasive hydrothermal recrystallization and by localized development of pegmatitic vugs and a greisen-bordered sheeted vein complex. A greisen-bordered sheeted vein complex has developed in part of the muscovite-biotite granite south of Sandwich Point, and although this zone shows all of the features characteristic of the mineralization elsewhere in the batholith, it is barren.

Une nouvelle cartographie, pétrographie et géochimie, comprenant des analyses REE, indiquent une région plus étendue de granite de muscovite-biotite et moins de dikes d'alaskite qu'on ne le pensait auparavant, dans la region de Halifax-St. Margarets Bay. Les roches de cette région ont été formées par le cristalisation fractionnée de quartz, de plagioclase, de biotite, de zircon, d'ilmenite, d'apatite, et de la monazite. La présence de monazite dans l'assemblage de cristallisation fractionnée est essentielle pour expliquer le fort épuisement du contenu d'élément terre-rare, et le fractionnement des éléments légers terre rare, qui ont été relevés dans ces roches. Elles ont été affectées par la recristalisation hydrothermale perméable et par des développements locaux de Druses pegmatitiques et par un complexe stratifé de veines à bordures greisen. Un complexe de veines stratifées, à bordures greisen s'est formé dans une partie du granite muscovite-biotite, au sud de Sandwich Point, et même si cette zone montre tous les traits caracteéristiques de la minéralisation d'autres parties du batholithe, elle est stérile.

INTRODUCTION

The South Mountain Batholith outcrops over much of southwestern Nova Scotia, from just west of Yarmouth to Halifax (Fig. 1). The early workers suggested that it is made up of two suites of granites characterized by different petrography and mode of occurrence (Gossip 1864, p. 49, Honeyman, 1883, p. 60, Malcolm, 1914, pp. 78-79, Wright 1931, p. 384). Zoned plutons of coarse-grained biotite granodiorite, biotite granite and muscovite-biotite granite are cut by large dykes of finer grained alaskite and leucogranite (Cormier and Smith, 1973, Smith 1974, McKenzie and Clarke, 1975, Smith and Turek, 1976, Smith 1979a,b). These rocks are stanniferous, peraluminous (S-type) granites (Smith and Turek 1975, 1976, McKenzie and Clarke, 1975, Smith 1979a, b, Smith et al., 1982). The magmas from which they formed were derived from a (largely) metasedimentary source area (Smith and Turek, 1976, Smith, 1979a, b, Longstaffe and Smith ,1978, Longstaffe et al., (1980). There is evidence that tin and uranium mineralization is associated with the most highly differentiated rocks of the suite, and especially with a paraintrusive suite of rocks (biotite leucogranites, argillized and sericitized granites, albitized granites, albitites, and

MARITIME SEDIMENTS AND ATLANTIC GEOLOGY
22, 101-116 (1986)

0711-1150/86/010101-16$3.40/0

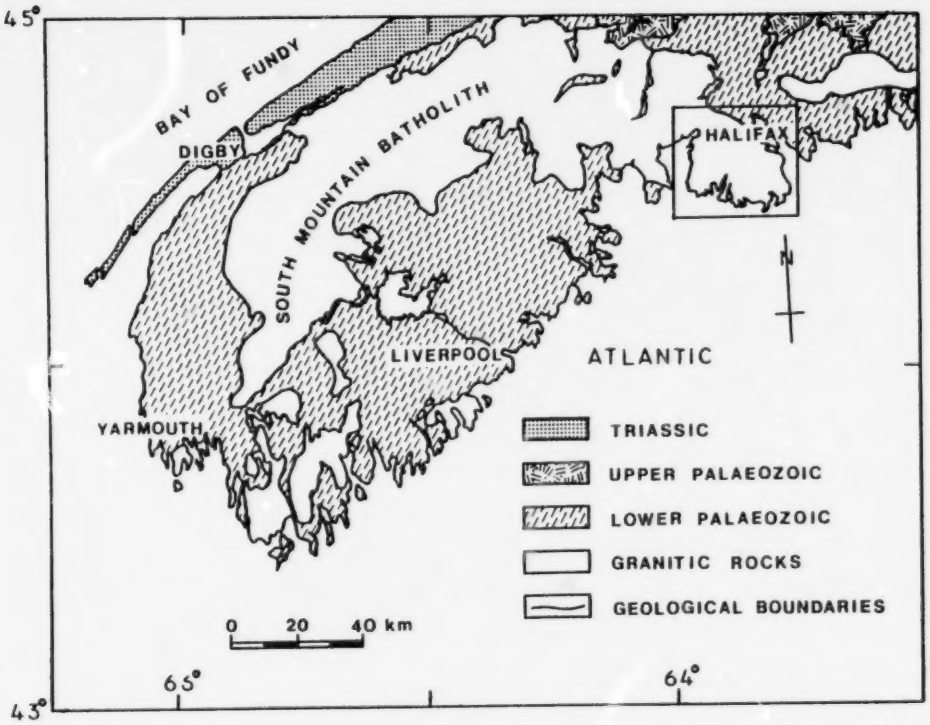

Figure 1 - The geology of southwestern Nova Scotia, showing the outcrop area of the South Mountain Batholith.

greisen) (Smith and Turek, 1976, Chatterjee and Muecke 1982, Smith et al., 1982).

The field relationships have generally been confirmed by geochronological studies (Fairburn, et al., 1960, 1964, Lowdon, 1960, Lowdon, et al., 1963, Cormier and Smith 1973, Clarke and Halliday, 1980), which also suggest that intrusion took place in a series of episodes extending from the early Devonian into the Carboniferous. The details of the intrusive sequence are still poorly known because the majority of the batholith has not yet been mapped. There may be two separate suites of granites in the batholith, only the later of which produced tin and uranium mineralization (Chatterjee et al., 1983).

The best exposed part of the batholith is in the vicinity of Halifax, where a complete suite of the granitic rocks, and paraintrusive rocks are present. Geochemical, geochronological, and stable isotope studies have already been carried out one some of these rocks (Cormier and Smith, 1973; Smith, 1974, 1975, 1979a, b; Smith and Turek, 1976; Longstaffe et al., 1980; Smith et al., 1982). In this study new field and petrographic observations, together with new geochemical data including rare-earth elements (REE) are used to clarify the evolution of the granitic rocks and the paraintrusive suite in this area.

GEOLOGICAL SETTING

The South Mountain Batholith is intruded into a conformable pile of lower Paleozoic metasedimentary and metavolcanic rocks at least 12 km thick (Taylor and Schiller, 1966). The stratigraphic relationships indicate that intrusion, crystallization, uplift and erosion of the batholith took place between Emsian and Tournaisian (?) times (Clarke and Halliday, 1980;

Chatterjee and Muecke, 1982). The available geochronological data confirm that the emplacement of the granites took place during this time interval. The ages cluster around 370-380 Ma (Reynolds et al., 1980) and range from 395-336 Ma (Cormier and Smith, 1973, recalculated by Keppie and Smith, 1978, using decay constants and isotopic abundances after Steiger and Jager, 1977).

GRANITIC ROCKS OF THE HALIFAX - ST. MARGARETS BAY AREA

a) Mineralogy and Petrography

The initial mapping of this area was carried out in detail on the well exposed, eastern side of the peninsula (Smith, 1974). The conclusions drawn from this work were used to interpret the reconnaissance mapping of the poorly exposed, western half of the peninsula (Smith, 1974, Fig. 1). It was suggested that a zoned pluton, comprising biotite-granodiorite, porphyritic biotite-granite, and muscovite-biotite granite occupied the whole peninsula and was cut by five large dykes of alaskite, four of which occur in the western half of the area.

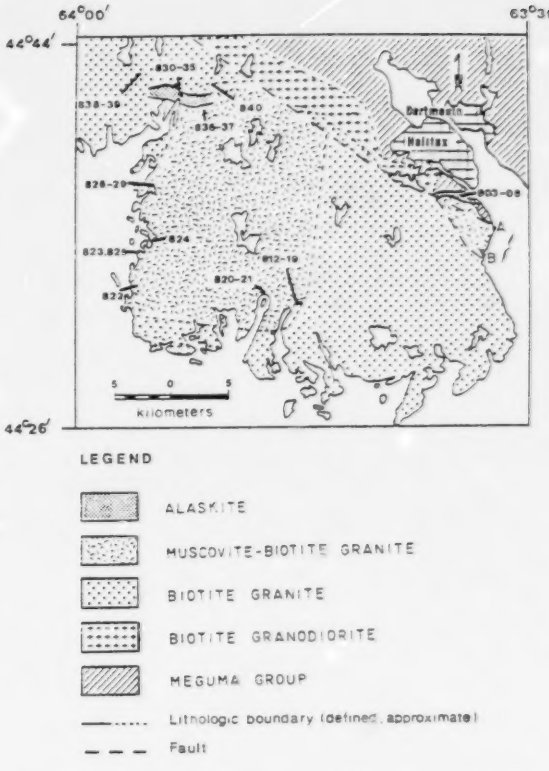

Figure 2 - Geological map of the area between Halifax and St. Margarets Bay, showing sample locations NS 803-806 Ferguson Cove, 812-821 Shad Bay, 822-825 Hacketts Cove, 826-829 Seabright, 830-840 Upper Tantallon. A - Sandwich Point, B - Herring Cove.

Recent mapping, combined with airborne gamma ray spectrometric patterns (Ford, 1982), and supported by petrographic and geochemical data, has led to a complete revision of the distribution of the rock types in the western half of the peninsula (Fig. 2). The interpretation of the relationships between the rock types remains unchanged. Most of this area is underlain by a leucocratic, even-grained to sparsely porphyritic, muscovite-biotite granite. It is surrounded by a comparatively narrow zone of porphyritic biotite granite to the north and south and a much wider zone. The porphyritic biotite granite grades into biotite granodiorite to the north and south (Fig. 2). The boundary between the muscovite-biotite granite and the porphyritic biotite granite is only exposed near Halifax where the two rocks appear to grade into each other (Smith 1974, p. 651). Elsewhere the boundary on the map is approximate. This gradation is confirmed by the variation in the proportions of the principal minerals and accessories present in the rock. There is a systematic decrease in quartz, plagioclase, and biotite and increase in potash-feldspar from the granodiorite to the muscovite-biotite granite (Table 1). Two large porphyritic alaskite dykes occur, one at the north eastern edge of the intrusion and another in the northwest (Fig. 2, Table 1). This pattern of rock distribution is well established through much of the South Mountain Batholith (Smith, 1974, 1979a, b; McKenzie and Clarke, 1975).

New samples were collected from

Table 1

Modal mineralogy of the new rock samples from the area between Halifax and St. Margarets Bay and Mean compositions of the principal rock types determined by Cormier and Smith (1974). A = Alaskite, MBGr = Muscovite-biotite granite

	Sample	Qu%	Pl%	K-Sp%	Bio%	Chl%	Musc%	Acc%	Rock Typ
	803	35.2	11.1	47.8	0.1	3.1	2.0	0.6	A
Ferguson	804	35.7	12.6	43.4	0.2	2.7	5.3	-	"
Cove	805	47.7	17.0	26.5	0.1	3.4	5.2	0.1	"
	806	48.1	15.1	22.0	0.3	2.0	12.5	0.1	"
	812	46.8	17.2	23.9	5.2	1.7	4.9	0.1	MBGr
	813	34.6	17.2	39.0	2.7	0.9	5.5	-	"
	814	34.3	18.8	39.9	3.4	0.5	3.1	-	"
	815	39.4	14.8	35.7	7.3	1.5	1.3	-	"
Shad	816	53.7	15.7	22.2	5.8	0.7	2.0	-	"
Bay	817	41.4	27.4	20.4	6.1	1.4	3.3	-	"
	818	29.3	30.6	26.6	6.6	3.2	3.7	-	"
	819	44.3	28.7	16.4	5.1	1.9	3.5	-	"
	820	25.2	26.3	39.8	3.2	2.5	3.0	-	"
	821	36.5	24.4	28.8	4.3	1.9	4.0	-	"
	822	35.5	28.1	28.4	0.4	2.9	4.7	-	MBGr
Hacketts	823	41.3	23.3	25.6	1.9	1.6	6.3	-	"
Cove	824	39.8	22.7	28.4	2.2	1.3	5.6	-	"
	825	34.1	23.6	34.6	1.0	2.0	4.5	0.1	"
	826	37.2	34.1	19.4	5.6	1.1	2.6	-	MBGr
Seabright	827	41.3	24.5	27.2	1.9	0.6	4.6	-	"
	828	35.3	33.5	19.7	5.8	0.9	4.7	-	"
	829	25.6	29.3	38.2	3.0	1.5	2.5	-	"
	830	43.7	22.0	25.4	1.3	0.9	6.6	-	A
	831	38.6	20.1	31.5	0.1	1.7	7.9	-	"
	832	34.9	22.3	36.3	0.3	1.2	4.9	-	"
	833	34.0	22.9	34.8	0.9	0.6	6.8	-	"
Upper	834	37.1	20.7	32.7	2.2	-	7.4	-	"
Tantallon	835	40.0	19.5	29.6	0.6	0.9	9.3	-	"
	836	37.7	23.8	27.3	4.0	0.8	6.3	0.1	MBGr
	837	36.1	26.0	29.1	1.0	1.7	6.1	-	"
	838	34.7	22.6	37.0	2.2	0.2	3.2	-	A
	839	36.9	19.1	39.5	1.5	0.6	2.5	-	"
	840	27.7	28.2	34.5	2.5	0.5	6.6	-	MBGr
	Means[a]								
Biotite Granodiorite		34.4	34.5	14.1	16.0	0.4	0.4	0.4	
Biotite Granite		28.6	29.6	34.0	3.0	2.0	2.6	0.3	
2-Mica Granite[b]		34.7	24.9	30.8	3.6	1.4	4.5	-	
Alaskite[b]		39.8	22.9	28.1	0.9	1.3	7.0	0.1	

[a] From Cormier and Smith, 1979, Table 1
[b] Includes Samples from this Study

Ferguson Cove (NS 803-806), Shad Bay (NS 812-21), Hacketts Cove (NS 822-825), Seabright (NS 826-829), and Upper Tantallon (NS 830-840) (Fig. 2) and used to establish the nature of the rocks exposed at each locality. The petrography and modal mineralogy (Table 1) of the Ferguson Cove and Upper Tantallon rocks shows that they belong to the alaskite dyke suite. Those of the other three areas belong to the muscovite-biotite granite suite exposed at Indian Harbour and Ferguson Cove (Table 1). Details of these suites have already been given in several places (Cormier and Smith, 1973; Smith, 1974, 1975, 1979) and only tabulated data and important similarities and differences are noted here.

The mineralogy of the alaskites and muscovite-biotite granites is very similar, the muscovite-biotite granite is made up principally of quartz, plagioclase (An_{7-15}) potash feldspar, biotite and muscovite, and the alaskites contain phenocrysts of quartz, plagioclase (An_{7-12}), and biotite set in an anhedral matrix of quartz, albite, potash feldspar, and muscovite. Micrographic intergrowths of quartz and alkali feldspar occur in the matrix of the Upper Tantallon dyke but not in the dyke at Ferguson Cove.

Accessory minerals in both suites include apatite, ilmenite (partically or completely replaced by rutile), zircon, monazite, and uraninite, all of which are included in or aggregated with the biotite, and are more abundant in the muscovite-biotite granite. In addition, pinite after cordierite is abundant in the muscovite-biotite granite and rare in the alaskite, only occurring in the dyke exposed at Upper Tantallon. Minor andalusite occurs in a few of the samples from each rock suite. The same accessory minerals (except andalusite) occur in greater abundance in the biotite granodiorite and the porphyritic biotite granite.

The gradational relationships noted in the field and in mineralogy between the biotite granodiorite, porphyritic biotite granite and the muscovite-biotite granites of the Halifax - St. Margarets Bay area show that they are all genetically related. The spatial and temporal association and mineralogical similarities shown by the alaskites to these other rocks suggest that they too belong to the suite.

The muscovite-biotite granite and alaskite suites show the same wide variety of pervasive alteration effects which are patchily developed throughout both rock types. These effects are noted to a lesser degree in the biotite granodiorite and biotite granite. Plagioclase crystals and phenocrysts have saussuritized cores and show minor sericitic alteration. The potash feldspars have been made turbid by incipient kaolinization, most obvious in the alaskites. Large crystals of patch perthite replace plagioclase phenocrysts in the alaskites. Muscovite occurs as large ragged flakes, surrounding and penetrating all the other major minerals, and much of it is considered secondary. All of the biotite is partially or completely replaced by chlorite.

Members of the paraintrusive suite are very well developed in the muscovite-biotite granite in the area extending from Sanwich Point to Herring Cove (section A to B on Fig. 2). These include lenticular miarolitic pegmatites, aplite/pegmatite dykes and a greisen-bordered sheeted quartz-vein complex. The greisens comprise principally quartz-sericite-pyrite-arsenopyrite with very rare sphalerite, and are notably different in composition to the precursor muscovite-biotite granite. They have been studied (Smith et al., 1982) and are interpreted as resulting from the effects of the localized release of large quantities of hydrothermal fluids which have largely escaped from the system. This contrasts with the pervasive but patchy alteration described above which produces mainly hydrous (secondary) minerals in the granitic rocks, and which is most

pronounced in the muscovite-biotite granite and alaskite. The pervasive alteration results from subsolidus recrystallization, promoted by the release of small quantities of aqueous fluid at the end stages of crystallization. The absence of associated quartz veining over most of the rock outcrops suggests that in contrast to the greisenization, no material escaped from the system during the pervasive recrystallization, but the elements were redistributed during the recrystallization (Smith et al., 1982).

Thus, the mineralogy and field relationships of these rocks suggest that three separate processes were involved in their evolution. The major rock types and their distribution were controlled by magmatic (crystal-melt) processes. The rocks produced were affected by a pervasive hydrothermal event followed by localized intense hydrothermal veining and alteration. These events should be reflected in the geochemistry of the rocks.

b) Geochemistry

Thirty-one representative samples of the alaskite (12) and muscovite-biotite granite (19) were analyzed for their major and trace element contents by X-ray fluorescence techniques. The sample locations are given on Figure 2. Major elements were analyzed on fused glass discs and trace elements were determined on rock powder pellets. Full details of the methods and their precision are given elsewhere (Peck, 1984).

Table 2 summarizes the results of these analyses and also compares the new data with previous work on this pluton (Smith 1979b). The mean contents of TiO_2, MnO, MgO, CaO, Al_2O_3, and Fe_2O_3, P_2O_5, Ba, and Zr decrease and K_2O and Rb increase systematically (Figs. 3 and 4). Smith (1974) reported a break in the systematic variation of Na_2O, Rb, Ba, K/Rb, K/Ba, and Ca/Sr ratios between the muscovite-biotite granite and alaskites. When the additional data is plotted the break is seen to be more apparent than real (Figs. 3 and 4), but the distribution of Na_2O, Rb, and Ba is more irregular than that of other elements.

The systematic variations in whole rock geochemistry can be readily accounted for by fractional crystallization of quartz, plagioclase, and biotite (Smith, 1974, 1979a, b; McKenzie and Clarke, 1975). However, it is not possible to model the evolution of the rocks mathematically, using the measured Rb, Ba, and Sr contents of feldspar and micas separated from them (Smith et al., 1982). This observation together with the increase in concentration dispersion shown by K_2O suggests that the distribution of these elements is not controlled by crystal melt equilibria but by some other process. Since the whole rock chemistry is unaffected it is suggested that the five elements have been redistributed by the pervasive subsolidus recrystallization described above.

c) Rare-earth element distribution

The concentrations and distributions of the rare-earth elements (REE) are commonly used in igneous petrogenesis to define the processes leading to the formation of the magmas and to trace the evolution of the magma (Alburquerque, 1977; Muecke and Clarke, 1981; Mahood and Hildreth, 1983; Mittlefeldh and Miller, 1983). These elements may also be used to define the nature of the hydrothermal processes affecting granitic rocks (Taylor and Fryer, 1982).

The concentrations of 6 rare earth elements in fifteen rock samples from the granitic and paraintrusive rock suite of the Halifax area were measured by INAA techniques. The work was carried out at Michigan State University. The relative error and normalization concentrations, from Yoder (1976) are given in Table 3.

Two very different groups of REE

Table 2.

Major element and trace element geochemistry of the muscovite-biotite granites and alaskites from the Halifax - St. Margarets Bay area.

Sample	FERGUSON COVE							SHAD BAY										HACKETTS COVE			
No. NS	211	216	217	803	804	805	806	812	813	814	815	816	817	818	819	820	821	822	823	824	825
SiO_2	74.39	76.82	75.99	75.80	76.43	75.81	78.13		74.14	75.33	73.13	74.03	72.31	72.64	73.49	74.92	71.74	71.96	72.41	71.97	75.28	72.68
TiO_2	0.21	0.14	0.09	0.16	0.17	0.17	0.18	0.31	0.20	0.34	0.24	0.32	0.30	0.32	0.26	0.34	0.31		0.18	0.18	0.15	0.18
Al_2O_3	14.08	12.99	13.46	12.71	12.83	12.86	11.39	13.44	13.37	13.41	13.32	13.72	13.69	13.46	12.96	13.65	13.39		14.12	14.10	13.74	14.58
Fe_2O_3	1.66	1.66	1.23	1.41	1.24	1.82	1.69	2.38	1.76	2.44	1.75	2.28	2.27	2.40	1.88	2.44	2.34		1.47	1.54	1.52	1.51
MnO	0.06	0.07	0.03	0.04	0.03	0.05	0.06	0.05	0.05	0.04	0.04	0.05	0.04	0.05	0.05	0.04	0.05		0.04	0.04	0.04	0.03
MgO	0.51	0.49	0.36	0.16	0.18	0.35	0.29	0.44	0.25	0.46	0.11	0.42	0.31	0.54	0.36	0.45	0.34		0.70	0.24	0.04	0.05
CaO	0.80	0.60	0.36	0.39	0.39	0.56	0.46	0.74	0.55	0.87	0.63	0.96	0.85	0.85	0.82	0.85	0.70		0.65	0.62	0.47	0.65
Na_2O	3.55	2.54	3.37	3.09	3.36	3.39	2.21	3.53	3.69	3.29	3.67	3.68	3.36	3.44	3.37	3.49	3.52		3.49	3.54	3.44	3.99
K_2O	4.44	4.34	4.62	4.59	4.33	4.61	4.10	4.48	4.28	4.33	4.47	4.48	4.10	3.99	4.08	4.58	4.46		4.43	4.48	4.07	4.66
P_2O_5	0.24	0.18	0.18	0.17	0.18	0.18	0.17	0.25	0.23	0.23	0.21	0.22	0.26	0.26	0.25	0.23	0.22		0.32	0.30	0.26	0.33
LOI	0.71	0.73	0.89	0.81	0.95	0.78	0.64	0.50	0.89	0.81	1.02	0.77	1.12	1.08	0.93	0.89	1.04		1.13	1.08	1.06	1.08
V				11	11	10	11	21	12	16	26	27	23	24	20	27	24		11	13	9	13
Co				2	-	1	1	2	1	3	1	4	3	4	2	5	3		1	2	1	1
Ni				2	2	2	3	3	-	1	4	1	1	3	3	2	2		2	3	3	2
Cu	6	5	5	4	2	-	4	4	1	-	4	-	1	2	3	34	23		13	5	8	5
Zn	49	39	27	-	-	21	12	26	13	6	35	35	37	34	22	27	36		5	17	7	9
Rb	254	254	253	232	228	262	234	267	300	250	258	249	241	255	224	240	253		218	214	464	215
Sr				18	16	25	21	56	20	27	62	69	59	60	57	76	66		52	55	24	57
Y				23	18	13	19	17	12	13	17	17	16	17	14	17	17		12	8	3	9
Zr				71	72	63	64	112	63	77	130	124	106	120	93	127	115		56	59	43	59
Nb				9	10	8	9	14	13	12	15	14	13	15	11	13	13		10	11	15	12
Sn	10	20	15	1	2	3	5	-	4	2	3	-	3	3	2	3	4		6	6	-	6
Ba	276	276	108	74	67	78	58	184	35	63	240	276	201	204	206	279	244		269	270	43	286

For sample location and lithology, see Appendix 1

Table 2 (cont'd).

Sample No. NS	SEABRIGHT 826	827	828	829	UPPER TANTALLON 830	831	832	833	834	835	836	837	838	839	840	Averages+ B.Gd	B.Gr	MBGr.*	Alaskite*
SiO_2	75.28	75.47	73.74	75.02	74.71	75.05	74.54	75.54	74.81	75.58	74.90	76.60	75.67	75.43	74.69	69.27	73.09	74.00	75.55
TiO_2	0.16	0.14	0.16	0.13	0.11	0.11	0.11	0.12	0.11	0.10	0.17	0.12	0.11	0.13	0.23	0.64	0.32	0.21	0.13
Al_2O_3	13.16	13.44	13.39	13.76	13.90	13.78	13.56	13.70	13.58	14.02	13.09	13.70	13.31	12.95	13.57	15.52	14.33	13.59	13.37
Fe_2O_3	1.81	1.43	1.84	1.43	1.44	1.62	1.25	1.31	1.33	1.03	1.78	1.57	1.21	1.40	1.94	3.50	2.28	1.82	1.70
MnO	0.05	0.04	0.06	0.05	0.04	0.04	0.05	0.05	0.04	0.03	0.06	0.04	0.05	0.04	0.05	0.10	0.07	0.05	0.04
MgO	0.07	0.15	0.09	0.08	0.05	0.18	0.25	0.06	0.02	0.03	0.14	0.06	0.13	0.08	0.33	1.22	0.69	0.25	0.28
CaO	0.48	0.56	0.61	0.55	0.44	0.43	0.44	0.42	0.40	0.42	0.78	0.39	0.40	0.40	0.58	2.18	1.17	0.68	0.50
Na_2O	3.54	3.41	3.59	3.42	3.68	3.72	3.40	3.45	3.58	3.60	3.14	3.48	3.62	3.53	3.54	3.00	3.21	3.45	3.37
K_2O	4.25	4.40	4.26	4.43	4.08	4.12	4.13	4.17	4.32	3.79	4.22	4.32	4.53	4.76	4.35	4.12	4.55	4.47	4.36
P_2O_5	0.20	0.20	0.27	0.20	0.24	0.24	0.23	0.21	0.22	0.20	0.20	0.22	0.18	0.14	0.24	0.22	0.22	0.24	0.20
LOI	0.82	0.88	0.90	0.87	1.05	0.99	1.01	1.01	1.10	1.20	1.08	1.13	0.91	0.83	1.11	0.39	0.50	0.89	0.82
V	10	9	11	9	7	9	6	6	9	6	12	7	6	7	19			16	8
Co	2	1	2	2	-	-	2	-	3	-	3	2	2	-	2	23	22	2	1
Ni	1	1	1	-	-	-	3	-	2	-	-	3	-	-	2	25	23	2	1
Cu	2	3	7	-	1	3	9	1	13	12	3	6	2	33	-	10	9	6	7
Zn	23	8	25	10	-	-	11	12	-	-	28	-	-	16	13	66	52	10	17
Rb	384	328	353	342	431	413	424	417	417	405	320	324	311	279	327	159	216	281	323
Sr	23	26	34	39	7	7	7	8	7	5	23	12	8	15	38	156	84	43	18
Y	13	13	7	10	7	7	7	7	5	3	14	14	10	14	15	-	-	13	11
Zr	52	48	53	46	41	38	37	36	32	29	59	48	33	36	80	-	-	80	46
Nb	13	9	10	9	12	13	10	11	11	8	12	12	9	9	13	-	-	12	10
Sn	7	9	5	8	14	12	12	12	10	9	9	7	9	7	7	6	-	6	11
Ba	52	82	72	53	5	6	3	8	6	-	58	34	2	10	116	731	389	161	65

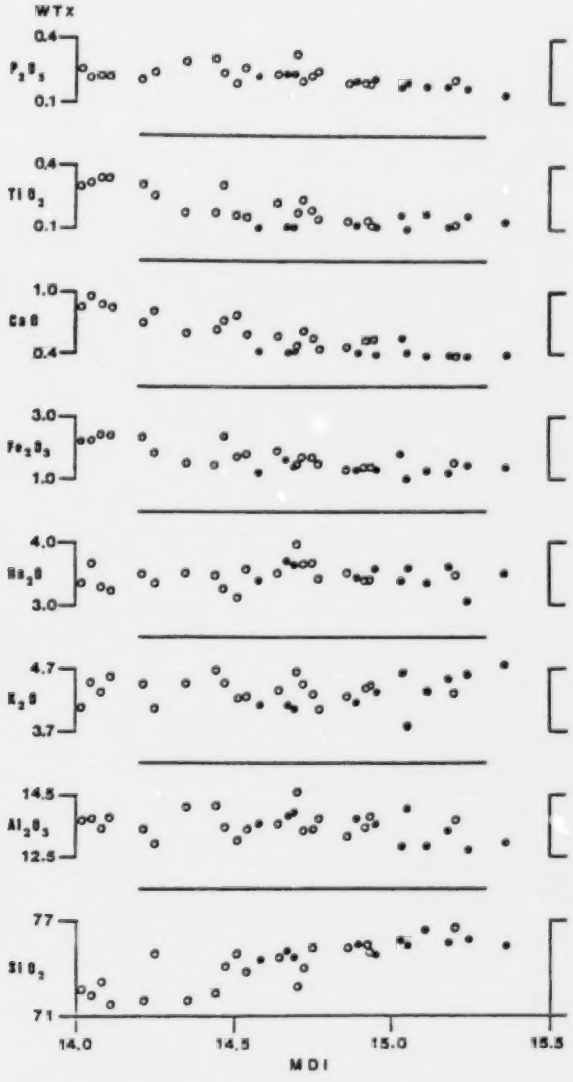

Figure 3 - Major element chemistry of the muscovite-biotite granites (o) and alaskites (●) of the Halifax - St. Margarets Bay area plotted against the Modified Larsen Differentiation Index (MDI = 1/3 Si + K - (Ca + Mg)).

pattern are noted. The first is typical of the biotite-granodiorite, biotite-granite, muscovite-biotite granite and alaskite suite, and is used to model the magmatic processes qualitatively. The second is typical of the paraintrusive suite and is used to define the nature of the hydrothermal processes affecting these rocks. Samples selected to illustrate the magmatic processes show minimum effects of pervasive alteration. No REE data is available from mineral separates so it is not possible to define the changes produced by the pervasive alteration.

The grandiorite, porphyritic biotite granite, muscovite-biotite granite and alaskite show broadly similar patterns, with decreasing ΣREE, La/Sm ratios,

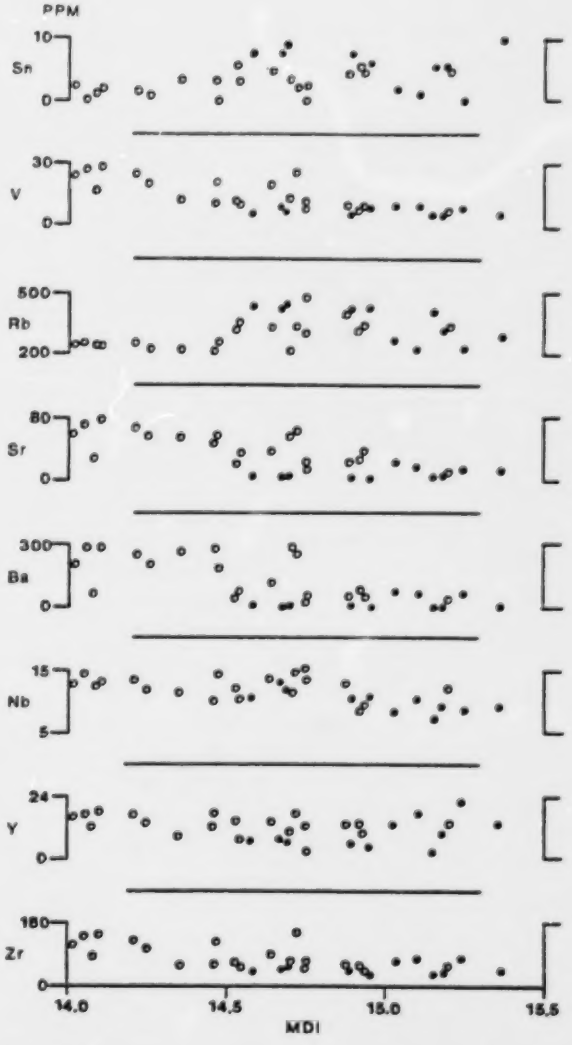

Figure 4 - Trace element chemistry of the muscovite-biotite granites (o) and alaskites (●) of the Halifax - St. Margarets Bay area, plotted against the Modified Larsen Differentiation Index.

Table 3.

Rare earth element contents of the principal granitoid rock types including the paraintrusive suite, from theHalifax - St. Margarets Bay area. Normalization concentrations from figs. 5 and 6 from Yoder (1976). Relative error calculated from:

$$RE = \frac{\text{(standard concentration)} - \text{(measured concentration)}}{\text{standard concentration}} \times 100$$

RE for La = 10%, for Ce = 6%, for Sm = 5%, for Tb = 20%, for Lu = 20%, Yb could not be determined because of Ta interference

	Biotite Grandiorite		Biotite Granite		
	NS 231	NS 209	NS 213	NS 406	NS 219
	ppm	ppm	ppm	ppm	ppm
La	29	29	22	20	11
Ce	62	58	42	40	22
Sm	6.9	7.3	5.3	5.7	4.0
Eu	1.35	1.29	0.76	0.59	0.24
Tb	0.94	1.00	0.63	0.79	0.43
Lu	0.55	0.53	0.40	0.34	0.37
(La/sm)N	2.3	2.2	2.3	1.9	1.5
(Tb/Lu)N	1.2	1.4	1.1	1.7	0.8

	Muscovite-biotite Granite		Alaskite/Leucogranite		Pegmatite
	NS 210	NS 457	NS 216	NS 217	HX 28
	ppm	ppm	ppm	ppm	ppm
La	11	9	12	8	8
Ce	21	15	20	14	18
Sm	4.2	3.2	3.8	3.1	6.2
Eu	0.37	0.20	0.30	0.20	0.27
Tb	0.57	0.58	0.57	0.49	0.73
Lu	0.30	0.38	0.35	0.31	0.44
(La/sm)N	1.4	1.5	1.7	1.4	0.7
(Tb/Lu)N	1.4	1.1	1.2	1.1	1.2

	Pegmatite		Greisen		
	HX 114	HX 108	HX 124	HX 105	HX 125
	ppm	ppm	ppm	ppm	ppm
La	7	13	10	4	3
Ce	9	25	19	8	7
Sm	2.7	4.3	3.8	2.3	2.5
Eu	0.44	0.41	0.27	0.34	0.14
Tb	0.31	0.53	0.46	0.32	0.39
Lu	0.25	0.35	0.32	0.23	0.22
(La/sm)N	1.4	1.7	1.4	0.95	0.7
(Tb/Lu)N	0.9	1.1	1.0	1.0	1.3

and an increasingly large negative Eu anomaly (Table 3, Fig. 5) Σ6REE decreases from ∿100 ppm in the granodiorites to ∿60 ppm in the porphyritic biotite granite, and ∿35 ppm in the muscovite-biotite granite and the alaskite. The La/Sm ratios decrease from 2.3, through 1.9 to ∿1.4 in these rocks. The heavy rare-earth elements (HREE) in these rocks are relatively unfractionated (Tb/Lu 1.2) and show a decrease in concentration through the range of rocks from ∿20 to ∿10x chondrite (Table 3). Zircon, apatite, and monazite, are all included in, or aggregated with, the biotite.

These minerals must also be involved with the biotite in the fractionation process. The removal of ilmenite and zircon would lead to the observed depletion of TiO_2 and Zr. In addition REE preferentially enter both zircon (HREE) and apatite (LREE and HREE) (Hanson, 1978). However, these minerals are present in proportions on the order of 0.1% and the distribution coefficients are not large enough to cause effective depletion or fractionation of these elements. If apatite was the mineral controlling the REE patterns they should contain a positive Eu anomaly (Hanson, 1978) not a negative anomaly as noted.

Mittlefeldht and Miller (1983) have shown that up to 75% of the REE in felsic rocks may be present in monazite and that the removal of minute quantities of the mineral are sufficient to decrease LREE abundances by 10 or 20x. The LREE become increasingly strongly fractionated into monazite as the melt becomes more felsic (Miller and Mittlefeldht, 1982). In the Halifax suite the LREE are fractionated and decrease in abundance by ∿3X. The X-Ray spectrometry maps of the peninsula (Ford, 1982) show that the Th content decreases and the U content increases, and U/Th ratio generally increases, systematically as

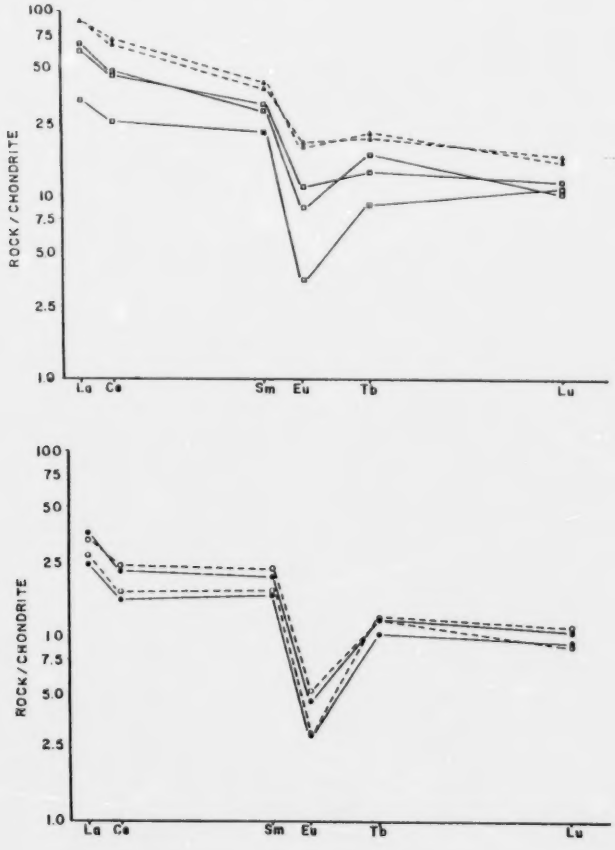

Figure 5 - Plot of chondrite normalized rare earth element abundances of selected granitic rocks from the Halifax - St. Margarets Bay area. Normalization concentrations from Yoder (1976). La = 0.330 ppm, Ca = 0.88 ppm, Sm = 0.181 ppm, Eu = 0.069 ppm, Tb = 0.047 ppm, La = 0.034 ppm. (a) Symbols. ▲ Biotite granodiorite, □ Biotite granite. (b) Symbols. ● Muscovite-biotite granite, ●Alaskite.

the rocks vary from biotite granodiorite, through biotite granite to muscovite-biotite granite and alaskite.

Monazite contains large quantities of Th and much less U and its early removal during fractional crystallization would account for the major trends described above, i.e., the depletion of Th, enrichment in U and increase in the U/Th ratio. These observations suggest that it is monazite which causes the strong depletion and fractionation of the LREE elements and that the depletion effects become greater as the melt becomes more felsic.

Thus, the removal of zircon, ilmenite, apatite, and monazite along with plagioclase, biotite, and quartz provides an adequate qualitative model for the evolution of this rock series by fractional crystallization. It is not possible to model the process quantitatively in the absence of precisely determined distribution coefficients for monazite.

The muscovite-biotite granite extending from Sandwich Point to the south (section A-B, Fig. 2), which is strongly greisened, is exceptional in that it contains high Th and relatively low U. In addition, the pattern of distribution of the REE changes abruptly in the pegmatites and greisens, marking the change in the processes controlling the evolution of the rocks. The pegmatites crystallized in miarolitic vugs within the muscovite-biotite granite in the presence of an aqueous phase (Burnham, 1979). The greisens formed by the phyllic alteration of the muscovite-biotite granite in narrow zones adjacent to large (up to 20 cm) quartz veins of the sheeted complex exposed at Sandwich Point (section A-B, Fig. 2).

One of the pegmatites (HX28) and two of the greisens (HX108, HX124) show REE patterns very similar to the muscovite-biotite granite, confirming their relationship to the granite. The remaining pegmatite and greisens show similar REE patterns which differ from the igneous patterns described above. The pegmatite (HX114) shows a greater depletion in the overall concentration of the REE, than the igneous rocks, especially La and Ce. The greisens (HX105, HX125) also show the overall depletion of the REE and especially a relative fractionation of La/Sm (Fig. 6). The negative Eu anomalies shown by these rocks are considered to be the result of the removal of plagioclase during fractional crystallization, and were inherited from the precursor muscovite-biotite granite.

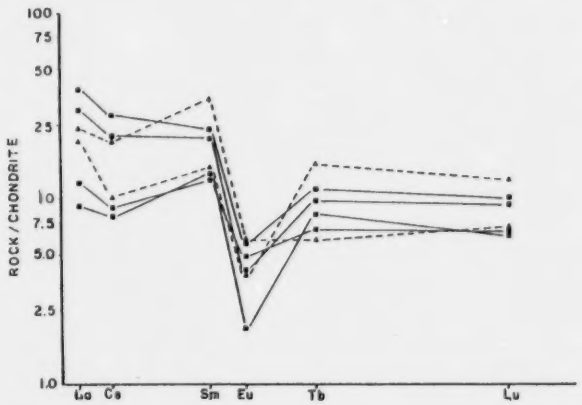

Figure 6 - Plot of chondrite normalized rare earth element abundances of selected paranitrusive rocks from the Sandwich Point - Herring Cove section. Normalization concentrations from Yoder (1976). Symbols. ▲Pegmatite, ■ Greisen.

The zone of muscovite-biotite granite and alaskite, noted above, trending E-W from Sandwich Point (A, Fig. 2) shows U-Th relationships which differ from those of the typical igneous trend, in particular they show strong Th enrichment (Ford, 1982). This unusual trend coincides in areal distribution with the only extensive occurrence of a greisen-bordered sheeted vein complex and is therefore considered to be related to this hydrothermal phenomenon.

The greisen consists of quartz- sericite -pyrite-arsenopyrite, sphalerite without fluorite or topaz. This mineral assemblage is indicative of a relatively low pH hydrothermal fluid interaction with the precursor rock. The most common low pH hydrothermal fluids are Cl^-, F^-, and CO_3^{2-} bearing. Since carbonate is not one of the minerals found in the hydrothermal assemblage it is not likely to be the dominant anion present in the fluid. Both Cl^- and F^- are capable of complexing with the LREE and removing them, increasingly so as they get lighter (Taylor and Fryer, 1982). In addition F^-, which is known to be comparatively high in these magmas (Smith and Turek, 1976), may complex with the HREE and remove them (Taylor and Fryer, 1982) in the hydrothermal fluid. The pegmatites and greisens are characterized by the depletion in the lightest and heaviest REE (Fig. 5) and Th enrichment, and the hydrothermal fluid producing these patterns is believed to be F-rich.

DISCUSSION

The data given above suggest that at least three processes have been important in the evolution of the granitoid rocks and their associated paraintrusive suite in the Halifax area. These are fractional crystallization which produces the biotite granodiorite, biotite granite, muscovite-biotite granite and alaskite suite, pervasive patchy recrystallization which produces mainly secondary chlorite, muscovite, and potash-feldspar, and localized hydrothermal activity which produces an unmineralized greisen-bordered sheeted vein complex and miarolitic pegmatites. In addition, there are at least two more sets of thin quartz veins which are important locally.

Chatterjee et al. (1983) have shown that an earlier suite of "non-specialized" and a later suite of "specialized" (equivalent to the paraintrusive suite of Chatterjee and Muecke, 1982) granites can be identified in the South Mountain Batholith. The granitic rocks of the Halifax area are initially rich in U and Th and have a U/Th ratio of ~1.0 and during fractional crystallization there is depletion in Sr, Ba, Zr (Fig. 4) and the REE (Fig. 5) and enrichment in Rb, Sn, and U (Fig. 4). These changes in trace element contents are typical of the Sn-mineralized suite (Chatterjee et al., 1983). The greisen-bordered sheeted vein complex is developed in the muscovite-biotite granite and is associated with a somewhat more widespread zone of Th enrichment. This enrichment is developed near the margin of the batholith, hence this zone shows all of the features of the highly mineralized Davis Lake and Plymouth Plutons (Chatterjee and Muecke, 1982) and yet lacks mineralization. The late stage alaskite dyke at Upper Tantallon has unusually low K/Rb ratios (average 95) and low Ba content (134 ppm) and hence belongs to the "specialized" suite (Chatterjee et al., 1983, Table 1, Fig. 2). It is patchily hematized and although hematization commonly precedes lode mineralization in Cornwall, is barren of mineralization. This dyke is the end product of fractional crystallization of rocks belonging to the Sn-mineralized suite, as shown above, but shows no evidence of Th enrichment.

Since the Upper Tantallon dyke does not show all of the features associated with known occurrences of Sn-mineralization, it is perhaps not surprising that it is barren of mineralization. However, the lack of mineralization in the Sandwich Point to Herring Cove area, which shows all of the necessary features, does require some explanation.

Many of the trends of geochemical change in these rocks are controlled by fractional crystallization, but the Sn-mineralization, which occurs in greisens, and the associated Th enrichment, are the results of hydrothermal activity (Smith et al.,

1982; Chatterjee et al., 1983). The hydrothermal activity has also caused the depletion of the lightest and heaviest REE by leaching. Under these conditions Cu, Mo, Sn and W are also expected to be mobile (Taylor and Fryer, 1982) and may also have been leached from the rocks. Redeposition of the REE and the metals may be caused by changes in pH, fluid/rock ratios and anionic activities caused by the interaction of the magmatic hydrothermal brine with meteoric hydrothermal fluids (Taylor and Fryer, 1982). However, oxygen isotope studies of these granitic rocks have demonstrated that meteoric water was not involved in their evolution (Longstaffe et al., 1980), perhaps because the present level of exposure is too deep. Sn - Cu - W deposits, if ever present, may have formed at higher levels where meteoric water would have been encountered, but have now been eroded away.

CONCLUSIONS

Data is presented above to show that a very large area of leucocratic muscovite-biotite granite is exposed on the western side of the peninsula between Halifax and St. Margarets Bay, and only two large alaskite dykes occur. These siliceous leucocratic rocks are affected by a pervasive hydrothermal alteration which causes redistribution of trace elements but little change in bulk composition. In addition, the muscovite-biotite granite is subjected to very strong localized alteration in a greisen-bordered sheeted quartz vein complex.

REE patterns show that the biotite granodiorite, porphyritic biotite granite, muscovite-biotite granite and alaskite dykes are related by fractional crystallization involving the removal of monazite in addition to quartz, plagioclase, biotite, ilmenite, apatite, and zircon.

The strong localized hydrothermal effects produce a marked change in REE patterns which suggest that the rock has been leached by a hydrothermal fluid having a low pH (<3.5) and containing F. This fluid may have deposited Sn-W-Cu ores on coming into contact with meteoric water, but if so they are now eroded away.

ACKNOWLEDGEMENTS

This work was supported by a research grant from the N.S.E.R.C. of Canada.

ALBUQUERQUE, C.A.R. DE, 1977. Geochemistry of the tonalitic and granitic rocks of the Nova Scotia southern plutons. Geochimica et Cosmochimica Acta, 41, pp. 1-13.

BURNHAM, C.W., 1979. The importance of volatile constituents. In: The evolution of the igneous rocks, Fiftieth Anniversary Perspectives, (ed.) H.S. Yoder Jr. Princeton: Princeton University Press. pp. 439-479.

CHATTERJEE, A.K., and MUECKE, G.K., 1982. Geochemistry and the distribution of uranium and thorium in the granitoid rocks of the South Mountain Batholith, Nova Scotia: Some genetic and exploration implications. In: Uranium in granites (ed.) Y.T. Maurice. Geological Survey of Canada, Paper 81-23, pp. 11-17.

CHATTERJEE, A.K., STRONG, D.F., and MUECKE, G.K., 1983. A multivariate approach to geochemical distinction between tin-specialized and uranium-specialized granites of southern Nova Scotia. Canadian Journal of Earth Sciences, 20, pp. 420-430.

CLARKE, D.B, and HALLIDAY, A.N., 1980. Strontium isotope geology of the South Mountain Batholith, Nova Scotia. Geochimica et Cosmochimica Acta, 44, pp. 1045-1058.

CORMIER, R.F., and SMITH, T.E., 1973. Radiometric ages of granitic rocks, southwestern Nova Scotia. Canadian Journal of Earth Sciences, 10, pp. 1201-1210.

FAIRBURN, H.W., HURLEY, P.M., PINSON, W.H. and CORMIER, R.F., 1960. Age of granitic rocks of Nova Scotia. Geological Society of America Bulletin, 71, pp. 399-413.

FAIRBURN, H.W., HURLEY, P.M., and PINSON, W.H., 1964. Preliminary age study and initial $^{87}Sr/^{86}Sr$ of Nova Scotia granitic rocks by the Rb/Sr whole rock method. Geological Society of America Bulletin, 75, pp. 253-258.

FORD, K.L., 1982. Investigation of regional airborne gamma-ray spectrometric patterns in

New Brunswick and Nova Scotia. Geological Survey of Canada, Paper 82-1B, pp. 117-194.

GOSSIP, W., 1864. The rocks in the vicinity. Proceedings and Transactions, Nova Scotia Institute of Science, 1, pp. 45-49.

HANSON, G.N., 1978. The application of trace elements to the petrogenesis of igneous rocks of granitic composition. In: Trace elements in igneous petrology, eds. C.J. Allegre and S.R. Hart. Developments in Petrology 5, pp. 26-43, Elsevier, New York.

HONEYMAN, D., 1883. Nova Scotia geology-Halifax and Colchester Counties. Proceedings and Transactions, Nova Scotia Institute of Science, 6, pp. 52-67.

KEPPIE, J.D. and SMITH, P.K., 1978. Compilation of isotopic age data from Nova Scotia. Nova Scotia Department of Mines, Report 78-4.

LEECH, G.B., LOWDEN, J.A., STOCKWELL, C.H., and WANLESS, R.K., 1963. Age determinations and geological studies. Geological Survey of Canada, Paper 63-17, 140 p.

LONGSTAFFE, F.J., and SMITH, T.E., 1978. Oxygen isotope evidence for the origin of Devonian granitoids, southwestern Nova Scotia. Geological Association of Canada/Mineralogical Association of Canada, Abstracts with Programs, 10, pp. 446-447.

LONGSTAFFE, F.J., SMITH, T.E., and MUEHLENBACHS, K., 1980. Oxygen isotope evidence for the genesis of Upper Paleozoic granitoids from southwestern Nova Scotia. Canadian Journal of Earth Sciences, 17, pp. 132-141.

LOWDON, J.A., 1960. Age determinations by the Geological Survey of Canada. Geological Survey of Canada, Paper 60-17, 127 p.

LOWDON, J.A., STOCKWELL, C.H., TIPPER, H.W., and WANLESS, R.K., 1963. Age determinations and geological studies. Geological Survey of Canada, Paper 62-17, 140 p.

MAHOOD, G., and HILDRETH, W., 1983. Large partition coefficients for trace elements in high-silica rhyolites. Geochimica et Cosmochimica Acta, 47, pp. 11-30.

MALCOLM, W., 1914. The goldfields of Nova Scotia. Geological Survey of Canada, Memoir No. 20. 329 p.

MCKENZIE, C.B., and CLARKE, D.B., 1975. Petrology of the South Mountain Batholith, Nova Scotia. Canadian Journal of Earth Sciences, 11, pp. 650-657.

MILLER, C.F., and MITTLEFEHLDT, D.W., 1982. Depletion of light rare earth elements in felsic magmas. Geology, 10, pp. 129-133.

MITTLEFEHLDT, D.W., and MILLER, C.F., 1983. Geochemistry of the Sweetwater Wash Pluton, California: Implications for "anomalous" trace element behaviour during differentiation of felsic magmas. Geochimica et Cosmochimica Acta, 47, pp. 109-124.

MUECKE, G.K., and CLARKE, D.B., 1981. Geochemistry of the South Mountain Batholith, Nova Scotia: Rare-earth element evidence. Canadian Mineralogist, 19, pp. 133-145.

PECK, D.C., 1984. A re-appraisal of the alaskite/muscovite-biotite granite suite of Halifax County, Nova Scotia. B.Sc. thesis, University of Windsor, 74 p.

REYNOLDS, P.H., CLARKE, D.B., MUECKE, G.K., and ZENTILLI, M., 1980. K-Ar and $^{40}Ar/^{39}Ar$ geochronology of the granitoid rocks from the Meguma Zone, southern Nova Scotia. Geological Association of Canada/Mineralogical association of Canada, Abstracts with Programs 5, pp. 77.

SMITH, T.E., 1974. The geochemistry and origin of the granitic rocks of Halifax County, Nova Scotia. Canadian Journal of Earth Sciences, 11, pp. 650-657.

SMITH, T.E., 1975. Layered granitic rocks at Chebucto Head, Halifax County, Nova Scotia. Canadian Journal of Earth Sciences, 12, pp. 456-463.

SMITH, T.E., and TUREK, A., 1975. Sn-bearing potential of some Devonian granitic rocks of S.W. Nova Scotia. Geological Association of Canada. Abstracts with program, 7, p. 861.

SMITH, T.E., and TUREK, A., 1976. Tin-bearing potential of some Devonian granitic rocks in southwest Nova Scotia. Mineralium Deposita, 11, pp. 234-245.

SMITH, T.E., 1979a. The geochemistry and origin of the Devonian granitic rocks of southwest Nova Scotia. Summary. Geological Society of America Bulletin, 90, pp. 424-426.

SMITH, T.E., 1979b. The geochemistry and origin of the Devonian granitic rocks of southwest Nova Scotia. Geological Society of America Bulletin, 90, pp. 850-885.

SMITH, T.E., MILLER, P.M., and HUANG, C.H., 1982. Solidification and crystallization of a stanniferous granitoid pluton, Nova Scotia, Canada. In: Metallization Associated with Acid Magmatism, (ed.) A.M. Evans. John Wiley and Sons Ltd., pp. 301-320.

STEIGER, R.H., and JAGER, E., 1977. Subcommission on Geochronology: convention on the use of decay constraints in geo- and cosmochronology: Earth and Planetary Science Leters, 36, pp. 359-362.

TAYLOR, F.C., and SCHILLER, E.A., 1966. Metamorphism of the Meguma Group of Nova Scotia. Canadian Journal of Earth Sciences, 3, pp. 959-974.

TAYLOR, R.P., and FRYER, B.J., 1982. Rare-earth element geochemistry as an aid to interpreting hydorthermal ore deposits. In: Metallization associated with Acid Magmatism (ed.) A.M. Evans. John Wiley and Sons, pp. 357-365.

WRIGHT, W.J., 1931. Data on the method of granitic intrusion in Nova Scotia. Royal Society of Canada, Transactions, Series 3, 25, pp. 309-327.

YODER, H.S., JR., 1976. Generation of Basaltic Magmas. National Academy Press, Washington, D.C., 353 p.

Appendix 1

Sample Location and Lithology

Sample No.-NS	Location	NTS[a] Grid Reference	Rock Type
211[b]	Ferguson Cove	11D/12-542396	Alaskite
216[b]	Ferguson Cove	11D/12-555393	Alaskite
217[b]	Ferguson Cove	11D/12-554394	Alaskite
803	Ferguson Cove	11D/12-553392	Alaskite
804	Ferguson Cove	11D/12-554392	Alaskite
805	Ferguson Cove	11D/12-556391	Alaskite
806	Ferguson Cove	11D/12-557388	Alaskite
812	Shad Bay	11D/12-393305	Muscovite-biotite granite
813	Shad Bay	11D/12-393298	Muscovite-biotite granite
814	Shad Bay	11D/12-392299	Muscovite-biotite granite
815	Shad Bay	11D/12-392301	Muscovite-biotite granite
816	Shad Bay	11D/12-388289	Muscovite-biotite granite
817	Shad Bay	11D/12-394312	Muscovite-biotite granite
818	Shad Bay	11D/12-394310	Muscovite-biotite granite
819	Shad Bay	11D/12-393308	Muscovite-biotite granite
820	Shad Bay	11D/12-371316	Muscovite-biotite granite
821	Shad Bay	11D/12-370315	Muscovite-biotite granite
822	Hacketts Cove	11D/12-256328	Muscovite-biotite granite
823	Hacketts Cove	11D/12-265347	Muscovite-biotite granite
824	Hacketts Cove	11D/12-276362	Muscovite-biotite granite
825	Hacketts Cove	11D/12-266350	Muscovite-biotite granite
826	Seabright	11D/12-267398	Muscovite-biotite granite
827	Seabright	11D/12-267398	Muscovite-biotite granite
828	Seabright	11D/12-267398	Muscovite-biotite granite
829	Seabright	11D/12-264407	Muscovite-biotite granite
830	Upper Tantallon	11D/12-303485	Alaskite
831	Upper Tantallon	11D/12-303485	Alaskite
832	Upper Tantallon	11D/12-303485	Alaskite
833	Upper Tantallon	11D/12-303485	Alaskite
834	Upper Tantallon	11D/12-307482	Alaskite
835	Upper Tantallon	11D/12-307482	Alaskite
836	Upper Tantallon	11D/12-313480	Muscovite-biotite granite
837	Upper Tantallon	11D/12-316481	Muscovite-biotite granite
838	Upper Tantallon	11D/12-280508	Alaskite
839	Upper Tantallon	11D/12-280508	Alaskite
840	Upper Tantallon	11D/12-325499	Muscovite-biotite granite

[a]National Topographic Series
[b]Samples from Smith, 1974

Maritime Sediments and Atlantic Geology

Vol. 22 April, 1986 No. 1

Application of Airborne Gamma Ray Spectrometric Surveys Meguma Terrane, Nova Scotia

K.L. Ford and J.M. Carson
Geological Survey of Canada
601 Booth Street, Ottawa, Ontario K1A 0E8

Between 1976 and 1983 a series of airborne gamma-ray spectrometric surveys with flight lines spaced at one kilometre intervals were carried out in the Province of Nova Scotia. These surveys covered most of the Meguma Terrane and have yielded radioelement distribution patterns that have proven useful in delineating various aspects of the region's geology.

Within a cogenetic suite of Devonian-Carboniferous peraluminous granitic rocks uranium concentrations are shown to increase progressively with increasing differentiation while thorium concentrations reflect two contrasting trends. The most prevalent trend, shown by the granitic rocks of the eastern part of the South Mountain Batholith (New Ross area) and Eastern Meguma Terrane, is one of decreasing thorium concentrations with increasing differentiation. A second, less prominent trend exhibited by the granitic rocks of the western part of the South Mountain Batholith shows increasing thorium concentrations with increasing differentiation. The more prevalent inverse relationship between uranium and thorium results in high eU/eTh ratios associated with the more differentiated phases of the granitic suite. In addition, certain slate units of the Meguma Group are shown to have distinctly higher radioelement contents, in particular thorium, compared to the other slate units and the remainder of the Meguma Group.

Follow-up investigations of these airborne gamma-ray spectrometric surveys have confirmed the relationships between uranium and thorium. Limited lithogeochemical sampling has shown that those phases of the granitic suite which exhibit a high eU/eTh ratio also exhibit increased levels of other lithophile elements, Sn and Be and occasionally Li and F.

Entre 1976 et 1983 une série de levées de terrains spectométrique aérien de rayons gamma, avec des lignes de vols éspacées à intervals d'un kilomètre, ont été effectuées dans la province de la Nouvelle Ecosse. Ces levées s'étendent sur la pluspart du terrain Meguma et ont fourni des pattrons de distribution d'éléments radioactifs qui ont été utiles pour décrire divers aspects de la géologie de la region.

Dans une suite Dévoniène-Carbonifère cogénétique de roches granitiques per-alumineuse, il a été démonté que les concentrations d'uranium augmentent progressivement avec des hausses de différenciations alors que les concentrations de thorium montrent deux tendences contrastantes. La tendence la plus dominante, démontrée par les roches granitiques du batholithe de la "South Mountain", (région de New Ross) et du terrain "Eastern Meguma", est une baisse de concentration de thorium avec un accroissement de différenciation. Une autre tendance, moins accentuée, exposée par les roches granitiques de la partie de l'ouest du batholithe de la "South Mountain" montre une hausse des concentrations de thorium avec une hausse de différenciation. Les relations inverses les plus dominantes entre l'uranium et le thorium donnent des rapports eU/eTh, qui sont associés avec les phases plus différenciées de la suite granitique. De plus, certaines unités d'ardoise du groupe Meguma, ont des teneurs d'éléments radioactif qui sont nettement plus élevées, surtout pour le thorium, comparé aux autres unités d'ardoise dans le reste du groupe Meguma.

De plus amples investigations de ces levées spectrometriques à rayons gamma, ont confirmé les relations entre l'uranium et le thorium. Des prévèlements d'échantillons limité de géochimie, ont démontré ces phases de la suite granitique, qui exposent de hautes proportions de eU/eTh, comprennent aussi des niveaux élevés d'autres éléments, lithophiles, Sn, Be, et desfois Li et F.

MARITIME SEDIMENTS AND ATLANTIC GEOLOGY
22, 117-135 (1986)

0711-1150/86/010117-19$3.85/0

INTRODUCTION

The purpose of this paper is to illustrate the variety of airborne gamma ray spectrometric patterns over the granites and metasediments of the Meguma Terrane of Nova Scotia and to correlate these patterns with bedrock petrographic and elemental variations.

Since 1976, the Geological Survey of Canada has been systematically collecting high sensitivity airborne gamma ray spectrometric data in the Province of Nova Scotia. These surveys have proven useful in mapping the regional radioelement distribution patterns, in showing a variety of geological relationships, and in outlining areas of potential uranium and lithophile element enrichment and mineralization. The general principles of gamma ray surveying, including instrumentation, electronics, and operational procedures have been described by Bristow (1979), Grasty (1979) and Killeen (1979).

Between 1976 and 1978, approximately 11,000 line kilometres of reconnaissance (5 km line spacing) airborne gamma ray spectrometric data were collected covering the entire province of Nova Scotia (Geological Survey of Canada, Geophysical Series Maps 35411G, 35511G, 35611G, 36111G and 35821G, and Open File 429). As well, between 1976 and 1983 a substantial portion of southern and central Nova Scotia, covering most of the Meguma Terrane, was reflown with approximately 28,000 line kilometres of surveys with one kilometre line spacing (Fig. 1). This more detailed coverage has

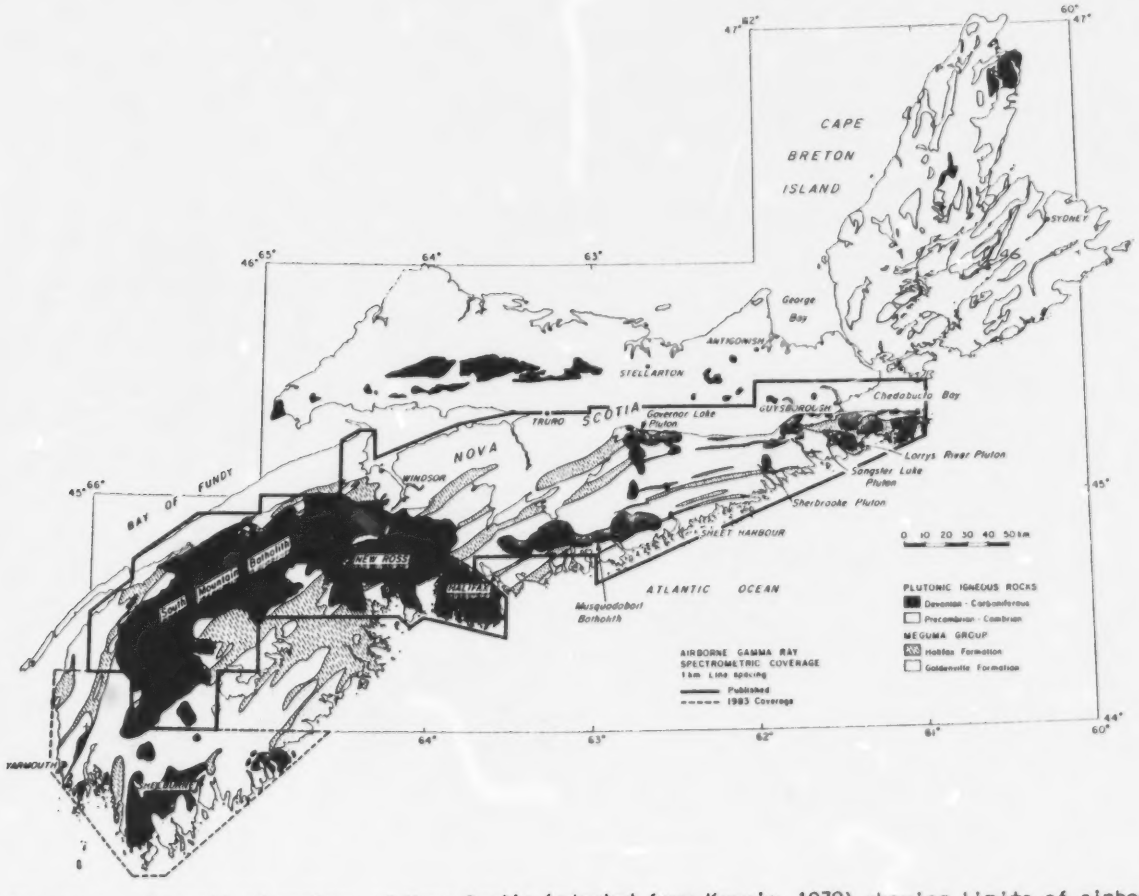

Figure 1 - Generalized geology of Nova Scotia (adapted from Kepple, 1979) showing limits of airborne gamma ray spectrometric coverage. Total area covered with reconnaissance, 5 km line spaced surveys.

provided increased resolution of the radioelement distribution patterns indicated by the reconnaissance surveys resulting in the delineation of several phases of the composite granitic intrusives.

Previously reported ground follow-up investigations (Ford et al, 1981; Ford, 1982; and Ford and Ballantyne, 1983) and data presented in this report have confirmed the radioelement variations within and between the Devonian-Carboniferous granites of southern and central Nova Scotia. In many cases these variations relate to varying degrees of differentiation and possibly autometasomatic alteration within the granites (Chatterjee and Muecke, 1982).

This report will focus on previously defined regional radioelement distribution patterns from the eastern Meguma Terrane with examples from the Governor Lake, Sherbrooke and Sangster Lake Plutons (Fig. 1). Previously unreported results of ground follow-up investigations conducted in 1982 on the Governor Lake and Sherbrooke Plutons along with some earlier results from the Sherbrooke and Sangster Lake Plutons (Ford and Ballantyne, 1983) are included.

REGIONAL GEOLOGY

The geology of the eastern Meguma Terrane is dominated by the Cambro-Ordovician Meguma Group which is divisible into the older Goldenville Formation (predominantly greywacke), and the younger Halifax Formation (predominantly slate) (Fig. 1). These metasedimentary units have been folded into a series of open to tight folds with east-west striking, steeply dipping axial planes. These major Acadian fold structures predate the intrusion into the Meguma Group of a series of Devonian-Carboniferous (c. 370 Ma) granitoid plutons (Smith, 1981; Keppie, 1979). The granitoids range in composition from granodiorite to monzogranite with minor amounts of muscovite-bearing leucogranite and associated aplitic and pegmatitic dyke rocks. Metamorphic grade within the eastern Meguma Terrane ranges from lower greenschist-chlorite grade to middle amphibolite-staurolite grade (Henderson, 1983).

Although not indicated on Figure 1, the geology to the north of the Meguma Terrane is dominated by Lower Carboniferous continental and marine sediments of the Horton and Windsor Groups, respectively. These groups, in part, onlap the Meguma Group (Shubenacadie and Musquodoboit Basins; Boehner, 1980) or are bounded by the West River - St. Mary's Fault.

AIRBORNE GAMMA RAY SPECTROMETRIC RESULTS

Airborne gamma ray spectrometric data acquired over the eastern Meguma Terrane with a line spacing of 1 kilometre are shown on Figures 2,3 and 4. The airborne patterns over the Governor Lake, Sherbrooke and Sangster Lake Plutons (Fig. 1) illustrate the variations generally observed over other granites of the Meguma Terrane. Figure 2 shows that the Sangster Lake Pluton has the highest equivalent uranium (eU) concentrations at slightly greater than 6 ppm while maximum values for the Sherbrooke and Governor Lake Plutons are slightly greater than 3 ppm. These differences may reflect variations in exposure as the Sangster Lake Pluton is well exposed relative to the Sherbrooke and Governor Lake Plutons.

The term equivalent, as reported by the International Atomic Energy Agency (IAEA, 1976) is used for reporting uranium concentration, measured by gamma ray spectrometry where, assuming the sample material is in radioactive equilibrium and appropriate corrections have been made, it is a correct measure of uranium concentration.

The effect of variation in bedrock exposure is further illustrated by comparing the average radioelement

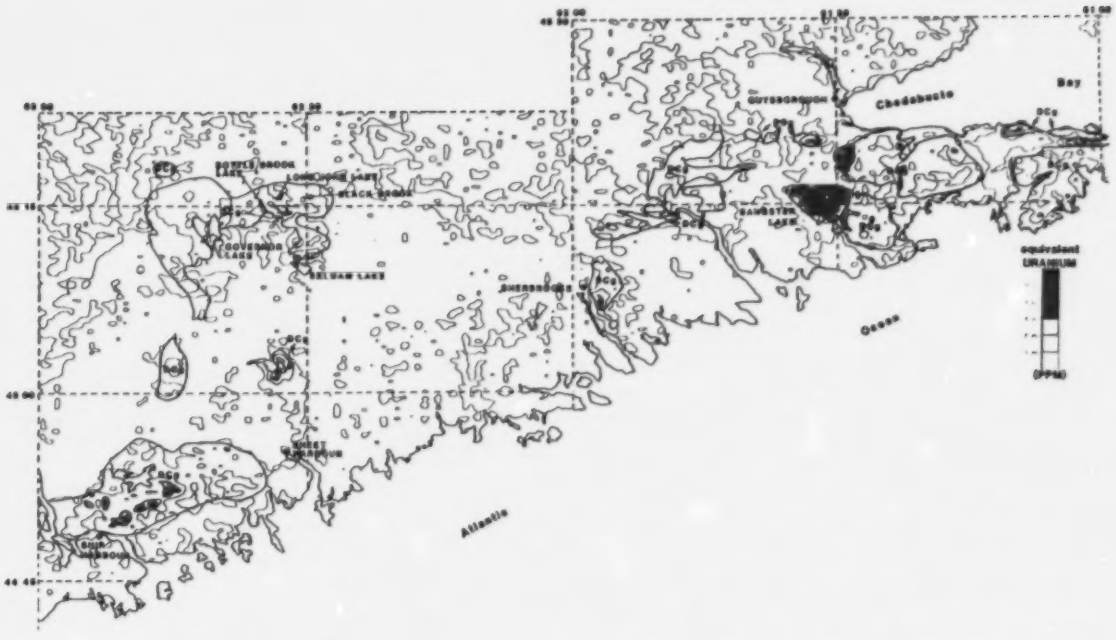

Figure 2 - Equivalent uranium (ppm) map for the eastern Meguma Terrane compiled from 1 km line spaced airborne gamma ray spectrometric surveys. Scale 1 cm = 6.8 km.

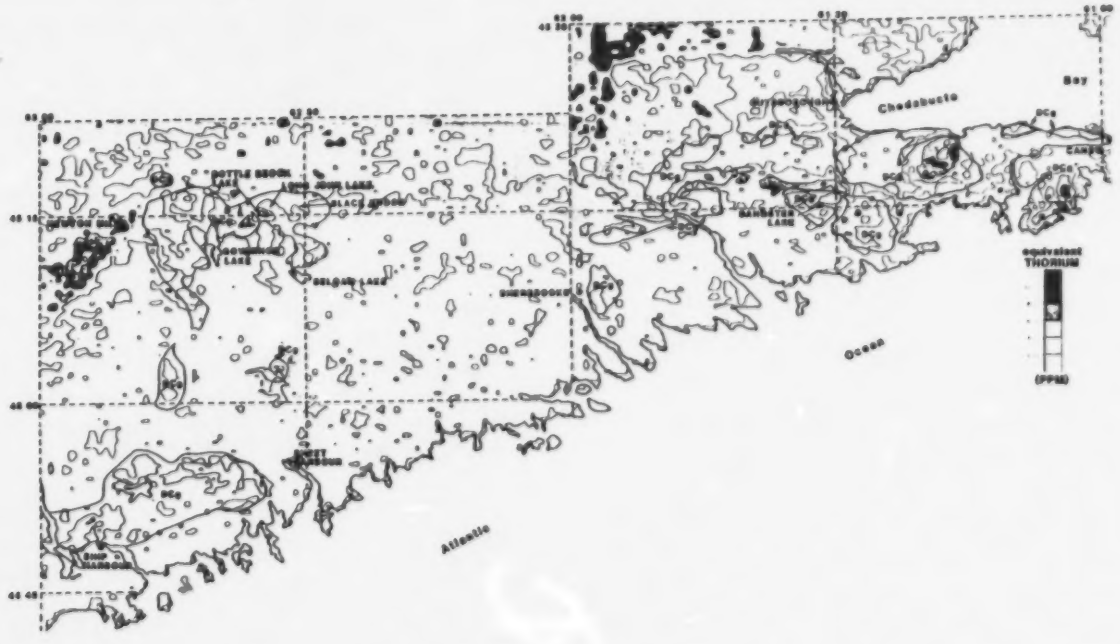

Figure 3 - Equivalent thorium (ppm) map for the eastern Meguma Terrane compiled from 1 km line space airborne gamma ray spectrometric surveys. Scale 1 cm = 6.8 km.

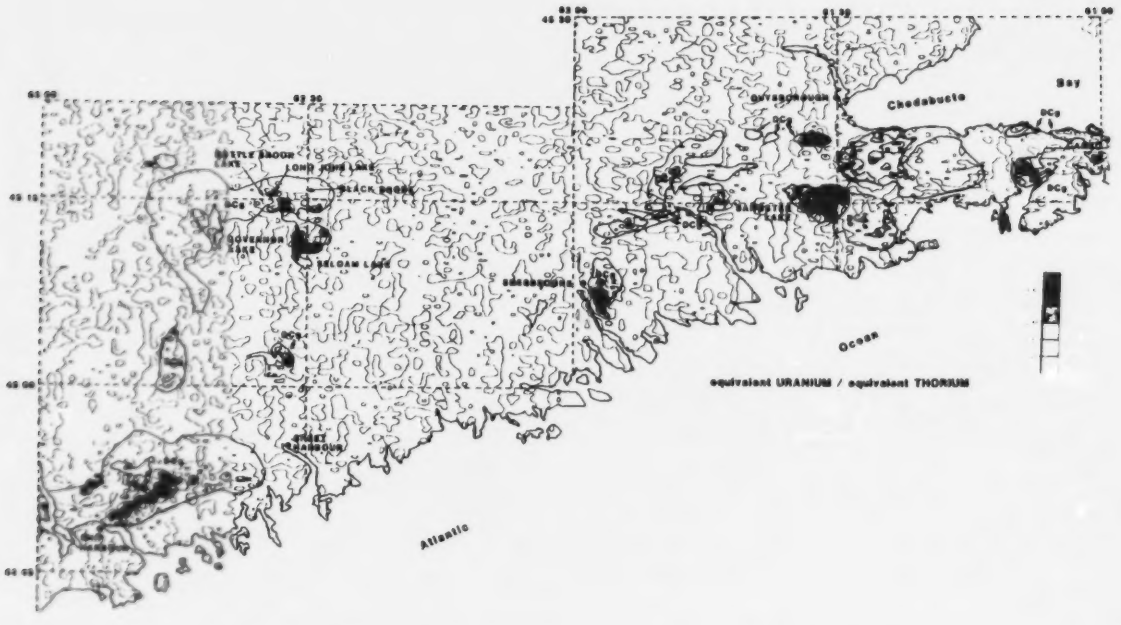

Figure 4 - Equivalent uranium/equivalent thorium ratio map for the eastern Meguma Terrane compiled from 1 km line spaced airborne gamma ray spectrometric surveys. Scale 1 cm = 6.8 km.

concentrations measured by in-situ gamma ray spectrometry for these three plutons (Table 1) with the airborne measurements. The extreme eastern portion of the Sangster Lake Pluton has a mean surface concentration of slightly greater than 6 ppm eU determined by airborne spectrometry and an average bedrock eU concentration of 12.3 ppm based on 19 in-situ gamma ray spectrometric measurements. Compare this with the southwestern portion of the Sherbrooke Pluton which has a mean surface concentration of just slightly greater than 3 ppm eU and an average bedrock concentration of 16.5 ppm eU based on 14 in-situ measurements. Usually airborne determinations of radioelement concentrations will be less than bedrock concentrations, due to the shielding effects of overburden, wetness, and vegetation, however the two measurements will be proportional (Charbonneau et al, 1976).

Figure 2 illustrates the variability of the eU concentrations within each pluton. The Sangster Lake Pluton shows concentrations ranging from 1 ppm near the western margin to greater than 6 ppm in the eastern part of the pluton. In the Sherbrooke Pluton, concentrations range from less than 1 ppm to greater than 3 ppm with maximum concentrations occurring towards the southwest margin. In the Governor Lake Pluton eU concentrations range from less than 1 ppm to greater than 3 ppm with the higher concentrations restricted to the eastern part of the pluton (Bottle Brook Lake - Long John Lake area) and the marginal parts of the pluton in the Seloam Lake area.

In contrast to the eU distribution patterns, those areas of the three plutons which have elevated concentrations of eU generally have the lowest concentrations of equivalent thorium (eTh) (Fig. 3). For example, the southwestern margin of the Sherbrooke Pluton which has eU concentrations of greater than 3 ppm, has eTh concentrations of less than 2 ppm compared with eTh levels for the northeastern portion of the pluton that reach 4 ppm. In the Governor Lake Pluton eTh levels range from less than

Table 1

Radioelement content of various granitic and metasedimentary rock of the eastern Meguma Terrane, Nova Scotia

Location	No. of Values	Arithmetic Mean and Range			Rock Type
		K (%)	eU (ppm)	eTh (ppm)	
GOVERNOR LAKE PLUTON					
- Bottle Brook Lake	15	4.43 (3.89-5.53)	7.9 (5.8-10.8)	30.4 (18.6-38.3)	Fine Grained, Biotite Monzogranite
- Black Brook	17	4.52 (3.69-5.87)	7.4 (4.3-10.2)	11.3 (8.5-13.3)	Coarse Grained, Biotite (±Musc.) Monzogranite
- Long John Lake	24	3.96 (2.52-5.12)	6.8 (3.5-10.5)	4.4 (1.8-7.4)	Medium Grained, Muscovite (±Bio.) Leuco-Monzogranite
- Seloam Lake	14	3.52 (2.84-4.56)	10.9 (6.6-16.3)	4.1 (2.7-7.1)	Medium Grained, Muscovite (±Bio.) Leuco-Monzogranite
SHERBROOKE PLUTON					
- Northeast	4	4.64 (4.30-5.03)	7.9 (7.23-9.16)	10.7 (9.7-11.4)	Medium Grained, Biotite-Muscovite Monzogranite
- Southwest	14	4.13 (3.31-4.99)	16.6 (7.16-31.8)	5.3 (3.2-9.1)	Medium Grained, Muscovite-Biotite Monzogranite
SANGSTER LAKE PLUTON					
- Western	8	3.99 (3.55-4.47)	3.2 (1.9-5.5)	5.1 (4.3-6.4)	Coarse Grained, Biotite-Muscovite Monzogranite
- Central	32	3.57 (2.83-4.68)	9.1 (5.5-13.7)	5.2 (3.4-7.0)	Medium Grained, Biotite-Muscovite Monzogranite
- Eastern	19	3.62 (3.11-4.17)	12.3 (8.6-17.5)	5.0 (4.1-6.1)	Fine-Medium Grained, Muscovite (±Bio.) Leucogranite
MEGUMA GROUP					
- Halifax Form.	31	3.51 (2.17-5.33)	4.9 (1.7-11.4)	17.4 (9.6-25.8)	Andalusite-Bearing Slate, Minor Pyrite
- Goldenville Form.	19	2.33 (1.21-3.66)	1.8 (0.4-4.0)	9.2 (4.9-15.9)	Metaquartzite and Metagreywacke
SOUTH MOUNTAIN BATHOLITH *					
- Granodiorite	31	3.6 (3.0-4.5)	3.6 (1.8-5.4)	12.9 (8.7-15.4)	
- 2 - Mica Monzogranite (New Ross)	54	4.3 (1.8-5.5)	6.9 (2.7-21.7)	10.9 (2.1-20.9)	
- Dike Rocks and minor Intrusives (New Ross)	20	4.1 (3.1-7.0)	8.5 (2.5-21.7)	6.4 (2.3-10.9)	
Average Granodiorite (Taylor, 1965)			3.0	10	
Average Granite (Taylor, 1965)			4.8	17	

Radioelement content of Nova Scotia lithologies measured by in-situ gamma ray spectrometry

2 ppm to greater than 7 ppm. Again, as with the Sherbrooke Pluton, areas of highest eU levels (Bottle Brook Lake - Long John Lake and Seloam Lake) generally have the lowest eTh levels. In the case of the Bottle Brook Lake - Long John Lake area however, eTh levels are somewhat higher at Bottle Brook Lake (7 ppm) than they are at Long John Lake (3 ppm). In-situ gamma ray spectrometric data (Table 1) confirms this relative variation determined by airborne measurements. The fine grained biotite monzogranite of the Bottle Brook Lake area contains on average, 7.9 ppm eU and 30.4 ppm eTh compared with 6.8 ppm eU and 4.4 ppm eTh for the medium grained muscovite leuco-monzogranite of tne Long John Lake area. Airborne eTh determinations over the Sangster Lake Pluton show no apparent zonation and range between 2 to 4 ppm compared with an average bedrock concentration of 5 ppm.

In Figure 4 the high eU/eTh ratios are restricted to those granitic areas which are characterized by either elevated concentrations of uranium and/or depleted concentrations of thorium. In the Sherbrooke Pluton, the high eU/eTh ratio developed along the southwestern margin is the result of increasing eU levels (1-2 ppm for the northeastern margin to greater than 3 ppm for the southwestern edge) superimposed on decreasing eTh levels (4 ppm to less than 2 ppm). In contrast to the Sherbrooke Pluton, the high eU/eTh ratio associated with the central and eastern portions of the Sangster Lake Pluton is the result of sharply increased eU levels (1 ppm in the west to greater than 6 ppm in the east) superimposed on relatively constant eTh levels. In still a third situation, the high eU/eTh ratio associated with the Long John Lake area of the Governor Lake Pluton appears to be the result of decreasing eTh levels superimposed on a relatively constant eU level.

These associations between uranium and thorium and the resulting high eU/eTh ratio are an unusual characteristic of most, but not all, granitoids of the Meguma Terrane.

An interesting additional feature of the airborne gamma ray spectrometric data is the distinction between the Halifax Formation and the Goldenville Formation. The primary difference is illustrated on Figure 3 in the Newton Mills area and along the northern margin of the Sangster Lake Pluton where some slate units of the Halifax Formation are shown to have higher eTh levels than the Goldenville Formation. Variation within and between different slate units may reflect differences in bedrock exposure or overburden variations. Differences in the radioelement concentrations of the Halifax and Goldenville Formations, based on in-situ gamma ray spectrometry are shown in Table 1. Measurements on roadside outcrops of the Halifax Formation southeast of Newton Mills (Fig. 3) reveal eTh concentrations as high as 62 ppm. This high thorium concentration was found to be associated with a narrow (10 cm) quartzitic unit within the slate. Chemical analysis of a sample from this unit (Table 2) shows high Zr with elevated concentrations of TiO_2, Ce, La and Th. Petrographic and microprobe analysis reveal a relatively abundant, apparently detrital, accessory mineral suite composed of zircon-rutile-tourmaline-garnet and thorite.

GROUND FOLLOW-UP INVESTIGATIONS

Bedrock Radioelement Contents

One hundred and fifty seven in-situ gamma ray spectrometric measurements were made on bedrock exposures of the granites and metasediments of the eastern Meguma Terrane of Nova Scotia using a portable Disa 400 (Exploranium) gamma ray spectrometer. Since the airborne measurements represent an average surface concentration which is dependent on the percentage of outcrop and overburden, the relationship between the bedrock and overburden radioelement contents, the percentage

Table 2

Major, Minor and Selected Traces Element Analysis of the Halifax Formation
From The Newton Mills Area, Nova Scotia

Sample	FIA-82-132	FIA-82-133	FIA-82-135		FIA-82-132	FIA-82-133	FIA-82-135
	Black, Pyritic Slate	Grey-Green Non-Pyritic Slate	Fine Grained Grey-Green Quartzitic Unit				
Weight%				PPM			
SiO_2	63.4	61.2	82.0	Sr	110	100	52
TiO_2	.91	.96	1.47	Ba	860	850	170
Al_2O_3	19.9	21.0	7.7	Rb	130	210	40
Fe_2O_3	2.3	.9	.9	Zr	210	130	3470
FeO	2.5	4.8	2.1	Cu	12	13	10
MnO	.03	.40	.32	Pb	8	—	--
MgO	1.42	1.29	.66	Zn	68	90	27
CaO	.06	.16	.47	Li	80	81	44
Na_2O	1.2	.8	1.0	B	47	57	84
K_2O	3.27	4.60	.79	Ce	34	114	230
H_2O	4.2	4.1	1.3	La	16	54	104
CO_2	0.0	0.0	.3	U	5.0	3.0	11.0
P_2O_5	.07	.13	.09	Th	8	16	70
S	.03	.00	.00				
L.O.I.	0.7	--	--				
TOTAL	100.2	100.8	99.6				

Analytical Methods: Major and minor oxides, Rb and Zr by x-ray influorescence except FeO by a modified Wilson's method and H_2O and CO_2 by infra-red spectrometry; Sr, Ba and B by optical emission spectrometry; Cu, Pb, Zn and Li by atomic absorption; Ce, La, U and Th by neutron activation analysis.

of surface water and soil moisture, and the density of vegetation (Charbonneau et al, 1976), the airborne determinations will usually be less than, although proportional to the corresponding bedrock concentrations.

Table 1 lists the average radioelement concentrations in the various phases of the three granites investigated along with the radioelement concentrations of the Halifax and Goldenville Formations of the Meguma Group. For comparison, the average radioelement concentrations of the South Mountain Batholith in the New Ross area are also included (Ford, 1982) along with the average uranium and thorium contents for granodiorite and granite as reported by Taylor (1965).

These averages reflect the generally low eTh concentrations and high eU/eTh ratios for some phases of the Nova Scotia granites. Few phases actually show an enrichment of thorium beyond Taylor's average of 17 ppm for granite. The 30.4 ppm average eTh concentration of the fine grained biotite monzogranite of the Bottle Brook Lake area is the second highest average eTh concentration found for granitoids in the Meguma Terrane of Nova Scotia. As previously reported (Ford, 1982) the highest average concentration of 36.6 ppm, is associated with biotite granite of the Wedgeport Pluton south of Yarmouth.

In Figure 5, the radioelement variation within and between individual plutons is shown to be considerable. Of the three plutons represented in Figure 5, the Governor Lake Pluton shows the greatest variability with individual eU determinations ranging from 3.5 to 16.3 ppm and eTh determinations ranging from 1.8 to 38.3 ppm.

As indicated by the airborne gamma ray spectrometric surveys and confirmed by the bedrock determinations presented in Figure 5 each pluton appears to show a slightly different relationship between the two radioelements. In the Sherbrooke Pluton, average bedrock radioelement concentrations range from 7.9 ppm eU and 10.7 ppm eTh in the northeast to 16.6 ppm eU and 5.3 ppm eTh in the southwest. This inverse relationship is not accompanied by any

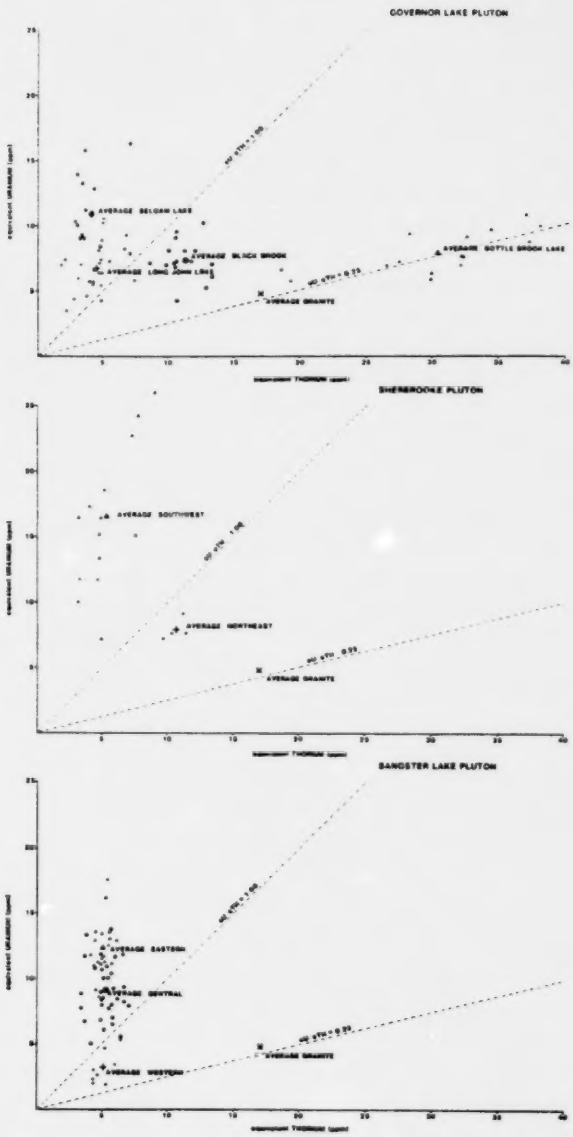

Figure 5 - Variation in equivalent uranium and equivalent thorium contents based on in situ gamma ray spectrometry for the Governor Lake, Sherbrooke and Sangster Lake Plutons. Also shown are the average uranium and thorium contents for granite from Taylor (1965).

obvious change in mineralogy or texture in the Sherbrooke granite except for an increase in the muscovite-biotite ratio with muscovite becoming the predominant micaceous phase in the high eU/eTh ratio portions of this pluton. It has been suggested (Plant et al, 1980) that such an increase in the muscovite-biotite ratio may reflect a high temperature water-rock interaction or autometasomatic alteration. As will be discussed in the next section on lithogeochemistry, the southwest portion of the pluton appears to be more evolved chemically than the northeast portion.

Figure 5 illustrates the restricted range of eTh concentrations for the Sangster Lake Pluton. For the 59 in-situ gamma ray spectrometric measurements, the eTh concentrations exhibit a narrow range from 3.4 to 7.0 ppm while the eU concentrations range from 1.9 to 17.5 ppm. These data and the corresponding averages reflect a sharp increase in the eU concentrations superimposed on a constant eTh concentration resulting in a high eU/eTh ratio for the eastern portion of the pluton. These variations do not correspond with any obvious mineralogical or textural variation in the pluton with the exception of a slight increase in the muscovite content associated with the high ratio portion of this two-mica monzogranite (O'Reilly, personal communication, 1983). A limited number of measurements taken on outcrop of a small leucogranite phase in the eastern portion of the Sangster Lake Pluton show eU concentrations as high as 51.7 ppm with a corresponding eTh concentration of 4.6 ppm. However, measurements considered to be more representative of this phase show eU concentrations of between 9.0 and 19.4 ppm with corresponding eTh concentrations between 1.2 and 3.5 ppm. These values suggest only slight differences between this more evolved (O'Reilly, 1983) leucogranite phase and the less evolved monzogranite, and may not be enough to distinguish these two separate phases on the airborne data.

In the Governor Lake Pluton the radioelement variations shown in Figure 5 correspond with distinct petrographic variations. As will be shown in a discussion of the lithogeochemistry of these phases the low eTh and high eU/eTh ratio phases at Long John Lake and Seloam Lake are more evolved than the Black Brook and Bottle Brook Lake phases. In both the Long John Lake and Seloam Lake areas the predominant rock type is a medium grained, muscovite leuco-monzogranite with minor biotite, while at Black Brook and Bottle Brook Lake the predominant rock type is a biotite monzogranite with minor muscovite.

In the New Ross area of the South Mountain Batholith, Chatterjee and Muecke (1982) have noted similar variations in uranium and thorium concentrations which they have related to differentiation within a cogenetic suite of granitic rocks. Uranium concentrations were shown to increase and thorium concentrations decrease with progressive differentiatiion from a biotite granodiorite, through biotite-muscovite and leucocratic monzogranite to minor intrusions of aplite, pegmatite and porphyries. The range or rock types encountered in the South Mountain Batholith was not encountered in the plutons from the eastern Meguma Terrane reported here although granodioritic phases may be present in the western portion of the Governor Lake Pluton and have been recorded in other plutons of the Chedabucto Bay area (O'Reilly, 1983; Ham, 1983).

The variations in radioelement concentrations measured by in-situ gamma ray spectrometry clearly verify the relative variations observed in the regional airborne survey data and show a correlation with differentiation and possibly autometasomatic alteration.

Lithogeochemistry in Relation to Radioelement Variation

Based on a limited rock sampling program, Ford et al. (1981) showed that

Table 3
Means and ranges of major, minor and trace element analysis
of the various phases of the Governor Lake Pluton, Nova Scotia

	GOVENOR LAKE PLUTON						
	Bottle Brook Lake (N=5)	Black Brook (N=6)	Long John Lake (N=6)	Seloam Lake (N=6)	Dyke Rocks (N=4)		
	Fine Grained Biotite Monzogranite	Coarse Grained Biotite (±Musc.) Monzogranite	Medium Grained Muscovite (±Bio.) Leuco-Monzogranite	Medium Grained Muscovite (±Bio.) Leuco-Monzo granite		Specialized or Stannigene Granites (Tischendorf, 1977) Group I	Normal Granites (Tischendorf, 1977) Group III
SiO_2	72.48	72.30	75.90	74.18	75.38	73.38	70.84
	(71.20-73.30)	(71.40-73.50)	(73.70-77.00)	(73.50-74.60)	(73.90-78.00)		
TiO_2	.35	.28	.07	.05	.02	.16	.34
	(0.33-0.37)	(0.18-0.37)	(0.03-0.10)	(0.02-0.09)	(0.01-0.03)		
Al_2O_3	14.28	14.72	14.05	15.25	15.30	13.97	14.33
	(13.90-15.30)	(14.20-15.30)	(13.00-15.30)	(14.80-15.90)	(13.50-16.10)		
Fe_2O_3	.74	.32	.18	.30	.22	.80	1.31
	(0.40-1.30)	(0.00-0.90)	(0.00-0.30)	(0.00-0.60)	(0.10-0.30)		
FeO	.90	1.23	.38	.22	.25	1.10	1.78
	(0.40-1.20)	(0.30-1.80)	(0.20-0.50)	(0.00-0.40)	(0.20-0.30)		
MnO	.03	.03	.02	.04	.04	.045	.064
	(0.02-0.03)	(0.02-0.04)	(0.01-0.02)	(0.01-0.17)	(0.01-0.06)		
MgO	.63	.62	.20	.16	.14	.47	.81
	(0.57-0.68)	(0.28-0.84)	(0.07-0.26)	(0.09-0.23)	(0.10-0.19)		
CaO	.69	.91	.43	.31	.51	.75	1.89
	(0.55-0.86)	(0.61-1.27)	(0.33-0.60)	(0.14-0.55)	(0.34-0.71)		
Na_2O	2.72	3.00	3.27	4.07	4.58	3.20	3.44
	(2.20-3.60)	(2.50-3.30)	(2.40-4.10)	(3.60-4.50)	3.20-5.70)		
K_2O	5.04	4.56	4.04	4.95	2.26	4.69	4.34
	(4.68-5.17)	(3.86-5.06)	(3.49-4.54)	(3.68-4.170	(0.73-3.15)		
H_2O	.96	.93	.85	.82	.82	—	—
	(0.80-1.20)	(0.90-1.00)	(0.60-1.10)	(0.70-0.90)	(0.40-1.30)		
CO_2	.26	.07	.20	.35	.08	—	—
	(0.00-0.70)	(0.00-0.10)	(0.10-0.60)	(0.10-0.50)	(0.00-0.10)		
P_2O_5	.28	.27	.32	.28	.46	—	—
	(0.25-0.31)	(0.19-0.36)	(0.26-0.37)	(0.19-0.37)	(0.29-0.54)		
Total	99.90	99.24	99.91	99.98	100.06	A	B
Sr	51	67	10	15	50	7	100
	(43-60)	(37-93)	(3-13)	(3-29)	(13-95)	(2-31)	
Ba	448	422	60	84	46	68	840
	(440-480)	(210-610)	(21-87)	(11-190)	(17-100)	(3-356)	
Rb	294	437	287	347	338	651	170
	(270-330)	(220-300)	(210-370)	(200-480)	(160-500)	(300-1,080)	
Zr	142	118	42	38	45	177	175
	(130-170)	(60-150)	(30-40)	(30-50)	(40-50)	(58-400)	
F	760	567	550	383	375	4330	850
	(400-900)	(400-700)	(300-700)	(200-500)	(100-500)	(2,200-6,000)	
Li	99	110	114	95	32	84	40
	(66-143)	(92-147)	(79-168)	(36-156)	(8-51)	(50-200)	
Be	3.2	4.1	4.0	5.7	156.2	14	3
	(1.0-4.9)	(2.0-5.8)	(2.3-6.3)	(3.8-10.0)	(26.0-410.0)	(2-50)	
Sn	7.2	11.0	13.5	28.7	50.0	22	3
	(4-12)	(5-16)	(9-19)	(12-43)	(42-65)	(2-114)	
Ce	60.0	39.0	9.0	5.3	5.5	111	97
	(54-66)	(24-50)	(6-14)	(2-10)	(2-8)	(47-293)	
La	22.0	16.0	3.0	2.2	1.8	99	55
	(20-25)	(9-22)	(2-5)	(1-4)	(1-3)	(24-330)	
U	6.9	4.8	5.4	4.8	14.0	—	4.7
	(5.0-8.0)	(3.5-6.5)	(2.5-10.0)	(3.5-8.0)	(2.0-25.0)		
Th	27.0	10.0	2.0	1.0	1.0	46	20
	(23-30)	(7-12)	(1-4)	(1-2)	(1-1)	(3-105)	
U/Th	0.26	0.48	2.70	4.80	14.00	—	0.24

A - Means and ranges of trace elements in stanniferous granites, Younger Granites, Northern Nigeria: Olade (1980)

B - Low-calcium granites: Turekian and Wedepohl (1961)

Analytical methods: Major and minor oxides, Rb, Zr and Sn by x-ray fluorescence except FeO by a modified Wilson's method and H_2O and CO_2 by infra-red spectrometry; Sr, Ba and Be by optical emission spectrometry; Ce, La, U and Th by neutron activation analysis; F by fusion and specific-ion electrode; Li by atomic absorption.

Table 4
Means and ranges of major, minor and trace element analysis of the various phases of the Sherbrooke and Sangster Lake Plutons, Nova Scotia

	SHERBROOKE PLUTON				SANGSTER LAKE PLUTON				
	Northeast (N=4)1	Southwest (N=4)2	Leucogranite Dykes (N=8)3	Albitized Dyke (N=3)	West (N=3)	East I (N=13)	East II (N=11)		
	Medium Grained Biotite-Muscovite Monzogranite	Medium Grained Muscovite-Biotite Monzogranite	Fine Grained Muscovite Leuco Monzogranite		Coarse Grained Biotite-Muscovite Monzogranite	Medium Grained Biotite-Muscovite Monzogranite	Fine-Medium Grained Muscovite (+Biotite) Leucogranite	Specialized or Stanniferous Granites (Tischendorf, 1977) Group I	Normal Granites (Tischendorf, 1977) Group III
SiO_2	73.67 (71.80-75.00)	73.45 (72.60-74.20)	74.76 (73.30-76.60)	74.27 (74.00-74.50)	74.13 (73.10-75.50)	72.55 (69.40-76.30)	73.57 (67.90-75.30)	73.84	70.84
TiO_2	.17 (0.11-0.23)	.08 (0.04-0.13)	.06 (0.01-0.09)	.02 (0.01-0.03)	.17 (0.14-0.23)	.20 (0.11-0.27)	.06 (0.02-0.17)	.16	.34
Al_2O_3	14.17 (14.30-15.10)	14.78 (14.30-15.30)	14.60 (13.40-15.90)	15.36 (15.00-15.70)	14.30 (13.50-15.00)	15.49 (13.80-17.30)	15.61 (14.60-18.90)	13.97	14.33
Fe_2O_3	.21 (0.20-0.30)	.15 (0.00-0.20)	.22 (0.10-0.30)	.31 (0.30-0.31)	1.06 (0.91-1.38)	1.52 (0.84-2.12)	.89 (0.33-2.10)	.80	1.31
FeO	.94 (0.59-1.17)	.61 (0.40-0.80)	.31 (0.10-0.50)					1.10	1.78
MnO	.02 (0.02-0.03)	.03 (0.02-0.03)	.04 (0.01-0.08)	.03 (0.02-0.04)	.03 (0.02-0.04)	.05 (0.02-0.06)	.04 (0.01-0.23)	.045	.064
MgO	.35 (0.08-0.53)	.21 (0.16-0.27)	.07 (0.00-0.17)	.05 (0.02-0.09)	.33 (0.26-0.46)	.36 (0.20-0.48)	.13 (0.03-0.37)	.47	.81
CaO	.65 (0.53-0.78)	.52 (0.46-0.64)	.37 (0.23-0.64)	.39 (0.30-0.39)	.64 (0.60-0.69)	.38 (0.28-0.47)	.29 (0.14-0.49)	.75	1.89
Na_2O	3.54 (3.00-3.81)	4.06 (3.80-4.50)	4.84 (3.13-5.90)	6.96 (6.40-7.85)	3.66 (3.45-3.76)	3.88 (3.07-4.51)	4.49 (3.56-5.29)	3.20	3.44
K_2O	4.67 (4.23-5.11)	4.16 (3.93-4.55)	3.25 (2.02-4.53)	1.35 (0.89-2.20)	4.55 (4.37-4.70)	4.16 (3.49-4.98)	3.95 (3.16-4.69)	4.69	4.34
H_2O	.73 (0.40-0.90)	.70 (0.60-0.80)	.60 (0.40-0.80)	.43 (0.30-0.60)	.60 (0.60-0.60)	.70 (0.10-1.00)	.52 (0.30-1.00)	—	—
CO_2	.13 (0.00-0.20)	.30 (0.10-0.60)	.19 (0.10-0.30)	.07 (0.00-0.10)	—	—	—	—	—
P_2O_5	.22 (0.16-0.27)	.30 (0.25-0.37)	.29 (0.14-0.62)	.31 (0.30-0.34)	.29 (0.24-0.36)	.35 (0.23-0.48)	.38 (0.30-0.44)	—	—
Total	99.41	99.35	99.60	99.95	99.76	99.64	99.73	A	B
Sr	71 (54-97)	17 (3-36)	28 (12-75)	31 (10-50)	67 (30-100)	18 (3-50)	47 (3-120)	7 (2-31)	100
Ba	310 (110-430)	25 (10-55)	34 (10-71)	34 (13-40)	245 (120-360)	80 (50-130)	92 (20-320)	68 (3-356)	840
Rb	224 (199-242)	294 (210-350)	387 (257-610)	497 (390-690)	207 (160-280)	335 (240-510)	412 (280-600)	651 (300-1,080)	170
Zr	90*	40** (40-40)	53*** (30-70)	37 (10-70)	27 (10-40)	45 (20-60)	11 (10-40)	177 (58-400)	175
F	452 (290-600)	587 (460-690)	465 (280-900)	595 (200-850)	342 (270-400)	800 (600-1050)	538 (390-710)	4330 (2,200-6,000)	850
Li	115 (61-187)	166 (103-263)	51 (28-80)	6 (4-8)	52 (4-8)	180 (27-362)	64 (21-168)	84 (50-200)	40
Be	6.9 (2.6-11.0)	11.3 (2.7-26.0)	53.5 (7.9-140.0)	128.0 (100.0-182.0)	3.8 (3.5-4.0)	10.5 (3.5-28.0)	25.3 (3.0-61.0)	14 (2-50)	3
Sn	9.6 (6.5-14.0)	19.8 (8.0-35.0)	39.1 (12-72)	248.0 (126.0-400.0)	8 (4-10)	21 (1-33)	32 (16-48)	22 (2-114)	3
Ce	34*	9.0** (8-10)	7.0*** (4-16)	6*	—	—	—	111 (47-293)	57
La	13*	2.5** (2-3)	2.5*** (1-6)	3*	—	—	—	99 (24-560)	55
U	2.7 (1.6-3.6)	9.0 (2.9-17.5)	8.7 (1.9-16.5)	8.8 (7.0-12.0)	3.7 (2.5-5.0)	9.5 (5.5-16.7)	9.8 (2.5-21.0)	—	4.7
Th	4.8 (2-8)	2.2 (1-4)	1.0 (1-2)	1.0 (1-1)	3.0 (2-4)	4.1 (1-7)	1.7 (1-6)	46 (3-105)	20
U/Th	0.56	4.09	8.70	8.80	1.23	2.32	5.76	—	0.24

* - One analysis only; ** - Two analyses only; *** - Four analyses only

1 - Three analyses supplied by P.K. Smith, Nova Scotia Dept. of Mines and Energy
2 - Two analyses supplied by P.K. Smith, Nova Scotia Dept. of Mines and Energy
3 - Four analyses supplied by P.K. Smith, Nova Scotia Dept. of Mines and Energy

A - Means and ranges of trace elements in stanniferous granites, Younger Granites, Northern Nigeria; Olade (1980)
B - Low-calcium granites: Turekian and Wedepohl (1961)

Analytical methods: Sherbrooke Pluton - Major and minor oxides, Rb, Zn and [illegible] by x-ray fluorescence, except FeO by a modified Wilson's method and H_2O and CO_2 by infrared spectrometry; Sr, Ba and Be by optical emission spectrometry; Ce, La, U and Th by neutron activation analysis; F by fusion and specific-ion electrode; Li by atomic absorption. Sangster Lake Pluton - Major and minor oxides, Sr, Ba, Rb, Zr and Sn by x-ray fluorescence, Be and Li by atomic absorption; F by fusion and specific-ion electrode; U and Th by neutron activation analysis.

the Sangster Lake Pluton was enriched in U, Sn, Rb, Li and Cs and depleted in Sr, Ba, Zr and Th compared to the average abundances of these elements for low-Ca granites as given by Turekian and Wedepohl (1961). Additional work by Ford and Ballantyne (1983) on the Sangster Lake Pluton correlated these enrichment and depletion trends with variation in the radioelement concentrations and showed that in general the high U/Th ratio phases exhibited the characteristics of increased differentiation and possible autometasomatic alteration.

Table 3 and 4 provide a summary of the major, minor and selected trace element analyses for the Governor Lake, Sherbrooke and Sangster Lake Plutons along with major and minor element data from Tischendorf (1977) and trace element data from Olade (1980) and Turekian and Wedepohl (1961) for comparison. These analyses do not represent all of the phases, styles of alteration or mineralization which may be present in these granites.

Compared to the "Normal Granite" group of Tischendorf (1977) the various phases of the three plutons presented in Tables 3 and 4 generally show elevated concentrations of SiO_2, Al_2O_3 and Na_2O, and depleted concentrations of TiO_2, Fe (Total), MnO, MgO and CaO. Many of these elemental abundances compare closely with Tischendorf's "Specialized or Stannigene granite" group. The selected trace element data show enrichment in Rb, Li, Be, Sn and U, and depletion in Sr, Ba, Zr, F and Th compared to Turekian and Wedepohl's average abundances for low-Ca granites.

Variations in elemental concentrations between the various phases sampled from each pluton can generally be correlated with the radioelement variations. In particular, certain elements are shown to increase and others to decrease with an increasing U/Th ratio (Figs. 6, 7 and 8). With an increasing U/Th ratio, the major and minor element variations reflect increasing differentiation and possible autometasomatic alteration in the form of pervasive albitization. This albitization trend, while not obvious petrographically is obvious chemically. Figures 6, 7 and 8 all show that with an increasing U/Th ratio, the K_2O concentrations decrease progressively while the Na_2O concentrations increase. This albitization trend and the associated radioelement variations may reflect the cumulative effects of increasing igneous differentiation and autometasomatic alteration. Albitization trends have been described elsewhere, as in the Nigerian Younger Granite Province by Olade (1980) and in the Tin Granites of the Seward Peninsula, Alaska by Hudson and Arth (1983).

This albitization trend and the associated U/Th ratio increases are both accompanied by enrichment and depletion of other elements. For example, CaO, Fe (Total), MgO and TiO_2 all show a general reduction in concentration with increasing U/Th ratio. These variations reflect the generally increasing leucocratic appearance of each successive phase. Selected trace element variations show similar enrichment and depletion trends associated with the increasing U/Th ratio although in each example their relative variations may be slightly different. For example, Rb generally shows a progressive enrichment with increasing U/Th although in the Governor Lake Pluton, Rb concentrations appear relatively constant in all phases sampled. Barium concentrations generally decrease and in some situations quite sharply (i.e. Governor Lake and Sherbrooke Plutons). Lithium concentrations appear to increase initially but then decrease sharply in the more evolved phases. Tin and beryllium both show progressive enrichment with increasing U/Th ratio although in the Governor Lake Pluton, Be enrichment is only slight until the final phases are encountered. Uranium and thorium concentrations follow the same relative variations as indicated

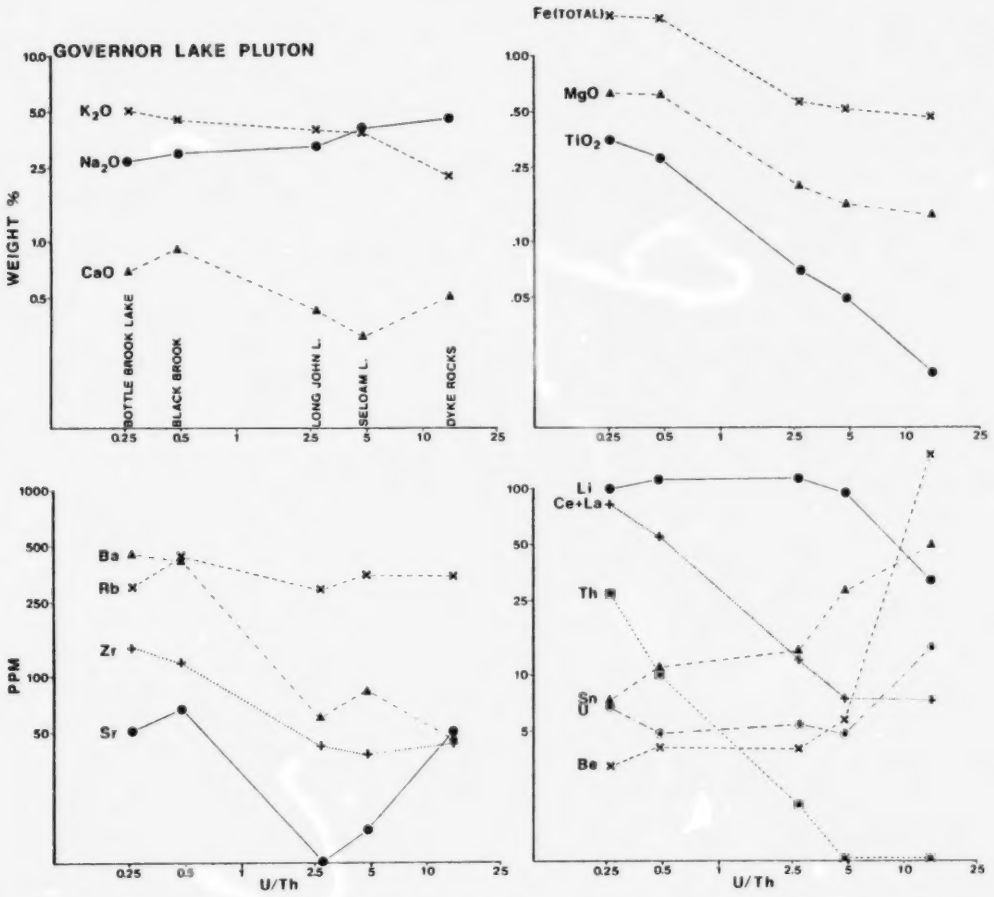

Figure 6 - Variation in selected major and minor oxides, and trace elements as a function of increasing U/Th ratio for the various phases of the Governor Lake Pluton. Uranium and thorium analysis by delayed neutron counting and neutron activation analysis, respectively.

by the airborne and ground gamma ray spectrometric surveys. Uranium concentrations either increase or remain relatively constant while thorium concentrations generally decrease, although in the Sangster Lake Pluton they remain relatively constant.

A relationship between the albitization trend and possible mineralization processes is suggested by comparison of the chemical analyses from the various phases for the Sherbrooke Pluton. Figure 7 illustrates the progressive increase in Na_2O, Rb, Sn and Be and decrease in K_2O, CaO, Fe (Total), MgO, TiO_2 and Ba with increasing U/Th ratio from the northeastern portion of the pluton to the southwestern portion and into the leucogranite dyke rocks. However, samples from an albitized dyke situated near the western margin of the pluton show extreme enrichments and depletions. Tin and beryllium concentrations reach maximums of 400 and 180 ppm respectively with associated Na_2O concentrations reaching a high of 7.8 wt. % while K_2O concentrations are depleted to a low of 0.9 wt. %. Ford and Ballantyne (1983) report the presence of cassiterite in samples from this albitized dyke but could not identify discrete Be-bearing mineral phases. Muscovite separates from this dyke were found to contain Be concentrations of 700 ppm. This is considerably higher than Be concentrations of muscovite reported by Beus (1965) which ranged from 30-140

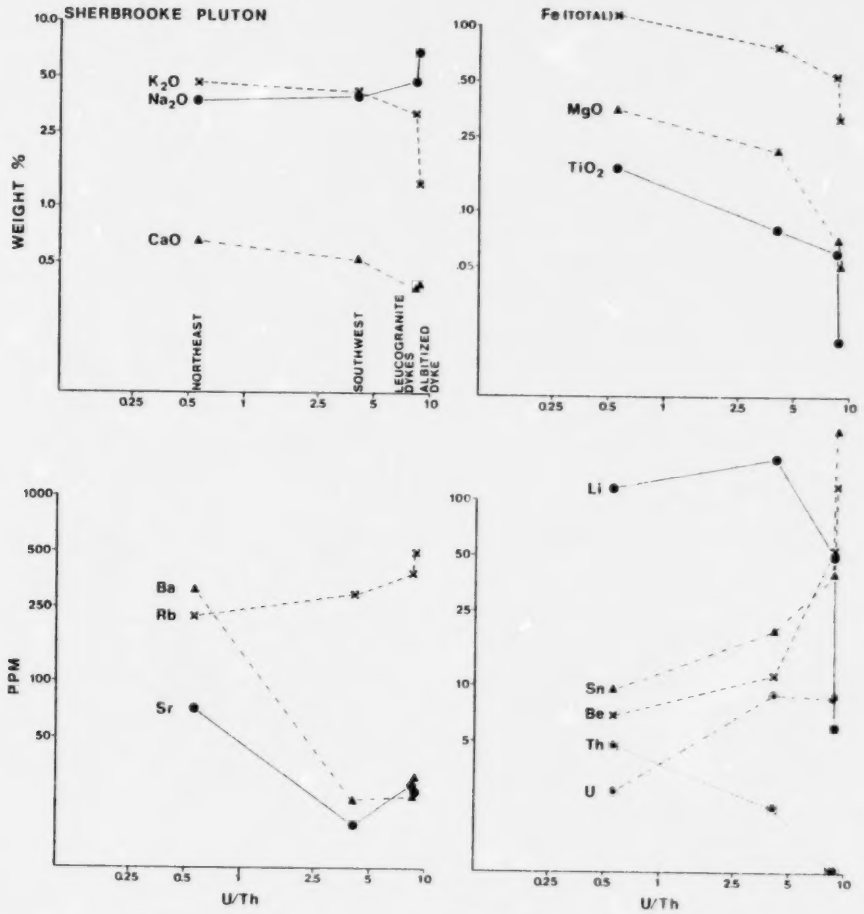

Figure 7 - Variation in selected major and minor oxides, and trace elements as a function of increasing U/Th ratio for the various phases of the Sherbrooke Pluton. Uranium and thorium analysis by delayed neutron counting and neutron activation analysis, respectively.

ppm. Beryl was identified in boulder samples of leucogranite dykes collected along the eastern margin of the Seloam Lake portion of the Governor Lake Pluton. Beryllium concentrations reached highs of 410 ppm in these samples.

Ford and Ballantyne (1983) reported the presence of the mineral phases, ixiolite, $(Ta, Nb, Fe, Mn, Sn)_4O_8$ and tapiolite, $(Fe^{+2}(Ta, Nb)_2O_6)$ in samples of the Sangster Lake Pluton which contained relatively high concentrations of Sn, Be, Nb and Ta. The presence of such mineral phases may explain the anomalous Sn concentrations in other phases of the granites of the eastern Meguma Terrane. It has also been reported (Imeokparia, 1982) that biotites from stanniferous granites of the Amo Younger Granite in Nigeria contain anomalous levels of Sn however those phases of the eastern Meguma Terrane granites reported here that have the highest Sn concentrations are often depleted in biotite.

Fission track and scanning electron microprobe studies on samples from the uranium-enriched phases of the Sangster Lake Pluton indicate that the most abundant uranium-bearing phases include Fe-oxide, principally coating fractures and a variety of phosphate-rich phases which include Fe, rare-earth and chlorine-bearing varieties (Figures 9A and 9B). In addition, apatite (Figures

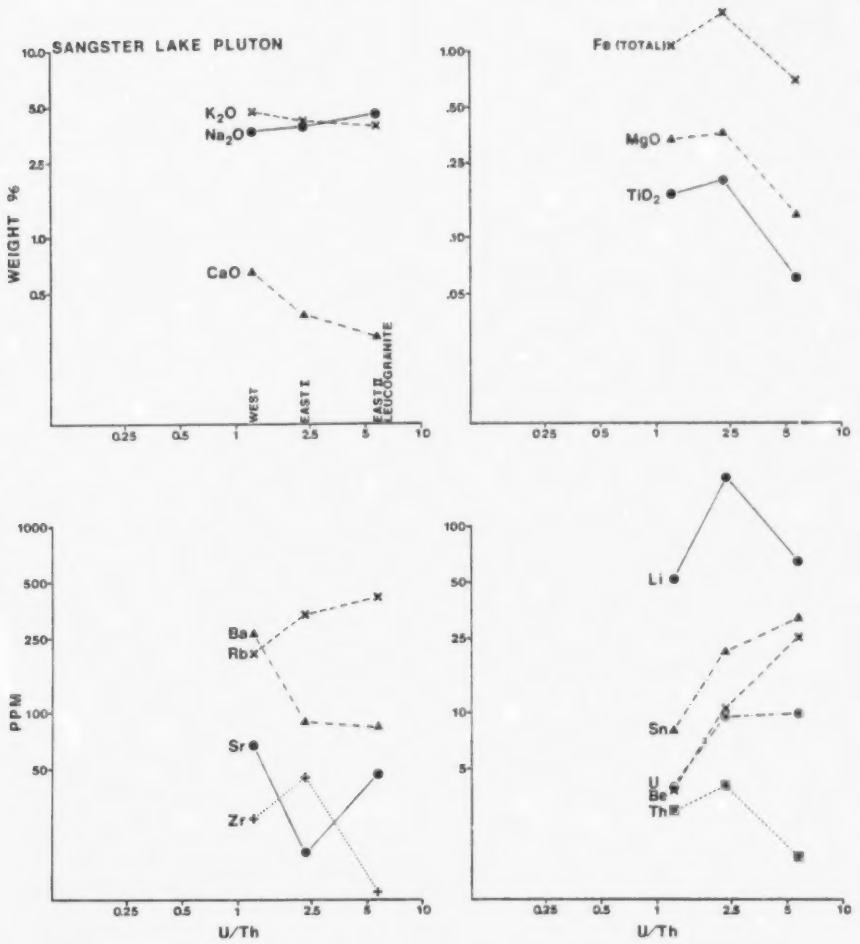

Figure 8 - Variation in selected major and minor oxides, and trace elements as a function of increasing U/Th ratio for the various phases of the Sangster Lake Pluton. Uranium and thorium analysis by delayed neutron counting and neutron activation analysis, respectively.

9C and 9D) with or without monazite and zircon inclusions show particularly strong fission track responses. In addition, minute monazite and zircon grains as inclusions in biotite show particularly strong fission track responses.

SUMMARY

Ground follow-up investigations not only confirm the relative variations in radioelement concentrations that are indicated by the airborne gamma ray spectrometric surveys, but they also illustrate the capability of the airborne results to delineate those granites or phases of larger composite granitic plutons that exhibit the characteristics of increased differentiation and/or autometasomatic alteration. In the eastern Meguma Terrane, the more evolved or differentiated granites generally show higher eU/eTh ratios than those less evolved phases. The high ratios are usually the result of an inverse relationship between the radioelements with U concentrations generally increasing and Th concentrations decreasing with increasing differentiation. The reasons for the unusually high eU/eTh ratios is not clearly understood but may be related to the cumulative effects of igneous

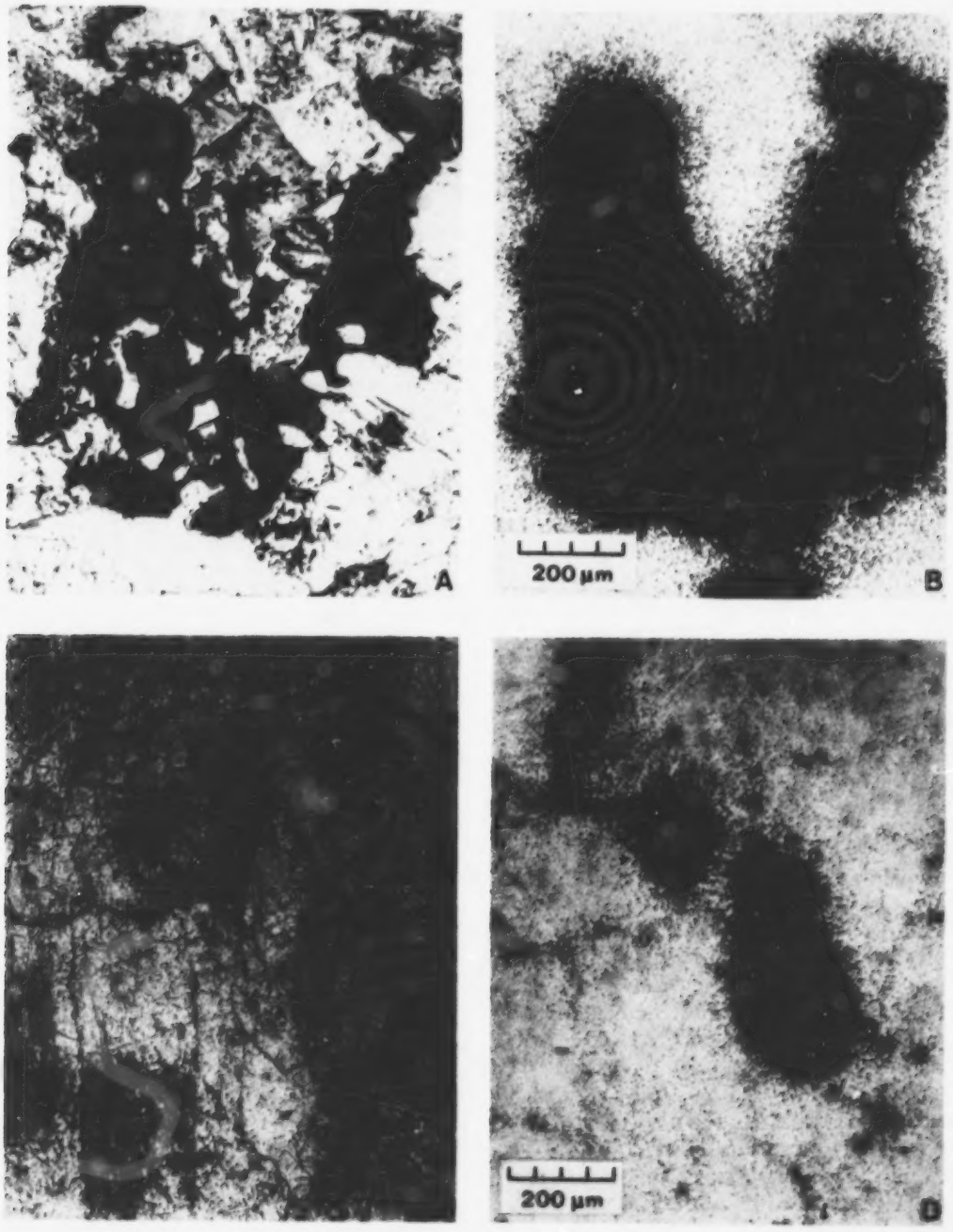

Figure 9 - Photomicrographs of Fe-bearing phosphate phase - 9A and apatite (A) -9C along with their associated fission track responses - 9B and 9D, respectively.

differentiation and some degree of late-stage autometasomatism. This is suggested by the correlation between the increasing U/Th ratios and the "albitization" trend. Associated with the increasing U/Th ratios and the albitization trend are enrichments and depletions in other elements. Of particular significance in the eastern Meguma Terrane is the enrichment of Sn and Be in the more evolved, high U/Th ratio phases.

The application of gamma ray spectrometry as a technique for delineating various phases of a composite suite of granitic rocks and for exploring for lithophile element mineralization in granitic environments has also been suggested by Yeates et al. (1982). It has been shown here that airborne and ground gamma ray spectrometric surveys are not only useful in delineating various phases of composite granite plutons but that they are also useful as a potential exploration technique in the regional exploration for granite-related lithophile elements. Those phases that are delineated by gamma ray spectrometry as having characteristics of increased differentiation (high eU/eTh ratios) and confirmed by bedrock sampling as having elevated levels of other lithophile elements may be precursors to, or are spatially related to potential economic concentrations.

ACKNOWLEDGEMENTS

We would like to thank Mrs. G.M. LeCheminant and Mr. G.R. LaChance, both of the Central Laboratories and Technical Services Division of the Geological Survey of Canada for carrying out mineral identification and microprobe analyses, and for supervising the chemical analysis of rock samples. We would also like to extend our appreciation to Mr. P.K. Smith of the Nova Scotia Department of Mines and Energy for providing additional analysis of samples from the Sherbrooke Pluton and for valuable discussions relating to geology of the area. Discussions with Mr. S.B. Ballantyne and Mr. B.W. Charbonneau of the Geological Survey of Canada were invaluable as were their critical reviews of this paper.

BEUS, A.A. 1965. Geochemistry of beryllium and genetic types of beryllium deposits; ed. L.R. Page; W.H. Freeman and Company, San Francisco, 401 p.

BOEHNER, R.C. 1980. Geology, geochemistry and geophysics of the Shubenacadie-Stewiacke salt deposit, Hants and Colchester Counties, Nova Scotia. Nova Scotia Department of Mines and Energy, Report 80-1, pp. 165-186.

BRISTOW, Q. 1979. Gamma ray spectrometric methods in uranium exploration: airborne instrumentation. In Geophysics and Geochemistry in the Search for Metallic Ores; ed. Peter J. Hood; Geological Survey of Canada, Economic Geology Report 31, pp. 135-146.

CHARBONNEAU, B.W., P.G. KILLEEN, J.M. CARSON, G.W. CAMERON and K.A. RICHARDSON. 1976. Significance of radioelement concentration measurements made by airborne gamma ray spectrometry over the Canadian Shield. IAEA Symposium on Exploration for Uranium Ore Deposits, Vienna, Austria, 1976, ST1/PUB/434, IAEA-SM 208/3, pp. 35-53.

CHATTERJEE, A.K. and G.K. MUECKE. 1982. Geochemistry and the distribution of uranium and thorium in the granitoid rocks of the South Mountain Batholith, Nova Scotia: some genetic and exploration implications. In Uranium in Granites, ed. Y.T. Maurice; Geological Survey of Canada, Paper 81-23, pp. 11-17.

FORD, K.L., J.M. CARSON and P.B. HOLMAN. 1981. Preliminary airborne gamma ray spectrometric maps and ground investigations, central Nova Scotia. Geological Survey of Canada, Open File 789.

FORD, K.L. 1982. Investigation of regional airborne gamma ray spectrometric patterns in New Brunswick and Nova Scotia. Geological Survey of Canada, Paper 82-1B, pp. 177-194.

FORD, K.L. and S.B. BALLANTYNE. 1983. Uranium and thorium distribution patterns and lithogeochemistry of Devonian granites in the Chedabucto Bay area, Nova Scotia. Geological Survey of Canada, Paper 83-1A, pp. 109-119.

GRASTY, R.L. 1979. Gamma ray spectrometric methods in uranium exploration - theory and operational procedures. In Geophysics and Geochemistry in the Search for Metallic Ores; ed. Peter J. Hood; Geological Survey of Canada, Economic Geology Report 31, pp. 147-161.

HAM, L. 1983. The Halfway Cave - Queensport Pluton, Guysborough County, Nova Scotia. Nova Scotia Department of Mines and Energy, Information Series No. 6, p. 61.

HENDERSON, J.R. 1983. Analysis of structure as a factor controlling gold mineralization in Nova Scotia. Nova Scotia Department of Mines and Energy, Report 83-1, pp. 265-282.

HUDSON, T. AND J.G. ARTH. 1983. Tin granites of Seward Peninsula, Alaska. Geological Society of American Bulletin, 94, pp. 768-790.

INTERNATIONAL ATOMIC ENERGY AGENCY. 1976. Radiometric reporting methods and calibration in uranium exploration. Technical Report 174, IAEA, Vienna, 57 p.

IMEOKPARIA, E.G. 1982. Tin content of biotites from the Afu Younger granite complex, Central Nigeria. Economic Geology, 79, pp. 1710-1724.

KEPPIE, J.D. 1979. Geological map of the Province of Nova Scotia. Department of Mines and Energy, Nova Scotia, Scale 1:500,000.

KILLEEN, P.G. 1979. Gamma ray spectrometric methods in uranium exploration - application and interpretation. In Geophysics and Geochemistry in the Search for Metallic Ores; ed. Peter J. Hood; Geological Survey of Canada, Economic Geology Report 31, pp. 163-229.

OLADE, M.A. 1980. Geochemical characteristics of tin-bearing and tin-barren granites, Northern Nigeria, Economic Geology, 75, pp. 71-82.

O'REILLY, G.A. 1983. Geology of the Sangster Lake, Larry's River, and Forest Hill Granitoid Plutons. Nova Scotia Dept. of Mines and Energy, Information Series No. 6, pp. 57-59.

PLANT, J., Brown,C.G., SIMPSON, P.R. and R.T. SMITH. 1980. Signature of metalliferous granites in the Scottish Caledonides. Institution of Mining and Metallurgy Transactions, Section B, Applied Earth Science, 89, November 1980, pp. B198-B120.

SMITH, P.K. 1981. Geology of the Sherbrooke area, Guysborough County, Nova Scotia. Nova Scotia Department of Mines and Energy, Report 81-1, pp. 77-94.

TAYLOR, S.R. 1965. The application of trace element data to problems in petrology. In Physics and Chemistry of the Earth, V. 6, ed. L.H. Ahrens, F. Press, S.K. Rumom and H.C. Usey, pp. 135-213.

TISCHENDORF, G. 1977. Geochemical and petrographic characteristics of silicic magmatic rocks associated with rare-earth mineralization. In Metallization Associated with Acid Magmatism, ed. M. Stemprok, L. Burnal and G. Tischendorf; International Geological Correlation Programme, 2, pp. 41-96.

TUREKIAN, K.K. and K.H. WEDEPOHL. 1961. Distribution of the elements in some major units of the earth's crust. Geological Society of America, Bulletin, 72, pp. 175-191.

YEATES, A.N., B.W. WYATT and D.H. TUCKER. 1982. Application of gamma-ray spectrometry to prospecting for tin and tungsten granites, particularly within the Lachlan Fold Belt, New South Wales. Economic Geology, 77, pp. 1725-1738.

MARITIME SEDIMENTS AND ATLANTIC GEOLOGY

INSTRUCTIONS TO AUTHORS

GENERAL - Two copies of the completed manuscript (paper, note, or discussion) must be submitted to one of the Editors (c/o The Acadia University Institute, Box 67, Acadia University, Wolfville, N.S. B0P 1X0), who will send them out to two appropriate reviewers.

Manuscripts should be typed on white bond paper measuring 8 1/2 x 11 inches (21 x 28 cm), with margins of a minimum of 1 inch (2 1/2 cm). Every part of the manuscript (text, figure captions, references etc.) should be double spaced. Material to be set in italics should be underlined.

The first page of the manuscript should contain only the title, the authors' names, authors' complete business address, and relevant footnotes. Page numbers begin with the title page and all subsequent pages should be numbered accordingly.

Maritime Sediments and Atlantic Geology publishes papers, notes, discussions and miscellanea in ENGLISH and FRENCH.

ABSTRACT - An abstract of approximately 200 words or less is required for all papers and a shorter one for notes. No abstract for discussion and miscellanea sections is necessary. Authors who can submit abstracts in both fluent English and French are encouraged to do so; otherwise a translation will be provided prior to publication. References should not be cited in the abstract.

REFERENCES - should be typed double spaced and listed alphabetically by authors names. Reference to unpublished work should be made as follows: (Pajari, G.E., pers. comm. 1981). Titles of journals should be written in full.

ILLUSTRATIONS - All figures and illustrations should be planned to fit (after reduction) into one column of the text (width 3 1/4 ins. or 8 1/4 cm) or two (width 6 3/4 ins. or 17.1 cm); the length of the columns is 9 ins. (22.4 cm). Illustrations should be numbered consecutively and each one should be referred to, in order, in the text. Authors' names and figure number should be written in the lower right corner of each illustration.

Plates should be submitted on glossy paper with strong contrast. Only black and white plates are acceptable.

All figures and illustrations must include a scale which may be on the figure or illustration or alternatively in the figure caption.

REPRINTS - Reprints must be ordered at the same time as the paper is submitted for publication. The following rates will be used:-

25 reprints (max. 10 pages)	$20.00	50 reprints (max. 10 pages)	$35.00
25 reprints (max. 15 pages)	25.00	50 reprints (max. 15 pages)	45.00
25 reprints (max. 20 pages)	30.00	50 reprints (max. 20 pages)	55.00
25 reprints (over 20 pages)	30.00 + $1.00 per page		

Postage is extra.

It is our policy to allow author(s) to substantiate their thesis with photographs and figures. But increasing costs have made it necessary to now charge a fee for more than an average number of photographs and figures. The editor will inform authors of the charges at the time of submission of their article.

ATLANTIC GEOSCIENCE SOCIETY SPECIAL PUBLICATION: ISSN 0832-7025

SOCIÉTÉ GÉOSCIENTIFIQUE DE L'ATLANTIQUE PUBLICATION SPECIALE: ISSN 0832-7033

1. GEOLOGICAL HIGHWAY MAP OF NOVA SCOTIA
By Bujak J.P. and Donohoe H.V. Jr. 1980 $3.50 Available from: Nova Scotia Government Bookstore, 1597 Hollis Street (P.O. Box 637) Halifax, Nova Scotia, B3J 2T3

2. GEOLOGICAL HIGHWAY MAP OF NEW BRUNSWICK AND PRINCE EDWARD ISLAND / CARTE ROUTIERE GEOLOGIQUE DU NOUVEAU-BRUNSWICK ET D L'ISLE DU PRINCE EDOUARD
By Ferguson Laing and Fyffe L.R. 1985 Members $4.00, non-members $5.00 Available from: Nova Scotia Department of Mines and Energy, 1960 Hollis Street (P.O. Box 1087) Halifax, Nova Scotia, B3J 2X1

3. OCCUPATIONAL SAFETY IN THE GEOSCIENCES (Programme with papers, from a seminar, September 25, 1985)
Ed: Lyttle N. 1985 $2.00 for postage only. Available from: Nova Scotia Department of Mines and Energy, 1960 Hollis Street (P.O. Box 1087) Halifax, Nova Scotia, B3J 2X1

4. FIELD TRIP OF CARBONIFEROUS-JURASSIC SEDIMENTATION AND TECTONICS: MINAS, CUMBERLAND, AND MONCTON BASINS, NOVA SCOTIA AND NEW BRUNSWICK
Boehner R., Donohoe H., Ryan D. and Carter D. (In press) Available from: Nova Scotia Department of Mines and Energy, 1960 Hollis Street (P.O. Box 1087) Halifax, Nova Scotia, B3J 2X1